Cross-layer Energy-efficient Schemes for Multimedia Content Delivery in Heterogeneous Wireless Networks

by

Shengyang Chen

A Dissertation submitted in fulfilment of the requirements for the award of Doctor of Philosophy (Ph.D.)

Dublin City University

School of Electronic Engineering

Supervisor: Dr. Gabriel-Miro Muntean

November, 2014

Declaration

I hereby certify that this material, which I now submit for assessment on the programme of study leading to the award of Ph.D is entirely my own work, that I have exercised reasonable care to ensure that the work is original, and does not to the best of my knowledge breach any law of copyright, and has not been taken from the work of others save and to the extent that such work has been cited and acknowledged within the text of my work.

Student ID:_____58124055_____

Signed: _____

Date: _____

To my dear parents

ACKNOWLEDGEMENT

The first and foremost thank is given to my dearest parents, who have been making great effort to raise me up as a person with good quality, giving me the opportunity to be where I am at this moment. It is the strongest and warmest support from them that enables me to get over with the toughest moments in the past. It is the most precious and honest love from them that I will benefit for the future of my life. They have always been and will forever be my beloved ones.

An extra special acknowledgement is given to my supervisor, Dr. Gabriel-Miro Muntean, who has always been extremely kind, helpful and patient during my postgraduate studying period. Without his lead, there is no way for me to complete this hard path. Without his experienced suggestions, there is no way for me to improve my abilities to be a qualified researcher. Without his great effort to make the best atmosphere in the lab, the past years wouldn't be so mind-engraving. I would like to pay my greatest respect and regard at this moment to Gabi, who has been and will always be my dearest friend.

Also I would like to sincerely acknowledge my colleague and close friend, Dr. Zhenhui Yuan, who have kindly offered me great help countless times when I was confronting with important choices in my academic years. It has been joyful during the past moments with Zhenhui. All the best to his future career in China and the most wonderful wishes to his wife, Ms. Xin Zhang and their about-to-born son!

Great thanks are also given to everyone who used to be in PEL, who is at the moment in PEL and who will soon join PEL, including Bogdan, Ramona, Faisal, Hrishi, Arrthy, Sebastian, Irina, Quang, Ronan, Ruiqi, Yang, Ting, Longhao, Yi, Martin and Leija. It's lucky for me to know you all and to spend the past years together, trying our best to progress on research. Special thanks to Bogdan, Ramona, Faisal and Hrishi, who I was lucky enough to co-operate together with. I have really learnt a lot from the wisdom and experience of you.

Appreciations are also sent to the great technical staff from School of Electronic Engineering, Dublin City University, Ireland, who have been very supportive with the issues in the lab.

Special thanks to the Irish Research Council and Mr. Alan O'Herlihy, the CEO of Everseen Ltd., who generously offers me financial support to complete this degree.

Last but not least, I gratefully acknowledge Dr. Pascal Landais, Prof. Adlen Ksentini and Dr. Cathal Gurrin for their time organizing the PhD defence.

Dublin, Sept.2014

Shengyang Chen

LIST OF PUBLICATIONS

[Journals]

- Z. Yuan, **S. Chen**, G. Ghinea and G.-M. Muntean, "User Quality of Experience of Mulsemedia Applications", *ACM Transactions on Multimedia Computing, Communications and Applications (ACM TOMM)*, May 2014

[Conference Papers]

- R. Andreucetti, Z. Yuan, **S. Chen** and G.-M. Muntean, "Smartphone Energy Consumption of Multimedia Services in Heterogeneous Wireless Networks", *IET Irish Signals & Systems Conference (ISSC)*, Aug. 2014
- T. Ding, **S. Chen**, Z. Yuan and G.-M. Muntean, "Smartphone Energy Consumption Models for Multimedia Services using Multipath TCP", *IEEE Consumer Communications and Networking Conference (CCNC)*, January 2014
- **S. Chen**, Z. Yuan and G.-M. Muntean, "A Traffic Burstiness-based Offload Scheme for Energy Efficiency Deliveries in Heterogeneous Wireless Networks", *IEEE Globecom Workshop*, December 2013
- **S. Chen** and G.-M. Muntean, "AOC-MAC: A Novel MAC-layer Adaptive Operation Cycle Solution for Energy-awareness in Wireless Mesh Networks", *IEEE Vehicular Technology Conference (VTC)*, September 2013
- **S. Chen**, Z. Yuan and G.-M. Muntean, "An Energy-aware Multipath-TCP-based Content Delivery Scheme in Heterogeneous Wireless Networks", *IEEE Wireless Communications and Networking Conference (WCNC)*, April 2013
- **S. Chen** and G.-M. Muntean, "E-Mesh: An Energy-efficient Cross-layer Solution for Video Delivery in Wireless Mesh Networks", *IEEE International Symposium on Broadband Multimedia Systems and Broadcasting (BMSB)*, June 2012

TABLE OF CONTENTS

ABSTRACT

The wireless communication technology has been developed focusing on fulfilling the demand in various parts of human life. In many real-life cases, this demand directs to most types of commonly-used rich-media applications which – with diverse traffic patterns - often require high quality levels on the devices of wireless network users. Deliveries of applications with different patterns are accomplished using heterogeneous wireless networks using multiple types of wireless network structure simultaneously. Meanwhile, content deliveries with assuring quality involve increased energy consumption on wireless network devices and highly challenge their limited power resources. As a result, many efforts have been invested aiming at high-quality and energy-efficient rich-media content deliveries in the past years.

The research work presented in the thesis focuses on developing energy-aware content delivery schemes in heterogeneous wireless networks. This thesis has four major contributions outlined below:

1. **An energy-aware mesh router duty cycle management scheme (AOC-MAC)** for high-quality video deliveries over wireless mesh networks. AOC-MAC manages the sleep-periods of mesh devices based on link-state communication condition, reducing their energy consumption by extending their sleep-periods.

2. **An energy efficient routing algorithm (E-Mesh)** for high-quality video deliveries over wireless mesh networks. E-Mesh evolves an innovative energy-aware OLSR-based routing algorithm by taking energy consumption, router position and network load into consideration.

3. **An energy-aware multi-flow-based traffic load balancing scheme (eMTCP)** for multi-path content delivery over heterogeneous wireless networks. The scheme makes use of the MPTCP protocol at the upper transport layer of network, allowing data streams to be delivered across multiple consequent paths. Meanwhile, this benefit of MPTCP is also balanced with energy consumption awareness by partially off-loading traffic from the paths with higher energy cost to others.

4. **A MPTCP-based traffic-characteristic-aware load balancing mechanism (eMTCP-BT)** for heterogeneous wireless networks. In eMTCP-BT, mobile applications are categorized according to burstiness level. eMTCP-BT increases the energy efficiency of the application content deliveries by performing a MDP-based distribution of traffic delivery via the available wireless network interfaces and paths based on the traffic burstiness level.

LIST OF FIGURES

LIST OF TABLES

LIST OF ABBREVIATIONS

3G: Third Generation Cellular Networks

3GPP: Third Generation Partnership Project

4G: Fourth Generation Cellular Networks

ARF: Auto Rate Fallback

AARF: Adaptive Auto Rate Fallback

AP: Access Point

AMP: Adaptive Media Player

AVC: Advanced Video Coding

BER: Bit Error Rate

BSC: Base Station Controller

BSS: Basic Service Set

BTS: Base Transceiver Station

CAC: Call Admission Control

CART: Classification And Regression Tree

CBR: Constant Bit Rate

CDMA: Code Division Multiple Access

CSMA/CA: Carrier Sense Multiple Access with Collision Avoidance

CN: Core Network

CSN: Connectivity Service Network

DCCP: Datagram Congestion Control Protocol

DCF: Distributed Coordination Function

DCT: Discrete Cosine Transform

DS: Distribution System

DVB: Digital Video Broadcasting

EDCF: Enhanced Distributed Coordination Function

EDCA: Enhanced distributed channel access

EDGE: Enhanced Data Rates for GSM Evolution

EGPRS: Enhanced GPRS

E-UTRAN: Evolved-UTRAN

FTP: File Transfer Protocol

GOP: Group of Pictures

GPRS: General Packet Radio Service

GSM: Global System for Mobile Communications

HD: High Definition

HSPA: High-Speed Packet Access

HSDPA: High-speed Downlink Packet Access

HSUPA: High-speed Uplink Packet Access

HTTP: Hypertext Transport Protocol

iBE: intelligent Bandwidth Estimation

IEEE: Institute of Electrical and Electronics Engineers

IEC: International Electro technical Commission

IETF: Internet Engineering Task Force

IMS: IP Multimedia Subsystem

IP: Internet Protocol

ISO: International Organization for Standardization

ITU: International Telecommunication Union

LAN: Local Area Network

LTE: Long-Term Evolution

MAC: Medium Access Control

MAN: Metropolitan Area Network

MBE: Model-based Bandwidth Estimation

MDP: Markov Decision Process

MH: Mobile Host

MIHF: Media Independent Handover Function

MICS: Media-Independent Command Service

MIES: Media-Independent Event Service

MIIS: Media-Independent Information Service

MIMO: Multiple Input Multiple Output

MIP: Mobile IP

MIPv4: Mobile IPv4

MIPv6: Mobile IPv6

MN: Mobile Node

MOS: Mean Opinion Score

MPEG: Moving Picture Experts Group

MPTCP: Multi-path TCP

MSSSIM: Multi-scale Structural Similarity Index

OFDMA: Orthogonal Frequency-Division Multiple Access

OLSR: Optimized Link State Routing

PAN: Personal Area Networks

PCF: Point Coordination Function

PDA: Personal Digital Assistants

PDF: Policy Decision Function

PDN: Packet Data Network

PEVQ: Perceptual Evaluation of Vide Quality

PGM: Probe Gap Model

PRM: Probe Rate Model

PMIP: Proxy Mobile IP

PMIPv6: Proxy Mobile IPv6

PSNR: Peak-Signal-to-Noise-Ratio

PSTN: Public Switching Telephony Network

QoE: Quality of Experience

QoS: Quality of Service

RAN: Radio Access Network

RAT: Radio Access Technology

RRM: Radio Resource Management

RSS: Received Signal Strength

RTP: Real Time Transport Protocol

RTCP: RTP Control Protocol

RTMP: Real Time Messaging Protocol

RTMFP: Real-Time Media Flow Protocol

RTSP: Real Time Streaming Protocol

RTT: Round-Trip Time

SAMMy: Signal Strength-based Adaptive Multimedia Delivery

SCTP: Stream Control Transmission Protocol Mobile

ST-DEV: Standard Deviation

SIM: Subscriber Identity Module

SINR: Signal to Interference plus Noise Ratio

SIP: Session Initiation Protocol

SIR: Signal-to-Interferences Ratio

SMS: Standard Message Service

SNR: Signal to Noise Ratio

SS: Subscriber Station

SSIM: Structural Similarity Index

STA: Station

TDMA: Time Division, Multiple Access

TD-SCDMA: Time Division Synchronous CDMA

TFRC: TCP-Friendly Rate Control

TCP: Transmit Power Control

UDP: User Datagram Protocol

UMB: Ultra Mobile Broadband

UMTS: Universal Mobile Telecommunications System

UTRAN: UMTS Terrestrial Access Network

UWB: Ultra-Wideband

VoD: Video on Demand

VoIP: Voice over IP

VQM: Video Quality Metric

VSQI: Video Streaming Quality Index

VTQI: Video Telephony Quality Index

WAN: Wide Area Network

WCDMA: Wideband CDMA

Wi-Fi: Wireless Fidelity

WiMAX: Worldwide Interoperability for Microwave Access

WLAN: Wireless Local Area Networks

WMAN: Wireless Metropolitan Area Networks

WP: Weighted Product

WPAN: Wireless Personal Area Networks

WRAN: Wireless Regional Area Network

WSNR: Weighted-Signal-to-Noise-Ratio

WWAN: Wireless Wide Area Networks

CHAPTER 1

Introduction

1.1 Research Motivation

Over the past decades, the demand for support for data communications has increased significantly. This demand has been fueled by the increasing popularity of network-based services such as file transfer, web browsing, voice over IP (VoIP) and video streaming, which are responsible for large amounts of data exchange. In terms of the quality of communications, different types of network services usually have a range of requirements. For example, online shopping via web browsing involves a process of fast exchange of short messages such as order information, payment details and receipts which need very short delays. On the other hand, video conferencing involves long-term communication sessions between the attendees and requires as much as possible reliable network connectivity for continually exchanging large amounts of data packets. Figure 1.1 presents an example of possible network services accessible from an end user device (smartphone) over two network options.

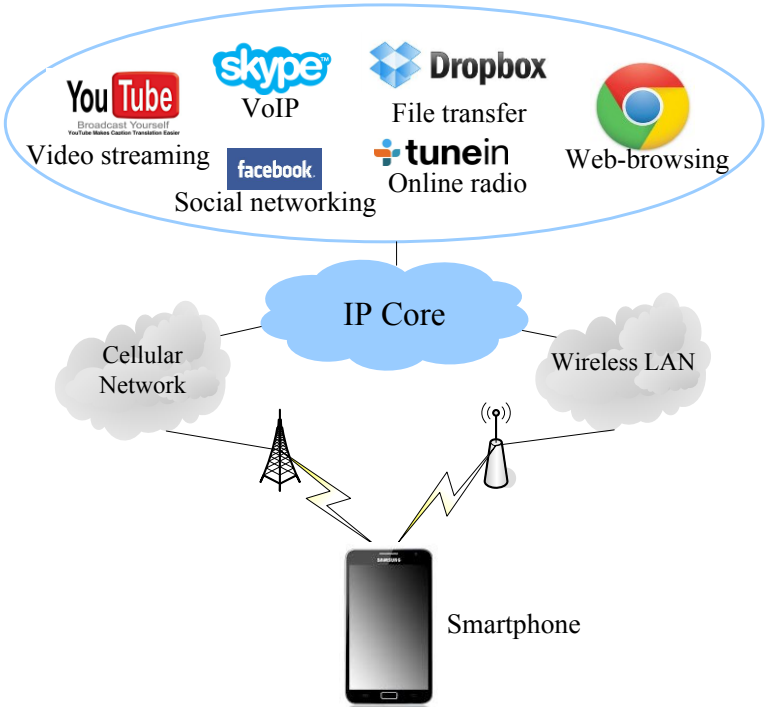

Figure 1.1 Example of possible network applications

The basis of network services is a connection with the Internet, which can be achieved via wired or wireless solutions. Compared with wired networks, wireless networks have been with an important impact in mobile communications and have been adopted by many network service providers. Wireless connection accessibility is enabled by using different Radio Access Technologies (RATs), including broadband wireless networks such as Wireless local/Personal/Metropolitan Area Networks (WLAN/WPAN/WMAN) [1], Universal Mobile Telecommunications System (UMTS) [2] and Long-Term Evolution (LTE) [3]. Nowadays, various RATs with difference in signal coverage range, capacity and data rate are used to overlap various locations.

With the advances in wireless network technology, usage of end user mobile devices such as smartphones, tablets and laptops has increased rapidly, accompanied by the significant growth of data traffic of high-level rich network services. Investigation done by Cisco [4] on the impact of network application shows that the number of mobile devices has grown from 6.5 billion to 7 billion in 2013, with the growth of associated global data traffic reaching 81% from 820 petabytes per month to 1.5 exabytes per month. It is noticeable that over 50% of the grown data traffic is video, representing the highest rate of increase among all the application categories [4]. The investigation also forecasts that within the next five years, the number of mobile devices will grow to over 10 billion and the associated global data traffic will increase approximately 11-fold, reaching 15.9 exabytes per month by 2018 [4]. Moreover, as the next generation wireless networks will be able to support high traffic load over the communication channels, the mobile network connection speed is expected to increase two-fold. As a result, over 66% of the global mobile traffic will be video traffic by 2018 [4].

As many companies aspire to enhance their marketing strategies for business competition by taking advantage of the significant growth of mobile device usage, the popularity of rich media content on mobile devices of users is expected to be substantially increasing, especially for advertising. According to the report on rich media monitor insights proposed by Celtra Inc. [5], native advertisements deliver over four times higher expansion rates in comparison with static mobile banners. In addition, the report reveals that rich media mobile ads generate 12 times more clicks than desktop banner ads [5].

Summarizing the aspects discussed above, the main goal of current and future

developments in wireless networking is to propose solutions for mobile devices to meet the demand on high network loads.

1.2 Problem Statement

High user Quality of Service/Experience (QoS/QoE) for various network services, especially while performing wireless communications, is considered essential for further development of these services. It has been a challenge over the past years to provide high quality video-related mobile services with QoS/QoE provisioning over wireless networks, as the network resources involved, such as channel bandwidth and signal strength, are often constrained. Moreover, several factors commonly used for video quality evaluation, such as bit rate, resolution and frame rate, are severely affected by changes of the wireless network condition, especially user mobility that changes the entire topology of the wireless network. Connections between the devices and the Internet in such conditions are unstable and mobile video services are easily interrupted or delayed, which degrades the video quality and user experience. This issue opens up the demand for solutions to ensure the stability of mobile application service in order to provide a best user-perceived quality. Many associated research efforts have already been done in terms of wireless network self-adaptation so that the smoothness of the services is ensured.

The energy consumption of wireless radio access technologies on user devices is another important research issue nowadays. Several advanced wireless radio access technologies such as UMTS and LTE have been designed for supporting large data transmission services with good quality as they offer support for large bandwidth and wide signal coverage. However, the usage of such radio access interfaces severely increases the total energy consumption of the end user device in comparison with traditional interfaces such as the IEEE 802.11 protocol family (Wi-Fi) [6], as they need higher levels of signal strength. This makes the batteries of mobile devices drain faster and shortens the active time of the devices, which is inconvenient for users and consequently degrades QoS/QoE. Although developments in terms of increasing battery power capacity are excellent [7], they do not keep up with the development of the wireless communication technologies as well as application services which have increasing energy requirements [8]. The issue of the increasing energy consumption is even

more serious in the case of using multiple wireless communication technologies, which has already happened in terms of hardware deployment for several types of popular smartphones on the market. For example, the newly released iPhone 5s and Samsung Galaxy SIII provide support of wireless network access via both Wi-Fi and LTE interfaces at the same time. Despite the benefits in terms of performance improvement of wireless-communication-based services, dual radio usage reduces the life-span of the wireless device battery, further affecting user QoE.

With the availability of multiple wireless radio access technologies and the fast growth of multimedia application usage, it is more and more common to see such a scenario in daily life: a user with several different types of application running on his mobile device, which is connected to the Internet via multiple sorts of wireless networks (LTE and Wi-Fi, for example). The user expects both good application service quality and long battery life span for the mobile device, while the operators of the wireless devices in the multiple networks also expect energy saving and connection stability. Most of the existing network solutions do not fulfill these expectations simultaneously.

Considering the aspects mentioned above, there is a need for investigating solutions that makes use of multiple wireless communication technologies in a more efficient manner in terms of energy consumption and application service quality, especially quality of rich-media type of services and the related QoE. The balance between the energy consumption of wireless network devices and the application service quality remains one of the main research challenges, as many important factors such as network load, user/device mobility, active time of devices and cooperation between various radio access technologies need to be considered within different priorities for different situations.

1.3 Solution Overview

In this thesis, four separate solutions are proposed in order to achieve high energy efficiency for network operators of wireless mesh networks and for end user mobile devices in heterogeneous wireless networks, and also to obtain high QoS benefit for application services on both. The solutions are distributed in different layers of a heterogeneous wireless network topology integrating a wireless mesh network and a LTE network, providing multi-connections for an end user mobile device, as shown in Figure 1.2:

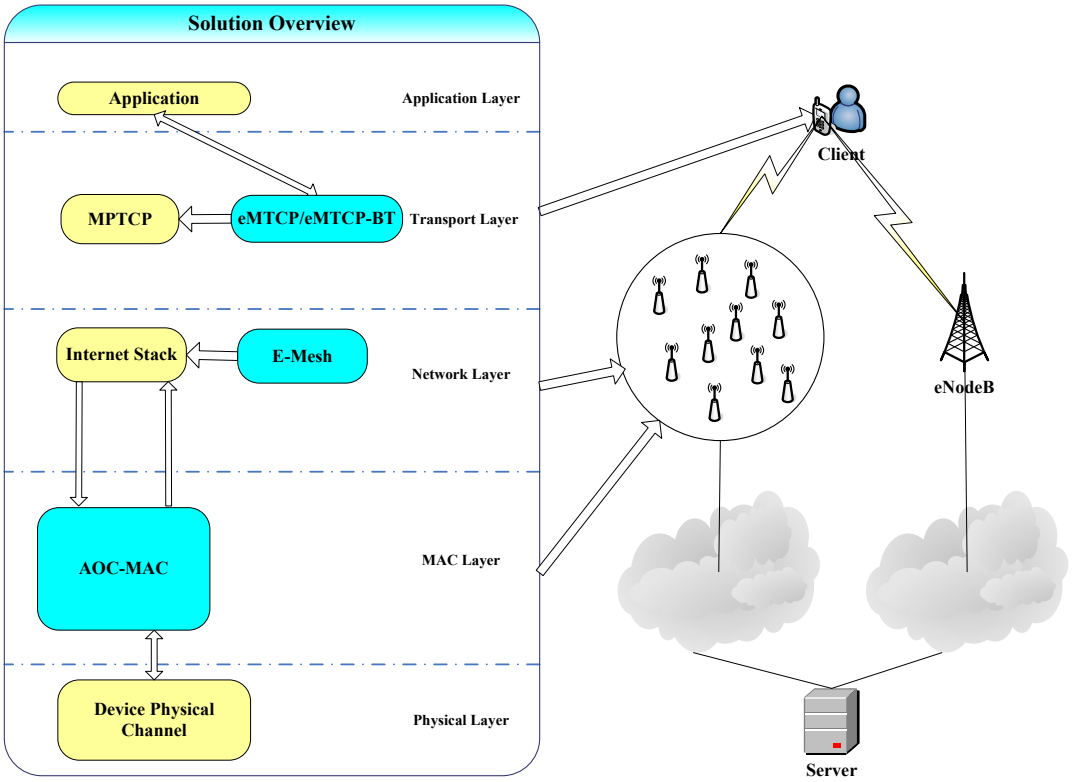

Fig.1.2. Overview of contributions in a heterogeneous wireless network environment

1) AOC-MAC: an energy-aware mesh router duty cycle management scheme deployed at MAC layer for high-quality video deliveries over wireless mesh networks. AOC-MAC manages the sleep-periods of mesh devices in a smarter way based on link-state communication condition, reducing the energy consumption of mesh routers by extending their sleep-periods.

2) E-Mesh: an energy efficient routing algorithm for high-quality video delivery over wireless mesh networks. E-Mesh is deployed at network layer and evolves an innovative energy-aware routing algorithm which extends the Optimized Link State Routing (OLSR) [9] algorithm by taking energy consumption, changes of router position and network load into consideration.

3) An energy-aware multi-flow-based traffic load balancing scheme (eMTCP) deployed at the upper transport layer for heterogeneous wireless networks. The MPTCP-based scheme makes use of the IETF-proposed **Multipath TCP (MPTCP)** protocol [10] at the upper transport layer of network, allowing single data stream to be delivered across multiple simultaneous wireless consequent paths. Meanwhile, this benefit of MPTCP is also balanced with energy

consumption awareness by partially offloading traffic from the radio access channels with higher energy cost to others.

4) A MPTCP-based traffic-characteristic-aware load balancing mechanism (eMTCP-BT) deployed at the upper transport layer for heterogeneous wireless networks. In eMTCP-BT, mobile applications traffic is categorized according to its burstiness level, including some most widely-used services such as Voice over IP (VoIP) service, video streaming, large file downloading and web browsing. eMTCP-BT increases the energy efficiency of the application content deliveries by performing an innovative machine-learning-based mathematical distribution of the overall traffic for its delivery via the available wireless network interfaces and paths based on the traffic burstiness level.

1.4 Thesis Contributions

This thesis contributes the current state of the art as follows:

- **AOC-MAC**: an energy-aware mesh router duty cycle management scheme which adaptively adjusts the sleep-periods of router devices in a wireless mesh network. AOC-MAC is a MAC-layer solution which controls the sleep-periods of mesh routers according to the condition of application traffic delivery detected by the E-Mesh solution. In general, the sleep-periods of idle mesh routers are increased in order to save energy. On the other hand, the sleep-periods are reduced for the mesh routers changing from idle to busy, in order to maintain the stability of network connection and traffic delivery for good QoS levels.
- **E-Mesh**: an energy-adaptive routing algorithm for router devices in a wireless mesh network. E-Mesh consists of a novel utility function for obtaining the optimal route for traffic delivery in terms of energy consumption level, network load and connection stability for each mesh router, based on the classic OLSR algorithm. E-Mesh also works in conjunction with AOC-MAC via informing it with the detection result of the network connection condition and traffic delivery state.
- **eMTCP**: an energy-aware traffic load balancing scheme for rich-media content

delivery to end-user mobile devices in heterogeneous wireless networks. eMTCP makes use of the IETF-proposed multi-path TCP transport-layer protocol for multi-path wireless connection maintenance, by which the transmission bandwidth is significantly increased. The issue of extra energy consumption on MPTCP-based mobile devices is caused by using multiple wireless radio access technologies and is solved by off-loading traffic from the more energy-consuming radio interfaces to others. Traffic off-loading is achieved by the co-operation of the sub-flow interface state detector module and the off-loading controller module of eMTCP. The sub-flow interface state detector observes the physical-layer traffic receiving and idle states of the wireless radio interfaces used on mobile devices. The off-loading controller module performs the off-loading activity according to the state observation results from the sub-flow interface state detector module. As a result, eMTCP makes increase in energy efficiency on mobile devices.

- **eMTCP-BT**: an energy-efficiency-oriented traffic load balancing scheme extending the traffic off-loading scheme of eMTCP. eMTCP-BT performs an innovative distribution of the overall traffic for its delivery via the available wireless radio interfaces and paths on mobile devices, according to the traffic characteristics of the running applications. The traffic distribution on each wireless content delivery path is adaptively managed for obtaining the highest energy efficiency for mobile devices. The adaptive management of traffic distribution in eMTCP-BT is provided by adding a traffic classification module to co-operate with the sub-flow interface state detector module and the off-loading controller module of eMTCP. The traffic classification module categorizes the burstiness level of the application traffic on mobile devices and the classified traffic burstiness level information is sent to the off-loading controller module as an important factor for traffic off-loading percentage decision making. By using this mechanism, eMTCP-BT further increases energy efficiency on mobile devices as the energy-efficiency-optimal traffic off-loading percentage is adaptively achieved.

1.5 Thesis Structure

The thesis was structured in chapters as follows:

- *Chapter 1* – introduces motivation of the research, states the research challenges, presents a brief overview of the solution and lists the contributions of the research.
- *Chapter 2* – introduces the technical background of the research involved in this thesis.
- *Chapter 3* – presents a detailed review of the related works in the research area of this thesis.
- *Chapter 4* – describes the overall system architecture of the four proposed solutions.
- *Chapter 5* – presents the simulation-based test bed setup, design of scenarios, tests and result analysis for the four proposed solutions.
- *Chapter 6* – presents the real-life experimental test bed setup, design of scenarios, tests and result analysis for the four proposed solutions.
- *Chapter 7* –concludes the thesis and presents possible future work directions.

1.6 Chapter Summary

This chapter presents the research motivation and includes the problem statement for the work repeated in this thesis. The solution overview, research contributions to advancement of the state of the art as well as the thesis structure are also included.

CHAPTER 2

Technical Background

Abstract

This chapter introduces the technical background of the work reported in this thesis. First, the evolution of the wireless network environment and the corresponding communication technologies is reviewed. Next, the application layer, transport layer and MAC/PHY layer protocols relevant to this work are briefly introduced. The concepts of user Quality of Experience (QoE) and Quality of Service (QoS) are also described together with quality assessment methods, especially in the context of video over wireless networks. Finally, a brief investigation of the current situation of energy efficiency of the wireless devices is presented.

2.1 Evolution of Wireless Networks

During the past years, the wireless networks have experienced an astonishing evolution process towards offering support for various application services at high quality levels [11]. Wireless communications are based on a set of global wireless network standards to support both broadband wireless networks and cellular networks. Among the broadband wireless networks, efforts were made to propose technologies behind Wireless Personal Area Networks (WPANs), Wireless Local Area Networks (WLANs), Wireless Metropolitan Area Networks (WMANs), Wireless Wide Area Networks (WWANs). In cellular network space, various technologies from different generations have been proposed with increasing bit rate, range and service support.

2.1.1 Generic Overview of Broadband Wireless Networks

In general, broadband wireless networks are based on extensions of point-to-point wireless solutions utilized for fixed connectivity. Broadband wireless networks are used for high-speed and high-capacity delivery tasks such as voice, multimedia and Internet access services between fixed positions, without some support for user mobility needs. In terms of network topology scale, broadband wireless networks are briefly divided into WPANs, WLANs,

WMANs and WWANs. In this thesis, efforts based for WLAN support are focused on.

2.1.1.1 Brief Overview of Wireless PANs/MANs/WANs

WPANs are used to provide wireless interconnections between multiple computing and communicating devices centered on the workspace of an individual, based on the IEEE 802.15 standard [12]. Devices in WPANs are able to communicate to each other directly within close distance with each other, or to communicate via a central wireless server when in its range. Interference or unexpected access to certain information from other devices in the same WPAN can be selectively blocked by the current device. A connection made through a WPAN involves little or no infrastructure or direct connectivity to the world outside the link, which allows small, power-efficient, inexpensive solutions to be implemented for a wide range of devices. State-of-the-art WPAN-based technologies include Bluetooth [12] and Infrared Data Association [13].

WMANs are with much larger intended coverage area within urban areas in comparison with WPANs. WMANs provide individual connections that span far distances for backhaul applications while also support last-mile connectivity. The Worldwide Interoperability for Microwave Access (WiMAX) standard [14], released as the interoperable implementations of the IEEE 802.16 family, is an attempt to employ multiple spectrum usage of WMANs. The earlier version of WiMAX offers data rates of up to 75 Mbps for users with fixed positions and the later implementation of the IEEE 802.16e [15], referred to as the Mobile WiMAX, offers date rate of up to 30 Mbps for users with mobility. The newer released IEEE 802.16m standard aims at achieving the data rate level of 1 Gbps for users with fixed position and 100 Mbps for users with mobility [16].

WWANs involve larger geographical size of network topologies in comparison with WMANs and WPANs, in which application services are delivered via large-scale mobile telecommunication cellular network technologies. Devices are able to get access to the Internet anywhere within the regional boundaries of WWANs if the corresponding hardware is integrated with the support of regional, national or global wireless service providers. Some WWANs incorporate with message encryption and authentication mechanisms to provide secure connection paths for radio communication systems.

2.1.1.2 Wireless LANs

Wireless LAN (Wi-Fi) is one of the most successful wireless network technologies, allowing cheaper deployment of LANs, including in places where cables cannot be deployed, such as historical buildings and outdoor areas. It was first proposed by the IEEE 802.11 standard group for offering communication bit rates about 1-2 Mbps in year. It has been amended over the past years in terms of available channel bandwidth. Table 2.1 shows the data rate supports for some of the improved versions of the original IEEE 802.11 standard:

TABLE 2.1 Data Rate of Different IEEE 802.11 WLAN Standards

802.11 protocol	Year	Frequency (GHz)	Bandwidth (MHz)	Data rate per stream (Mbit/s)
802.11a	1999	5	20	54
802.11b	1999	2.4	22	11
802.11g	2003	2.4	20	54
802.11n	2009	2.4/5	20/40	600
802.11ac	2013	5	20/40/80/160	866.7
802.11ad	2012	60	2160	7000

As Table 2.1 shows, the first improved version of the original IEEE 802.11 standard is the IEEE 802.11a proposed in 1999 [17], which offers support for various data bandwidths: 6, 9, 12, 18, 24, 36, 48 and 54 Mbps, using a 52-subcarrier Orthogonal Frequency-Division Multiplexing (OFDM) with 5 GHz frequency. While the theoretical value of the maximum available raw data rate of 802.11a is 54 Mbps, the actual achievable network throughput of 802.11a in real-life cases is around 20 Mbps [17]. The higher carrier frequency band of 802.11a in comparison with 802.11 significantly increases the band capacity and avoids channel disconnections and service degradation to certain degree, yet it also has some disadvantages in terms of signal strength and cover range due to the proportional signal path loss.

Another widely-used amendment of the original 802.11 specification is the 802.11b [18] with significant increase in bandwidth support and substantial decrease in price. 802.11b uses the Complementary Code Keying (CCK) modulation technique in the same 2.4 GHz frequency band with 802.11 and extends the available bandwidth to cover 1, 2, 5.5 and 11 Mbps. In real-life cases, the actual enabled throughput is approximately 5.9 Mbps with TCP and 7.1 Mbps

with UDP [18]. One of the main disadvantages of 802.11b is that the usage of 2.4 GHz frequency band leads to massive interference from other devices using the same frequency band, such as cordless telephones and Bluetooth devices.

The third amendment of the original 802.11 specification is the 802.11g [19] which uses the same OFDM modulation scheme with 802.11a (hence supported the same bandwidth range from 6 Mbps to 54 Mbps), but operates in the 2.4 GHz frequency band. The actual throughput in a real network scenario is approximately 22 Mbps, which is similar with that of 802.11a with only some latency overhead brought by the backwards compatibility with the 802.11b devices [19]. 802.11g offers data rates of 6, 9, 12, 18, 24, 36, 48 and 54 Mbps with the OFDM modulation scheme and reverted to CCK for 5.5 and 11 Mbps and DBPSK/DQPSK+DSSS for 1 and 2 Mbps, respectively, for backward compatibility.

The IEEE 802.11n standard proposed in 2009 [20] improves the network bandwidth very much in comparison with 802.11a and 802.11g as the maximum data rate increases from 54 Mbps to 600 Mbps. 802.11n achieves this improvement by adding the Multi-Input Multi-Output (MIMO) feature and multiple 40 MHz channels to the physical layer of the original IEEE 802.11. MIMO uses Spatial Division Multiplexing (SDM) to transfer multiple independent data streams simultaneously within one spectral channel so that the data throughput is significantly increased. On the other hand, the usage of 40 MHz channels (available for both 2.4 GHz and 5 GHz frequency bands) doubles the original channel bandwidth in the 802.11 physical layer.

The IEEE 802.11ac standard released in 2011 [21] further improves the network bandwidth in comparison with the original 802.11 on the 5 GHz frequency band, with 500 Mbps maximum data rate for a single link and up to 1 Gbps maximum data rate for multi-station WLAN. This is achieved by using the following new technologies:

- *Extended channel binding*: RF channel bandwidth extended from 40 MHz in 802.11n to 80 MHz (and optionally 160 MHz in some cases)
- *Increased MIMO spatial streams*: number of available spatial streams extended from 4 in 802.11n to 8
- *Multi-user MIMO*: multiple stations transmit/receive independent data stream simultaneously

- *High-density modulation*: up to 256-Quadrature-Amplitude-Modulation (QAM) with rate 3/4 and 5/6 was supported in comparison with 64-QAM and rate 5/6 in 802.11n

To upgrade the wireless communication speed to multi-gigabit level, the Wi-Fi alliance has promoted the introduction of the IEEE 802.11ad standard in 2009 [22]. This addition enables support for multi-gigabit transmission speeds between wireless devices that operate in the 2.4, 5 and unlicensed 60 GHz frequency band. The maximum data rate available in this specification is 7 Gbps.

In general, WLANs can be divided into two types in terms of network structure: ad-hoc and infrastructure/non-ad-hoc. In the ad-hoc wireless networks, mobile devices exchange data directly through data forwarding between each other based on certain routing mechanisms, without making use of any centralized structures. In the infrastructure wireless networks, on the other hand, communication between wireless mobile devices is enabled via central components like base stations or access points. One of the benefits of the ad-hoc networks over the infrastructure networks is the elimination of any existing infrastructure with central components, which saves management and maintenance cost and adds flexibility. However, in many cases the ad-hoc networks involve increased overhead in comparison with the infrastructure networks.

2.1.1.3 Wireless Mesh Networks

One of the most widely used ad-hoc WLANs is the Wireless Mesh Network (WMN). A typical WMN consists of multiple radio nodes referred to as mesh points (MPs) organized in a mesh topology. Mesh points are categorized into three types: mesh clients, mesh routers and gateways. The mesh clients are usually wireless terminal devices of end users, such as laptops, smartphones and tablets, serving both as data sender and receiver. The mesh routers forward traffic through the gateways, which may (but do not have to) be connected with the Internet. A single mesh link is shared by two independent mesh points which exchange data directly with each other through the wireless medium. The pair of such two mesh points is defined as neighbor nodes. Some power constraint mesh points are able to communicate with their neighbor nodes only and do not have congestion control services. This structure offers reliability to communication services as nodes that fail to operate do not affect the communication of the other active nodes.

WMNs can be implemented with various network technologies, among which the IEEE

802.11s standard [23] is of particular interest to this thesis. The IEEE 802.11 task group introduces extension of the 802.11 MAC layer in 802.11s by introducing radio-aware metrics over self-configuring multi-hop technologies to support unicast, multicast and broadcast data delivery at the same time. It defines the Hybrid Wireless Mesh Protocol (HWMP) as the routing protocol, within which mobile devices communicate with each other in a mesh manner and get access to the devices outside the mesh network through gateway devices. The 802.11 standards (802.11a/b/g/n) carry the actual data traffic,

The following aspects of the 802.11s standard are specifically of interest:

- *Path selection and routing* – HWMP is used as the default routing protocol, providing hierarchical schemes for data forwarding through the tree-like logical structure in mesh networks and on-demand routing schemes for addressing mobility of mesh points.
- *Medium Access Control* – mesh points synchronize their timers with time stamp and offset information included in beacons and probe response messages from other mesh points. Enhancement on the Network Allocation Vector (NAV) has been introduced, including new types of NAVs such as the packet-by-packet NAV (which protects until the receipt of an ACK), for the Enhanced Distributed Channel Access (EDCA) mechanism, which provides service differentiation allowance by using multiple channel access functions to control the backoff counters, timers and contention windows.
- *Congestion control* – mesh points regulate the received and transmitted data amount to minimize queue size which is used as congestion detection metric and notification of congestion on one mesh point is broadcast to one-hop neighbor mesh points so that they can rate limit the transmission.
- *Power management* – Mesh points with power supply could switch from awake state to sleep state to save energy. The mesh point stays awake and listens to incoming beacons for the time period specified in the Announcement Traffic Indication Message (ATIM). When it goes to sleep, the neighbor mesh points could send special packages to it to make it reactive or send traffic during the ATIM window to request it to stay awake past the ATIM window, so that unnecessary congestion is avoided.

2.1.2 Cellular Networks

Despite the rapid development of the WLAN technologies, the cellular networks are still highly popular. Powered by technologies of different generations, cellular networks are the most important communication technologies that cover large geographic areas and have relative large capacity and reduced interference to/from other signals. The evolution of cellular networks is specifically striking in the entire history of the evolution of wireless networks. It is investigated in detail in this section.

The evolution of cellular networks started from the proposal of the first generation (1G) used by analog mobile phones in the 1980s. 1G used analog transmission for basic voice communication services with certain level of support for handover and roaming capabilities. Examples of the 1G systems included the Nordic Mobile Telephones (NMT) [24] and the Total Access Communication Systems (TACS) [25], which were both popular in Europe, and the later proposed Advanced Mobile Phone System (AMPS) in the United States [26]. Diverse types of 1G systems were deployed in different areas with different frequency bands. For example, the NMT system operated in the 450 MHz frequency band, the TACS used the 900 MHz frequency band and the AMPS ran in the 800-900 MHz frequency band. As a result, it was challenging for multiple 1G systems to interoperate between different countries, which was one of its main disadvantages.

After the development of 1G, the second generation (2G) of cellular transmission technologies was launched at the end of the 1980s. Transmission between mobile devices in 2G changed from analog to digital, using multiple access technologies such as Time Division Multiple Access (TDMA) and Code Division Multiple Access (CDMA). The new access technologies of 2G enabled supports for extra low-throughput data communication services upon the existing basic voice-IP service of 1G. Other benefits including higher spectrum efficiency, better data services and more advanced roaming were also provided. Examples of the 2G systems included the widely-used Global System for Mobile Communications (GSM) operated in 900 MHz frequency band in Europe, the CDMA One system in the United States and Personal Digital Cellular (PDC) system in Japan [27].

To meet the growing requirements of data traffic services, the GSM system has gradually evolved. A typical GSM system consists of the following components, as illustrated in

Figure 2.1:

- Mobile Station (MS): contains the mobile equipment and the corresponding Subscriber Identity Module (SIM) card which stores the information of the subscribers
- Base Station Subsystem (BSS)
  - Base Transceiver Station (BTS): maintains the air interface used for communication with the MS
  - Base Station Controllers (BSC): manages the radio network
- Network Switching Subsystem (NSS)
  - Mobile Switching Center (MSC): controls the calls in a large geographical area
  - Visitor/Home Location Register (VLR/HLR): VLR holds information about the users and HLR holds permanent information about subscribers and the current location
  - Authentication Center (AC): deals with authentication and encryption parameters for information security
  - Equipment Identity Register (EIR): holds information of valid mobile equipment

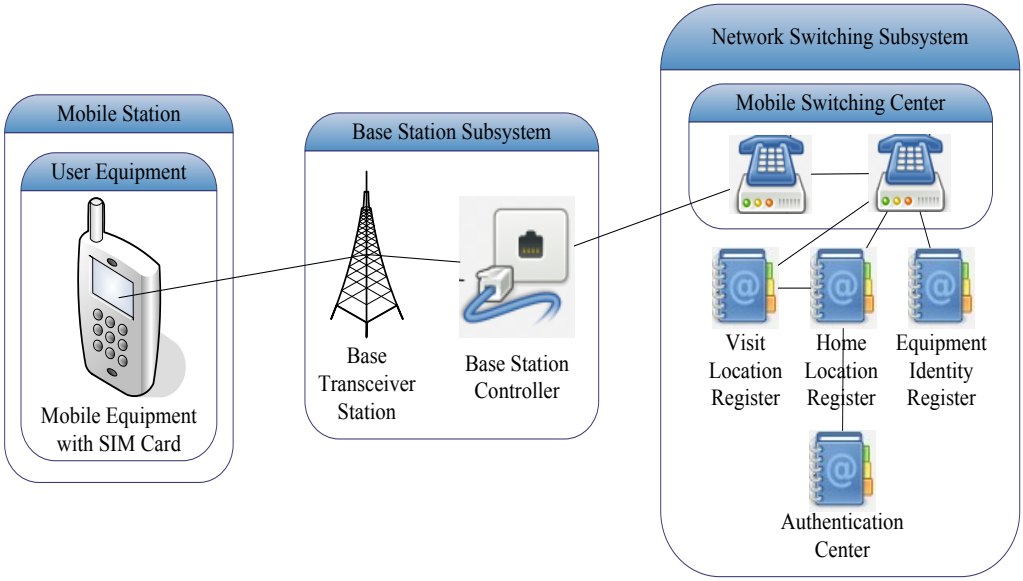

Fig.2.1 GSM Structure

New technologies were developed based on the GSM system to address the need for communication services over the air interfaces. One of the examples of such technologies was the General Packet Radio Service (GPRS) [28] which offered higher data rates than GSM (up to 160 Kbps). It introduced packet switching protocols to break up information to be sent into

packets with addressing data, and made use of the Serving GPRS Support Node (SGSN) and the Gateway GPRS Support Node (GGSN) elements for position management of MSs when logging at different places. To further increase data rates, the Enhanced Data rate in GSM Environment (EDGE) technology [28] was implemented using the same TDMA framework that increased the data rate of voice and data communication services up to 384 Kbps. The development process of technologies such as GPRS and EDGE was referred to as the 2.5 generation (2.5G).

The continuous growth of the data stream quantity in network resulted in the invention of the third generation (3G) technologies for wireless networks to offer higher data rates for communication services. Immediately following the first version of the global 3G standard defined by the International Telecommunication Union (ITU) as ITU-2000, the 3rd Generation Partnership Project (3GPP) proposed the Universal Terrestrial Mobile System (UTMS) [29] for use in Europe. UMTS uses the Wideband CDMA (WCDMA) inherited from GSM as the air interface technology with a new infrastructure composed of the following components, as shown in Figure 2.2:

- User Equipment (UE): UE refers to the mobile equipment of user authenticated via SIM card, playing the same role as the MS in GSM.
- UMTS Terrestrial Radio Access Network (UTRAN): UTRAN in UMTS consists of several different terrestrial air interfaces for the UE. It is a collective term for the Node B which works as base station and Radio Network Controller (RNC) which provides control functionalities for Node Bs.
- Core Network (CN): UMTS uses the same core network as GSM/EDGE with the Mobile Application Part (MAP), in order to offer support for existing GSM operations.

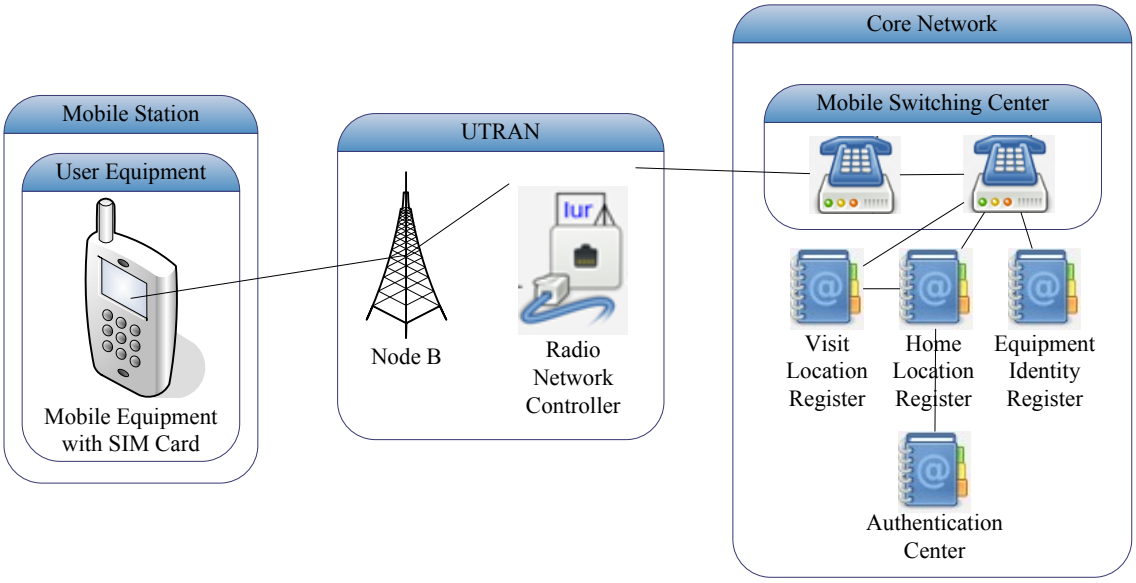

Fig.2.2 UMTS Structure

An earlier version of UMTS offered data rates of up to 384 Kbps on both uplink and downlink, within the same level of GSM/EDGE. As the High Speed Downlink/Uplink Packet Access (HSDPA/HSUPA) technology has been implemented into the upgraded UMTS since 2006, the downlink data rates have been increased up to 14.4 Mbps and the uplink data rates have reached up to 5.76 Mbps.

Other types of 3G technologies include the CDMA 2000 family [27] developed from its previous 2G iteration IS-95 (CDMA One). CDMA 2000 is used in North America and Asia with CDMA channel access, offering average data rate support of around 40-80 Kbps.

The continuous evolution of cellular networks has led to the proposal of the 3.5 generation (3.5G) technologies as an interim step towards the fourth generation (4G). Examples of 3.5G solutions include the Evolved High Speed Packet Access (HSPA+) technology [30], which offers an improved maximum data rate of 168 Mbps for downlink and 22 Mbps for uplink in comparison with HSDPA/HSUPA, by adding MIMO and higher order modulation (64 QAM) support.

Due to the emergence of new multimedia applications accompanied by the increasing growth of user demands, the concept of 4G has been proposed and is expected to be thoroughly developed over the following years to offer optimized bandwidth, reduced communication delay and wider signal coverage range. One of the goals of the 4G framework is to provide a common platform which integrates all the existing mobile technologies so that multi-service capacity is

enabled and user experience is improved. This is achieved by using the all-Internet-Protocol (IP)-based communication to replace traditional circuit-switched communication. Following this goal, 4G aims at offering enhanced roaming capabilities, unified messaging, broadband multimedia and most importantly, faster data transfer rates. The International Telecommunications Union-Radio communications sector (ITU-R) first defined several 4G standards as the International Mobile Telecommunications Advanced (IMT-Advanced) specification in 2008 [31], in which the peak data rate was defined as 100 Mbps for high mobility communication and 1 Gbps for low mobility communications.

One of the earliest released versions of 4G systems is the Long Term Evolution (LTE) standard [32]. LTE inherits parts of the GSM/UMTS architecture with the introduction of the Orthogonal Frequency-Division Multiple Access (OFDMA) and the Single-Carrier FDMA (SC-FDMA) instead of WCDMA as transmission schemes for downlink and uplink. The first released version of LTE was commercially deployed in 2009, offering support for up to 100 Mbps data rate for downlink and 50 Mbps data rate for uplink, if the 20 MHz channel is used. Although being a significant improvement in comparison with the 384 Kbps data rate of WCDMA and the 14 Mbps data rate of HSPA, the LTE data rate still fails to reach the 1 Gbps requirement of IMT-Advanced and there are debates on whether LTE should be considered as 4G or beyond 3G technology. Later the LTE-Advanced (LTE-A) technology [33] was proposed as an IMT-Advanced compliant backwards compatible version of LTE and was submitted by 3GPP in 2009 and finalized in 2011. By using multiple transmit antenna solutions for MIMO and up to 128 QAM for downlink, LTE-A is able to provide a theoretical peak data rate of 3.3 Gbps.

As a major phase of mobile telecommunication standard beyond 4G, the concept of the 5^{th} generation (5G) has already been introduced. It has been debated that the benefits of 5G over 4G should pay more attention to aspects like higher number of simultaneously supported devices, higher spectrum and energy efficiency, larger signal coverage and lower latency other than simply increased bandwidth [34]. These aspects have been objectives of several existing research works at the moment, but no particular official specification has been released by any telecommunication standardization bodies so far.

2.2 Network Protocols

Network protocols play an essential role in defining basic rules for governing communication behaviors in networking in general, and in wireless networks in particular. The rules include guidelines that regulate diverse network characteristics such as access principle, physical topology, cabling type, data transfer speed, packet formatting and signaling. Network protocols are grouped into separate abstraction layers by the Open Systems Interconnection (OSI) model proposed by the International Organization for Standardization (ISO) [35], in which lower layer protocols serve upper layer protocols.

2.2.1 Application Layer Protocols

As the top layer in the OSI model, the application layer protocols directly interact with end users to provide full access to a variety of shared network application services. The responsibilities of application layer protocols include displaying data to the end users, passing data flow over networks and error handling/recovery. Application layer protocols are commonly involved in end user activities like remote login, file transfer, electronic mailing and service support.

One of the most widely-used application layer protocols is the Hypertext Transfer Protocol (HTTP)[1], which plays a key role of data communication in the World Wide Web (WWW). HTTP defines rules for transferring intermediate network elements which contain hypertext content with hyperlinks between text items. These elements are used as request/response messages for a basic client-server network model. Previously used messages can be cached by web browsers on end user devices and reused to reduce unnecessary network traffic. The Uniform Resource Locators (URLs) are used to identify HTTP resources by combining the Hypertext Markup Language (HTML) document and the hypertext elements.

2.2.2 Transport Layer Protocols

Data transmission between wireless mobile devices via different wireless network structures is handled by transport layer protocols, with the use of ports and sockets in the IP hosts. Transport layer protocols provide essential functionality regarding data delivery, such as:

- Congestion control: the transmission is controlled by the transport layer protocols to

[1] Hypertext Transport Protocol - http://www.ietf.org/rfc/rfc2616.txt

avoid exceeding link capacities. The packet sending rate is adjusted according to available network transport capacity.

- Reliable data delivery: some transport layer protocols provide transmission error detection mechanisms such as checksum to ensure that the received data is not corrupted, and receipt verification mechanisms based on acknowledgement packets to check whether data is lost. Retransmission of lost or corrupted data is also supported.
- Flow control: to avoid the buffer at the receiver side to overflow or to be empty, the data transmission rate is managed by transport layer protocols.
- Multiplexing: multiple endpoints on a single node could be supported by using different ports for different applications. Hence multiple synchronous services are enabled.

Transport layer protocols can be simply divided into two categories: connection-oriented and connectionless. For services with simple message transmissions, connectionless transport layer protocols are used more frequently. The **User Datagram Protocol** (UDP)[2] provides the basic checksum property for error detection and port numbers for message identification at the source and destination, while it has no mechanisms such as handshaking communication to ensure connection quality and exposes unreliability to the application services. UDP is used more often with applications that have no or low requirements in terms of error rate and corresponding correction schemes, such as real-time applications that prefers packet loss to serious delays.

If the application running on the wireless mobile device is error-sensitive, it is better to use the **Transmission Control Protocol (TCP)**[3] at the network interface level as it is designed with error detection and correction mechanisms. As investigations in [36] shows that more than 95% of the total traffic over the Internet nowadays is delivered using TCP, it actually has become one of the most popular and fundamental transport layer protocols at the moment. In comparison with UDP, TCP provides reliable connections between the wireless terminals and the network and ensures data stream to arrive at the receiver with correct packet order, while affecting the network overhead and latency. TCP splits application data into a series of TCP

[2] User Datagram Protocol - https://www.ietf.org/rfc/rfc768.txt

[3] Transmission Control Protocol - https://www.ietf.org/rfc/rfc793.txt

packets, each of which consisting of a header including the source, destination and control message of the packet and a body containing the application payload data. The control messages in the header of every TCP packet determine almost all the functionalities of TCP. For example, the 32-bit *acknowledgement number* (ACK) flag is used for connection establishment confirmation together with the 32-bit *sequence number* (SYN) flag, while the *window size* flag indicates the amount of window size units that the sender is willing to receive.

With the usage of all the control messages in TCP header, the TCP protocol operation could be divided into three phases:

- *Connection establishment*: involves a handshake process exchanging ACK/SYN control messages via sockets on a client and a server which are bound to certain ports. The process starts by the client sending a SYN to the server. Next the server replies with a SYN-ACK in response. Finally, the client sends an ACK back to the server. The sequence number is updated according to the acknowledgement values during this process. At the end, the parameters on both directions of the connection are set and acknowledged and a full-duplex connection is established.
- *Data transfer*: the sender transmits data via a series of TCP packets to the receiver.
- *Connection termination*: the connection is closed and the related resources are released.

The specific benefits of TCP appear in all of the three phases. For example, in the data transfer phase, TCP checks the sequence numbers of the transferred packets to identify their order so that possible disorder or packet loss could be detected and retransmission is done accordingly. Another example is the end-to-end flow control mechanism of TCP, which specifies the amount of additional data the receiver could buffer in the *window size* flag of the TCP packet header. The sender stops sending data for a period when the control message from the receiver includes a window size with the value 0, implying that the receiver buffer is full. When this period is expired, the sender slowly recovers the data sending rate.

TCP is designed for accurate delivery as it ensures the identical order of the received data through mechanisms like retransmission, especially for streaming services that have high requirements on bit rate and delay as these services usually involve sending a considerable amount of data in a short period while keeping the completeness, the order and the quality of the

data content. Unfortunately, the performance of TCP is severely limited for streaming services in many types of wireless networks due to their unpredictable unreliability caused by radio effects such as fading, shadowing and hand off that do not exist in wired networks [36].

Some alternative transport layer solutions have been proposed to help solve the TCP performance issue on streaming services in wireless networks, such as the **Stream Control Transmission Protocol** (SCTP) [37]. SCTP is specifically designed for real-time applications which have also reliability requirements. It provides concurrent and reliable multipath data transfer via data duplication detection and retransmission. In comparison with TCP, whose transfer unit is based on series of bytes, SCTP transfers a sequence of messages in one complete operation to the receiver. It also supports multi-streaming in parallel, combining several connections in a single session between the sender and the receiver. Each SCTP host selects a primary IP address from a list of IP addresses it maintains as part of identification of SCTP associations which are protocol relationships between endpoints. A SCTP association consists of one primary connection and several secondary connections. When the primary connection fails, switchover is triggered to a secondary connection. For each message, SCTP assigns a sequence number similar with TCP for ordering of the messages and the receiver could optionally decide to process the messages in the order of the sequence number, or in the order as they are received. However, SCTP is still unable to fulfill the raising requirements on the performance of streaming services, especially with the growth of the size and complexity of the content being streamed. Moreover, SCTP needs support from the application layer hence incurs increased implementation costs, while in many real-life cases the SCTP packets might be blocked by middle boxes (i.e. network address translator) or firewalls.

In order to address some of the shortcoming of existing transport layer protocols, the **Multipath TCP (MPTCP)** protocol [10] has been proposed. MPTCP enables data transmission via multiple channel paths simultaneously, instead of using a single path as in the classic TCP protocol, in order to increase bandwidth resource usage, redundancy and throughput via statistical multiplexing resources. In classic TCP, a connection is built by the hand-shaking process via sockets before data exchange, referred to as a TCP session. MPTCP makes use of the idea of TCP session and redefines it as sub-flow, representing the underlying transport per path. One single MPTCP connection contains a set of sub-flows, each of which acts similar to a

regular single-path TCP connection to the network. Multiple sub-flows are managed by MPTCP at the upper transport layer with the following mechanisms:

- *Path management*: when the connection is established, MPTCP options are included in the SYN segments to verify that the receiver host is capable of using MPTCP. Next the connection is uniquely identified with a token containing multiple pairs of different IP addresses and ports, in which each sub-flow uses an independent pair of IP addresses and ports at the sender and receiver. The purpose of this is to learn about alternative addresses to one or both hosts. Moreover, it provides convenience for setting up new sub-flows and joining them to existing MPTCP connections via the previously exchanged token during the three-way handshake process similar to TCP, which is especially important for mobile networks. The availability of each sub-flow is also detected and reported to other components.
- *Packet scheduling*: MPTCP uses a data sequence mapping scheme to associate segments delivered via multiple available sub-flows with global sequence numbers so that they could be correctly re-ordered after arriving at the receiver. The data sequence mapping scheme specifies the mapping from sub-flow sequence space to connection-level data sequence space to be used by the receiver. The segments on each of these available sub-flows are generated by dividing the byte streams obtained from the application layer into several parts. The information on the availability of the sub-flows is obtained from the path management component, based on which the packet scheduler is set to transfer the queued segments. The packet scheduling component on the receiver end then obtains the reassembled segments and re-orders them in the complete byte stream according to the data sequence mapping of the packet scheduling component at the sender.
- *Sub-flow interface*: after the segments are scheduled and queued by the packet scheduling component, the sub-flow interface transmits them via its specific path to the receiver and ensures their delivery by using the classic TCP reliable delivery detection mechanisms. Only one sub-flow is used on any wireless interface in order to improve the reaction to failures and to increase throughput.
- *Congestion control*: coordinates the congestion control mechanism in classic

single-path TCP across each sub-flow.

In general the multi-sub-flow management mechanisms cooperate in the manner described next. The path management mechanism establishes multiple paths between the sender and the receiver with independent mark (IP address and port) for each individual path. If the receiver has additional addresses, it sends a SYN segment with a JOIN option to the sender to inform the possibility of extra sub-flow. If the sender has additional addresses, it sends an *add-address* option on an existing sub-flow to indicate the availability of a new address and the receiver will establish a new sub-flow for the new address. The process of removing an unavailable sub-flow is similar. The packet scheduling mechanism obtains data from the application layer, breaks it into connection-level segments and pre-orders the segments with the data sequence mapping scheme before sending them to the sub-flows. The sub-flow interface mechanism obtains the pre-ordered segments and sends them to the receiver while maintaining the reliability of the delivery. Finally the congestion control and packet scheduling mechanisms work together to determine the time interval and the sending rate for each segment.

The connection-level receive buffer of MPTCP also plays an important role in maintaining the reliability of the data delivery, as it is the place where received segments are located waiting to the re-ordered and reassembled into data streams. In classic single-path TCP, the size of the receiver buffer is usually recommended as twice the product between channel bandwidth and round-trip time, allowing for re-ordering of the segments and maintenance of the connection during the fast retransmission. The requirements on the receive buffer might be different in MPTCP, as one of the basic goals of MPTCP is to avoid the transmission failure on one sub-flow affecting the throughput of other sub-flows and hence the receive buffer needs to be capable of capturing data from all the sub-flows for the duration of the retransmission timeout. Moreover, avoiding the stalls in the absence of timeout is also important. As a result, the ideal size of the receive buffer in MPTCP is twice the product between the sum of bandwidth of all the sub-flows and the maximum round-trip time across all the sub-flows.

One of the latest concerns when using MPTCP for wireless data transmissions is the energy consumption of the battery-powered mobile devices due to their limited power resources. It is obvious that the total energy consumption increases when multiple wireless network interfaces on a mobile device are active waiting for remote data transmission at the same time.

However, the current implementation of MPTCP has not taken this important factor into consideration, making it necessary for researchers to propose energy-aware solutions for MPTCP usage with wireless mobile devices.

2.3 Rich-media Content Delivery in Heterogeneous Wireless Networks

Over the years, the goal of wireless network solutions was to increase application user perceived quality on various devices, including when content is delivered over wireless networks. The rich-media content has been an important part of all the content delivered via wireless networks due to its wide usage in commerce, education and entertainment of human life. Evaluations on user perceived quality of delivered rich-media content usually involve multiple aspects. Some of them are affected by wireless network conditions such as packet loss, end-to-end delay and throughput. Other aspects are related to the properties of the delivered content itself, such as resolution, frame rate and bit rate for video content. It has been a challenge to deliver various types of contents over wireless networks while ensuring high quality for as many of them as possible.

To ensure high quality level of applications, particularly of rich-media content delivery, several solutions have been proposed by different academic/industrial organizations based on multiple wireless network access technologies. Meanwhile, mathematical metrics for user perceived quality measurement on different types of content have been invented.

2.3.1 Multimedia Streaming

High-quality video streaming has become the main part of common rich-media delivery over wireless networks. In general, this type of rich-media content is with high data volume and is sensitive to the following conditions of wireless networks: fluctuating network behavior and mobility of the end users.

Typical streaming protocols include the Real-Time Transport Protocol (RTP)[4] which is often used in conjunction with the Real-Time Control Protocol (RTCP)[4] and the Real-Time Streaming Protocol (RTSP)[5]. RTP is designed for real-time streaming between end-to-end devices, which requires timely rich-media content delivery. For this reason, it is normally used

[4] Real-time Transport Protocol - https://www.ietf.org/rfc/rfc3550.txt

[5] Real Time Streaming Protocol - http://www.ietf.org/rfc/rfc2326.txt

with transport layer protocols like UDP which focuses on timeliness, instead of TCP which sees connection reliability as more important. Information provided by RTP includes timestamps used for synchronization, sequence numbers used for packet loss detection and reordering and payload format used for content encoding. Synchronization between media streams is handled by the control protocol RTCP which also includes network QoS-related information such as loss, delay and jitter. RTSP is used to provide remote multimedia playback control such as play/pause commands from the end user devices. In RTSP, the playback state on the device is monitored by the multimedia stream server during the connection period so that the server could encode the multimedia data packets at a suitable data rate according to the available bandwidth before streaming them to the device.

2.3.2 Content Delivery Quality Measurement

2.3.2.1 QoS and QoE

The concept of QoS has been used since first defined in the ITU-T recommendation E.800 in 1994 [38], for assessing the overall performance of networks and associated application services and data flows experienced by users. QoS comprises requirements on many aspects of the network communication reserving ability and the subjective metrics used for service quality measurements (for video streaming in particular), listing components like support, operability, accessibility, reliability, integrity and security. Several enhanced definitions, including the recommendation X.902 [39] with a definition of the OSI reference model and X.641 [40] with a means of enhanced standards, have been released with several improved concepts and terminologies for maintaining the consistency of QoS-related standards.

In terms of traffic performance in wireless networks, common factors that affect QoS include the transmission bit rate, packet loss, end-to-end delay, jitter and packet un-ordering. The influences of these factors are listed as follows:

- Transmission bit rate: low bit rate may result in long service time (transmission time) and low user perceived quality especially for real-time services, when various traffic loads to users are sharing the same network resources without scheduling priorities.
- Packet loss: dropped packets due to possible corruption or full-buffer at the receiver may cause severe user perceived quality degradation as parts of the delivered content are missing. Meanwhile, some dropped packets might be retransmitted by the network,

causing extra delays in the overall transmission.

- End-to-end delay: end-to-end packet delay caused by queuing or taking inappropriate routes extends the time waiting for service to end users. It also renders specific application that involves online communications.
- Jitter: obvious jitter in wireless networks indicates unstable levels of end-to-end delay for different packets, which seriously affects user perceived quality.
- Packet un-ordering: packets passing through different routes may arrive at the receiver in a different order with when they are sent. The un-ordering of packet sequence may cause serious quality issues for video and VoIP related applications.

Most of the QoS-related factors focus on the performance of delivery from a network perspective without much concern of the performance at the end device (from the user's perspective).

For measuring the user's experience on the service quality, the concept of the Quality of Experience (QoE) has been introduced. QoE offers metrics for users to be perceived as quality assessment parameters with respect to different types of applications services and focuses on the assessment results on the end user devices instead of on the network as in QoS. In this context, the most relevant concern of application services are the video-related services which are compressed and with low entropy.

2.3.2.2 Subjective and Objective Quality Assessment

There are two major methods for evaluating the user perceived quality in general and in wireless networks in particular: subjective and objective. Subjective quality evaluation methods require judgment from human with multiple scoring options for the users. In general these methods need large human resources to be performed, cannot be used in real time and are time-consuming. Objective quality evaluation methods, on the other hand, are based on the use of metrics and the calculation processes are performed by algorithms. The disadvantages of objective quality evaluation methods include poor correlation with human perception or judgments.

One of the most common subjective measurement metrics is the Mean Opinion Score (MOS). It is used in multimedia delivery quality measurement in perceptual tests when users score the video quality individually. The score of video quality is generated by averaging the

results of a set of subjective tests, in the form of single numbers ranged from 1 (the lowest) to 5 (the highest). MOS is standardized in the ITU-T recommendation P.800 as shown in Table 2.2 [41].

TABLE 2.2 Mean Opinion Score

MOS	PSNR Range	Quality	Impairment
5	>37	Excellent	Imperceptible
4	31-37	Good	Perceptible but not annoying
3	25-31	Fair	Slightly annoying
2	20-25	Poor	Annoying
1	<20	Bad	Very annoying

MOS categorizes accurate subjective test results within simple number of scores which precisely shows the difference between different levels of video/image quality.

The metrics used in objective quality assessment can be divided into three types in terms of the presence of reference images: full reference, reduced reference and no reference. The full reference metrics rely on comparison between the original video (before transmission) and the delivered video. The reduced reference metrics require a feature vector derived from the statistical models of reference image for quality evaluation. The no reference metrics use information contained in the delivered video only, which are easier to be deployed in real-time tests. The quality evaluation result is more precise for full reference metrics in comparison with reduced/no reference metrics. However, more complex calculation process is also involved. As the full reference metrics are more precise, they will be discussed more in this thesis.

Typical full reference objective quality assessment metrics include Peak Signal to Noise Ratio (PSNR) [42], Mean Square Error (MSE) [43], Structural Similarity Index Measurement (SSIM) [44] and Video Quality Metric (VQM) [45]. PSNR is mainly used for accessing video quality. The PSNR value is computed via MSE according to formula (2.1) and (2.2), given a noise-free $m \times n$ monochrome image and its noisy approximation K:

$$MSE = \frac{1}{mn}\sum_{i=0}^{m-1}\sum_{j=0}^{n-1}[I(i,j) - K(i,j)]^2 \quad (2.1)$$

And

$$PSNR = 20\,log_{10}(\frac{MAX_I}{\sqrt{MSE}}) \quad (2.2)$$

In which MAX_I is the maximum possible pixel value of the image. When the pixels are represented using B bits per sample, the value is 2^B - 1.

As one of the first released objective quality assessment metrics, PSNR is simple in terms of mathematical complexity and accessibility. However, PSNR does not consider the affect from visual masking, i.e., any pixel error will cause decrease of PSNR even if it is not perceived [42].

SSIM is another video quality assessment metric based on similarities between images of video. Unlike PSNR which uses estimation of perceived image errors in videos, SSIM measures the video image quality based on an initial raw image without any distortion as reference and considers image degradation as perceived change in inter-dependencies of spatially close pixels inside the image. Suppose there are two windows $\boldsymbol{x}$ and $\boldsymbol{y}$ of common size $N \times N$ pixels, the metric of SSIM is shown in formula (2.3):

$$SSIM(x,y) = \frac{(2\mu_x\mu_y+((2^n-1)k_1)^2)(2\sigma_{xy}+((2^n-1)k_2)^2)}{(\mu_x^2+\mu_y^2+((2^n-1)k_1)^2)(\sigma_x^2+\sigma_y^2+((2^n-1)k_2)^2)} \quad (2.3)$$

In which μ_x represents the average of $\boldsymbol{x}$ and μ_y the average of $\boldsymbol{y}$; σ_x^2 represents the variance of $\boldsymbol{x}$, σ_y^2 the variance of $\boldsymbol{y}$ and σ_{xy} the covariance of $\boldsymbol{x}$ and $\boldsymbol{y}$; n represents the amount of bits per pixel; k_1 and k_2 are two constant variables used for stabilization of the division with weak denominator, with the values 0.01 and 0.03.

The result of SSIM metric calculation sits between [-1, 1] and the value 1 represents two identical sets of data. SSIM is accurate and with high correlation with subjective quality assessment methods. However, it is clear from formula (2.3) that the mathematical complexity of SSIM is high in comparison with that of PSNR.

VQM is provided by ITS as a novel objective measurement for perceived video quality. In VQM, the perceptual effects of video impairments such as blurring, noise and distortion are assessed and combined into a single metric which takes the original and received video as inputs. The calculation process of VQM involves the following steps:

- Calibration of the received video with respect to the original video, in terms of the spatial/temporal shifts and the contrast and brightness offsets.
- Extraction of perceptual changes in the spatial-temporal video sub-region properties.

- Computing of quality parameters representing the perceptual changes in video quality by comparing the received video with the original video.
- Calculation of the previous steps with a linear combination.

VQM is with even higher mathematical complexity in comparison with SSIM, yet the correlation with subjective quality assessment method is better.

Other objective quality assessment metrics include the PSNR estimation model proposed in [46]. In this research work, the PSNR value of multimedia streaming service is estimated as shown in formula (2.4):

$$PSNR = 20\,log_{10}(\frac{MAX\_Bitrate}{\sqrt{(EXP\_Thr-CRT\_Thr)^2}}) \tag{2.4}$$

In formula (2.4), *MAX_Bitrate* is the average bit rate of the data stream transmitted, *EXP_Thr* is the average throughput expected to be obtained and *CRT_Thr* is the actual average measured throughput.

2.4 Energy Consumption Issues During Content Delivery

As end user terminal devices in wireless networks are deployed with limited-amount battery-based power resources, the energy conservation of wireless devices has become a critical issue to extend life spans of devices. Therefore, pursuing high energy efficiency will be the trend for the design of future wireless communications. Energy efficiency is generally defined as information bits per unit of transmission energy. A typical function of energy efficiency calculation for an Additive White Gaussian Noise (AWGN) channel is shown in formula (2.5) [47]:

$$\eta_{EE} = \frac{2R}{N_0(2^{2R}-1)} \tag{2.5}$$

In which the channel capacity *R* is defined as [47]:

$$R = \frac{1}{2}\log_2(1+\frac{P}{N_0B}) \tag{2.6}$$

In formula (2.6), *P* represents the transmit power, N_0 represents the noise power spectral density and *B* represents the system bandwidth. It is obvious that with this energy consumption model, the energy efficiency decreases monotonically with the channel capacity.

The energy consumption model implied by formula (2.5) and (2.6) is based on the assumption that the information block size is infinite. However, in real-life cases where the

information block size is always finite, the situation is different. Energy conservation on wireless devices results from various aspects such as data transmission, traffic encoding/decoding, content playback and radio access interface switching. Among these sources, most of the energy is conserved during data transmission over wireless devices when their radio access interfaces are active, yet the state transition of these interfaces also consume considerable amount of energy. For example, a typical commercial 802.11g network consumes 990 mW energy at the idle state and 1980 mW at the transmitting state [48]. On the other hand, the energy consumption from circuits on the devices differs according to the type of radio access technology used. For example, telephony and data over WCDMA network is more power-intensive on many types of mobile devices with widely-known manufacturers, such as HTC and Samsung smartphones, in comparison with comparable GSM network. HSPA+ delivers significant improvement on the battery life of wireless devices by maintaining a long-term active connection which allows shorter time for the device to transfer from wake to idle.

Apart from the effect of circuit energy consumption, recent research efforts have indicated that the amount of energy consumed by the devices in wireless networks is closely related to the amount of data transferred [49]. Usually, the higher network traffic indicates the larger energy consumption. This makes it more necessary to increase energy efficiency for content delivery services in wireless networks as most of these services, especially when involved with rich-media content, are with high traffic load so that the QoS/QoE requirements of these services can be achieved.

2.5 Chapter Summary

This chapter presents a review of the technical background involved in the thesis, including wireless network evolution history, commonly-used application-layer and transport-layer protocols in wireless networks, rich-media content delivery, QoS/QoE, subjective/objective quality assessment methods and energy consumption issues of wireless devices.

CHAPTER 3

Related Works

Abstract

This chapter presents a comprehensive investigation on the start-of-the-art research works on the following topics: MAC-layer duty cycle management strategies for wireless sensor/mesh networks, QoS-related and energy-aware wireless MAC-layer schemes, network routing algorithms, multi-path/multi-homing communications approaches, multipath-TCP-based optimization approaches, mobile traffic load balancing, and multimedia traffic characteristics-aware mobile energy optimization. In each of the topics, the advantages and disadvantages of the existing standards, research approaches and industry solutions are presented, compared and analyzed, separately.

3.1 MAC-layer Duty Cycle Management Strategies for Wireless Sensor/Mesh Networks

3.1.1 Research Approaches on MAC-layer Duty Cycle Management

To adapt duty cycle for wireless devices to achieve optimal energy efficiency in terms of energy consumption and communication performance, various duty cycle management schemes have been proposed in the research literature, which can be categorized into two types: synchronous schemes and asynchronous schemes. The synchronous duty cycle management schemes align the sleep-periods of wireless sensor/mesh devices so that packet transmission proceeds in common active periods of multiple sensor/mesh devices, enabling their radio channels to be asleep for most of the time to save energy. Synchronous schemes significantly reduce idle time of sensor nodes and hence decouple the duty cycle, but the scheduling synchronization process introduces extra overhead and complexity into the network. Asynchronous schemes, on the other hand, allow each individual sensor/mesh device to handle its own duty cycle independently by using low-power listening mechanisms with special preambles working as channel wake-up notification messages. As a result, the asynchronous

scheme achieves energy saving by enabling sensor nodes to sleep longer while avoiding the negative effects caused by synchronization overhead as in synchronous schemes. However, asynchronous schemes are specifically suitable for the situations when the network traffic is light. When traffic load increases, the benefits of asynchronous schemes in terms of energy efficiency, latency and throughput would decrease, as the preamble transmission may occupy the wireless channels for much longer time than actual data transmission.

3.1.1.1 Synchronous Duty Cycle Management Schemes

One of the earliest examples of synchronous duty cycle management schemes is S-MAC [50], which aims at reducing extra energy consumption caused by the following factors at the cost of some reduction in both pre-hop fairness and latency:

- Retransmission of lost packets
- Overhearing of regular packets and control packets
- Idle listening state of channels

In order to achieve energy saving, the following components have been proposed by S-MAC:

- Periodical listening and sleeping duty cycle scheduling of the wireless nodes: radio access channels of devices are inactivated for a fixed duration when idle and re-activated by messages notifying incoming packets. Synchronization of inactivated channel timer between neighboring nodes is done periodically by exchanging timestamps relatively.
- Collision and overhearing avoidance: the existing IEEE 802.11 RTS/CTS mechanism is used for collision avoidance, overcoming the hidden terminal problem. The overhearing avoidance is solved by setting the interfering nodes to go to sleep after they hear incoming RTS/CTS packets.
- Message passing: a long-length message segment is separated into smaller fragmentation segments and transmitted in bursts in one RTS/CTS round, in order for both energy efficiency and latency efficiency.

In comparison with the IEEE 802.11 protocols, S-MAC is able to obtain significant energy saving in the case with heavy traffic in which gaps between arriving packets are short. The energy saving benefit increases when the gaps between arriving packets become longer.

However, S-MAC causes extra delay as the outgoing packets have to wait for the destination node to wake up, which might severely impact the QoS for time-sensitive applications services.

To reduce the sleep-delay issue of S-MAC, another contention-based MAC protocol for wireless sensor networks called T-MAC [51] has been proposed. In T-MAC, packets are transmitted in bursts of variable length and the sleeping periods of channels set between the bursts, replacing the fixed-length periods in S-MAC. The active time of the channels in each burst end when no incoming data stream is detected after a certain period, determining the minimal amount of idle listening period for each packet. Packets between active periods of channels are buffered and the capacity of the buffer determined the maximum burst length. Moreover, RTS packet retransmission and contention interval management for collision avoidance are also introduced in T-MAC for reducing network load and packet loss.

The disadvantage of T-MAC mainly occurs in the case of unidirectional network traffic. When the node between the sender and the receiver overhears CTS packets from its previous node, its channels remain inactive, causing the channels of the next node to be inactive while the current node still has packets to send out and has to wait until the next active period of the channels of the next node. This severely decreases the throughput in comparison with S-MAC. T-MAC has proposed two mechanisms to solve this issue: the future-RTS and full-buffer priority. The future-RTS mechanism uses a message packet containing the length of the blocking data information to notify nodes that are expected to receive data packets in the future to keep their channels active for a certain period. The full-buffer priority mechanism enables nodes with full buffer to send its RTS packet to other nodes after receiving RTS packets from other nodes, instead of replying with CTS packets, in order to release the buffer. These two mechanisms improve network throughput but also cause additional energy consumption and collision possibility.

Another synchronous duty cycle management scheme D-MAC [52] has been proposed for improving data transmission performance in wireless sensor networks for unidirectional traffic. Unlike S-MAC, D-MAC solves the high sleeping delay issue caused by the data forwarding interruption problem, in which some of the wireless nodes in the middle of the unidirectional path are not notified of the data delivery due to the limited overhearing ranges of radio channel. To solve this issue, D-MAC introduces different offsets into the duty cycle

schedule of each wireless node according to the depth of the node along the data delivery path and meanwhile sequentially staggers this schedule with consideration of several traffic-load-related factors: back-off period, contention window and data/ACK packet transmission time. As a result, intermediate nodes start sending packets immediately after receiving all packets and data delivery is done in a single direction towards the sink node.

This schedule staggering scheme in D-MAC has the following advantages:

- Sleeping delay is reduced since nodes along the data delivery path sequentially wake up to forward data to the sink node.
- Synchronization of scheduling for multiple nodes along the data delivery path is convenient as the request for changing the duty cycle could be propagated all the way down to the sink node.
- Contention is reduced as the active periods between multiple nodes are separated.
- Only nodes on the data delivery path need to update their scheduling while the remaining nodes in the network could keep short duty cycle by default so that energy consumption is reduced.

D-MAC also includes a duty cycle extension mechanism for sending multiple packets in one sending state, which enables fast reaction to traffic rate variations with energy efficiency and low transmission latency. The overhead brought by holding the extra receiving state periods is minor in comparison with the reduction of the sleep delay. To further avoid the interference between nodes on different branches of the data gathering tree, an explicit control packet called *More-to-Send* (MTS) is introduced in D-MAC. The duty cycle scheduling update request by MTS packets is forwarded through the staggered schedule to all the nodes along the multi-hop path. Using these mechanisms, D-MAC is capable of reducing latency but it is only applicable under the specific data gathering tree scenario for unidirectional communication flow from multiple sources to a single sink.

To overcome the limitation of D-MAC, RMAC [53] is put forward as a novel duty cycle MAC protocol aiming at saving energy at nodes in wireless sensor networks by using cross-layer routing information to avoid the latency and contention issues in S-MAC. RMAC uses more intelligent schemes for duty cycle scheduling of multiple nodes in the network, with a small setup control frame sent along the data delivery path on which all the nodes are informed

the time they needed to be awake for data receiving and forwarding respectively. The duty cycle schedule synchronization between multiple nodes is done by using a series of controls frames called Pioneer frames (PIONs) which serve as the RTS packet of the next hop of the current node and the CTS packet of the last hop. Each node includes a separate period in its duty cycle to send out the PIONs to its last and next hop. Upon receiving the PION from its next hop, each node holds the unsent data packets until it reaches the sleeping timestamp, instead of immediately sending out the packets as in the RTS/CTS mechanism. Cross-layer information such as the destination address of the current data flow and the number of hops it passes by is also included in the PIONs exchanged between nodes.

Compared with other duty cycle scheduling schemes, RMAC is unique as the algorithm is directly integrated into the medium access mechanism and the duty cycle scheduling scheme in RMAC is fully distributed and semi-on-demand by using the PION control frame multi-hop forwarding mechanism. However, one of the main issues with RMAC was brought by the possible loss of the PION frames which caused the next hop to wake up and receive no packets as the last hop failed to hear the lost PION and stopped forwarding packets. Usually the next hop would go back to sleep after a predefined timeout, but in the worst case when the PION successfully traversed several nodes along the data delivery path before getting lost, all these nodes would experience the same extra waking-up period before going back to sleep after the timeout and the amount of wasted energy increased much in total.

3.1.1.2 Asynchronous Duty Cycle Management Schemes

PMAC [54] is one of the typical examples of asynchronous duty cycle scheduling schemes for wireless sensor/mesh networks. The main contribution of PMAC is the determination of the duty cycle schedule based on the network load of individual device and the traffic pattern of its neighbors, replacing the fixed duty cycle as in S-MAC and the bursts with various lengths as in T-MAC. In PMAC, the length of duty cycle slot of each node is determined by the pattern of network traffic passing through the node. The traffic pattern is defined as a binary string started with a number of 0s and ended with a single 1, in which the higher number of 0s indicates lower traffic load. This pattern is updated by using the local traffic information at the node and exchanged at the end of each transmission period between nodes. For this type of duty cycle, any node in the network keeps its channels to be inactive if no incoming traffic is

predicted in a long period according to the traffic pattern of its neighboring nodes and back to be active when there is transmission in the neighborhood. Meanwhile, the active/inactive state switch of each node is controlled by a pair of 0-1 bit strings that indicate the active/inactive intention of the node itself and its neighbor.

The advantages of PMAC are concluded as follows:

- Adaptation to the traffic condition: when the network load is not heavy, nodes are able to stay longer periods in inactive mode, saving more energy than S-MAC. When network load becomes heavy, the pattern is updated so that the corresponding sleeping node could wake up in time.
- Power savings according to node locations: only the nodes involved in packet transmission switch their states between active and inactive while other nodes keep inactive for longer periods.
- Power savings from reducing idle listening.
- Time synchronization: small clock drifts do not affect time synchronization in PMAC as large time scale is used.

PMAC is proved to be able to save more energy in comparison with S-MAC and to improve transmission throughput in the case when the traffic load is heavy. The improvement on throughput is less for light traffic load. However, communication using state control bit strings in PMAC brings excess latency.

Another example of the asynchronous duty cycle management schemes is X-MAC [55], which improves energy efficiency based on the following principles:

- A series of short preambles are introduced, embedded with the address information of the destination node so that other nodes not involved in the transmission can get rid of overhearing incoming packets and go to sleep quickly.
- A strobed preamble is designed by inserting pauses between short preambles to allow the destination node to interrupt long preamble when it wakes up and receives packet. During each pause the sender node stopped listening to the medium and acknowledgement packets are sent from the intended receiver node to inform the sender node to stop sending preambles and to start sending data packets instead.

Apart from the short preamble mechanism proposed for shortening the overhearing

period, an adaptive algorithm is also included in X-MAC, which estimates the optimal values of different state periods in the duty cycle of the nodes in order to vary from traffic patterns of different nodes in the network to achieve better performance.

The advantage of X-MAC on reducing overhearing occurrence is obvious, especially in the case of high network density. The battery life of the receiver nodes in X-MAC can be extended by up to 3 times and the data delivery latency is significantly reduced.

RI-MAC [56] is proposed as another example of asynchronous duty cycle management schemes. RI-MAC guarantees good performance under heavy loads and bursty traffic by reducing the preamble transmission time using a different attempt with X-MAC on the rendezvous time determination mechanism for data transmission between nodes. In RI-MAC, data transmission is initiated by the notification from the receiver node instead of the sender node, using a short beacon frame to replace preambles in typical asynchronous schemes. The beacon frame contains several fields holding information such as source/destination node address and back-off window size. In the first duty cycle round of nodes, the initial beacon is sent out by the receiver node after doing a back-off when it detects that its wireless medium is busy. Meanwhile another sender node keeps active channels to sense this beacon from the intended receiver node until the beacon arrives. The sender node then starts transmitting the pending data at once and sends another beacon to acknowledge the receiver node. New duty cycle between beacons for one node is updated according to the length of the duty cycle before the last beacon.

To solve the issue of the increased resource cost from data collision detection/retransmission and extended active time of the receiver node in the case of multiple data senders, RI-MAC proposes the following mechanisms:

- Beacon frames are employed to coordinate data transmission from contending sender nodes;
- Beacons are broadcasted after the clear channel assessment (CCA) check in which the availability of the wireless medium is detected to prevent any sender node to use it when the receiver node is generating ACK beacons;
- The dwell time of the receiver node, which refers to the extra active period of the receiver node waiting for queued data packets from the sender nodes, is determined by

the back-off window size of the newest beacon, the short inter-frame space (SIFS) [6] and the maximum propagation delay, instead of a fixed duration in X-MAC.

In comparison with other asynchronous MAC-layer duty cycle management schemes, RI-MAC is beneficial in terms of the following aspects:

- The receiver-initiated design reduces unnecessary overhearing as a receiver node expected incoming data only within a small window after beacon transmission.
- Energy efficiency remains comparable with the lower cost for collision detection and data retransmission, especially when the network load increased.
- Transmission throughput is significantly improved especially for bursty traffic or transmission from hidden nodes.

A summary of the advantages and disadvantages of the synchronous and asynchronous MAC-layer duty cycle management schemes, as identified in section 3.1.1.1 and 3.1.1.2, is illustrated in Table 3.1.

TABLE 3.1SUMMARY OF ADVANTAGES AND DISADVANTAGES OF THE SYNCHRONOUS AND ASYNCHRONOUS MAC-LAYER DUTY CYCLE MANAGEMENT SCHEMES

Category	Scheme	Advantages	Disadvantages
Synchronous schemes	S-MAC	Significant energy savings with heavy traffic	Extra delay for time-sensitive applications
	T-MAC	Energy savings with traffic of all bursty levels	Decreased throughput and extra energy consumption in unidirectional channels
	D-MAC	Short sleep delay	Only applicable under unidirectional communication flow scenarios
		Convenient scheduling synchronization for multiple nodes along the data delivery path	
		Reduced contention	
		High energy efficiency	
	RMAC	Ensures energy savings without issues of latency, contention and usage limitation	Extra energy consumption in the case of semi-on-demand control message loss
Asynchronous schemes	PMAC	Significant energy savings from reducing idle listening, which are adaptive to node locations	Less obvious improvement on throughput with light traffic load
		Time synchronization	Control messages bring excess latency
	X-MAC	Reduced overhearing occurrence with high network density	
		Reduced latency	
		Significantly extended battery life span	
	RI-MAC	Reduced overhearing occurrence	
		Comparable energy efficiency with the lower cost for collision detection and data retransmission	
		Improved throughput especially for bursty traffic	

3.2 QoS/Energy-related Wireless Mesh MAC-layer Schemes

3.2.1 QoS-related Wireless Mesh MAC-layer Schemes

To solve some existing QoS performance issues specifically for wireless mesh networks using the IEEE 802.11 MAC protocol, several novel MAC protocols have been proposed in the research literature.

One of the first MAC solutions for improving the QoS performance of single-channel wireless mesh networks is introduced in [57], including three steps: extending the contention window size; express forwarding; express retransmission. Increasing the size of the contention window decreases the possibility of collision occurring at hidden nodes. Express forwarding involves increasing the duration field value of the current data frame being sent so that the neighbor nodes stop being active and the receiver node is able to access the channel, and the ACK packet of this data frame derives the extended duration field value from it, adjusted for elapsed time. Express retransmission allows immediate retransmission of the packet once the ACK timer expires. In this way, the end-to-end delay occurred in regular retransmission of a multi-hop flow is shortened. These three schemes are all based on existing mechanisms, such as CSMA/CA [6] proposed in the IEEE 802.11 MAC protocol and TXOP proposed in the IEEE 802.11e protocol [58], so the complexity of any required modifications is low. Performance evaluation of the three schemes is done with a wireless mesh network structure together with three WLAN structure, using VoIP applications and high/low-resolution videos as traffic. Results have proven that the proposed schemes are able to reduce end-to-end retransmission delay in an obvious level and to decrease the occurrence of dropped data frames.

2P [59] aims at improving the performance of the IEEE 802.11 MAC protocol by redesigning the CSMA/CA mechanism to enable data transmission and reception along all links of a node simultaneously, making full use of the available channel capacity and supporting low-cost rural connectivity. The basic principle of 2P is based on the synchronous transmitting/receiving operation state (SynTx/SynRx) [6] of the links at a node switching between these two states, which are not enabled in the IEEE 802.11 MAC protocol. 2P modifies the immediate ACK and the carrier-sense-based back-off mechanism in the IEEE 802.11 MAC protocol to enable SynTx/SynRx. Meanwhile, 2P introduces a timeout mechanism to handle

temporary synchronization loss and link recovery on each individual link and a SynTx notification mechanism to coordinate the state switching of multiple nodes. In terms of performance, 2P offers significant throughput improvement within a wireless mesh network topology containing 25-30 nodes and the throughput benefit is robust against losses, in comparison with the IEEE 802.11 MAC protocol with CSMA/CA.

Another contention-based MAC solution is the DBTMA [60] protocol, which aims at solving the hidden/exposed terminal problem. In DBTMA, two narrow-bandwidth and out-of-band busy tones are used together with the RTS packet at the receiver node and RTS transmitter node of data packet transmission. The busy tones are used to provide protection for the RTS packets so that the chance of successfully reception of RTS packets increases and the throughput increases consequently. As a result, the exposed terminal nodes can initiate data packet transmission and the hidden terminal nodes are able to reply to RTS packets and initiate data packet reception. DBTMA is proven to have better performance in terms of channel throughput in comparison with traditional RTS/CTS-based MAC protocols, such as ALOHA [6]. However, the usage of multiple busy tones requires extra incorporation of circuits into wireless devices and also increases bandwidth consumption.

An advanced MAC-layer protocol used for parallelism packet transmission in wireless mesh networks is proposed in [61] as an extension of the Medium Access via Collision Avoidance with Enhanced Parallelism (MACA-P) [62] protocol. The MACA-P protocol supports concurrent transmission on any mesh node by scheduling transmitting data packets and receiving ACK packets in the outgoing RTS packets to the neighbor mesh nodes. The neighbor mesh nodes schedule their data transmissions and ACK receptions according to the schedule included in the RTS packets received from that node. The main modifications made by the extended solution based on MACA-P include consideration of whether the remaining time is long enough for transmitting frames and the usage of a pair of query/query reply signals and an associated two-way handshake mechanism for connection setup. The information of neighbor mesh nodes is collected and the network allocation vector table is created after connection establishment. The control gap between RTS/CTS packet exchanges is calculated with the prediction of packet transmission time based on the send-out time included in the query signal and the arrival time of the query reply signal. The RTS sender mesh node retransmits its RTS

packets with the value of control gap, causing its neighbor mesh nodes to reschedule the reception time accordingly. By continuously adjusting the value of control gap, the solution tries to synchronize maximum number of mesh nodes in a parallel transmission without the unnecessary growth of wait time for control packets. However, the protocol has some performance issues when detecting different numbers of neighbors at different nodes.

The MAC-layer scheme proposed in [63] works as a part of a cross-layer solution which contains an overlay network structure for improving delay-constrained video streaming service quality in multi-hop wireless mesh networks. The scheme uses an algorithm to optimize different control parameters at mesh nodes, especially transmission retry limits, together with an IEEE 802.11e HCCA-based [58] traffic scheduling mechanism. The optimized parameters are exchanged between different layers in the overlay network structure to be further used as essential information for pre-building the mesh topology before the initialization of video streaming. As a result, negative network reconfiguration effects such as additional delays and link failures are minimized for the application service. Experimental results based on simulations have shown that the scheme provides significant improvement on received video quality as frequent feedback via the overlay network and end-to-end optimizations with different set of utility functions are used. The results also indicate that 1) the balancing between overhead in the overlay network and improvement brought by the feedback and 2) the prioritization of video packets with respect to distortion reduction and the received video quality.

The TDMA-mini-slot-based scheme proposed in [64] improves the performance of the IEEE 802.11 MAC protocol. To solve the issues of packet loss, bandwidth decrease and transmission delay caused by contention in traditional MAC protocols, this scheme allocates channel resource in mini-slots synchronized within two-hop neighborhood mesh nodes to avoid packet transmission corruption. Each individual mesh node is assigned a unique mini-slot within a two-hop neighborhood and all the slots are synchronized so that data packets from different node do not corrupt each other during transmission. Moreover, it provides priority access to extend cooperative communication to multi-hop cases, which is always reserved by a mini slot as needed. This is achieved by using an instantaneous SNR-based helper selection algorithm in the case of faulty wireless channels. The proposed scheme improves the end-to-end throughput

in a multi-hop manner in comparison with the IEEE 802.11 MAC protocol and offers generally steady performance when packet size varies during transmission.

MAC-ASA [65] is another MAC-layer scheme aiming at the following improvements based on the IEEE 802.11 MAC protocol: the enhancement of end-to-end transmission throughput for both single-hop and multi-hop wireless mesh networks; scalability; collision avoidance capability. MAC-ASA combines a distributed link scheduling algorithm and a power control mechanism for router-to-router communication together. It also uses a modified version of the IEEE 802.11 CSMA/CA contention handling procedure within a coordinate dynamic TDMA-like protocol to reduce collision and to enable data aggregation pipeline. In the case of communication between mesh clients and routers, MAC-ASA provides good throughput improvement and robustness to increasing packet size. However, MAC-ASA does not increase performance significantly when there is only mesh traffic in the network (only mesh routers are involved in data transmission).

3.2.2 Energy-related Wireless Mesh MAC-layer Schemes

The MAC-layer solutions discussed above mainly focus on transmission performance in wireless mesh networks and take little consideration of the energy consumption of the mesh devices, especially energy consumption during data packet transmission. Factors such as access delay and packet collision have impact on the energy consumption of wireless device during data packet transmission, which cannot be ignored. In this context, several energy-related MAC solutions for wireless mesh networks are also presented and discussed in this section.

DSMA-S [66] is proposed to solve the control packet collision problem. DSMA-S is based on the contention-based scheme in DBTMA and uses two out-of-band busy tone signals at the receiver node to indicate successful transmission and packet collision to other nodes. Meanwhile, control packets and data packets in DSMA-S are transmitted separately on the common wireless channel, which is divided into time-synchronized slots, to maximize the channel efficiency. The busy tone signals are sensed only at the beginning of the time slots so that the idle listening state of mesh devices is reduced to save energy. As no busy tones are broadcasted by the sender nodes, losing normal functionality, the improvement on throughput performance of DSMA-S in comparison with DBTMA is more significant in the case of hidden terminals in the network than no hidden terminals. In terms of energy consumption, DSMA-S

offers better performance than DBTMA with larger ratio of data packet duration and control packet duration.

The energy-efficient wireless mesh node monitoring scheme proposed in [67] tries to ensure continuous and complete detection coverage for wireless mesh network intrusion and to save energy for the non-monitoring mesh nodes via duty cycle management. In this scheme, each node in the wireless mesh network is integrated with an intrusion detection engine for wireless link monitoring. The intrusion detection engines on nodes selected for wireless link monitoring consume more energy than others, as they detect traffic in the entire network while others detect only traffic from/to the mesh client. A centralized and a distributed monitoring mesh node selection algorithm are proposed at the mesh gateway with trade-off between the time and message complexity for intrusion detection rate, respectively. Meanwhile duty cycle management schemes are used on the mesh nodes which are not selected as monitoring nodes, without affecting the intrusion detection process. Simulation-based results show that the mesh node monitoring scheme proves full wireless link coverage regardless of the network capacity, while the level of residual energy of nodes in the wireless mesh network is increased.

3.3 Routing Algorithms

Apart from MAC-layer solutions, routing algorithms during data transmission also play an important role in data packet transmission performance. In wireless networks, nodes between the sender node and the receiver node are responsible for data forwarding, working as routers. The principle of routers on how to generate data forwarding path determines the overall performance and resource cost of the wireless network, as each individual router has different states in terms of power supply, network load, mobility and duty cycle. It is essential that routing algorithms considering both energy efficiency and performance should be employed for wireless networks. Reviews on some of the state-of-the-art routing algorithms are presented in this section.

3.3.1 Classic Routing Algorithms

Many classic routing algorithms have been widely used in various network scenarios with significant benefits. One of the earliest routing schemes is the classic Dijkstra's algorithm [68]. It is originally designed for solving the shortest path problem in graph searching: finding

the path with the lowest cost between any endpoint to others in a graph structure. In the Dijkstra's algorithm, the cost calculation starts from one end node of the structure and recursively updates for each unvisited neighbor node of the current node in the structure until the destination node is visited. In wireless sensor/mesh network, the cost of finding the shortest path is determined by multiple network-condition-related factors such as network latency, traffic load and energy consumption. The principle of the Dijkstra's algorithm is commonly used in many more advanced path-searching algorithms for generating traffic routes with the lowest cost in wireless networks. These algorithms can be divided into two main categories: **global** and **distributed**, according to whether any node in the network has the information of all the other nodes, or just the nodes that are adjacent.

One of the common examples of global routing algorithms is the Link State (LS) routing protocol [69] used in packet-switching networks. In LS protocol, all the switching node in the network, i.e. the routers, construct a connectivity graph structure showing connection states between nodes. Each individual node in the graph structure has the knowledge of connectivity of the entire network. Based on this, each node in the LS protocol calculates the optimal path to other possible destination nodes independently, similar with the principle of the Dijkstra's algorithm. This is done by broadcasting short messages called link-state advertisements throughout the network in order to update routing information such as sequence numbers. The global routing table is updated when the shortest path calculations of nodes are complete.

The Optimized Link State Routing Protocol (OLSR) [9] is an IP-based extension of the classic Link State routing protocol and is mainly designed for mobile ad-hoc networks but also useful for other wireless ad-hoc networks. It is a typical proactive routing algorithm that exchanges control messages periodically between nodes in the network, optimizing the classic Link State protocol in terms of control packet size and control traffic load from the following two aspects:

- Only a subset of links is declared in OLSR instead of all the links with neighbor nodes in the classic Link State routing protocol. The neighbor nodes of the subset of links are multipoint relay selectors.
- Only the multipoint relays (the selected nodes) are used for retransmission in OLSR.

In OLSR, the multiple relays for any nodes are chosen from the range of its one-hop neighbor nodes when they have a bi-directional link toward any existing multipoint relays. Next at each node, the routes to all known destinations through its multipoint relays are calculated by periodically exchanging information of the relays with other nodes. One the routes are built, unicasting packets are forwarded hop by hop along the optimal route from the source node to the destination node. Broadcasting packets, on the other hand, are forwarded by the multipoint relays based on the rule that retransmission occurs only when the first copy from any multipoint relay selector node is received.

For distributed routing algorithms, one common example is the Distance Vector (DV) routing protocol defined in RFC 1058[1]. It uses distance and direction as the two main parts of the route calculation information exchanged between adjacent nodes. Each node in the network keeps a routing database with one entry for every possible destination. Information options such as address, gateway and timer are included in the database which is updated according to information received from neighboring gateways. The update of information is done in each node by periodically broadcasting a set of routing table messages to its neighbor nodes according to its own clock, so the update of information in the entire network is asynchronous. The optimal route from the source node to the destination node is determined by recursively judging the sum of cost for individual hops along the route. The cost could be (but not limited to) message delay, sending power, loss rate, etc.

Although small amount of drops of updated information is tolerant to the DV routing protocol, which moves to a new equilibrium when the drops of updated information cause changes of network topology, rules such as split horizon and triggered update are applied in the real implementation of the DV routing protocol to ensure the stability of route calculation. It is also worth to mention that the determination of the maximum cost value in the DV routing protocol is a trade-off between the speed convergence and capacity of the network, as the value has to be larger than any possible real route but not exceeding the information update time limit.

To ensure the stability of the route calculation, the real implementation of the DV routing protocol applies the following rules:

[1] Routing Information Protocol: http://tools.ietf.org/html/rfc1058

- To set the default “infinite” value as small as possible: this is to avoid the “counting to infinity” problem. However the “infinite” value has to be set larger than any possible real route at meanwhile. Hence the choice of the “infinite” value is a tradeoff between the speed of network convergence and the network capacity.
- Split horizon: this is a scheme used to avoid problems caused by including routes in updates sent to the node from which they are learned by setting the cost metrics of such routes to infinity or omitting the metrics learned from one neighboring node in updates sent to that neighboring node.
- Triggered updates: this scheme is applied for decreasing the time of network convergence in order to avoid the problem that three nodes might engage in mutual deception, making a looping route. Triggered update is done by adding the rule that whenever a node changes the metric for a route, it has to send the update information as soon as possible so it is not likely that after the triggered updates has gone through a node, regular updates from other nodes happen at the same time, causing nodes that haven’t received the triggered updates to send out information based on the routes that no longer exist.

Most classic routing algorithms derived from Dijkstra’s algorithm, including OLSR and the DV routing protocol just discussed, determine the shortest path by iteratively considering every node with the lowest cost. This involves complicated iterative calculation process resulting in slowness and ineffectiveness for large-scale wireless network topologies. Another issue caused by such algorithms is the count-to-infinity problem, in which parts of the network become completely inaccessible before the network realizes from the update of route information, as the time spent on the update is not short enough due to the definition of large “infinite” route cost values on certain nodes in the network.

3.3.2 Advanced Routing Algorithms

Many advanced routing algorithms have been proposed lately to endure the issues of classic routing algorithms based on the Dijkstra’s algorithm. As an example, the Recursive Best-First Search (RBFS) algorithm [69] uses linear space in the maximum search depth to expand nodes in the best-first order. The RBFS algorithm considers all the nodes in the network as a tree structure, in which every node has an upper bound value on the cost defined as the

minimal cost value among its parent and sibling nodes. The principle of the RBFS algorithm is briefly described as follows:

- The expansion starts from the sender node by searching all its neighboring nodes for the one with the minimal cost as the parent node of the sub-tree in the next recursive call. When the neighboring node with the minimal cost is found, the upper bound value is defined as the minimal cost value among its parent (the sender node, in this case) and all sibling nodes (all the other neighbors of the sender node, in this case).
- In every recursive call, the sub-tree below the current parent node is explored when it contains frontier nodes with cost not exceeding the upper bound value, which is updated according to the cost value of the current parent node and all of its children nodes.
- To avoid inefficiency caused by the redundant expansion in the recursive process, every child node in each recursive call inherits the cost value of its parent node as its own if this value is greater than its original own cost value. In order to be expanded, the upper bound of a node must be at least as large as its updated cost value. If a node has been previously expanded, its updated cost value will be higher than its original cost value. In this case its updated cost value is the minimum of the last updated cost values of its child nodes. In general, the updated cost value of a parent node is passed down to its child nodes, which inherit this value only if it exceeds both the original cost value of the parent node and itself.

Research efforts have proved that the RBFS algorithm has better performance than the classic routing algorithms based on the Dijkstra's algorithm with shortest-path problems for direct graph network topologies. However, the performance benefit is limited when it comes to other issues related to routing and optimization, such as the travelling salesman problem [70], the graph coloring and scheduling problem [71] and the knapsack problem [72].

The Simulated Annealing Arithmetic (SAA) algorithm [73] has been proposed as a better solution for the combinatorial optimization problems which determine the principle of the cost function in routing issues. The SAA algorithm uses a discrete-time inhomogeneous Markov chain [74] with the updated states of each node in the network whose neighbor states (new

states of the problem produced after altering a given state in an optimal way) are considered. At each iteration step, the algorithm probabilistically makes decision whether to move to the neighbor state. Moving to the neighbor state results in minimal alterations of the last state in order to help the algorithm keep the better results and change the worse results. After a tour of successive neighbor states comes the final solution considering all the neighbors of one state to explore the state space. States that are more optimal during this process are preferred when the algorithm is making decisions for the final solution, yet other states are also possibly accepted in certain circumstances in order to avoid the local optimum problem from simple heuristic algorithms.

In the SSA algorithm, the probability for a node to move to neighbor states is determined by an acceptance probability function which depends on the state results and a global parameter that varies according to time. States with smaller results are considered more optimal. If the difference between the results of moving/not moving to neighbor state becomes more significant after passing a period of time, the probability of moving decreases accordingly. This process ends with a global optimal solution as the annealing schedule is extended.

It is obvious that for the SSA algorithm, the choice of parameters such as the state space, the cost function, the acceptance probability function and the annealing schedule, has significant impact on the benefit of the algorithm. However, as there is no general way to define a generally optimal choice of the parameters for different situations, in real-life usage the choice depends on the given problem.

3.3.3 Network-layer Routing-related Research Efforts

This section investigates some research efforts which have been made specifically for advanced routing mechanisms in wireless mesh networks, apart from the general routing algorithms introduced in the previous sections, which are widely developed in research area and used in industry.

SOAR [75] is a proactive link-state-based routing protocol proposed for explicitly supporting multi-flow in wireless mesh networks. It attempts to improve the network throughput and fairness by introducing the following mechanisms: adaptively selecting forwarding paths to leverage path diversity and reducing duplicate transmissions; determining optimal forwarding nodes in terms of priority timer; local loss recovery to handle dropped packet detection and

retransmission; adaptively controlling data sending rate according to network conditions. With these mechanisms, SOAR offers better tolerance on the instability of wireless network medium with the hop-by-hop data forwarding in comparison with traditional shortest-path routing protocols. The performance of SOAR is evaluated through simulations and real test-bed experiments for single-flow and multi-flow scenarios with various network topologies. Results show the SOAR achieves higher improvement on the network throughput under symmetric losses than asymmetric losses with single-flow scenarios, and significant improvement on the flow index fairness with multi-flow scenarios.

The multi-flow joint optimization routing algorithm proposed in [76] works as the key part of a cross-layer cross-overlay architecture. It provides fast information exchange during cross-layer parameter update in order to enable proactive traffic performance optimization using a mesh internetworking system with network centric computing. The routing algorithm gathers link-state information of multiple traffic flows from a global database deployed in the mesh internetworking system and makes a joint optimization to meet the constraint of every flow. Factors utilized in the joint optimization for route decision differ according to constraints of different flows. Examples of such factors include the end trip time over the link (for applications with strict end-to-end delay constraints) and the effective throughput of the flow (for applications with significant bandwidth demand constraints). The preferred routing choice is decided independently by each flow based on the result of the joint optimization using extensions of the Dijkstra's algorithm.

In [77], a QoS-aware backup routing algorithm is proposed to work with an available bandwidth estimation mechanism to accommodate stable QoS for multimedia flows in mobile wireless mesh networks. The bandwidth estimation of any node in a network is based on the effective channel capacity and the total occupied bandwidth of this node and its neighbor nodes that share a common channel. The backup routing algorithm includes such information of the node into route calculation information packets to be broadcasted to neighboring nodes sharing the same channel for bandwidth estimation. Meanwhile, to reduce overhead caused by frequent route discovery in mobile wireless mesh networks with unstable link quality, a backup piggybacked path (whose available bandwidth is the second maximal among all the paths) is selected apart from the primary path when route is established after exchange of route

request/reply messages between nodes, in order to provide more reliable connectivity. Multimedia stream are transmitted via the primary path by default unless it is disconnected, in which case the backup path is activated for transmission. Simulation-based results have proven that the backup routing algorithm successfully shortened the route establishment and re-built time, which is beneficial for real-time multimedia communications.

3.4 Energy-Aware Mechanisms for Content Delivery in Heterogeneous Wireless Networks

In previous sections we have described the limited power resource issue with devices in wireless sensor/mesh networks and corresponding state-of-the-art solutions. For end user terminal devices in wireless networks, this issue is more severe, as the commonly-used wireless mobile devices such as laptops, smartphones and tablets are usually deployed with small-capacity batteries. Most of the energy consumed by end user mobile devices is due to large amount of data delivery. Therefore, the high requirements on QoS are supported by the IETF MPTCP protocol introduced in Chapter 2.

3.4.1 Multi-path and Multi-homing Related Solutions

Before MPTCP is proposed, support for multi-path and multi-homing feature in heterogeneous wireless networks is provided by SCTP, enabling seamless and transparent communication sessions over multiple network connections. In [78], the performance of SCPT-based multimedia delivery over single-path transfer (SPT) mode and concurrent multi-path transfer (CMT) mode is investigated, using diverse retransmission policies and network condition parameter sets for achieving best effort of multimedia delivery. Network modeling and simulation is used for evaluation of the SCTP SPT/CMT performance with implementations of delivery algorithms and user perceived quality measurement metrics. The multimedia content is encoded before SCTP-based delivery simulation and the corresponding trace file is processed after delivery to calculate packet loss, delay and user perceived quality metric. The performance of retransmission policies and Path Maximum Retransmissions (PMR) [37] in symmetric and asymmetric path conditions is also investigated.

The work in [79] presents performance evaluation of several different retransmission

policies of the CMT mode in SCTP with an amendment to the timeout retransmission mechanism. The retransmission policies in this work differ from each other in terms of the schedule of data chunk retransmission and path selection based on loss rate, congestion window size and slow-start threshold. The congestion window update algorithm for CMT is also modified to maintain multiple left edges for the Transmission Sequence Number (TSN) which works for SCTP in the same way as regular sequence number for TCP, so that the retransmitted TSNs are distinguished from the ones that are not. In the amendment of the retransmission policies, timeout of each retransmission is not triggered until the TSN has been sent for at least one Round-Trip Time (RTT) to avoid spurious retransmission caused by possible loss of TSNs. Evaluation results demonstrate the best and worst retransmission policies in terms of transmission time and retransmission timeout frequency, indicating the importance to consider loss in retransmission policies for load distribution.

For existing MPTCP-based research efforts, the multi-path and multi-homing feature is one of the key concerns as well, as strict requirements in terms of throughput reliability and timeliness are increasingly common in network applications. One example of proposed research solutions related to this feature is the IPv6 multi-homing solution Shim6 [80], approved by IETF in RFC 5533 and designed between the IP endpoint sub-layer and the IP routing sub-layer under the transport layer. It uses the concept of “locater” which refers to the network-layer routing and forwarding properties of an IPv6 address selected in initial contacts with the remote host as the preserved upper-layer identifier (ULID). The purpose of Shim6 is to handle path failures independently from a number of IP addresses for two hosts in communication. Hence in Shim6, a host maintains a list of IPv6 addresses, each of which is given by its service provider.

The REAchability Protocol (REAP) [81] is utilized in Shim6 to deal with data transfer failures. Whenever failures are detected, REAP recommends an alternative pair of IPv6 addresses that enable the two hosts to communicate with each other. After receiving the recommendation, Shim6 immediately modifies the content of the packets on transmit and tags the packets with the payload extension header with the receiver’s context tag. This context tag is used by the receiver to find the context state which determines the addresses to put in the IPv6 header before passing the corresponding packet up to the upper layer. The context is generated during a four-way exchange of Shim6 control messages, including a locator verification process

through HBA/CGA techniques. As a result, the packet is sent to the correct end host although the locator is different according to the IP routing infrastructure.

Shim6 is more effective in the case of locator preference when a best path is selected for packet delivery. For instance, when a communication path is established between two Shim6 hosts, packets can be delivered through that path with low delay by pairing appropriate addresses. In this case, the change of locator preference is notified to the host which records the information of the newly preferred locators, after which the address switching process is triggered according to the current preference.

Nokia has proposed another MPTCP-based solution in [82] for generating multi-path scheduler via Markov-Decision-Process-based [83] formalization for traffic handover between wireless interfaces of mobile devices in order to save energy. Energy models for different wireless radio access technologies and application models with different traffic patterns are first generalized into parameter sets based on measurement with real devices and then used as inputs for the formalization process. Based on the inputs, the multi-path scheduler generated from the formalization process periodically chooses one radio access interface on the device for the current active application, based on the throughput/energy state of the interface. Performance evaluation of the solution is explored by running realistic traffic traces on real mobile devices, which are generated from a large number of random application models including low/high-quality video streaming, application downloading and text-based browsing. Results have proved the benefit of minimizing energy consumption by switching between different MPTCP-based wireless radio interfaces based on different traffic patterns, as well as the robustness of the Markov-Decision-Process-based multi-path scheduler against random application models with various traffic patterns.

3.4.2 Traffic-optimization-based Solutions

A lot of research works on MPTCP-related traffic optimization have been proposed. One of such examples is ecMTCP [84], an energy-aware congestion control algorithm for MPTCP. ecMTCP aims at reducing energy consumption for devices using MPTCP by moving traffic from the links with higher energy cost to the others and maintains throughput level by moving traffic from the more congested links to the others, with the following features included:

- An energy cost measurement model for the hosts within a communication. In this

model, the energy cost for data packet transmission and ACK receipt is measured at the sender and the energy cost for data packet receipt and ACK transmission is measured at the receiver. The energy cost at the receiver is calculated and sent back to the sender periodically and the sender calculates the end-to-end energy cost with a short-term variation smoothed by an exponentially weighted moving average formula.

- A traffic off-loading scheme considering energy consumption. The scheme makes an inversely proportional increase of the link window size of a MPTCP sub-flow to the energy cost on it when it receives a positive ACK. The link window size is decreased by half every time a duplicate ACK is received, indicating a packet loss. The energy efficiency is controlled by a factor that determines the trade-off between fluctuation and load-balancing so that the path with higher energy cost is less aggressive with the increase of its congestion window. The congestion window increment recompense for multiple paths with divergent round-trip times is also determined with factors in order to ensure the improvement of throughput, as the congestion window of the sub-flows with the lightest load increases more slowly than expected.

The benefits of ecMTCP include the improvement on throughput, fairness to both classic single-path TCP and MPTCP flows, load-balancing and potential energy saving. On the other hand, ecMTCP requires considerable modifications of the original MPTCP and needs implementation at both the sender and the receiver.

NC-MPTCP [85] is another example of the MPTCP-based solution for solving the issue of goodput degradation in the presence of diverse network conditions on the available sub-flows in MPTCP. It introduces a network coding scheme into the sub-flows and transfers the original data on these sub-flows into linear combinations to be used for compensating for lost or delayed data so that congestion on the receiver is avoided. The network coding scheme maps linear encoded packets with continuous sequence number for decoding, after the packets are received via multiple sub-flows. When the linear encoded packets are sent via multiple sub-flows, some of them go through the sub-flows with the network coding scheme while the rest and some redundant packets go through the sub-flows with regular TCP within the same time interval, during which innovative packets arrived at the receiver are calculated and carried in each ACK packet forwarded back to the sender.

NC-MPTCP also includes a packet scheduling algorithm and a redundancy estimation algorithm to allocate data among different MPTCP sub-flows in order to optimize the overall goodput. In the packet scheduling algorithm, packet transmission is coordinated between different sub-flows from the shared buffer at the sender according to the sub-flow characteristics, during which the sequence numbers of the packets are estimated based on the transfer rate and the round-trip time. With this scheme, different sub-sockets are able to finish the transmission of packets from the same generation within the same time interval. The number of redundant packet sent through each sub-flow is determined by the redundancy estimation algorithm to ensure the complete decoding process at the receiver. The algorithm uses the estimated packet loss probability on specific sub-flow to calculate the amount of redundant vectors of packet to be sent. The feedback of the decoding matrix status is included in the ACK packets on fast sub-flows to the sender in order to avoid the underestimation of the packet loss rate and the sender decides whether to retransmit the lost packet or to continue transmitting the next unsent packet according to the feedback.

Experimental results have shown that NC-MPTCP achieves higher goodput compared to MPTCP in the presence of different sub-flow qualities. However in the worst case, the performance of NC-MPTCP is almost the same as that of single-path TCP.

The research work [86] investigates the energy consumption and handover performance of MPTCP for mobile traffic in Wi-Fi and 3G networks. The feasibility of using MPTCP in such networks is proved by real-time experiments, which are done on a test bed including a Nokia smartphone with a MPTCP-enabled operating system. Evaluations on download goodput, application delay and energy consumption of the smartphone are provided during the handover from Wi-Fi to 3G using MPTCP. Experiment results show that MPTCP allows applications to continue to function during the handover from Wi-Fi to 3G. In terms of the goodput and the energy consumption, using MPTCP mode results in shorter battery life as the 3G interface is costly in terms of energy consumption in comparison with the Wi-Fi interface, yet it brings the modest performance improvements over single-path connections.

3.5 Mobile traffic off-loading and smartphone energy optimization

3.5.1 Mobile Traffic Off-loading

Nowadays mobile devices might simultaneously operate one or more multimedia applications as shown in Figure 3.1. The explosion of mobile IP data traffic requires efficient off-loading solutions [87] [88], which aim to increase both network operators' revenues and customers' quality of experience levels. For instance, operators can off-load the traffic of high bandwidth applications (e.g. video streaming data) from cellular networks to broadband networks, protecting the key business of their cellular service (e.g. voice communication) with no additional infrastructure investments.

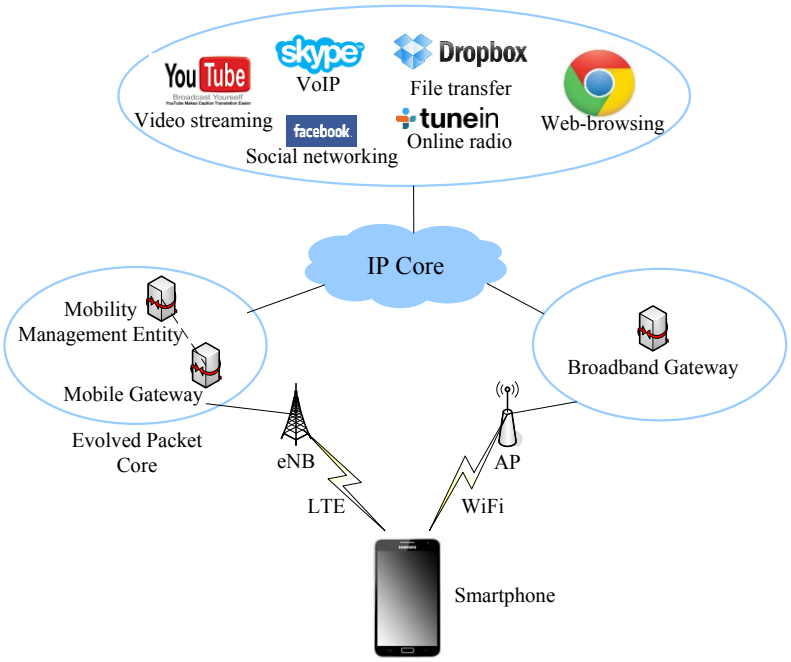

Fig.3.1. Smartphone applications with different traffic pattern

3GPP has released standards such as Local IP Access (LIPA) and Selected IP Traffic Off-load (SIPTO) [89], to support basic traffic off-load. For instance, mobile traffic based on LIPA and SIPTO is not necessarily delivered via mobile core cellular networks. However, advanced features such as user equipment mobility are still under development.

In [90], a mobile traffic off-loading solution for opportunistic communications is proposed in order to reduce operational costs. A selected set of users is assumed to receive delay-sensitive multimedia services (e.g. video streaming, on-line music, etc.) via mobile networks. These users can help to disseminate the information to the non-target users via

opportunistic communications, which are supported by Wi-Fi or Bluetooth. An extensive trace-driven simulation study has shown that mobile data traffic can be off-loaded by up to 73.66%.

In [91], the trade-off between the amount of traffic off-loaded and users' satisfaction was investigated. A novel incentive scheme is designed in which user traffic with high delay tolerance and large off-loading potential is given higher priority during off-loading. Comprehensive simulations validate the efficiency and robustness of the proposed framework.

To the best of our knowledge, none of the mobile traffic off-loading solutions considers the energy consumption at mobile devices for off-loading multimedia traffic services.

3.5.2 Multimedia Traffic Characteristics-aware Mobile Energy Optimization

Recently, the impact of emerging mobile internet applications (e.g. VoIP, video streaming, web-browsing, social networking, etc.) on the energy consumption at mobile devices has attracted very much attention [92]. Multimedia traffic pattern (e.g. burstiness level) acts as a key factor in the device energy consumption and consequently in the effort for its optimization.

In [93], the distribution of internet packet inter-arrival time of smartphone traffic was studied and the results have indicated that the network traffic is bursty in nature. The Low Energy Data-packet Aggregation Scheme (LEDAS) was proposed which buffered several upper layer packets into a burst at MAC layer. When using LEDAS, the radio interface is kept idle longer, saving energy at smartphones.

The energy consumption of diverse multimedia application traffic models on mobile devices in WCDMA and CDMA 2000 is investigated in [94]. Apart from the transition of activity states and the duty cycle scheduling, which are two major elements that determine the energy consumption of data transmission in WCDMA and CDMA 2000, the traffic model is also considered as the characteristics of traffic determine the transmission and reception of data packets on mobile devices. The traffic discussed is divided into two categories: non-real-time (e.g. web browsing, email, file downloading, etc.) and real-time (e.g. video streaming, online gaming, etc.). The characteristics of web browsing traffic are mainly indicated in the static distribution of the parameters including the intervals between browsing sessions and the consecutive data packets inside, the size of each packet and the number of total packets. The characteristics of video streaming traffic, on the other hand, mainly involve the access time of

one streaming video and the interval between two successive streaming videos, as the video streaming traffic is modeled in an on-off source. Based on these traffic characteristics, a Markov-chain-based analytical model is built for energy consumption calculation in the down-link and forward-link of WCDMA and CDMA 2000 for both non-real-time and real-time traffic. The numeric results of simulation show how energy consumption of mobile devices changes according to diverse set of traffic characteristic parameters for both WCDMA and CDMA 2000.

XEM [95] is an advanced energy saving mechanism based on the Power-Saving Mode (PSM) in the standard IEEE 802.11 protocol. PSM enables wireless interfaces of mobile devices to be active during data exchange only by exploiting the central role of the access points with beacons. However, PSM introduces high transfer delays for many applications due to the extra time spent on listening to beacons. Moreover, PSM does not consider the intervals between the traffic bursts called User Think Times (UTTs), which represent the main energy consumption source of wireless interfaces on mobile devices. Using a generic traffic model in which consecutive traffic bursts are downloaded from a remote mobile host separated with UTTs, XEM aims at turning off the wireless interface of the mobile device during UTTs for energy saving by exploiting information across different layer in the protocol stack. Two algorithms are invented for detecting the beginning of the consecutive traffic bursts and the UTTs, respectively. Based on the detection of the accurate start/end point of each traffic burst and UTT, XEM is able to shut down the wireless interface when not observing data traffic and to switch to PSM mode when traffic burst is arriving. Analytical results show that XEM has worse performance in terms of energy consumption in comparison with PSM in the case of UTTs as short as a few seconds. However, the possibility of such case is very low. For typical length of UTTs, XEM obtains significant improvement on energy saving with respect to PSM.

The interrupt direct memory access coalescing scheme proposed in [96] aims at reducing the wake-up time of wireless mobile platforms due to the incoming traffic in order to save energy on the platforms. The scheme is based on characteristic of diverse types of application workloads and investigation of their impact on energy consumption at different components of mobile platforms. Using the traffic characteristic information, the scheme sets up buffers at the MAC layer, which storing incoming packets in a short period as a chunk before

sending them to the CPU of the receiver mobile platform. Meanwhile, the scheme makes a change on the interrupt at the network interface card of the receiver mobile platform, which is triggered at the arrival of any packet. A short time threshold is set for postponing interrupt issuing after arrival of multiple packets, preventing the CPU of the receiver mobile platform from waking up several times which consumes more energy than in the sleep state. The advantages of the scheme include easy deployment as it needs no network support. Experimental results based on real test bed indicate the significant energy saving at the mobile platform when running application services with bursty traffic, without degradation of perceivable user experience of the services.

Several other mobile device energy optimization mechanisms based on traffic characteristics are also briefly introduced as follows. Q-PASTE [97] is a cross-layer solution which enables MAC layer to achieve energy savings by adjusting data delivery based on application-layer traffic pattern. In [98], the energy consumption of smartphone multimedia cloud computing (MCC) applications is studied. Extensive tests demonstrate that MCC services have positive impact on smartphone energy savings. Specifically, uploading and downloading a video document by using HTTP and FTP via both 3G and Wi-Fi is considered. Results show how MCC enables smartphone energy savings up to 70%. A cross- layer smartphone battery and stream-aware adaptive multimedia delivery mechanism (BaSe-AMy) was designed in [99]. The solution monitors the mobile device remaining battery, the remaining video stream duration and the packet loss rate. Based on these values, a video quality adaptation module is proposed to achieve power savings. Experimental results show how BaSe-AMy increases the battery life by up to 18%.

3.6 Chapter Summary

This chapter presents the existing research works done in the following areas: MAC-layer duty cycle management strategies for wireless sensor/mesh networks, QoS/Energy-related wireless MAC-layer schemes, routing algorithms, multi-path/multi-homing communications mechanisms, multipath-TCP-based optimization approaches, mobile traffic load balancing solutions and multimedia traffic characteristics-aware mobile energy optimization techniques.

The chapter investigates the existing schemes for MAC-layer duty cycle management categorized as synchronous and asynchronous, with a brief survey on the advantages and disadvantages of each scheme in these two categories. In terms of QoS/energy awareness in wireless mesh networks, the chapter lists several advanced solutions. In terms of routing algorithms, the chapter summarizes commonly-seen classic routing algorithms with associated introduction on more advanced routing algorithms as well as research efforts on routing protocols for wireless networks. The chapter concludes an overview of the energy-efficient traffic delivery solution in heterogeneous wireless networks, including solutions for multi-path/multi-homing feature, traffic optimization, load balancing and mobile energy optimization based on traffic characteristics.

There are some limitations of the related research and industrial works discussed in this chapter. First of all, very few of these works consider the balance between energy consumption of wireless devices and performance of network application services for users in an innovative manner. Next, some of the works such as ecMTCP are with negative development friendliness due to the considerable amount of modifications of existing network features from them. Moreover, most of the works are with limited usability in specific network scenarios and they are not adaptable with the unpredictable change of network conditions. For example, D-MAC is beneficial only under the specific unidirectional communication flow scenarios with multiple sources and a single sink. The four contributions proposed in this thesis, on the other hand, offers good balance between energy consumption of wireless devices and user application performance. They are designed based on existing network features so no additional modification of network structure is needed. Last but not least, the four contributions are able to work independently from each other to offer a cross-layer manner for a common user scenario described in the next chapter together, in which each contribution is able to be replaced by other solutions based on the same OSI layer.

CHAPTER 4

Energy Efficiency Solutions for Wireless Video Delivery – Architectures and Algorithms

Abstract

This chapter presents a general description of the system architecture and details the principles behind the algorithms of the four contributions in this thesis. These proposed solutions are: (1) the MAC-layer energy-saving duty cycle management solution (AOC-MAC) for mesh router nodes in wireless mesh networks; (2) the energy-aware routing algorithm (E-Mesh) in wireless mesh networks; (3) the MPTCP-based traffic off-loading scheme (eMTCP) for wireless end user devices in heterogeneous wireless networks, and (4) the traffic-characteristics-aware energy-efficient load balancing solution (eMTCP-BT) for wireless end user devices in heterogeneous wireless networks.

4.1 Mobile Heterogeneous Wireless Networking Overview

The rapid development and diversification of hardware technologies and the market demand for both novel types of mobile devices and high quality content have resulted in an unpredicted proliferation of mobile traffic load on the wireless mobile networks. Among various categories of mobile traffic, rich-media traffic has experienced one of the highest growth rates mostly due to its popularity in entertainment, social networking and other businesses. The growth of rich-media traffic brings serious challenges to the wireless mobile networking for both end users and network operators in terms of maintaining long life-cycle with stable service performance at high quality levels.

One way to address such a challenge in heterogeneous network environments is to propose adaptive solutions in terms of balancing service quality and energy consumption. Figure 4.1 illustrates a scenario of wireless mobile device usage in such a heterogeneous network environment involving rich-media traffic. In this scenario, the wireless terminal device (the smartphone) owned by the end user runs a video streaming application in which the video

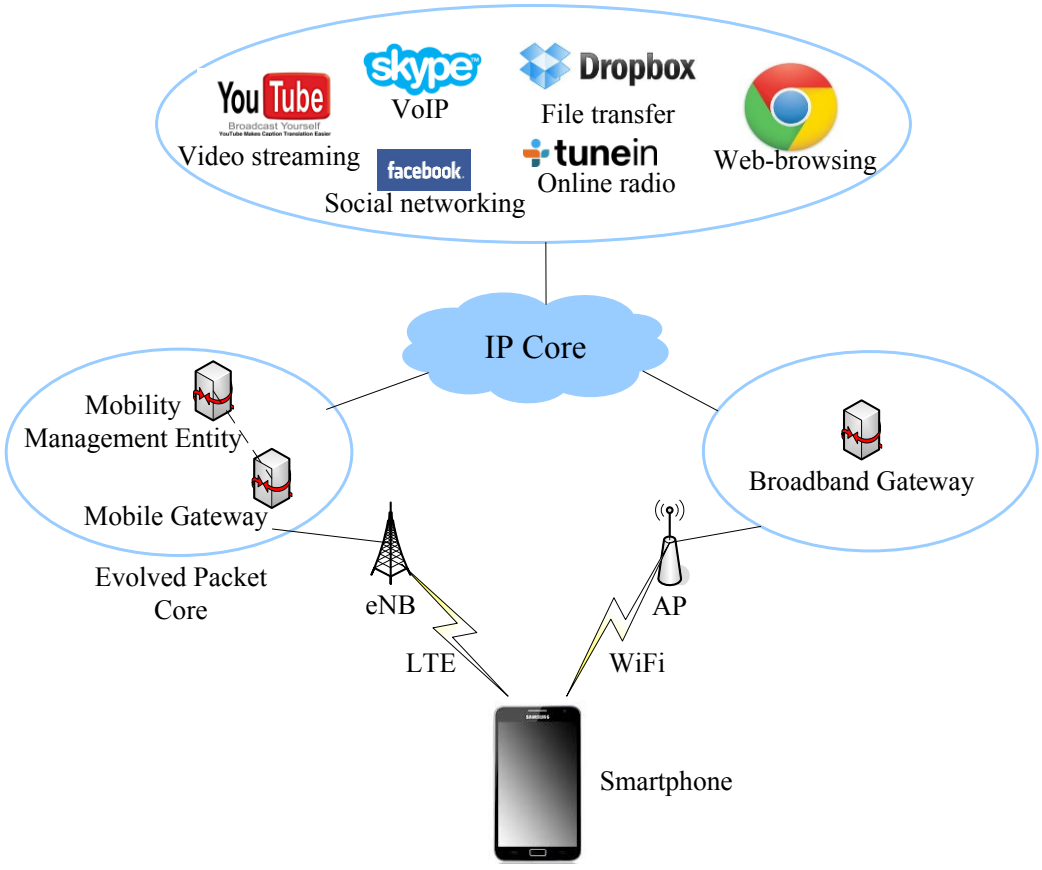

Fig.4.1. Rich-media usage on a mobile device in a heterogeneous wireless network

content is transmitted from a remote server and forwarded through several routers, over a wireless mesh network. The terminal device is connected to the wireless mesh network via Wi-Fi when within the communication range of the access point at the end user's home. The way from the end user's home to his office is within the signal coverage of a 4G LTE network. Both the wireless mesh network with Wi-Fi at the end user' home and the 4G LTE network on the way to the end user's office are parts of a heterogeneous wireless network, connecting the smartphone with the remote server where the video source is stored. There are several challenges in such a scenario when the end user is moving from his home to his office and running the video streaming service while mobile:

- If (some of the) wireless mesh routers are battery powered, the wireless mesh network operator desires support to extend the battery life-span of the routers.
- The network operator also wants to maintain good user-perceived quality of the video delivery during video traffic forwarding for users of wireless end devices.
- The end user expects good service quality on the smartphone during the mobility

from home to office, including mitigation of the handover from the wireless mesh network to the 4G LTE network.

- The end user desires a solution to increase the battery life-span on his smartphone.
- The end user desires a solution to provide high quality for the video streaming service.

Four adaptive solutions are proposed in order to help the user and the network operator to address these challenges in different situations:

- AOC-MAC: is an energy-aware mesh router duty cycle management scheme used for extending the battery life-span of the routers in the wireless mesh network. AOC-MAC adaptively adjusts the sleep periods of the routers in an innovative way, so the mesh router energy consumption is reduced while network connection stability is maintained. As a result, the battery life-span of the mesh routers is significantly extended regardless of whether the routers are mobile, at the cost of a slight decrease on the quality of the application traffic.
- E-Mesh: is an energy-efficient routing algorithm for balancing the energy consumption, load amount and router connectivity in the wireless mesh network, enabling the network operator on the mesh routers to maintain good video streaming service quality levels for the traffic traversing the routers, while also saving energy. By co-operating with AOC-MAC, E-Mesh achieves obvious reduction on energy conservation of the battery-powered mesh routers with some insignificant decrease on QoS.
- eMTCP: is a multi-path-enabled traffic load balancing scheme used for ensuring energy efficiency on the smartphone of the user. This scheme enables network connectivity via multiple wireless radio access interfaces (e.g. Wi-Fi and 4G LTE) so that the service quality of the video streaming is not affected by possible connection/disconnection processes, when the smartphone of the user moves out of the communication range of any particular technology. eMTCP also balances the energy and traffic load when considering multiple radio access interfaces, so that the high-energy-consuming interfaces (e.g. 4G LTE in this case) do not have high traffic load and therefore battery energy on the smartphone is saved. eMTCP

improves the energy efficiency of the smartphone in comparison with MPTCP, when multiple radio access interfaces are being used simultaneously.

- eMTCP-BT: is a traffic-characteristic-aware load balancing scheme based on eMTCP which adaptively provides the best traffic off-loading ratio between a high-energy-consuming radio access interface and a low-energy-consuming interface, based on the smartphone energy efficiency. eMTCP-BT enables setting of the energy-efficiency-optimal traffic off-loading ratio by predicting the traffic pattern of the application service running on the smartphone and adjusting the traffic off-loading amount, accordingly. By deploying eMTCP-BT, the energy efficiency of the smartphone is always adapted to the highest, regardless of the type of traffic.

The architectures of the four solutions are presented and the corresponding principles and algorithms are described in details in the next sections.

4.2 AOC-MAC: Energy-Aware MAC-layer Duty Cycle Management Scheme for Wireless Mesh Networks

In the scenario described in section 4.1, the end user starts the video streaming service on the smartphone while at home by connecting to the remote server via Wi-Fi and the wireless mesh network. The data traffic containing the video content is sent from the remote server and forwarded via the mesh routers to the user's smartphone. The network operators of the devices in the wireless mesh network expect reducing router energy consumption without affecting the video streaming performance. The proposed MAC-layer duty cycle management scheme, referred to as AOC-MAC, performs energy saving on the mesh routers by controlling the length of the sleep period of each router according to the information from the network layer, enabling the routers to sleep longer without severely decreasing the video streaming service quality.

4.2.1 AOC-MAC Architecture and Solution Overviw

The block architecture of the proposed MAC-layer mesh router duty cycle management scheme based on the OSI network model is shown in Figure 4.2. AOC-MAC architecture is composed of the following two modules:

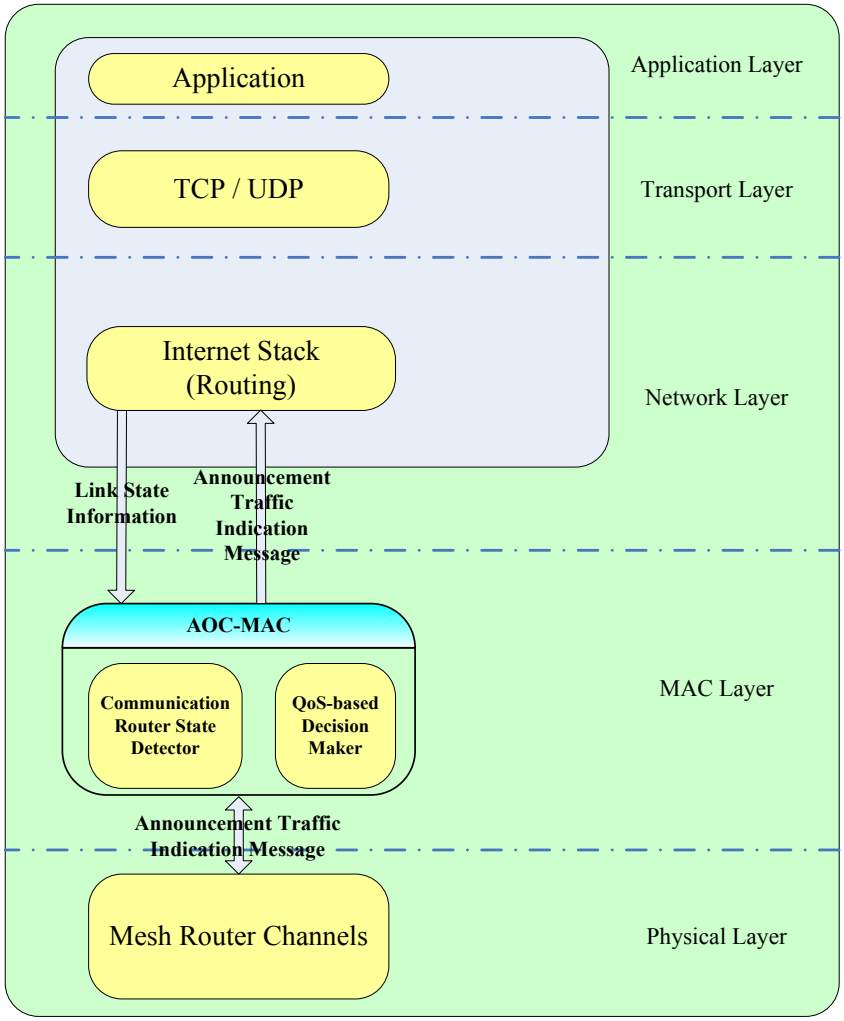

Fig.4.2. Architecture of AOC-MAC

1) ***Communication Route State Detector***: periodically checks the communication states of the mesh routers. The communication states of the mesh routers are obtained by using an external network-layer module which is in charge of routing during traffic delivery, based on a utility function with the energy consumption rate, the traffic load and the distance between mesh routers as the parameters.

2) ***QoS-based Decision Maker***: starts duty cycle adaptation based on the communication state detection result.

Figure 4.3 presents the UML class relationship between the AOC-MAC components. The *CommunicationRouteStateDetector* class defines functions to obtain link state information from the network layer (i.e. how many disconnections have happened during routing). The *QoSbasedDecisionMaker* class maintains a list of duty-cycle-related parameters and defines the function to adjust the duty cycles of mesh routers according to the link state information stored

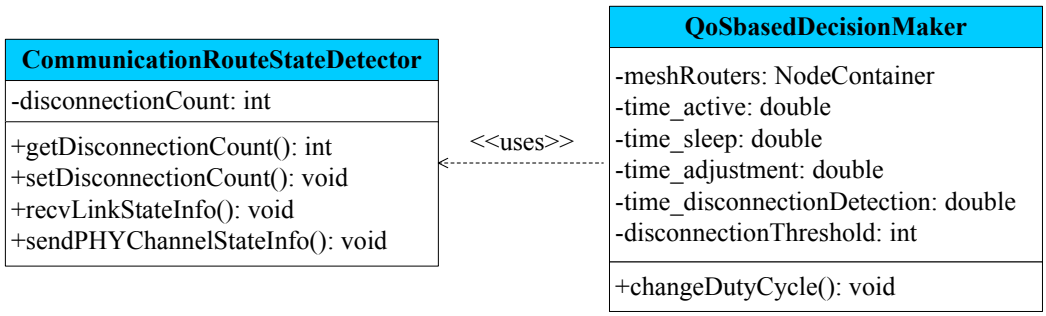

Fig.4.3. UML of classes for AOC-MAC algorithm implementation

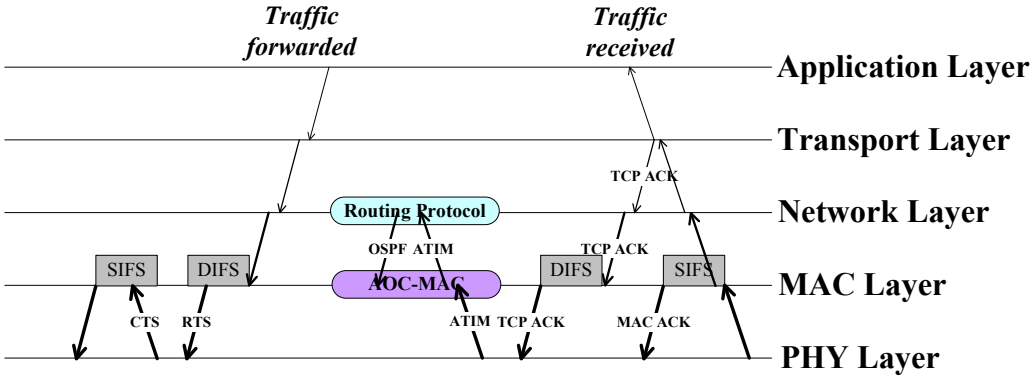

Fig.4.4. Network information exchange between different OSI layers

in the *CommunicationRouteStateDetector* class. The details of the modules are presented in section 4.2.1.1 and 4.2.1.2.

The work flow in the AOC-MAC architecture involves interactions between interfaces in different OSI layers, as shown in Figure 4.4. At each mesh router, after receiving traffic sent from the mesh client or another mesh router, the physical channel state information is contained in the Announcement Traffic Indication Message (ATIM) [23] packet and sent to AOC-MAC. The sleep/wake-up states of wireless channels of the mesh router are indicated in the ATIM packets, which are forwarded to the routing protocols in the network layer. The network layer sends back the routing-protocol-based packets such as the Open Shortest Path First (OSPF)[1] packets to the MAC layer, informing the link state information during the routing process. AOC-MAC uses the 0-1 bit mesh power mode message included in the header of each ATIM packet to indicate the physical channel state (sleep/wake-up) for routing protocols. Meanwhile, AOC-MAC obtains the link state information from the OSPF packets sent by the routing protocols in order to check whether there are disconnections along the route between two mesh

[1] Open Shortest Path First version 2 - http://tools.ietf.org/html/rfc2328

clients.

By default, the duty cycle of all routers in the wireless mesh network is controlled by the existing IEEE 802.11s DTIM beacon mechanism [23]. It defines a number of periodical beacon intervals within which traffic indication messages are exchanged to indicate different communication states such as pending traffic and re-instating stop flows and to guarantee the length of different states of the duty cycle of the mesh nodes (e.g. sleep/wake-up). The wake-up time of each mesh router is defined as the Mesh Awake Window in the 802.11s beacon frame. The sleep time of each mesh router is defined as the rest part of the beacon interval apart from the wake-up time. In the AOC-MAC algorithm (which is presented in the following sections), the default lengths of the sleep/wake-up periods of mesh routers defined in DTIM are used as the initial duty cycle states of them. The lengths of these periods are adaptively changed during traffic transmission using the AOC-MAC algorithm.

4.2.1.1 Communication Route State Detector

The basic functionality of this module is to gather the route/connection state information via feedback messages from the network layer module, in order for AOC-MAC to make decisions on how the duty cycles of the mesh routers are adjusted. It includes a *disconnection counter DCount* which calculates the number of disconnections occurred during the mesh router duty cycle adjustments. The disconnection occurs during the traffic data forwarding between routers when some of the routers are asleep. Suppose data packets are forwarded in the mesh network from router A to router B, which is in the sleeping state extended by AOC-MAC. As the channels of router B are inactive, no data packet from router A is received. As mentioned, the disconnections are recorded and included in the headers of the link state information packets sent by the routing protocols in the network layer. If such disconnections happen frequently in the mesh network, the quality of the traffic delivery in the entire mesh network is decreased. As a result, the duty cycles of the mesh routers need to be increased in order to maintain good traffic delivery quality. A threshold value of the disconnection number is defined. In general, higher threshold value indicates lower requirement on service quality level.

The detection on communication (disconnection) states and the calculation of disconnection numbers is done periodically by AOC-MAC. The length of the interval between

two detections is determined according to the frequency of the change of the wireless mesh network topology, which corresponds to the mobility of the mesh routers and the mesh clients. In this thesis, in the AOC-MAC experiments, the length of this interval is set to 20 seconds which proves to be satisfactory according to the test results illustrated in Chapter 5. The value of the disconnection counter is used as one of the key parameters of the QoS-based Decision Maker module, together with the length of the interval between two detections.

4.2.1.2 QoS-based Decision Maker

In each communication state detection period, the duty cycle (the active period) of each mesh router is lengthened or shortened depending on the value of the disconnection counter from the Communication Route State Detector mod ule. When the value of the disconnection counter is smaller than the threshold value set in the Communication Route State Detector module according to the demand on service quality level from the end user, the duty cycle of the mesh routers is decreased in length in order to save energy. Once the value of the counter exceeds the threshold, indicating possible decrease on traffic delivery service quality due to too many disconnections, the duty cycle of the mesh routers is reversed to their original lengths to maintain good service quality levels. This adjustment of mesh router duty cycles is performed during the entire duration of traffic delivery.

The biggest concern for the performance of the QoS-based Decision Maker module is the impact of the ping-pong effect caused by the back-forth adjustment of the mesh router duty cycle. AOC-MAC is aware of the extra overhead in the mesh network from the frequent change of mesh router duty cycle, which results in jitter and delay. However, the ping-pong effect does not affect the energy consumption rate on mesh routers, which is considered more important by the network operators. The impact on the service quality of the ping-pong effect does not overcome the benefit of energy saving from reducing duty cycles of mesh routers by AOC-MAC.

4.2.2 AOC-MAC Algorithm

AOC-MAC defines and adaptively controls the active/inactive period of mesh routers in details. The scheme uses the following parameters:

- $\boldsymbol{S}$ – a set of mesh nodes (mesh routers and clients). A neighbor mesh node of each mesh node n in $\boldsymbol{S}$ is defined as any mesh node in n's communication range not

already contained in $\boldsymbol{S}$.

- *DCount* – a counter of the disconnection times between the mesh client and any mesh router.
- TH_{DC} – an upper threshold value of *DCount* until which the communication disruption is considered normal.
- T_D – the time period in which the algorithm waits for the increase of *DCount*.
- T_A – the duty cycle (the ACTIVE time slot) of the router to wait for data request from other mesh nodes. It is clear that shorter T_A results in less energy consumption at the router.

The adaptive duty cycle management algorithm is described as follows:

- At the initialization, *DCount* is set to 0 and the length of T_A is set with the size of the Mesh Awake Window defined in DTIM by default. Meanwhile the communication route state detector starts keeping track of communication states for all the mesh nodes.
- When the communication route state detector finds that there are no neighbor mesh nodes waking up for any mesh node in $\boldsymbol{S}$, *DCount* is incremented by 1.
- When the value of *DCount* exceeds TH_{DC}, the length of T_A is increased by ΔT_A by the QoS-based decision maker, preventing severe decrement of the QoS level caused by over-extending the sleep period of mesh nodes. In this context, ΔT_A is set as $0.5 \times T_A$.

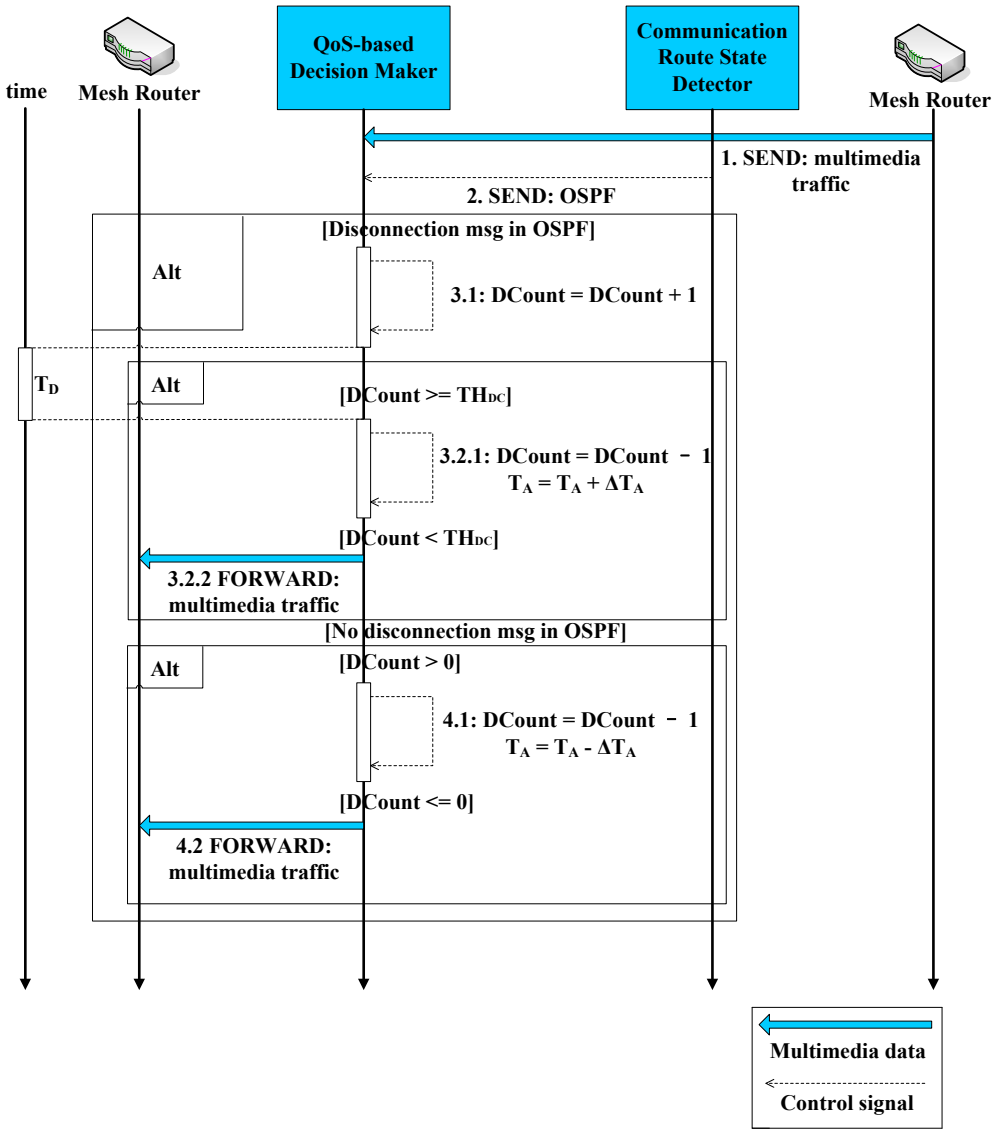

Fig.4.5. Sequence diagram of AOC-MAC

- When the value of *DCount* exceeds TH_{DC}, if after a period of time T_D, *DCount* does not increase, it is decreased by 1. *DCount* has the lowest limit 0.
- Every time when *DCount* decreases, the value of T_A is reverted to its previous value.

The scheme is detailed in Figure 4.5 and Table 4.1 in the form of sequence diagram and pseudo code, respectively.

By using this scheme, the duty cycle of each mesh node is able to be adapted according to the change of network communication states, which is indicated in the link state information in the network layer. This information exchange process is working independently together with the regular mechanism of interaction between the network layer and the MAC layer in IEEE

TABLE 4.1 PSEUDO CODE FOR THE AOC-MAC ALGORITHM

```
DCount = 0;
while (1)
{
    if (disconnection msg in OSPF)
    {
        DCount = DCount + 1;
        if DCount >= TH_DC
        {
            DCount = DCount – 1;
            T_A = T_A + ΔT_A;
        }
        else
            continue;
    }
    else
    {
        if DCount > 0
        {
            DCount = DCount – 1;
            T_A = T_A – ΔT_A;
        }
        else
            continue;
    }
}
```

802.11s, as shown in Figure 4.4.

4.2.3 Overhead and Complexity Analysis

The overhead of AOC-MAC mainly come from the link state information included in the OSPF packets and the duty-cycle-related state information included in the ATIM packets, which are used during the communication between the Communication Route State Detector module and the QoS-based Decision Maker module. The overhead consists of three aspects: 1) the link state information in the OSPF packets sent from the network layer; 2) the 0-1 bit mesh power mode message included in the headers of ATIM packets; and 3) the duty-cycle-related state information (e.g. $DCount$, TH_{DC}, T_A and ΔT_A). As the sizes of the link state information and power mode messages take only a few bits in the packet headers while the duty-cycle-related state information is transmitted inside each mesh router, the overhead is ignored in this thesis

due to the high processing ability of mesh routers.

As shown in Table 4.1, the algorithm runs linearly in each individual loop, with the information about each mesh router stored globally in a central place. Therefore, the complexity of AOC-MAC is only related to the number of mesh routers in the network. So for N mesh routers in the wireless mesh network, the complexity of the AOC-MAC algorithm is O(N).

4.3 E-Mesh: Energy-Load-Distance-Aware Routing Algorithm for Wireless Mesh Networks

Considering the scenario described in section 4.1, while the video content is being streamed from the remoter server to the user smartphone, the video data packets pass through multiple routers in the wireless mesh network along a traffic delivery route. Depending on the traffic conditions and network topology variation in the wireless mesh network, this delivery route may change. The network operators of mesh routers desire to reduce the energy consumption on their network, while ensuring the QoS provisioning of the video streaming services. To achieve this, the network operators of mesh routers can deploy the proposed Energy-Load-Distance-Aware Routing Algorithm for Wireless Mesh Networks (E-Mesh), which offers an innovative way to balance energy consumption, network load and connectivity for mesh routers during the video streaming service, using a novel utility function.

4.3.1 E-Mesh Principle

E-Mesh is an energy-aware routing solution which balances performance of video delivery with energy saving. The core aspect of E-Mesh is a novel utility function that takes multiple network-condition-related parameters into account to suggest the optimal option for route establishment in terms of both energy and performance. These parameters are:

- The remaining energy on each mesh router.
- The traffic load on each mesh router.
- The distance between any two mesh routers.

E-Mesh is based on the following assumptions:

- The maximum communication ranges of the mesh nodes (i.e. mesh router, mesh data source and mesh client) are with the same value defined as K.

- Each mesh node n_i has the capability to determine its position in terms of coordinate (X_i, Y_i) and to measure its remaining energy level E_i and traffic load L_i.
- The time for the client to get the information from the routers (such as their position and remaining energy level) is very short in comparison with the data transmission time and the time scale of the client movement.

Consider the wireless mesh network topology illustrated in Figure 4.6, in which the remote video server is a single mesh source node n_0. There are N mesh routers (n_1 to n_N) for data forwarding and at least one end user smartphone as the mesh client n_{N+1}. The position of each of these N routers is randomly distributed in a circular area with radius R. Some of the mesh routers move with a random velocity within the range of this circular area while others remain fixed. The ratio between the fixed and mobile routers is set to a specific value r. The mesh client n_{N+1} is moving with constant velocity when mobile, with its initial position at the edge of the circular area considered. The location of the mesh data source n_0 is fixed at the center of a circular area of consideration, as shown in Figure 4.6. This is a generalization of the situation in the scenario described in section 4.1 when the user was performing video streaming while travelling from home to office.

4.3.2 E-Mesh Architecture

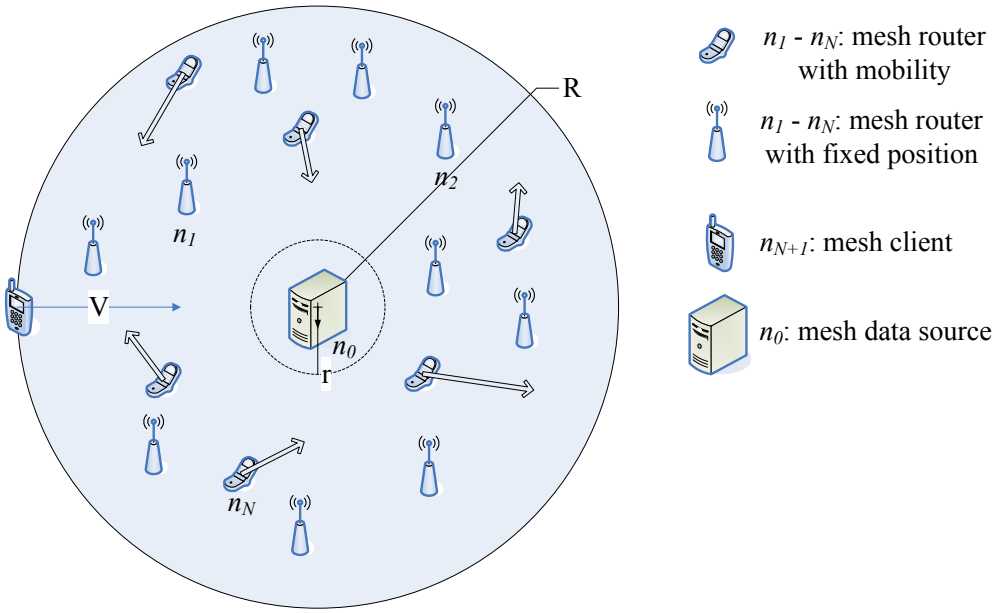

Fig.4.6. E-Mesh wireless mesh network topology

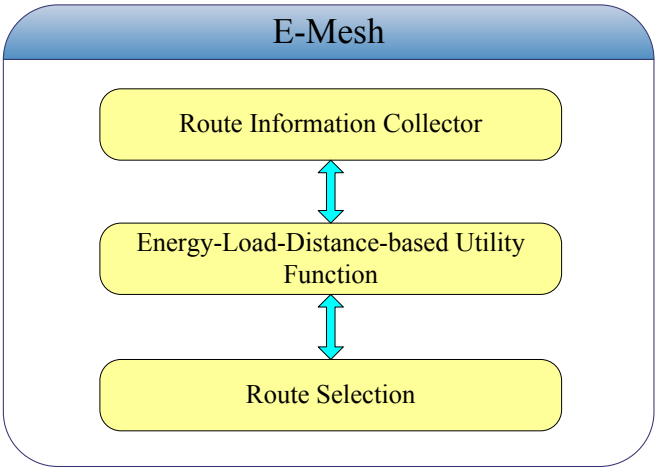

Fig.4.7. E-Mesh Architecture

The block architecture of E-Mesh is illustrated in Figure 4.7 and contains the following three modules:

1) ***Route Information Collector***: obtains router information such as remaining energy on each router, instant traffic load on each router and distance vectors between routers.
2) ***Energy-Load-Distance-based Utility Function***: computes the utility function for all the mesh routers based on the information from the Route Information Collector module.
3) ***Route Selection***: establishes the best route for traffic delivery based on a sequence of energy-load-distance-aware utility values provided by the utility function.

4.3.2.1 Route Information Collector

This module is in charge of collecting network/device-condition-based information from the mesh routers, including the remaining energy levels at each mesh router, current traffic load amount and distance between mesh routers, calculated using the position of each router. The information is used when computing by the utility function to assess the general condition of all the nodes in the wireless mesh network, in order to select the most suitable route for traffic delivery in terms of the least energy consumption on the mesh routers, optimal traffic load amount on the mesh routers and distance between routers within their maximum communication range.

The network/device-condition-based information is collected from the headers of the

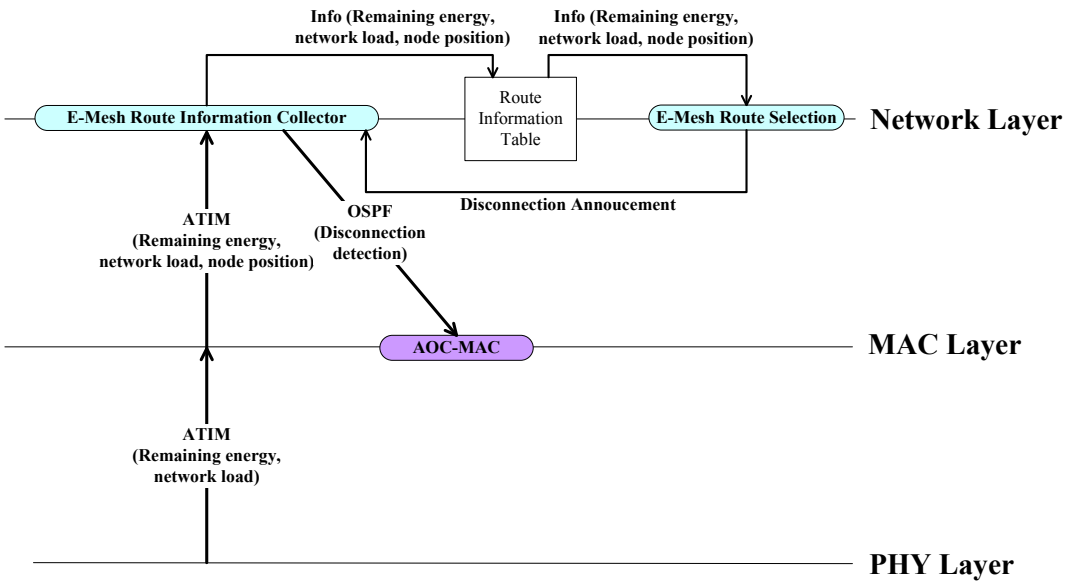

Fig.4.8. Network/device-condition-based information between different OSI layers

ATIM packets sent by the PHY layer and forwarded by the MAC layer. The messages are stored and updated in a global route information table in which the utility function obtains the information as it needs. The process of the information collection is illustrated in Figure 4.8. The information of remaining energy and current network load of each mesh router is included in the ATIM packets by the PHY layer and sent to the MAC layer. After the MAC layer receives the packets, the information of (X, Y) position of each mesh router is added to the headers and the packets are forwarded to the network layer where E-Mesh obtains such information and stores them in the global route information table.

4.3.2.2 Energy-Load-Distance-based Utility Function

The responsibility of the Energy-Load-Distance Utility Function module is to calculate the utility for each mesh router to enable choosing the next hop for the traffic from the neighbor mesh routers of the current mesh router. The neighbor mesh router with the optimal utility value will be selected as the next hop of the traffic and it will search for its next hop with the utility values of all its neighbor routes recalculated.

In the wireless mesh network topology shown in Figure 4.6, each mesh router n_i considers the following three key criteria for utility calculation: its local position in terms of the (X_i, Y_i) coordinates, its current network traffic load L_i and its remaining energy E_i. The remaining energy and network traffic load for each mesh router are updated periodically during the video streaming traffic delivery. Hence for each mesh router n_i, the

Energy-Load-Distance-based utility function relies on the following three utilities as described in equations (4.1), (4.2) and (4.3).

1) Remaining Energy Utility $E(n_i)$:

$$\mathrm{E}(\mathrm{n_i}) = \frac{E_i}{\mathrm{E_{imax}}} \qquad (4.1)$$

In equation (4.1), E_i represents the amount of current remaining energy on mesh router n_i and E_{imax} represents the full amount of battery energy capacity on mesh router n_i. The value of the remaining energy utility is in the [0, 1] range and has no unit. As the value of E_{imax} is constant for any mesh router n_i, higher values of E_i (more remaining energy) reflect directly into higher values of the utility $E(n_i)$, and are considered better in terms of energy saving than lower values.

2) Distance Utility $D(n_i)$:

$$\mathrm{D}(\mathrm{n_i}) = \frac{\mathrm{D}_i - \mathrm{D_{imin}}}{\mathrm{D_{imax}} - \mathrm{D_{imin}}} \qquad (4.2)$$

In equation (4.2), D_i represents the current distance from the mesh router n_i to the mesh client (the end user smartphone) and D_{imin}/D_{imax} represents the minimum/maximum distance from the mesh router n_i to the mesh client, respectively. The value of D_{max} is set to be the maximum communication range between any of the two mesh nodes in the mesh network. The value of D_{imin} depends on the initial position distribution of the mesh routers and is also constant. As the mesh client is mobile, the theoretical minimum value of D_{imin} is 0 in that case that the mesh client is at the position of one mesh router. The value of the distance utility is in the [0, 1] range and has no unit.

The default maximum communication range of mesh points in the IEEE 802.11s wireless mesh network topology is closely relevant to the default propagation model used during data delivery. In E-Mesh experiments, this range is estimated as 150 meters using the NS-3 log-distance propagation loss model [100] as illustrated in equation (4.3) and (4.4), as the user scenario described in Chapter 4 is a large-scale dense populated environment. The estimation is based on the relationship between the maximum communication range of the mesh point and its maximum transmission power level [101].

$$L = L_0 + 10n\log_{10}(\frac{d}{d_0}) \qquad (4.3)$$

$$d = d_0 \times 10^{\frac{L-L_0}{10n}} \qquad (4.4)$$

In equation (4.3) and (4.4), *n* represents the path loss distance exponent with the default value 3; d_0 represents the reference distance with the default value 1 meter; L and L_0 represent the pass loss at any distance and at reference distance, with the default value 111.96 dB and 46.6777 dB, respectively.

Different from the energy utility $E(n_i)$, lower values of the distance utility $D(n_i)$ are considered better than higher values, as they indicate shorter distances between the mesh router n_i and the mesh client, which results in better signal strengths.

3) Traffic Load Utility $L(n_i)$:

$$\mathrm{L(n_i)} = \frac{\mathrm{L_i - L_{imin}}}{\mathrm{L_{imax} - L_{imin}}} \qquad (4.5)$$

In equation (4.5), L_i represents the current amount of traffic load, measured in terms of the actual throughput at the mesh router n_i and L_{imin}/L_{imax} represent the minimum/maximum amount of traffic load on the mesh router n_i, respectively. The value of L_{imax} is the overall available bandwidth at the wireless mesh network, and is constant. The value of L_{imin} is 0 and corresponds to the case that no traffic is passing through the mesh router n_i. The value of the load utility is in the [0, 1] range and has no unit.

Higher values of the traffic load utility $L(n_i)$ indicate higher throughput on mesh router n_i, and are considered better for the overall E-Mesh utility function than lower values.

4) E-Mesh Utility Function

Making use of the three utilities described above, the utility function associated to route n_i is defined in equation (4.6):

$$C(n_i) = \frac{\mathrm{L(n_i)^{W_l} * D(n_i)^{W_d}}}{\mathrm{E(n_i)^{W_e}}} \quad 1 <= \mathrm{i} <= N \qquad (4.6)$$

In equation (4.6), W_e, W_d and W_l are adaptive weight factors for the utilities $\boldsymbol{E(n_i)}$, $\boldsymbol{D(n_i)}$ and $\boldsymbol{L(n_i)}$, respectively. The weights represent the importance of the different utilities in the route selection. The values of the weights are decided by the network operators of the mesh nodes in the wireless mesh network, depending on different possible demands on various situations. For example, the value of W_e is set higher in the case that the energy consumption is considered more important. On the other hand, if the network operator cares more about network load, the values of W_l can be set higher. As already mentioned, N represents the total

number of mesh routers in the wireless mesh network.

4.3.2.3 Route Selection

Based on the utility calculation results provided by the Energy-Load-Distance Utility Function module, the Route Selection module is responsible for picking the mesh routers with the optimal utility values hop by hop, starting from the router closest to the remote server and ending at the router closest to the mesh client, to build the optimal traffic delivery route balancing the energy-load-distance criteria. The utility-optimal route is updated periodically by this module, according to the change of network conditions and routing device characteristics. This is done by E-Mesh algorithm to be described next.

When no neighboring mesh routers are detected during the routing process, a disconnection announcement is made in the form of a 0-1 bit message (0 represents no disconnection and 1 represents disconnection) and sent to the Route Information Collector module. After receiving the disconnection announcement, the Route Information Collector module stores the 0-1 bit announcement message into the OSPF packet headers before sending the OSPF packets to the MAC layer where AOC-MAC is deployed. The disconnection announcement is then used by the MAC-layer protocol as the link state information. This process is illustrated in Figure 4.8.

4.3.3 E-Mesh Routing Algorithm

The proposed E-Mesh routing mechanism for energy-aware data routing in wireless mesh networks is an extension of the OLSR algorithm. As a link state protocol like OLSR, in E-Mesh the route is not decided by the source node, but the data forwarding neighbor router nodes. E-Mesh routing algorithm makes use of the neighbor sensing scheme in OLSR and replaces the original multipoint relay selection strategy with the E-Mesh utility function introduced in section 4.3.2.2. The details of the E-Mesh routing algorithm are described next.

Define $\boldsymbol{S}$ as a set of mesh points (mesh data source, router and client). A neighbor mesh point of each mesh point n in $\boldsymbol{S}$ is defined as any mesh point in n's communication range not already contained in $\boldsymbol{S}$.

Suppose there are m mesh points in $\boldsymbol{S}$ ($1 <= m <= N + 2$): $\boldsymbol{S} = \{n_1, n_2 \ldots\ldots n_m\}$. The algorithm detects all the neighbor mesh points of these m mesh points. Suppose mesh point n_x ($1 <= x <= m$) has y of these neighbor mesh points ($n_{x1}, n_{x2} \ldots\ldots n_{xy}$), some of which might also be

neighboring other different mesh points n_z ($1 <= z <= m$ and $y != z$) in ***S***.

For each of the neighbor mesh points of all the mesh points in ***S***, there are two possibilities for the mesh client (which is a mesh point in ***S***) to communicate with it: if it is in the mesh client's communication range, the client could set up direct communication with it, otherwise the client chooses one or more routers in ***S*** as intermediate nodes. Either way there is a route established from the client to this neighbor mesh point. In fact there are multiple possible routes from the mesh client to any of these mesh points in ***S***.

Suppose there are z nodes (n_{x1}, n_{x2} …… n_{xz}) on any one of these routes from the mesh client to mesh point n_x ($1 <= x <= m$) in ***S***. The concept of *routing weight factor* ***W(z)*** is introduced as the sum of the utility function values $\boldsymbol{C(n_{xz})}$ computed for the z nodes on this route. n_{xmin} is defined as the neighbor mesh point of any node n_x, in those z nodes which has associated the minimum value of $\boldsymbol{C(n_{xz})}$. In this context, the routing weight factor is described as follows:

$$W(z) = \min\left(\sum_{i=1}^{z} C(n_{xi}), W(n_{xmin}) + C(n_{xmin})\right) \quad (4.7)$$

With the above definitions, the process of data forwarding path generation from the source to the client is described below:

1) The algorithm starts when ***S*** contains the mesh client only.
2) The Energy-Load-Distance-based Utility Function periodically calculates the route selection utility ***C(n)*** for every mesh router n in the topology and searches for the mesh router n_{xmin} which has the minimum value of ***C(n)*** in the communication range of all the mesh points in ***S***.
3) If n_{xmin} is in AWAKE state, the routing weight factor from the client to n_{xmin} is computed and n_{xmin} is added to ***S***. If n_{xmin} is in AWAKE state, alternative mesh points in ascending order of ***C(n)*** are sought and this step is repeated. If no other mesh point can be found, the Communication Route State Detector in the MAC-layer router operation cycle management scheme notifies this situation to the QoS-based Decision Maker and waits until the next period of ***C(n)*** calculation comes.
4) If a new mesh point is added to ***S***, the algorithm checks if ***S*** contains the mesh data source. If so, it establishes the route with all the mesh points in ***S***, using the mesh client as the start point and the mesh data source as the end point. Once the route has been set up, the algorithm waits for the next period of ***C(n)*** calculation.

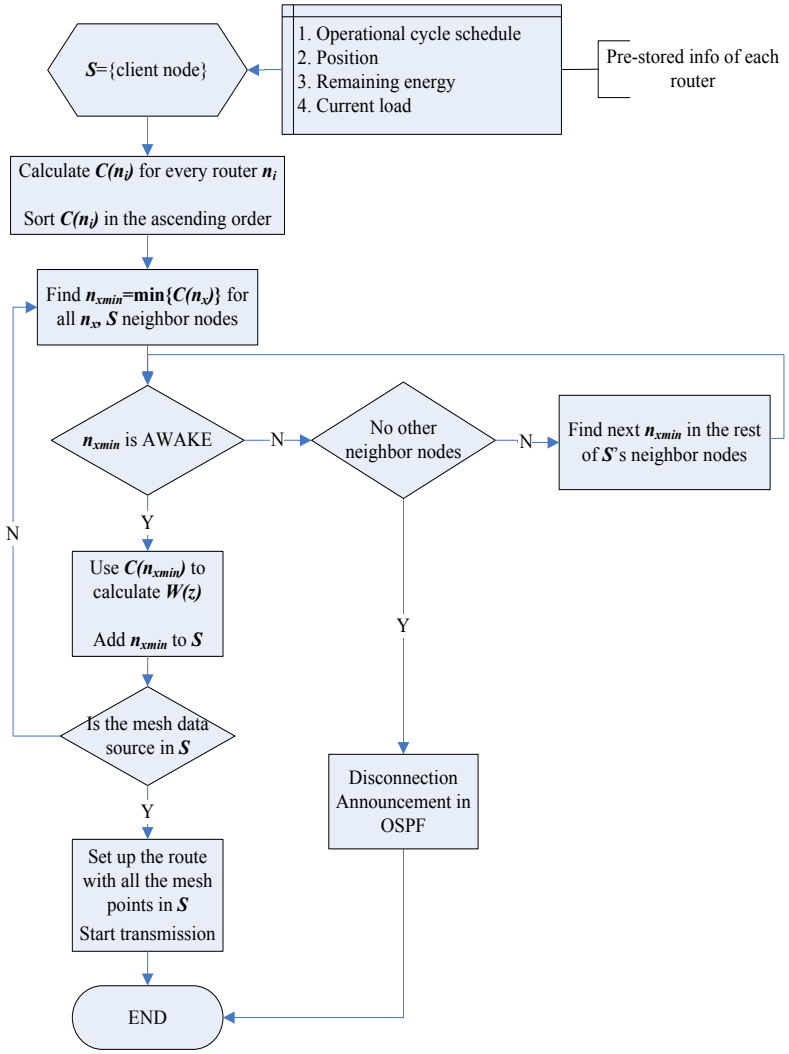

Fig.4.9. E-Mesh Algorithm

Figure 4.9 presents the diagram which details the E-Mesh energy-aware routing algorithm.

4.3.4 Overhead and Complexity Analysis

The overhead of E-Mesh mainly consists of the following aspects:

1) The remaining energy, (X, Y) position and network traffic load of each mesh router
2) The 0-1 bit disconnection announcement message stored in the headers of the OSPF packets information

The network/device-condition-based information are collected from the headers of the ATIM packets sent by the PHY layer and forwarded by the MAC layer, which are stored in a global route information table and used by the Router Information Collector module during the routing process. The disconnection announcement message are generated by the Route Selection

module and stored in the OSPF packet headers before sent to the MAC layer as the link state information. As the sizes of these information take only a few bits in the packet headers, the overhead is ignored in this thesis due to the high processing ability of mesh routers.

As described in section 4.3.3, the complexity of information collection depends on the number of routers only. So for N mesh routers in the wireless mesh network, the complexity of E-Mesh information collection is O(N). Similarly, in the utility calculation process, the usage of information is linear according to equation (4.6). So the complexity of E-Mesh utility calculation is O(N). Finally, the complexity of the OLSR-based routing is O(Nlog(N)) [9]. Therefore, the overall complexity of E-Mesh routing algorithm is O(N(log(N) + *1)*).

4.4 eMTCP: Energy-Aware Traffic Load Balancing Scheme for Heterogeneous Wireless Networks

Unlike E-Mesh which balances energy savings and quality awareness during video streaming from the network operator's point of view, next energy efficiency and service quality awareness is considered at the user device (e.g. smartphone).

Consider the scenario described in section 4.1 with a mobile user performing video streaming while travelling from home to office in a heterogeneous wireless network environment. As the user of the mobile device moves away from his home, the Wi-Fi connectivity will be interrupted when moving out of the communication range of the wireless mesh network. Moreover, if the user chooses to play high-quality video content when the wireless network does not support the additional bandwidth required to transfer such content to the mobile device, the service quality will be severely affected.

In order to ensure the connectivity to the server during the remote video streaming while the user is mobile and support for increasing bandwidth, MPTCP is used. When MPTCP is used, multiple sub-flows are established for video delivery, using different wireless network technologies. The usage of MPTCP not only avoids disconnection from the remote server during mobile video streaming, but also significantly increases the throughput when necessary by using more than one simultaneous sub-flows to transfer the required video data over multiple network technologies. This thesis considers a heterogeneous wireless network environment in

which Wi-Fi and 4G LTE technologies co-exist. However, the introduction of additional network connections comes with additional energy consumption on the mobile device, fact which is not taken into account by the classic MPTCP.

In this context, this thesis proposes an energy-efficiency-aware network load balancing scheme (eMTCP) which balances the energy consumption and data transfer for MPTCP-based video delivery. eMTCP ensures the multi-sub-flow usage in MPTCP and off-loads some amount of the delivered traffic from the sub-flows transported over the higher energy consumption network technology to the sub-flows carried by the lower energy consumption network technology, allowing energy saving. Wi-Fi and LTE are considered as the wireless radio access technologies, each allocated with one or more sub-flows. The energy efficiency of the traffic delivery using eMTCP is evaluated in terms of the energy consumption and traffic throughput on the smartphone on Wi-Fi and LTE. The evaluation of eMTCP performance is based on the condition of one sub-flow for each wireless technology (Wi-Fi/LTE) for simplicity.

4.4.1 eMTCP Energy Models

In this context, LTE and Wi-Fi are used as the wireless radio access technologies for the wireless multi-path data delivery. For each technology, the energy consumption level on the physical channel interface differs with others. Also, the overall energy consumption of the interface changes in different states of the wireless medium. To evaluate the eMTCP solution in terms of energy efficiency on mobile devices, it is necessary to define energy models for different states of wireless medium for LTE and Wi-Fi.

eMTCP makes use of a smartphone-battery-based LTE energy model defined in [102] and a Wi-Fi radio energy model defined in [103] to present the energy consumption levels of the two wireless technologies under various physical channel states during traffic delivery. The following parameters are defined in both energy models:

- *Current Intensity*
- *Voltage*

According to the default settings of both energy models, LTE is more energy-consuming than Wi-Fi in general.

4.4.2 eMTCP Architecture

The block architecture of the proposed eMTCP scheme is illustrated in Figure 4.10,

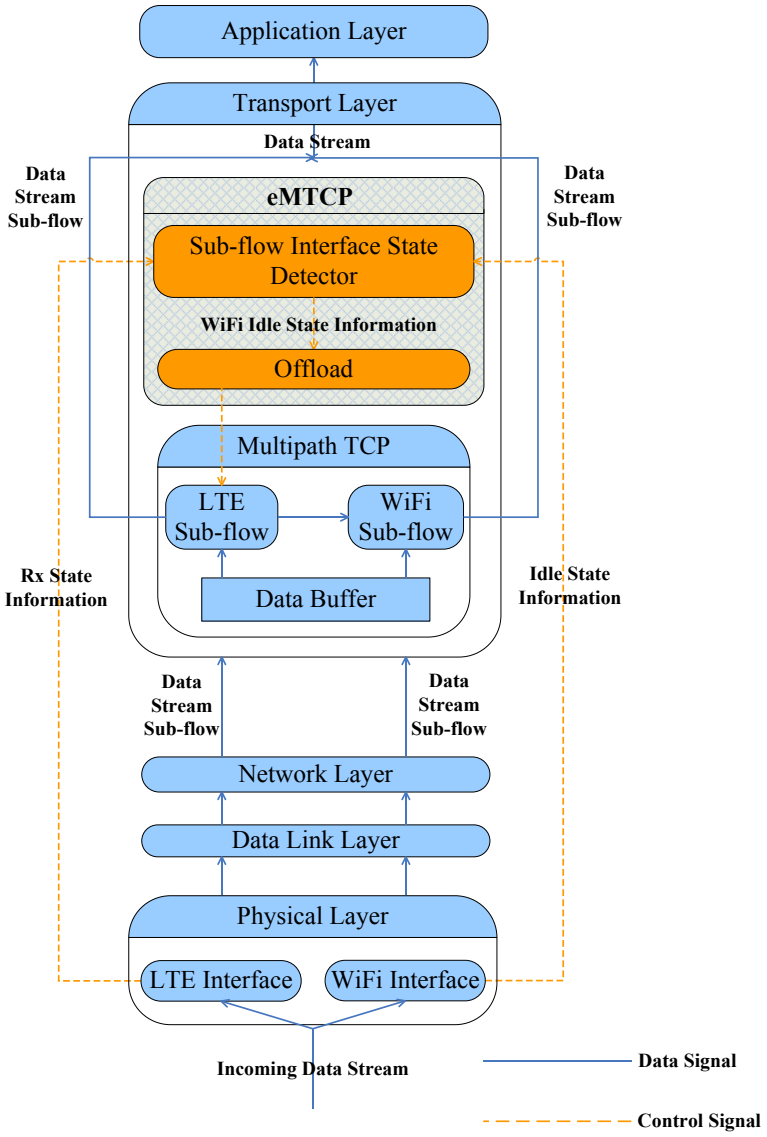

Fig.4.10. Architecture of eMTCP deployed on mobile devices

involving the following two modules deployed at the upper transport layer:

1) ***Sub-flow Interface State Detector (SISD)***: continuously observes the physical channel state of the Wi-Fi and LTE interfaces. These states can be:
   - *Receiving (RX)*: the interface receives data.
   - *Idle*: the interface waits for incoming data (no data is transferred).
2) ***Off-loading Controller***: prepares for off-loading some traffic from the LTE sub-flow to the Wi-Fi sub-flow. The off-loading amount is decided according to the current congestion window size of the LTE sub-flow and the feedback of interface channel state change from SISD.

As shown in Figure 4.10, the traffic flow is obtained from the TCP receive buffer on

the transport layer of the operating system of the smartphone, divided into two MPTCP sub-flows: the Wi-Fi sub-flow and the LTE sub-flow. In MPTCP, traffic data in the TCP receive buffer goes to the two sub-flows in a 50%-50% proportion by default [10]. The basic principle of eMTCP is to adjust the amount of traffic going through both sub-flows using the two modules, based on the channel states of the two interfaces in terms of balance between energy consumption and throughput.

4.4.2.1 Sub-flow Interface State Detector

The Sub-flow Interface State Detector (SISD) module is in charge of observing the physical channel state information for both the Wi-Fi and the LTE radio access interfaces. In general, when the transmission channels are active, the physical channel states of them are divided into the following categories: *transmitting* (*TX*), *receiving* (*RX*) and *idle*, managed by the Carrier Sense / Clear Channel Assessment (CS/CCA) mechanism of the 802.11 state machines [6]. As the smartphone of the user plays the traffic receiver role in the video streaming service, the focus is on the *RX* and *idle* states only.

During the video streaming process, the SISD module deployed at the upper transport layer keeps tracking the physical channel state information for Wi-Fi and LTE sub-flows. The information exchange between the OSI layers is illustrated in Figure 4.11. Once the SISD module senses the *RX* state at the LTE interface and *idle* state at the Wi-Fi interface, indicating that the streamed video traffic is going through the former, it informs the Off-load Controller module that the Wi-Fi interface is available to be used. As a result, the Off-load Controller module takes more traffic data out to the Wi-Fi sub-flow from the TCP receive buffer to reduce the RX period of the LTE interface, achieving energy saving.

4.4.2.2 Off-load Controller

The Off-load Controller module is responsible for the actual traffic data off-loading action from one sub-flow to the other, by making the decision of which sub-flow the current traffic data in the TCP receive buffer goes to. Once there is traffic data in the TCP receive buffer, the Off-load Controller module selects the next active sub-flow based on the physical channel state information sent from the SISD module. In general, the SISD module informs the Off-load Controller module the availability of the Wi-Fi sub-flow more frequently than the LTE sub-flow. As a result, the Off-load Controller selects the Wi-Fi sub-flow and puts traffic data to

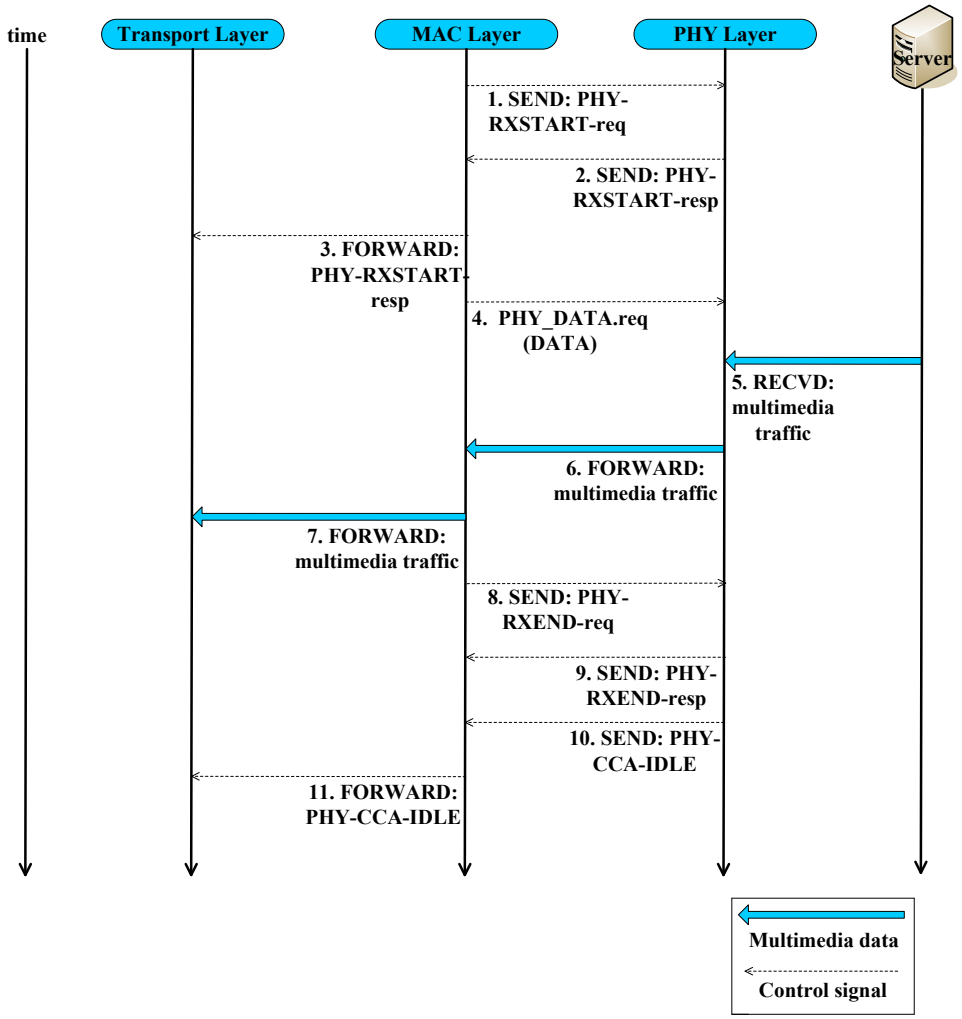

Fig.4.11. Sequence diagram of PHY channel state information exchange in eMTCP

it more frequently than the LTE sub-flow.

The traffic off-loading actions in eMTCP are also related to the status of the MPTCP congestion control mechanism which adaptively makes the decision which sub-flow to use to deliver data stream according to the alteration of the congestion window size. For example, in the case described in the last paragraph, the MPTCP congestion control mechanism decides to stop delivering data traffic to the Wi-Fi sub-flow and switch back to use the LTE sub-flow for containing traffic data when the congestion window size of the Wi-Fi sub-flow is 0. This occurs when the Wi-Fi sub-flow is over-off-loaded by traffic data originally going to the LTE sub-flow, as the congestion window size of the Wi-Fi subflow is much smaller than the LTE sub-flow due to the difference of available bandwidth of these two interfaces.

The UML class diagram in Figure 4.12 illustrates the cooperation of the SISD module

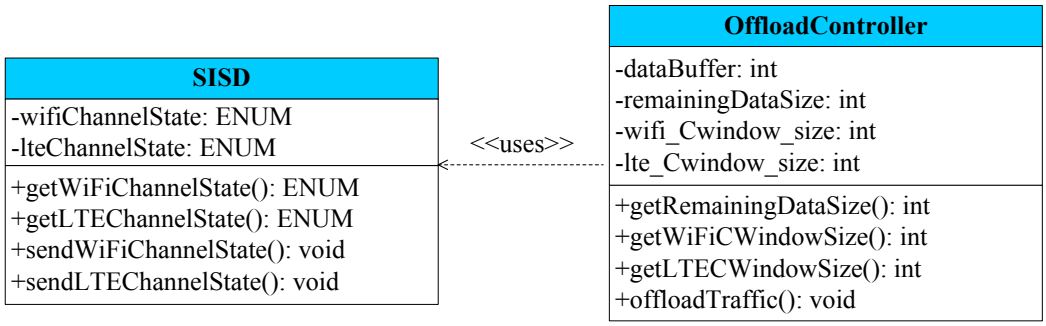

Fig.4.12. UML of classes for eMTCP algorithm implementation

and the Off-load Controller module. As a result, the energy consumption of the smartphone is reduced since more traffic data is carried via the Wi-Fi interface which consumes less energy than the LTE interface in the RX state, while also avoiding congestion in the overall traffic.

4.4.3 eMTCP Algorithm

This section describes the eMTCP algorithm, which uses the following parameters:

1) S_B – size of remaining data in the data buffer at the transport layer.
2) $S_{Wi\text{-}FiW}$ – congestion window size of the Wi-Fi sub-flow.
3) S_{LTEW} –congestion window size of the LTE sub-flow.
4) S – size of data obtained from the TCP receive buffer.
5) $ST_{Wi\text{-}Fi}$ – current channel state of the Wi-Fi interface.
6) ST_{LTE} – current channel state of the LTE interface.

The values of $S_{Wi\text{-}FiW}$ and S_{LTEW} are constant by default, based on the congestion window sizes of Wi-Fi and LTE channels defined in [23] and [32], respectively. The values of the rest parameters are changed during traffic delivery and are instantly updated by the SISD and Off-load Controller module functions.

Using the parameters listed above, the eMTCP data traffic off-loading process works in three steps as follows:

1) When the LTE channel is detected to be receiving traffic, SISD checks whether the Wi-Fi interface is in *idle* state. If so, *SISD* confirms the current availability of the Wi-Fi interface.
2) When the congestion of the Wi-Fi sub-flow is detected (the congestion window size is 0), the algorithm checks if the LTE sub-flow is in congestion as well. If so, the current data reception will be abandoned and the congestion control mechanism

TABLE 4.2 ALGORITHM PSEUDO CODE FOR EMTCP

```
S = 0;
while (1)
{
    if (ST_LTE == RX)
    {
        if (ST_WiFi == IDLE)
        {
            if (S_WiFiW > 0)
            {
                S = min(S_B, S_WiFiW);
                Off-load S amount of data to the WiFi sub-flow;
            }
            else
            {
                if (S_LTEW > 0)
                {
                    S = min(S_B, S_LTEW);
                    Take S amount of data from the TCP receive buffer to the LTE sub-flow;
                }
            }
        }
    }
}
```

will be triggered. If not, it takes the queued data from the TCP receive buffer out to the LTE sub-flow.

3) In step 2), when data traffic is not congested in the Wi-Fi sub-flow, the queued data in the TCP receive buffer is off-loaded from the LTE sub-flow to the Wi-Fi sub-flow.

By using eMTCP, multipath TCP-based delivery can be achieved with higher energy efficiency since the Wi-Fi interface is utilized when possible instead of the LTE interface which is responsible for larger energy consumption.

The pseudo code of eMTCP is presented in Table 4.2.

4.4.4 Overhead and Complexity Analysis

The overhead of eMTCP mainly comes from the physical channel state information for Wi-Fi and LTE sub-flows included in the 802.11 state machines from the PHY layer and used by the SISD module. As the sizes of these information take only a few bits in the packet headers,

the overhead is ignored in this thesis due to the high processing ability of the end user mobile device.

As described in section 4.4.3, the complexity of information collection depends on how many times data is obtained from the TCP receive buffer, which is determined by the size of remaining data in the buffer (S_B) and the amount of obtained data for each time (S). So the complexity of the information collection is $O(S_B/S)$. According to the algorithm, the complexity of traffic off-loading process is calculated as $O(S_B\log(S)/S)$. Therefore, the overall complexity of the eMTCP algorithm is $O(S_B(\log(S)+1)/S)$.

4.5 eMTCP-BT: Traffic-Characteristics-Aware Off-loading Scheme for Heterogeneous Wireless Networks

Recall the scenario described in section 4.1. The user starts a video streaming service from a remote server to his smartphone and uses MPTCP for multi-path data delivery. Unlike MPCP which does not consider energy efficiency during remote data transport, in a similar context, the eMTCP solution proposed and described in section 4.4 introduces a benefit in terms of smartphone energy efficiency. However, as different wireless technologies have different energy consumption rate associated with data transmission, it is important to note the impact on the overall energy efficiency of different traffic off-loading proportions between the multiple sub-flows. For example, in the dual LTE-Wi-Fi network scenario, both off-loading of no traffic (0%) and of all the traffic (100%) from the LTE-sub-flow to the Wi-Fi sub-flow achieve lower energy efficiency in comparison with off-loading some proportion of the data transfer. This is as no data off-loading results in high energy consumption at the LTE interface and off-loading of all the traffic leads to decreased throughput and high congestion. Hence it is essential to identify the suitable traffic off-loading proportion for eMTCP which achieves the highest energy efficiency for the smartphone.

An important factor that impacts the energy efficiency of the smartphone is traffic characteristics. Most of the widely-used mobile applications today are associated with various traffic patterns and have different requirements in terms of the network conditions. For example, video streaming and voice over IP (VoIP) services are sensitive to both delay and jitter and in

general require high bandwidth [104]. Web browsing and data transportation services, on the other hand, have low bandwidth requirements and less influenced by delay. As a result, the energy consumption of the smartphone is affected if the user switches between video streaming and a new application with a different traffic pattern, for instance, to check his emails with the browser. An additional adaptive mechanism is required in this case to augment eMTCP if used on the smartphone, in order to change the optimal traffic off-loading proportion according to the traffic type of the new application.

In this context, a traffic-characteristics-aware off-loading scheme, referred to as eMTCP-BT, is proposed as an extension of the eMTCP solution. eMTCP-BT categorizes of various types of applications on the smartphone according to their traffic patterns, and accordingly applies the best traffic off-loading proportions between sub-f lows in a multi-path data delivery context in a LTE-Wi-Fi heterogeneous network environment to save energy on the smartphone. In eMTCP-BT, four common application traffic types are investigated.

4.5.1 Traffic Burstiness Level Categorization

One of the typical patterns used for distinguishing different types of application traffic is the burstiness level (i.e., the degree of fluctuation in the traffic data rate). The natural burstiness of various types of IP traffic is considered the most important factor that affects the energy consumption of the smartphone, as the wireless network interfaces deployed on the smartphone are active whenever there are packet transmissions and idle if the transmission stops. The unpredictable arrival time of IP packets causes the interfaces to switch frequently from active to idle states, resulting in energy waste.

In this thesis we categorize the applications, based on their burstiness levels, into two classes: high bursty and low bursty, based on the standard terminology provided by IETF RFC 2212[2], IEFT RFC 2215[3] and IETF RFC 3290[4], for describing the behavior of the traffic source. The high bursty traffic data rate varies significantly throughout the transmission. The low bursty traffic data rate fluctuates very little during data exchange. However, both application type and deployed protocols impact traffic burstiness. In this thesis, as the eMTCP-BT solution is based

[2] Specification of Guaranteed Quality of Service - https://tools.ietf.org/rfc/rfc2212.txt

[3] General Characterization Parameters for Integrated Service Network Elements - https://tools.ietf.org/rfc/rfc2215.txt

[4] An Informal Management Model for Diffserv Routers - http://tools.ietf.org/html/rfc3290

on MPTCP, TCP traffic is specifically considered. Each of the two above-mentioned traffic burstiness classes has associated two different application types, respectively.

The high bursty traffic class includes the following application traffic types:

- *VoIP*:
  - Traffic content: voice conversation between multiple human beings
  - Characteristics: data rate varies a lot because of the irregular voice traffic source (the conversation), but in general the rate is low in comparison with the background, as audio data is contained
- *Web browsing*:
  - Traffic content: mixture of multimedia (video/audio) and texts
  - Characteristics: data rate fluctuates much because of the unpredictable content obtained by browser applications, but in general the rate is higher than that of VoIP, as possible multimedia contents with bigger data packet sizes are involved

The low bursty traffic class includes the following application traffic types:

- *Video streaming*:
  - Traffic content: video data packets
  - Characteristics: data packet sizes are relative constant on long term, but may experience short-term fluctuations
- *File downloading*:
  - Traffic content: regular data packets
  - Characteristics: smaller data packet size in comparison with video streaming; low bursty traffic except transitory periods

Generic illustrations of the traffic patterns for these four application types are shown in Figure 4.13 a) b) c) and d).

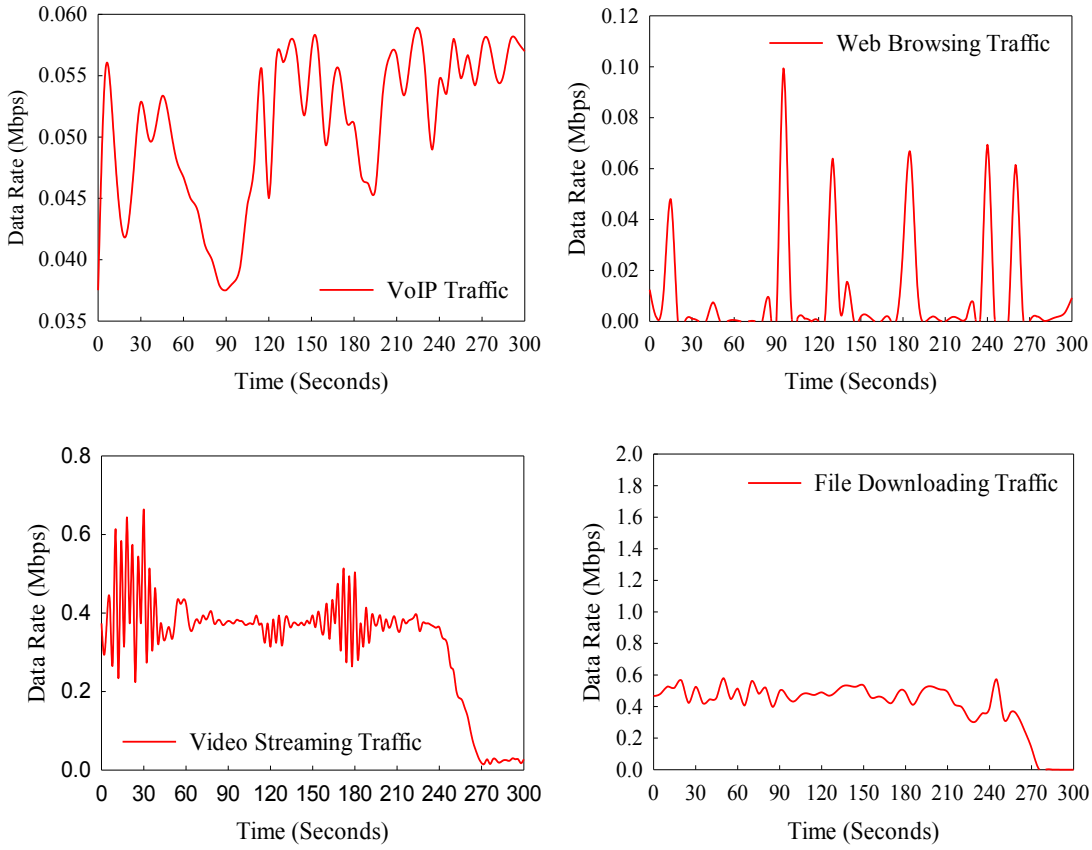

Fig.4.13. Comparative illustration of the traffic profiles for the different application types: a) VoIP; b) Web browsing; c) Video streaming; d) File downloading

4.5.2 eMTCP-BT Architecture

The block architecture of the proposed eMTCP-BT scheme, when considering a dual LTE-Wi-Fi-based heterogeneous network environment, is illustrated in Figure 4.14. The scheme is deployed at the upper transport layer, detecting the application traffic type which is delivered using multiple sub-flows. Each sub-flow is associated with one wireless radio access interface. Figure 4.14 illustrates how the application traffic flow is separated into two sub-flows: LTE and Wi-Fi sub-flows. The application traffic flow is a mix of more than one isolated data streams with different burstiness levels.

A more detailed block architecture of eMTCP-BT is presented in Figure 4.15, which includes the following major modules:

1) ***Traffic Classification***: categorizes the burstiness level (high, low or mix) of the incoming traffic from the TCP receive buffer.

2) ***Sub-flow Interface State Detector (SISD)***: this block has the same functionality as within eMTCP described in section 4.4.2.1.

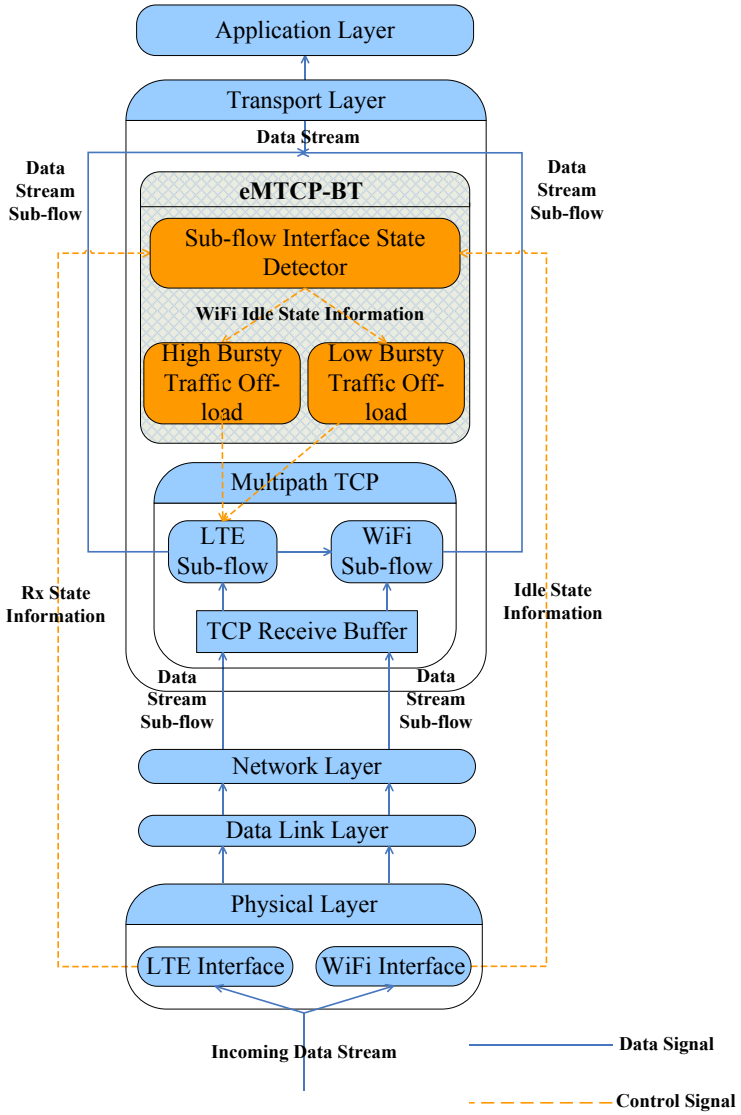

Fig.4.14. Architecture of eMTCP-BT

3) ***Traffic-Burstiness-Aware Off-load Controller*:** prepares for off-loading some traffic from the LTE sub-flow to the Wi-Fi sub-flow. Different with eMTCP, the off-loading amount is decided according to the current congestion window size of the LTE sub-flow, the feedback of interface channel state change from SISD and the burstiness level of traffic classified by the traffic classification module.

4.5.2.1 Traffic Classification

The Traffic Classification module categorizes the incoming data traffic into certain burstiness levels based on their traffic patterns. The traffic patterns used for the module to analyze the traffic burstiness level are included in the data packets. In this context, the following four traffic patterns from the application-layer protocol headers of data packets are chosen for

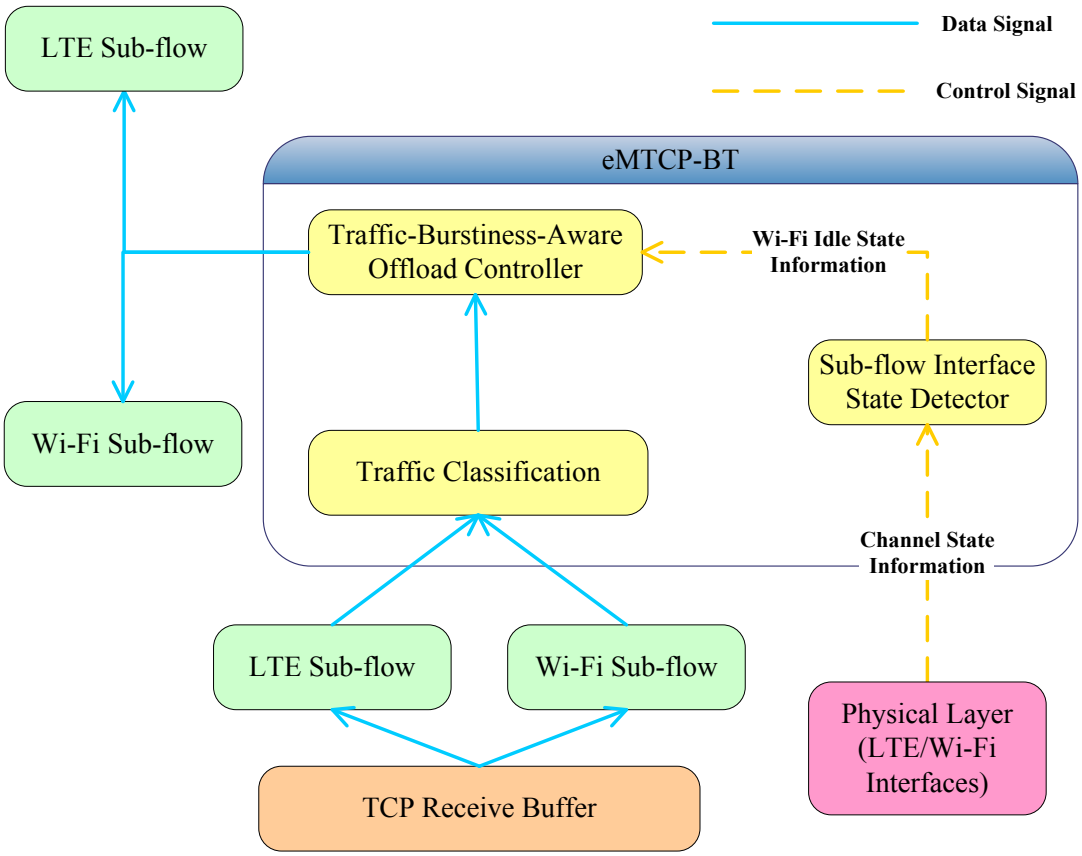

Fig.4.15. eMTCP-BT Modules

burstiness level analysis:

- *Content Type*: this information directly indicates the type of data contained in the packets.
- *Packet Size*: different types of application are usually with different ranges of packet size. For example, the size of packets in video streaming applications is usually larger than in text-based web browsing applications.
- *Sender IP Address*: indicating the source of data packets. This information is especially useful for applications mixing high/low burstiness at the same time, as data packets with the same sender IP address are very likely from the traffic of the same application.
- *Port Number*: in general, each individual application service uses a unique port. Hence the port number of the data packets indicates the type of application.

A Markov-Decision-Process-based mathematical model is integrated for traffic burstiness categorization. The model makes use of decision tree [105] as the core method for traffic pattern classification and prediction, using the four traffic patterns collected from the data packet headers as input data. The details of the MDP-based mathematical model are illustrated in Figure 4.16, involving co-operation of the following sub-modules of the traffic classification module:

- *Traffic Pattern Parsing*: parses the headers of data packets in the incoming application traffic and obtains the traffic patterns.
- *Data Splitting*: groups the parsed traffic patterns into metrics for the mathematical model to analyze.
- *Classification and Regression Tree (CART)* [106]: a non-parametric decision tree algorithm producing classification trees for traffic pattern categorization.

The MDP-related components of the mathematical model are defined as follows:

- Observation of the model
  - The IP address contained in the header of each data packet in the application traffic
  - The size of each data packet in the application traffic

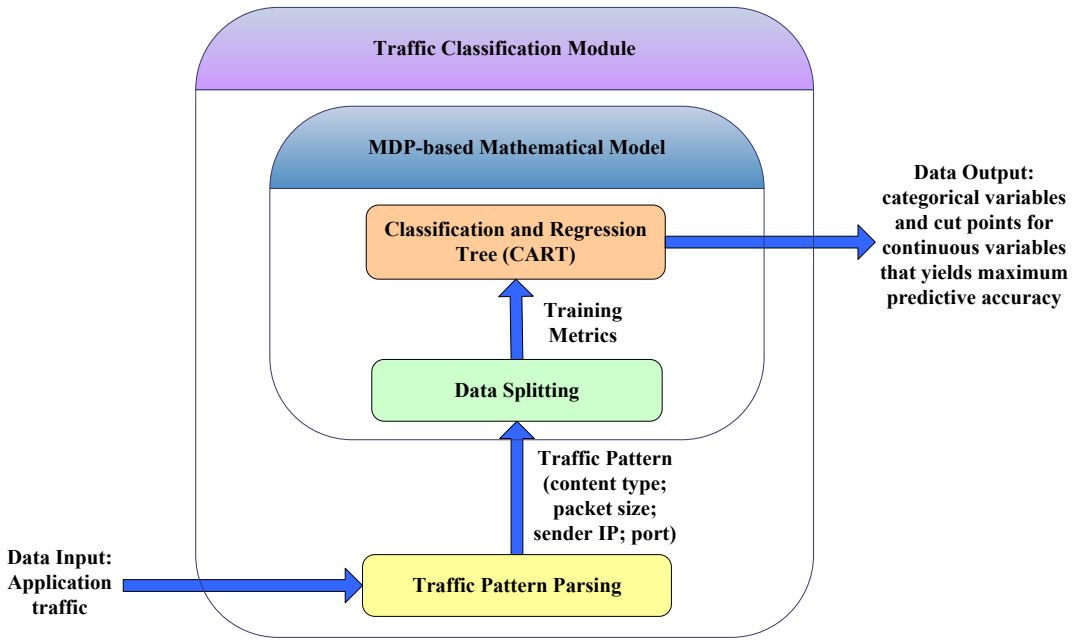

Fig.4.16. MDP-based mathematical model in eMTCP-BT

- The port number contained in the header of each data packet in the application traffic
- The content type of each data packet in the application traffic

- S – a finite set of states s_i, representing the arrival of data packet i, i = 1,2, … n (suppose there are n packets in traffic in total)
- A – a set of the following three types of actions:
  - a_{hi}: classify packet i into high burstiness
  - a_{ai}: classify packet i into average burstiness
  - a_{li}: classify packet i into low burstiness
- R – a reward function $R(s)$ defined as the accuracy of packet classification, with the value between [0, 1]
- P – the policy to specify a function $\pi(s_i)$ to select an action a for state s_i that maximizes the cumulative reward defined in equation (4.8)

$$V^{\pi}(\mathrm{s}) = R\big(s, \pi(s)\big) + E[\textstyle\sum_{t=1}^{\infty} R(s_t, \pi(s_t))] \tag{4.8}$$

The CART algorithm is selected as the key reward function for eMTCP-BT. It uses the Gini impurity metric [106] shown in equation (4.9) for data splitting during the decision tree construction. The Gini impurity metric is a measure of the incorrect labeling frequency of any item randomly chosen from a set of the items according to the distribution of labels in the subset. In this context, the combination of four traffic pattern parameters included in each data packet is considered as the item in the metric. The metric is computed by summing product between the probability of an item to be chosen and the probability of a mistake in categorizing it. A minimum value of 0 indicates that all the items belong to the same category. The resulting value of the metric is averaged to provide a measure of the data splitting quality.

$$I_G(f) = \sum_{i=1}^{m} f_i(1 - f_i) = \sum_{i=1}^{m} (f_i - {f_i}^2) = \sum_{i=1}^{m} f_i - \sum_{i=1}^{m} {f_i}^2$$
$$= 1 - \sum_{i=1}^{m} {f_i}^2 \tag{4.9}$$

In equation (4.9), i takes on values the set $\{1, 2, ..., m\}$ and f_i is the fraction of the items labeled with value i in the set.

The mathematical model evaluates the policy of the packet classification and generates

the classification results (s_i -> a_i). The classification results are sent to the Traffic-Burstiness-Aware Off-load Controller module for optimal off-loading proportion decision. The policy evaluation process is shown in Table 4.3.

In Table 4.3, $P_{ss'}^{a}$ is the possibility of taking action a when transitioning from state s to s'.

TABLE 4.3 POLICY EVALUATION OF THE MDP-BASED MODEL

Input π, the policy to be evaluated
$V^{\pi}(s)$= 0;
Set a gap Δ = 0

```
while (1)
{
    Δ = 0;
    For each s_i ∈ S
    {
        V = V^π(s);
        V^π(s) = ∑_a π(s,a) ∑_s' P^a_ss' [R^a_ss' + V^π(s')];
        Δ = max(Δ, |V - V^π(s)|);
    }
    if (Δ = 0)
        break;
}
```

4.5.2.2 eMTCP-Oriented SISD

The functionality of the SISD module remains the same as already described for eMTCP, involving investigation on the channel state information at the physical layer of the smartphone and notification to the Traffic-Burstiness-Aware Off-load Controller module when the channels are congested.

4.5.2.3 Traffic-Burstiness-Aware Off-load Controller

The Traffic-Burstiness-Aware Off-load Controller module is in charge with changings the off-loading proportion policy according to the traffic burstiness categorization result sent by the Traffic Classification module, apart from considering the congestion nature of the channels and channel state information.

Figure 4.17 illustrates the class diagram of the eMTCP-BT modules, indicating the information exchange between the eMTCP-BT modules.

4.5.3 eMTCP-BT Algorithm

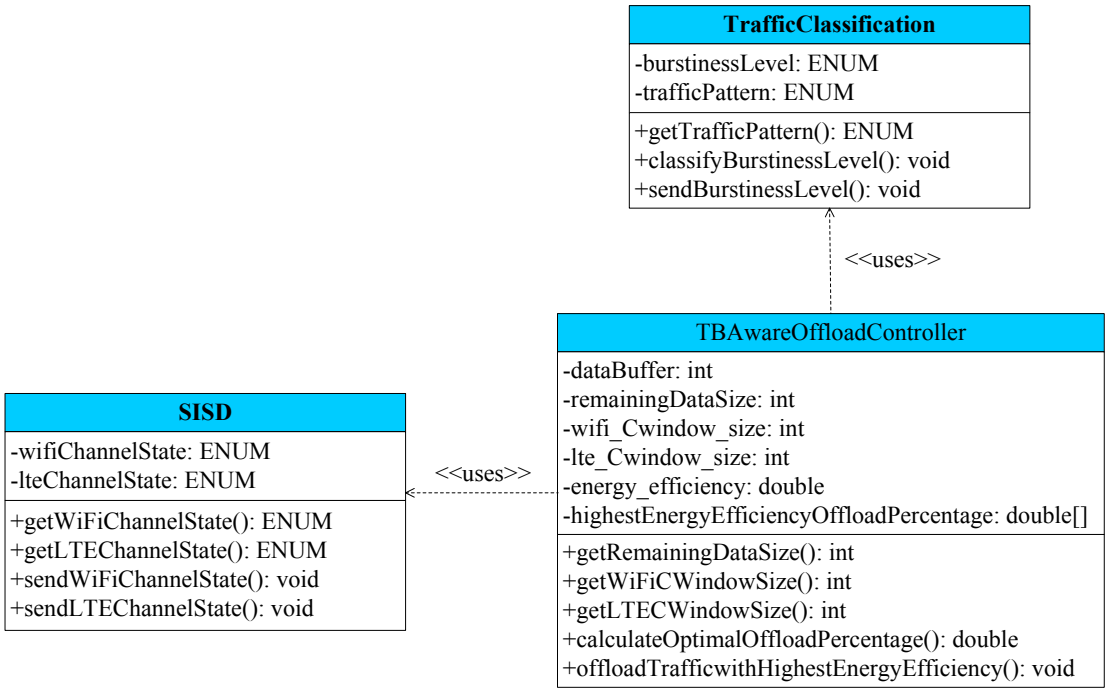

Fig.4.17. UML of classes for eMTCP-BT algorithm implementation

The parameters of eMTCP listed in section 4.4.2 are also used in eMTCP-BT. Meanwhile, eMTCP-BT includes the following extra parameters:

1) X_h – the traffic off-loading percentage with the highest energy efficiency for high bursty traffic.
2) X_l – the traffic off-loading percentage with the highest energy efficiency for low bursty traffic.
3) X_m – the traffic off-loading percentage with the highest energy efficiency for mixed bursty traffic.
4) BL_X – the burstiness level of the current traffic.

The values of X_h, X_l and X_m are determined by picking up the traffic off-loading proportion with the highest energy efficiency, based on measurement with different traffic off-loading proportions from 0% to 100%, for high/low/mixed burstiness level traffic, respectively. The value of BL_X is determined by the MDP-based mathematical model in the Traffic Classification Module.

TABLE 4.4 ALGORITHM FOR EMTCP-BT OFF-LOADING BETWEEN LTE AND WI-FI

```
while (1)
{
    BL_X = getBurstinessLevel();
    if (ST_LTE == RX)
    {
        if (ST_WiFi == IDLE)
        {
            if (S_WiFiW > 0)
            {
                X_h = calculateOptimalOffloadPercentage();
                X_l = calculateOptimalOffloadPercentage();
                X_m = calculateOptimalOffloadPercentage();
                Switch (BLx)
                {
                    case "high bursty":
                        Off-load X_h % data from LTE to Wi-Fi;
                        break;
                    case "low bursty":
                        Off-load X_l % data from LTE to Wi-Fi;
                        break;
                    case "mixed bursty":
                        Off-load X_m % data from LTE to Wi-Fi;
                        break;
                }
            }
            else
            {
                if (S_LTEW > 0)
                {
                    S = min(S_B, S_LTEW);
                    Take S amount of data from the TCP receive buffer to the LTE sub-flow;
                }
            }
        }
    }
}
```

Based on the parameters, the principle of eMTCP-BT is described in Table 4.4. Similar to eMTCP, eMTCP-BT detects the channel states of the LTE and Wi-Fi sub-flows and uses the MPTCP congestion control mechanism to check if either of the sub-flow is congested. When the Wi-Fi channel is idle and not congested, the mixed traffic from multiple applications is off-loaded to it to save energy for the device. However, if the Wi-Fi channel is congested in this

case, transmission continues through the LTE interface to maintain basic QoS level. If both channels are congested, then the transmission is interrupted and the congestion control mechanism is triggered. Based on this mechanism, for incoming application traffic with different burstiness levels (high bursty, low bursty or a mix), eMTCP-BT calculates the energy efficiency it could obtain by using different traffic off-loading percentages from 0% to 100%. It then determines the percentage for which the highest energy efficiency is achieved as the optimal off-loading percentage for the current bursty application type and uses this value.

4.5.4 Overhead and Complexity Analysis

The overhead of eMTCP-BT mainly consists of the following aspects:

- The physical channel state information for Wi-Fi and LTE sub-flows
- The traffic characteristics

Similar with eMTCP, the physical channel state information for Wi-Fi and LTE sub-flows information in eMTCP-BT are included in the 802.11 state machines from the PHY layer and used by the eMTCP-Oriented SISD module. The traffic characteristics are collected from the data packet headers by the Traffic Classification module. As the size of the physical channel state information take only a few bits in the packet headers while the traffic characteristics are transmitted inside the end user mobile device, the overhead is ignored in this thesis due to the high processing ability of the end user mobile device .

As described in section 4.5.3, assuming that there are n types of applications contained in the traffic input, the complexity of traffic classification is $O(n^2)$ according to the CART tree model. The complexity of information collection and traffic off-loading in eMTCP-BT are the same as for eMTCP: $O(S_B/S)$ and $O(S_B\log(S)/S)$. Therefore, the overall complexity of the eMTCP-BT algorithm is $O(n^2+S_B(\log(S)+1)/S)$.

4.6 Chapter Summary

This chapter describes the proposed system architecture, including the architecture, basic principle and detailed algorithm of the following four proposed solutions:

- **AOC-MAC**: an energy-aware mesh device MAC-layer duty-cycle management scheme which adaptively controls the length of duty cycle periods of mesh router in order to make them sleep as long as possible and meanwhile to keep traffic

delivery service quality.

- **E-Mesh**: an advanced routing algorithm which works in correlation with AOC-MAC, establishing the traffic delivery route which best balances the energy consumption, the connectivity and the network traffic load of mesh routers.
- **eMTCP**: an MPTCP-based traffic load balancing scheme for end user mobile devices, which off-loads data from more energy-consuming wireless radio access interfaces to less ones so that the former is less active.
- **eMTCP-BT**: a traffic-characteristics-aware extension of eMTCP , adaptively updating the energy-efficiency-optimal traffic off-loading proportion on the end user mobile devices to "always" ensure the highest energy efficiency for user application usage.

The benefit of the proposed AOC-MAC duty-cycle management scheme and E-Mesh routing algorithm is that energy savings and traffic delivery QoS levels are well-balanced on battery-powered mesh routers with heavy traffic loads so that device maintenance is convenient for network operators of the wireless mesh network. The benefit of the proposed eMTCP multi-path traffic load balancing scheme and its traffic-characteristics-aware extension eMTCP-BT is that high energy efficiency is ensured on end user mobile devices regardless of the type of application running.

CHAPTER 5

Simulation-based Testing: Environment Set-up, Scenarios, Testing Results and Result Analysis

Abstract

This chapter presents the details of simulation-based environment and scenarios for testing and the testing results with analysis of the results for the proposed four solutions presented in chapter 4. Two alternative wireless network topologies were designed for evaluating the performance of the proposed solutions, including a wireless mesh network topology and a MPTCP-based heterogeneous wireless network topology (with LTE and Wi-Fi selected as radio access technologies). The performance of AOC-MAC and E-Mesh was evaluated in terms of energy savings and QoS levels in the wireless mesh network topology. The performance of eMTCP and eMTCP-BT was evaluated in terms of energy efficiency and QoS in the heterogeneous wireless network topology. Several wireless scenarios with different sets of parameters are provided for the testing of each solution. The performances of the proposed solutions for wireless mesh networks are compared with the IEEE 802.11s routing and MAC protocols. The performances of the proposed solutions for multi-path heterogeneous wireless networks are compared with TCP and MPTCP. Meanwhile, the performances of several existing energy-aware research works for wireless network are compared against the corresponding proposed solutions.

5.1 Models - Implementation and Integration

Chapter 4 has introduced the four contributions of this thesis from which benefit either the network operators of the wireless devices or the end user mobile devices. These four contributions are:

(1). **The energy-aware MAC-layer duty-cycle management scheme** (AOC-MAC) which adaptively controls the length of sleep-periods of wireless mesh routers in

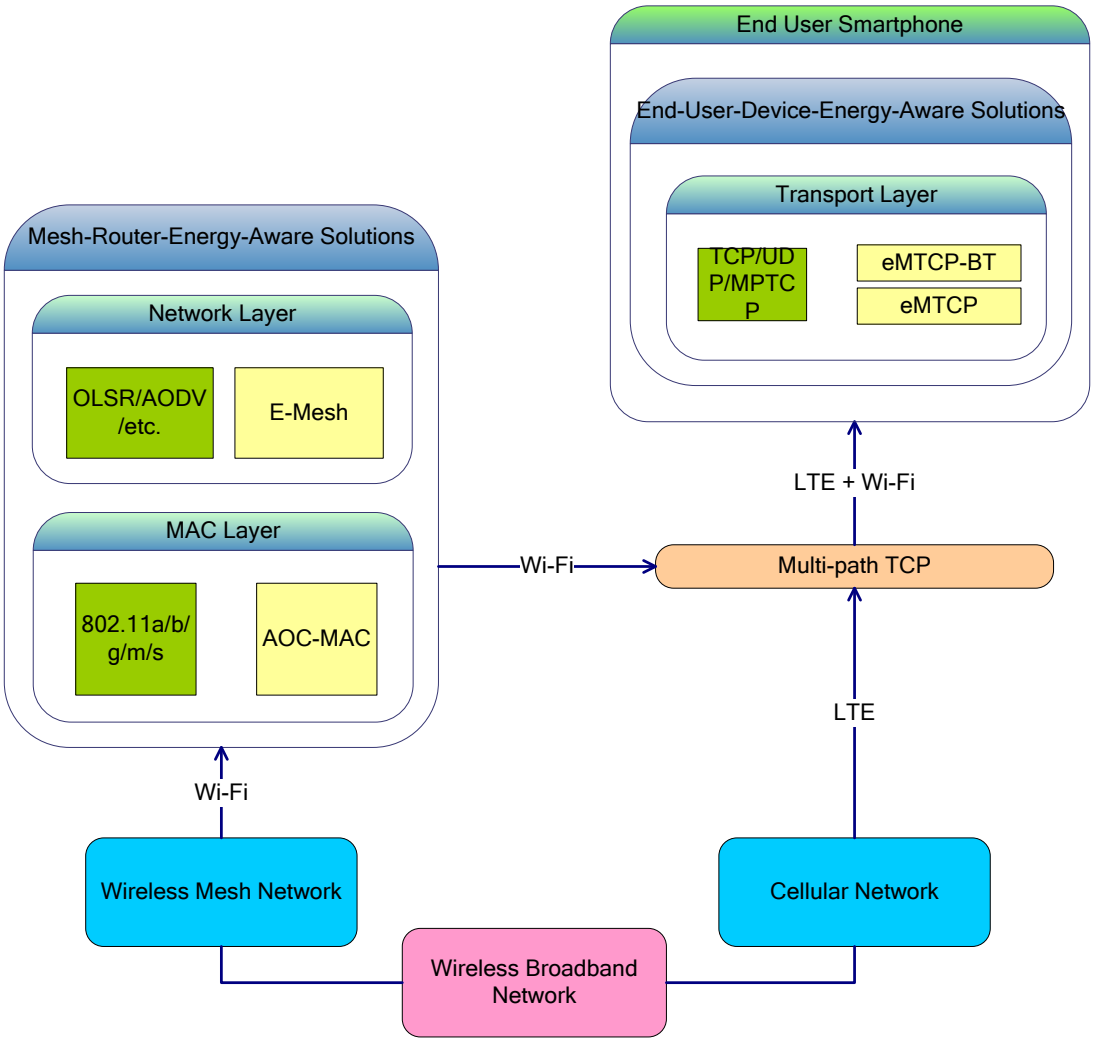

Fig.5.1. Integration of the solutions – layer model

order to reduce the mesh router energy consumption while maintaining network connection stability;

(2). **The energy-load-distance-aware routing algorithm** (E-Mesh) which balances energy consumption, traffic load and connectivity between wireless mesh routers;

(3). **The energy-aware multi-path traffic load balancing scheme** (eMTCP) which makes use of the cumulative bandwidth of multi-path connections and saves energy by off-loading traffic from high-energy-consuming wireless radio access interfaces to low-energy-consuming ones;

(4). **The traffic-characteristics-aware network load balancing scheme** (eMTCP-BT) which determines the optimal traffic off-loading proportion between multiple wireless connections on end user mobile devices according to

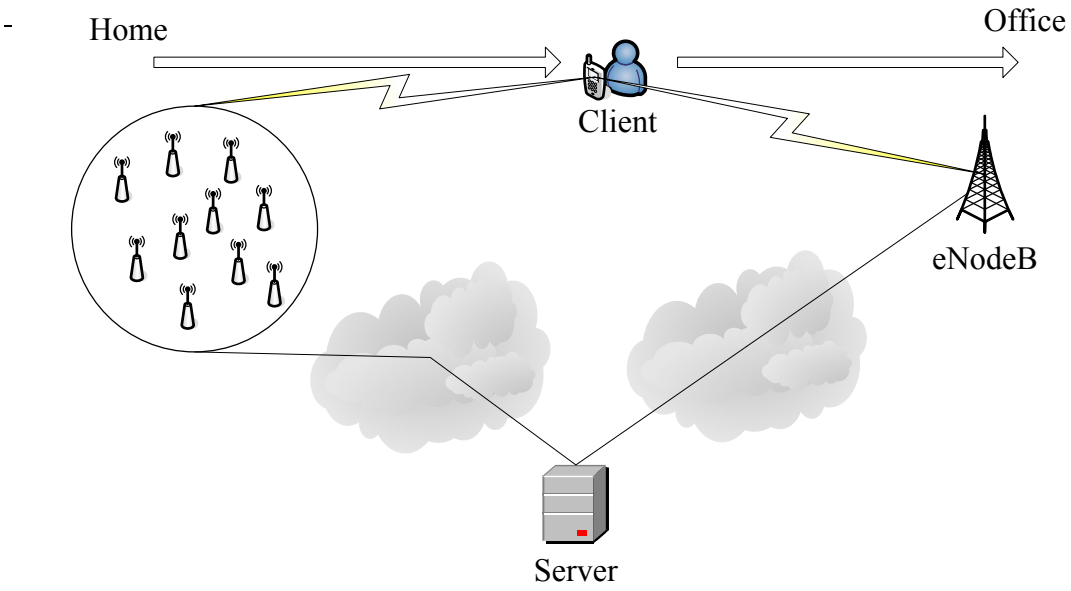

Fig.5.2. The heterogeneous wireless network topology for testing modeling and simulation

the prediction of traffic type, in order to achieve the highest energy efficiency for the mobile devices.

The performance of the four solutions is analyzed by modeling and simulation using Network Simulator 3 (NS-3) [107], which is a discrete-event simulator for different networking systems. NS-3 is open-source and publicly available for research and development.

Figure 5.1 illustrates the deployment of the four solutions. Models of AOC-MAC, E-Mesh, eMTCP and eMTCP-BT have been implemented according to the descriptions in chapter 4. AOC-MAC and E-Mesh are deployed at the level of the mesh routers in the wireless mesh network topology, while eMTCP and eMTCP-BT are implemented at the end user smartphone. Both a Wi-Fi-based wireless mesh network environment and a LTE-Wi-Fi heterogeneous wireless network environment are considered simultaneously to support data delivery to a smartphone, which has both Wi-Fi and LTE interfaces. Classic single-path TCP and MPTCP are used as transport-layer protocols, offering single-path or multi-path functionality support as required in the tests.

5.2 Simulation-based Testing Environment Set-up

The general wireless environment describing the user scenario in Chapter 4 is integrated using NS-3 and validated by the heterogeneous wireless network topology as shown in Figure 5.2. The server node represents the remote server holding the rich-media content,

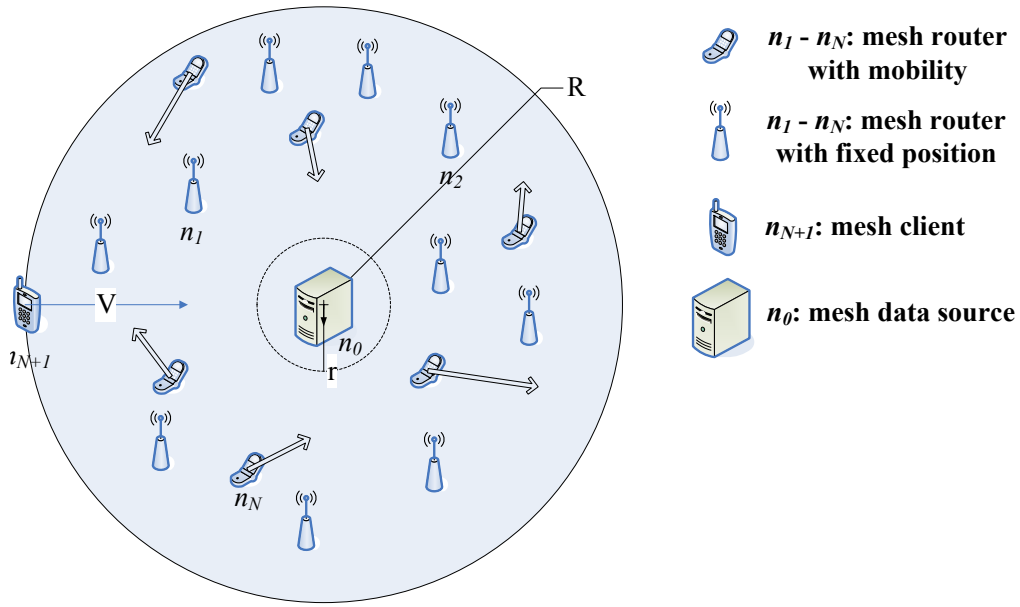

Fig.5.3. Wireless mesh network topology used in AOC-MAC/E-Mesh simulations

acting as data source of the content delivery. The client node represents the smartphone of the user, acting as data sink with mobility during the content delivery.

5.2.1 Set-up for the Wireless Mesh Network Topology

The wireless mesh network topology is illustrated in Figure 5.3. The topology offers the Wi-Fi part of the multi-path connectivity for the smartphone of the user when moving from home to office. It is used for performance evaluation of both AOC-MAC and E-Mesh.

The wireless mesh network topology contains the following components:

- N mesh routers $\{n_1, n_2, \ldots n_N\}$ for data forwarding.
- Two mesh clients n_0 and n_{N+1}, n_0 is used as the user-required video source, i.e., the sender, and n_{N+1} works as the end user device (the smartphone), i.e., the receiver.

The positions of the N mesh routers are randomly distributed in a circular area with radius R.

The YansWiFiPhy channel model [108] implemented in NS-3 is used for the default mesh router physical channel settings in the simulations. This model describes the physical layer based on IEEE 802.11s above 802.11a, with the parameters listed in Table 5.1:

TABLE 5.1 YANSWIFIPHY CHANNEL MODEL PARAMETERS

Symbol	Quantity	Value
EnergyDetectionThreshold	The energy of a received signal should be higher than this threshold to allow the PHY layer to detect the signal	-96 (dBm)
CcaMode1Threshold	The energy of a received signal should be higher than this threshold to allow the PHY layer to declare CCA BUSY state	-99 (dBm)
TxGain	Transmission gain	1 (dB)
RxGain	Reception gain	1 (dB)
TxPowerStart	Minimum available transmission level	16.0206 (dBm)
TxPowerEnd	Maximum available transmission level	16.0206 (dBm)
RxNoiseFigure	Loss in the Signal-to-Noise-Ratio due to non-idealities in the receiver	20 (s)
ChannelSwitchDelay	Delay between two short frames transmitted on different frequencies	0.25 (ms)
Frequency	The operating frequency	2407 (MHz)

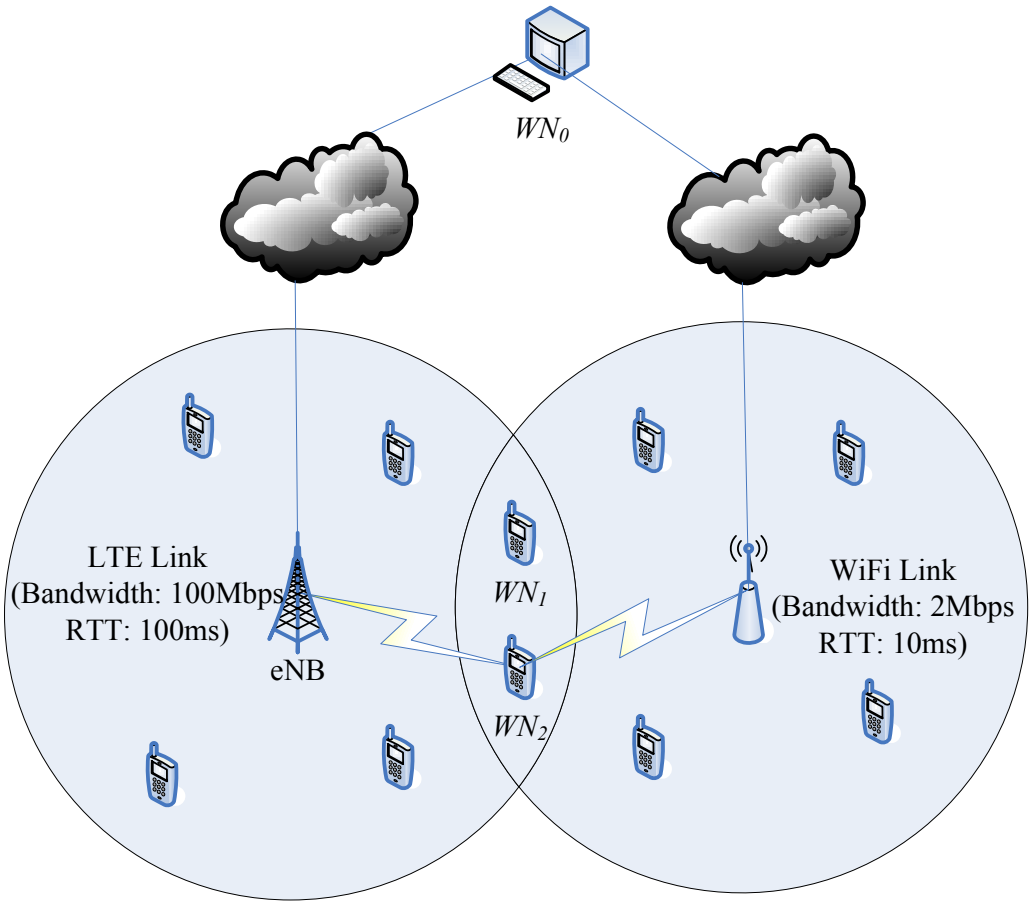

Fig.5.4. Heterogeneous wireless network topology used in eMTCP/eMTCP-BT simulations

5.2.2 Set-up for the Heterogeneous Wireless Network Topology

The heterogeneous wireless network topology is illustrated in Figure 5.4, offering multi-path (Wi-Fi and LTE) connectivity for traffic delivery to the mobile device of the user. This topology is used for performance evaluation of eMTCP and eMTCP-BT. The topology

involves the following components:

- One wireless node WN_0 used as data source.
- N wireless nodes $\{WN_1, WN_2, \ldots WN_N\}$ used as data sinks.
- One wireless node used as eNB node in the LTE network.

Parts of the N data sink nodes are within the signal coverage of the eNB node (the base station in LTE structure) only, while the rest data sink nodes are within the signal coverage of the Wi-Fi access point only. Two data sink nodes WN_1 and WN_2 are deployed in the overlapping area of both LTE and Wi-Fi coverage.

In our study we analyze data transmission performance of a single node (e.g. WN_2) which has both LTE and Wi-Fi connections simultaneously, representing an end user smartphone.

Figure 5.5 shows an updated heterogeneous wireless network topology for eMTCP-BT simulation experiments. This topology involves an additional wireless nodes used as the remote data source (referred to as SRC), and makes use of one of the nodes in the overlapping area as the data sink (referred to as DST) representing the mobile device. As mentioned, the position of the DST node is within the signal coverage of both the LTE and Wi-Fi networks, so that both LTE and Wi-Fi interfaces on the local wireless mobile device could be enabled simultaneously.

The LteSpectrumPhy channel model [109] implemented in NS-3 is used for the default physical channel settings for the LTE link in the eMTCP/eMTCP-BT simulations. This model describes the physical layer of LTE UE devices with a single antenna model instance providing both uplink and downlink connection, with the parameters listed in Table 5.2:

TABLE 5.2 LTESPECTRUMPHY CHANNEL MODEL PARAMETERS

Symbol	Quantity	Value
TxPower	Transmission power	10 (dBm)
NoiseFigure	Loss in the Signal-to-Noise-Ratio due to non-idealities in the receiver	9 (dB)
RsrpSinrSamplePeriod	The sampling period for reporting RSRP-SINR stats	1 (dBm)
RsrqUeMeasThreshold	Reception gain	-1000 (dB)
UeMeasurementsFilterPeriod	Time period for reporting UE measurements, i.e., the length of layer-1 filtering	200 (ms)

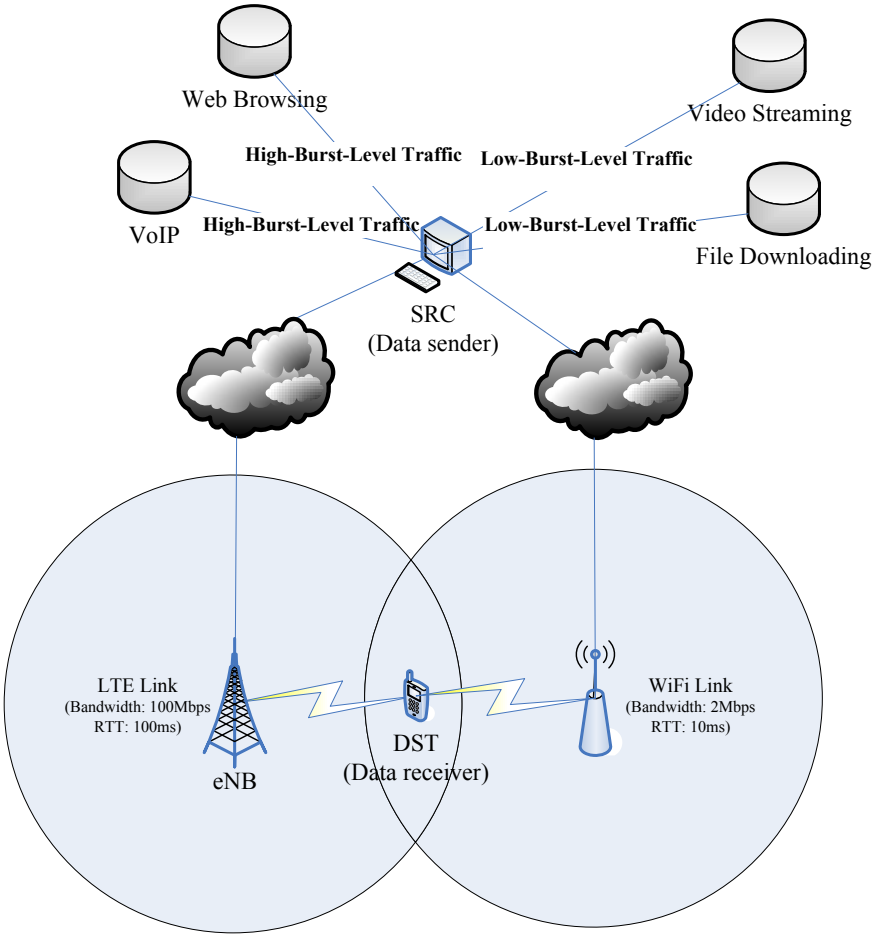

Fig.5.5. Heterogeneous wireless network topology used in eMTCP-BT application traffic simulations

5.3 Testing Overview

Next the simulation scenario settings and the performance analysis based on the test results for the four proposed solutions are described in details. The performance evaluation of the proposed AOC-MAC and E-Mesh solutions is based on the comparison with the classic IEEE 802.11s network mechanism in terms of ***data transmission performance*** (throughput, loss and QoS) and ***energy consumption level***. Data transmission performance of the proposed eMTCP and eMTCP-BT solutions during simulation is measured in terms of the ***remaining energy*** after certain time period (which represents the energy consumption), ***average throughput, energy efficiency*** (ratio between throughput and energy consumption), ***estimated battery lifespan*** and ***user perceived quality***. The performances of the four solutions are also compared against several existing research solutions correspondingly to illustrate the contributions.

5.4 AOC-MAC Testing Scenarios and Performance Analysis

To study the performance of AOC-MAC in wireless mesh networks with variable conditions, separate tests were performed to study the impact of traffic level, number of routers and router mobility. Each scenario included a specific experimental setup based on the topology illustrated in Figure 5.3.

In each scenario, the performance of AOC-MAC was evaluated and compared against the standard IEEE 802.11s MAC protocol and the synchronous duty cycle management scheme S-MAC [50]. The implementation of the IEEE 802.11s MAC protocol was included in the existing modules of NS-3. S-MAC was deployed via implementation in NS-3 using the algorithm described in [50] and involves the following modules:

- Periodic Listen and Sleep: this module provides the router duty cycle scheme with the length of the router sleep period. The duty cycle schedule of each router is broadcasted to its neighbor routers so that duty cycles of neighbor routers are exchanged.
- Collision and Overhearing Avoidance: The contention in the network in controlled by the existing RTS/CTS scheme implemented in NS-3. When the transmission starts, all neighbor routers of both the sender node and the receiver node will sleep after RTS/CTS is heard. The routers remain awake until the transmission of the current packet is over.

The performance of the AOC-MAC duty-cycle management mechanism is evaluated in terms of the following parameters on each mesh router:

- Average energy consumption rate
- QoS parameters such as frame loss rate and end-to-end delay
- Video quality assessment parameters: MSSSIM values

5.4.1 Impact of Traffic Data Rate on AOC-MAC Performance

This test was done in order to investigate the impact of various traffic data rate from the sender node on AOC-MAC performance. Too high data rate which exceeds the standard bandwidth of mesh network devices causes severe data packet drop and decreases QoS. Also,

TABLE 5.3 COMMON PARAMETERS USED IN AOC-MAC TESTING FOR DATA RATE IMPACT INVESTIGATION

Symbol	Quantity	Value
N	Number of mesh routers in the wireless mesh network	20
R	Radius of the circular coverage area of the wireless mesh network	180 (meters)
V	Moving speed of the mesh client n_{N+1}	2 (meters/s)
E	Initial battery energy of each mesh router	100 (Joule)
T	The overall simulation time	200 (s)
t	The SLEEP period of a mesh router	7.5 (s)
T_A	The WAKE-UP period of a mesh router	2.5 (s)
T_D	The period in which the algorithm waits for the increase of *DCount*	20 (s)
TH_{DC}	Threshold value of *DCount*	10

TABLE 5.4VIDEO PARAMETERS IN AOC-MAC TESTING FOR DATA RATE IMPACT INVESTIGATION

Video	Title	Size (Mbytes)	Duration (seconds)	Encoding Codec	Bit Rate (Kbps)	Resolution (pixels×pixels)	Frame Rate (fps)	Color Space
1	Cartoon	25	666	MPEG4	308	352×288	30	YUV
2	The Simpsons	50	399	MPEG4	1026	576×240	25	YUV
3	Jurassic Park	137.5	841	MPEG4	2000	1920×1040	23.976	YUV
4	Back to the future	250	1529	MPEG4	1339	1280×720	23.976	YUV

too high data rate indicates too frequent data transmission in the mesh network and the mesh routers are obliged to stay wake-up longer, which increases energy consumption.

As indicated in section 5.2.1, each mesh router in the network can be deployed with static position or with mobility. In this test, each mesh router was allocated with a **uniformly distributed** random mobility. At the initialization of the mesh network topology, each mesh router pauses for a random time value between [0, 2] (seconds) and chooses a random direction value between [0, 2π] and then moves with a random speed value between [1.0, 2.0] (m/s) towards this direction until it reaches the boundary of the mesh network with range R, as shown in Figure 5.3. When each mesh router reaches the boundary, it pauses again with a new random time between [0, 2] (seconds) and repeats the process above. The mesh client n_{N+1} moves with a constant speed 2.0 m/s from at the boundary towards the center of the wireless mesh network circular area where the mesh client n_0 is located and fixed.

Test was initialized with the parameters listed in Table 5.3.

The impact of four different data rates: 1) 1.0 Mbps; 2) 2.0 Mbps; 3) 5.5 Mbps and 4) 10.0 Mbps were investigated in this test, involving four corresponding test videos used for transmission with the corresponding parameters listed in Table 5.4, respectively.

In simulations the videos were transmitted using an extension of the EvalVid model [110], a tool-set used for measuring video quality during transmission through real-time or simulation networks. In order to avoid unnecessary ICMP traffic during transmission, EvalVid obtains video information by parsing the trace file of the video frames which are generated by the mp4trace tool inside. After transmission, QoS parameters such as frame loss rate, end-to-end delay, cumulative jitter and several video quality measurement matrices are generated as output for user-perceived video quality evaluation.

The estimation and measurement results of the data rate impact study are shown in Figure 5.6, Figure 5.7, Figure 5.8 and Figure 5.9 and further illustrated in Table 5.5. As shown in Figure 5.6, the energy consumption rates of the IEEE 802.11s MAC protocol, S-MAC and AOC-MAC on mesh routers increase along with the increase of traffic data rate, as higher data

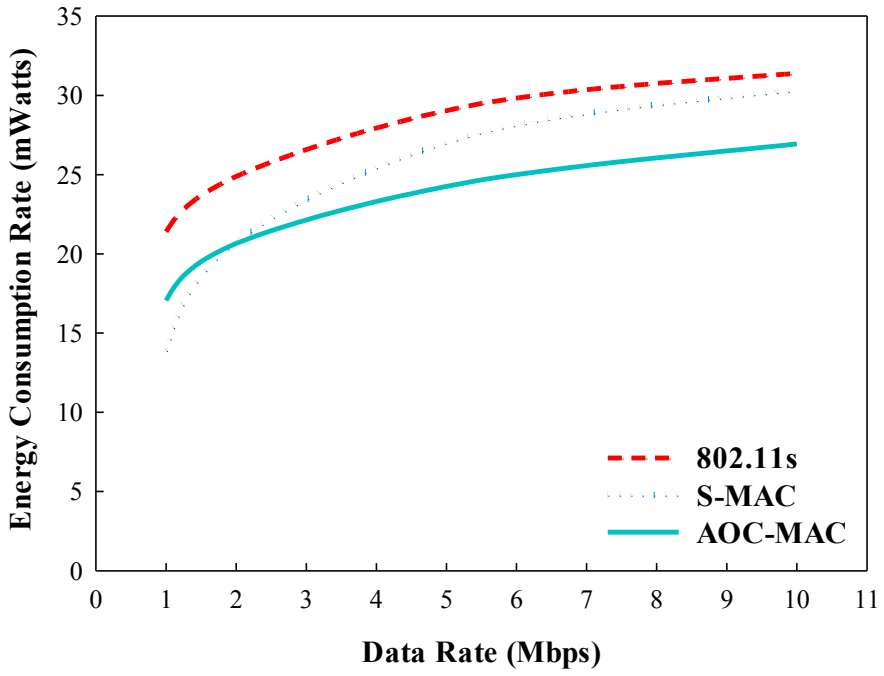

Fig.5.6. Energy consumption rates of 802.11s, S-MAC and AOC-MAC with variable data rates

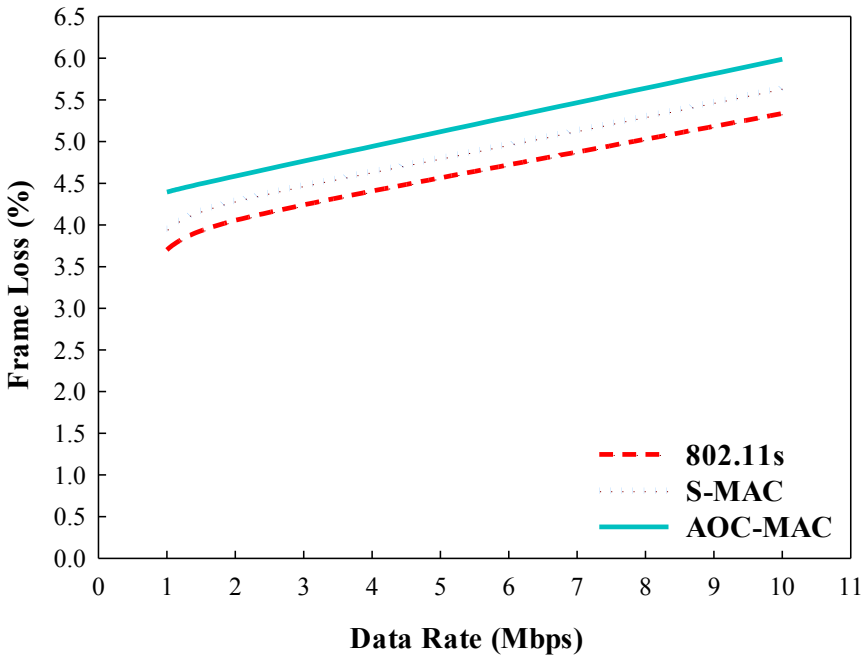

Fig.5.7. Frame loss rates of 802.11s, S-MAC and AOC-MAC with variable data rates

rate leads to more frequent transmissions and less sleep-period of mesh routers. With 1-Mbps data rate, AOC-MAC has obtained 20.23% decrease of energy consumption rate in comparison with the IEEE 802.11s MAC protocol, but the energy saving benefit is 18.63% less than S-MAC. With 2-Mbps data rate, AOC-MAC has obtained 17.03% and 5.44 % energy savings on mesh routers in comparison with the IEEE 802.11s MAC protocol and S-MAC, respectively. In this case the energy savings of AOC-MAC has started to overcome S-MAC, but the energy saving levels of the two solutions are approximately the same. With 5.5-Mbps data rate, the energy saving of AOC-MAC is approximately 16.37% in comparison with the IEEE 802.11s MAC protocol and 10.81% in comparison with S-MAC. With 10-Mbps data rate, AOC-MAC saves 14.2% more energy than the IEEE 802.11s MAC protocol and 11.18% than S-MAC. It is clear that in data transmission scenarios with low data rate, AOC-MAC provides energy saving benefit compared against the IEEE 802.11s MAC protocol, but the performance of S-MAC in terms of energy savings is better. However, the energy saving benefit of S-MAC shrinks severely in data transmission scenarios with high data rate, while AOC-MAC saves more energy.

As shown in Figure 5.7, the frame loss rates of the IEEE 802.11s MAC protocol, S-MAC and AOC-MAC increase along with the increase of traffic data rate, as higher data rate

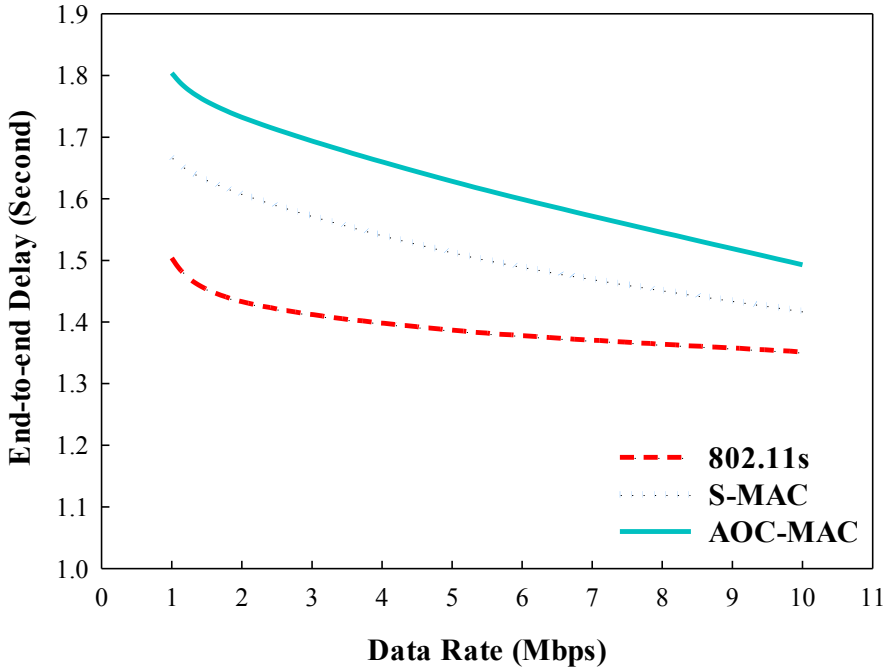

Fig.5.8. End-to-end delays of 802.11s, S-MAC and AOC-MAC with variable data rates

causes higher chances for data packet collisions and drops during traffic delivery. With 1-Mbps data rate, the average frame loss rate of AOC-MAC has increased to approximately 4.4% in comparison with the 3.7% rate of the IEEE 802.11s MAC protocol and the 3.95% rate of S-MAC. With 2-Mbps data rate, AOC-MAC has obtained 4.58% average frame loss rate in comparison with the 4.06% rate of IEEE 802.11s MAC protocol and the 4.293% rate of S-MAC, respectively. With 5.5-Mbps data rate, the average frame loss rate of AOC-MAC has increased to approximately 5.21% in comparison with the 4.65% rate of the IEEE 802.11s MAC protocol and the 4.89% rate of S-MAC. With 10-Mbps data rate, AOC-MAC has obtained 5.99% average frame loss rate in comparison with the 5.34% rate of IEEE 802.11s MAC protocol and the 5.64% rate of S-MAC, respectively. Although AOC-MAC increases the frame loss rate in comparison with the IEEE 802.11s MAC protocol and S-MAC, the value remains at a normal level for wireless communications.

Figure 5.8 illustrates the changes of end-to-end delay of the three MAC schemes, which decrease along with the increase of traffic data rate, as higher data rate indicates shorter sleep-periods of mesh routers which result in lower latency. With 1-Mbps data rate, the average end-to-end delay of AOC-MAC has experienced approximately 19.7% and 8.22% increase in comparison with the IEEE 802.11s MAC protocol and S-MAC, respectively. With 2-Mbps data

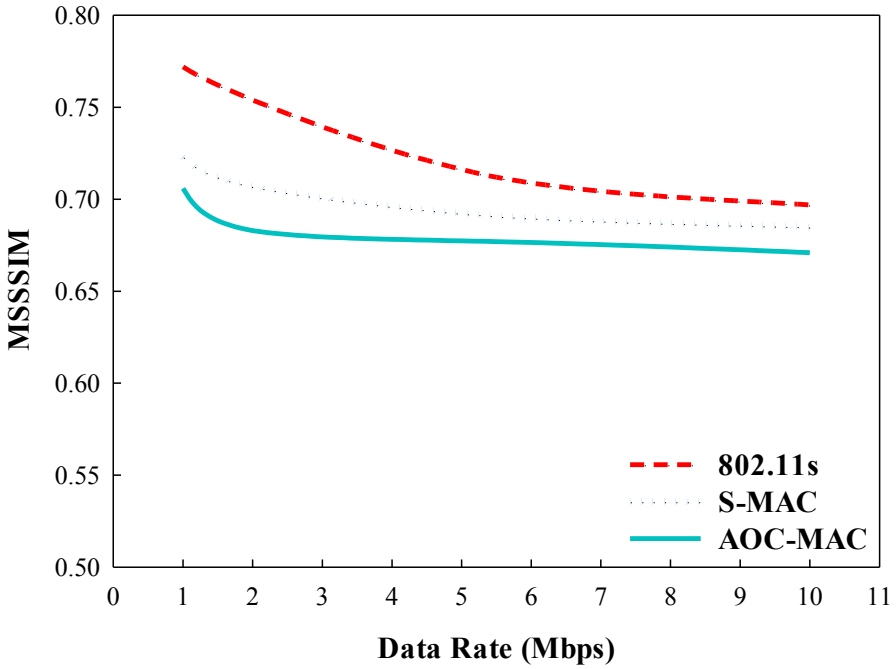

Fig.5.9.MSSSIM values of 802.11s, S-MAC and AOC-MAC with variable data rates

rate, AOC-MAC has experienced 20.87% and 7.7% increase of end-to-end delay in comparison with the IEEE 802.11s MAC protocol and S-MAC, respectively. With 5.5-Mbps data rate, the average end-to-end delay of AOC-MAC has experienced approximately 16.78% and 7.47% increase in comparison with the IEEE 802.11s MAC protocol and S-MAC, respectively. With 10-Mbps data rate, AOC-MAC has experienced 10.49% and 5.27% increase of average end-to-end delay in comparison with the IEEE 802.11s MAC protocol and S-MAC, respectively. It is clear that when the traffic data rate increases, the values of end-to-end delay of the three MAC schemes become closer. As the sleep-periods of mesh routers are decreased, the effect on delay is less obvious.

The video quality is estimated in terms of the Multi-scale Structural Similarity (MSSSIM) metric [44], measured by using the MSU video quality measurement tool [111]. As shown in Figure 5.9, the MSSSIM values of the IEEE 802.11s MAC protocol, S-MAC and AOC-MAC decrease along with the increase of traffic data rate. With 1-Mbps data rate, the average MSSSIM value of AOC-MAC has experienced approximately 8.55% decrease in comparison with the IEEE 802.11s MAC protocol, and approximately 2.35% decrease in comparison with S-MAC. With 2-Mbps data rate, AOC-MAC has experienced 9.42% and 3.4% decrease of the average MSSSIM value in comparison with the IEEE 802.11s MAC protocol

TABLE 5.5 EFFECT OF TRAFFIC DATA RATE ON AOC-MAC PERFORMANCE

Average Value		802.11s	S-MAC	AOC-MAC
Energy Consumption (mWatts)	Data Rate: 1 Mbps	21.4	13.89	17.07
	Data Rate: 2 Mbps	24.9	20.79	19.66
	Data Rate: 5.5 Mbps	29.5	27.66	24.67
	Data Rate: 10 Mbps	31.4	30.33	26.94
Frame Loss (%)	Data Rate: 1 Mbps	3.702	3.954	4.395
	Data Rate: 2 Mbps	4.057	4.293	4.586
	Data Rate: 5.5 Mbps	4.645	4.887	5.206
	Data Rate: 10 Mbps	5.338	5.644	5.987
End-to-end Delay (Seconds)	Data Rate: 1 Mbps	1.50	1.67	1.80
	Data Rate: 2 Mbps	1.43	1.61	1.73
	Data Rate: 5.5 Mbps	1.38	1.50	1.61
	Data Rate: 10 Mbps	1.35	1.42	1.49
MSSSIM	Data Rate: 1 Mbps	0.772	0.723	0.706
	Data Rate: 2 Mbps	0.754	0.707	0.683
	Data Rate: 5.5 Mbps	0.712	0.691	0.677
	Data Rate: 10 Mbps	0.697	0.685	0.671

and S-MAC, respectively. With 5.5-Mbps data rate, the average MSSSIM value of AOC-MAC has experienced approximately 4.92% decrease in comparison with the IEEE 802.11s MAC protocol, and approximately 2.03% decrease in comparison with S-MAC. With 10-Mbps data rate, AOC-MAC has experienced 3.73% and 2.04% decrease of the average MSSSIM value in comparison with the IEEE 802.11s MAC protocol and S-MAC, respectively. It is illustrated in Figure 5.8 that the decrease of data transmission QoS in terms of MSSSIM value is less obvious when the data rate is higher.

Test results indicate that both the energy saving benefit of AOC-MAC and the sacrifice of QoS (frame loss, delay, MSSSIM) are less obvious with higher traffic data rate, in comparison with the IEEE 802.11s MAC protocol and S-MAC, but in general the energy saving benefit overcomes the QoS decrease, regardless of the traffic data rate.

5.4.2 Impact of Number of Mesh Routers on AOC-MAC Performance

This test was done in order to investigate how different numbers of mesh routers included in the network affect AOC-MAC performance. The settings of mesh router mobility used in section 5.4.1 were used in this test. The traffic data rate was set to 2.0 Mbps and the video number 2 in Table 5.4 was selected as the corresponding source video. The number of mesh

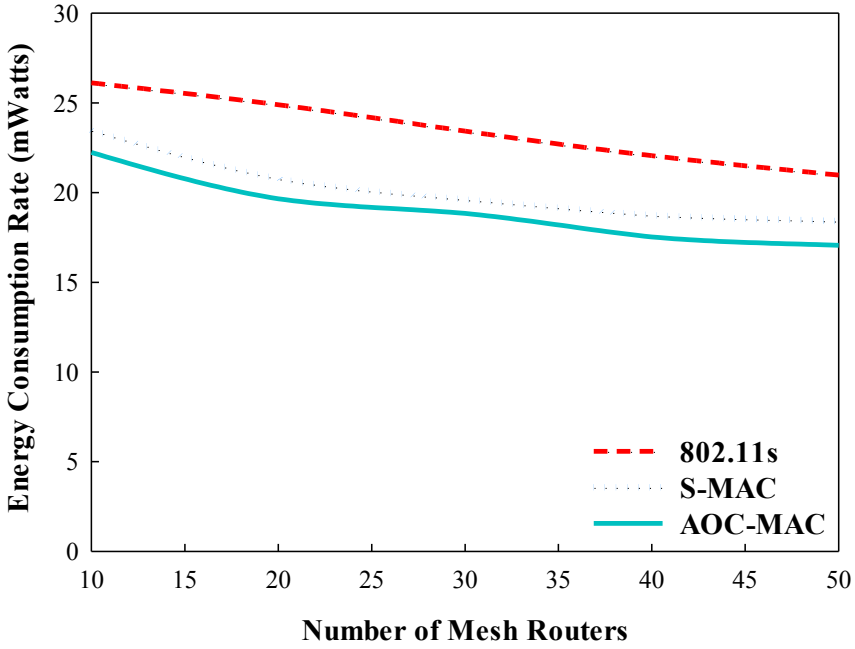

Fig.5.10. Energy consumption rates of 802.11s, S-MAC and AOC-MAC with variable router numbers

routers was varied from 10 to 50 with a step of 10 mesh routers in each test. The rest settings related to the mesh network topology remained the same as shown in Table 5.1.

The estimation and measurement results of the data rate impact study are shown in Figure 5.10, Figure 5.11, Figure 5.12 and Figure 5.13 and further illustrated in Table 5.6. As shown in Figure 5.10, the energy consumption rates of the IEEE 802.11s MAC protocol, S-MAC and AOC-MAC on mesh routers decrease along with the increase of number of mesh routers, as less mesh routers require each mesh router to stay in the wake-up state longer to maintain wireless connectivity. With 10 mesh routers, AOC-MAC has obtained 14.85% decrease of energy consumption rate in comparison with the IEEE 802.11s MAC protocol, and 5.28% decrease of energy consumption rate in comparison with S-MAC. With 20 mesh routers, AOC-MAC obtains 21.04% and 5.44% energy savings in comparison with the IEEE 802.11s MAC protocol and S-MAC, respectively. With 30 mesh routers, AOC-MAC saves approximately 19.59% and 3.97% more energy in comparison with the IEEE 802.11s MAC protocol and S-MAC, respectively. With 40 mesh routers, AOC-MAC provides 20.53% and 6.51% energy savings in comparison with the IEEE 802.11s MAC protocol and S-MAC, respectively. With 50 mesh routers, the energy saving of AOC-MAC is approximately 18.64%

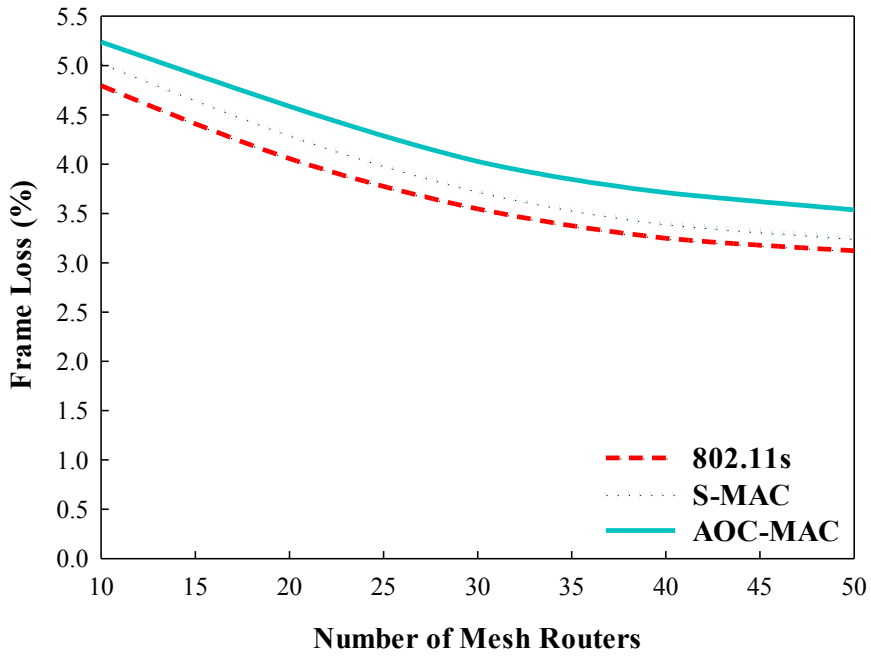

Fig.5.11. Frame loss rates of 802.11s, S-MAC and AOC-MAC with variable mesh router numbers

and 7.33% in comparison with the IEEE 802.11s MAC protocol and S-MAC, respectively.

As shown in Figure 5.11, the frame loss rates of the IEEE 802.11s MAC protocol, S-MAC and AOC-MAC decrease along with the increase of number of mesh routers, as less mesh routers with mobility cause in more unstable wireless connectivity and higher chance of packet drop. With 10 mesh routers, the average frame loss rate of AOC-MAC has increased to approximately 5.24% in comparison with the 4.8% rate of the IEEE 802.11s MAC protocol and the 5.03% rate of S-MAC. With 20 mesh routers, AOC-MAC has obtained 4.58% average frame loss rates in comparison with the 4.06% average frame loss rate of IEEE 802.11s MAC protocol and the 4.293% rate of S-MAC. With 30 mesh routers, the average frame loss rate of AOC-MAC has increased to approximately 4.03% in comparison with the 3.55% rate of the IEEE 802.11s MAC protocol and the 3.73% rate of S-MAC. With 40 mesh routers, AOC-MAC has obtained 3.72% average frame loss rates in comparison with the 3.25% average frame loss rate of IEEE 802.11s MAC protocol and the 3.4% rate of S-MAC. With 50 mesh routers, the average frame loss rate of AOC-MAC has increased to approximately 3.54% in comparison with the 3.12% average frame loss rate of the IEEE 802.11s MAC protocol and the 3.25% rate of S-MAC. It is illustrated in Figure 5.11 that with the increase of the number of mesh routers,

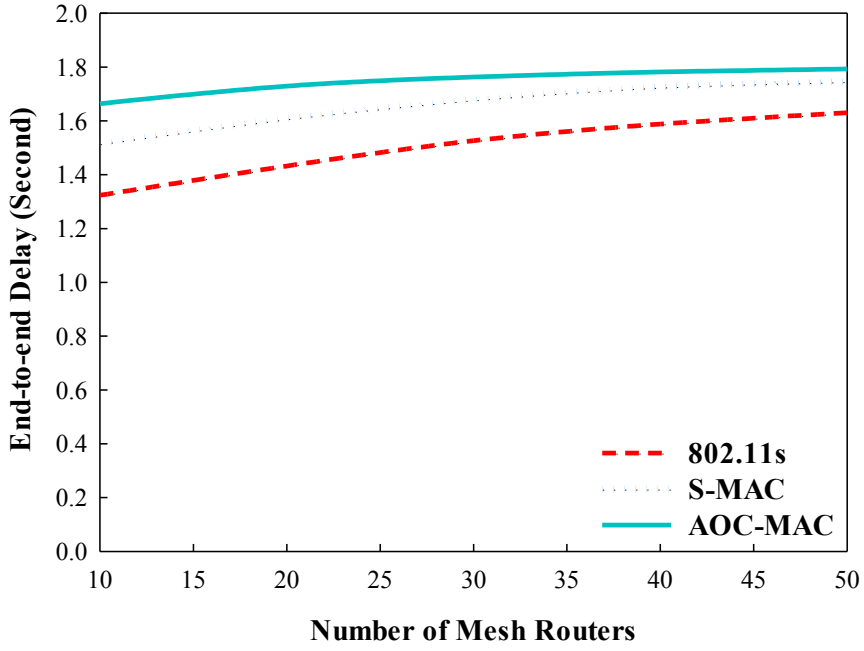

Fig.5.12. End-to-end delays of 802.11s, S-MAC and AOC-MAC with variable mesh router numbers

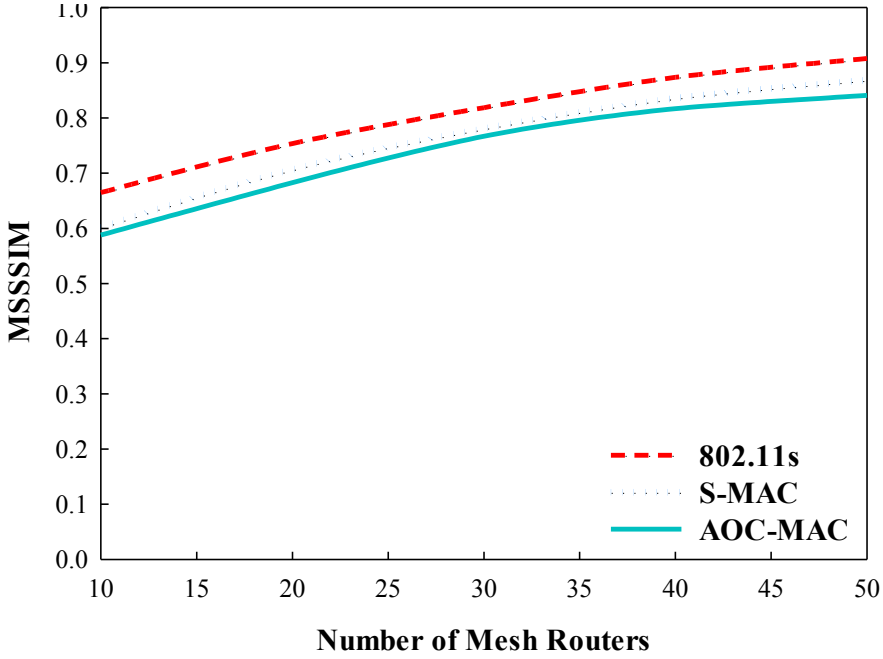

Fig.5.13.MSSSIM values of 802.11s, S-MAC and AOC-MAC with variable mesh router numbers

the frame loss rates of the three MAC schemes tend to be closer.

Figure 5.12 illustrates the changes of end-to-end delay of the three MAC schemes, which increase along with the increase of the number of mesh routers, but in general remain in a stable level. More mesh routers in the network indicate longer sleep-periods of each mesh router,

TABLE 5.6 EFFECT OF MESH ROUTER NUMBERS ON AOC-MAC PERFORMANCE

Average Value		802.11s	S-MAC	AOC-MAC
Energy Consumption (mWatts)	10 Mesh Routers	26.12	23.48	22.24
	20 Mesh Routers	24.9	20.79	19.66
	30 Mesh Routers	23.43	19.62	18.84
	40 Mesh Routers	22.06	18.75	17.53
	50 Mesh Routers	20.98	18.42	17.07
Frame Loss (%)	10 Mesh Routers	4.796	5.025	5.238
	20 Mesh Routers	4.057	4.293	4.586
	30 Mesh Routers	3.547	3.725	4.028
	40 Mesh Routers	3.249	3.396	3.712
	50 Mesh Routers	3.122	3.247	3.537
End-to-end Delay (Seconds)	10 Mesh Routers	1.324	1.516	1.664
	20 Mesh Routers	1.433	1.608	1.729
	30 Mesh Routers	1.527	1.679	1.763
	40 Mesh Routers	1.589	1.726	1.782
	50 Mesh Routers	1.631	1.747	1.793
MSSSIM	10 Mesh Routers	0.665	0.602	0.588
	20 Mesh Routers	0.754	0.707	0.683
	30 Mesh Routers	0.819	0.781	0.767
	40 Mesh Routers	0.874	0.836	0.817
	50 Mesh Routers	0.908	0.869	0.841

which causes extra latency. The MSSSIM values of the IEEE 802.11s MAC protocol, S-MAC and AOC-MAC are shown in Figure 5.13, in which the MSSSIM values increase along with the increase of traffic data rate, but in general remain in a stable level. The results in Figure 5.13 indicate that although AOC-MAC results in slight QoS decrease in comparison with the 802.11s MAC protocol (which does not overcome the energy saving benefit), it ensures similar quality level with S-MAC regardless of the number of mesh routers.

5.4.3 Impact of Mesh Router Mobility on AOC-MAC Performance

This test was done in order to investigate the impact of mesh router mobility on AOC-MAC performance. Different mobility settings of mesh routers result in different network structures in different periods, in which the condition of traffic delivery changes and the sleep/wake-up periods of mesh router change accordingly, affecting the throughput during traffic delivery and the energy consumption of mesh routers.

Two mesh router mobility test cases were introduced in this test, involving the mesh nodes illustrated in Figure 5.3:

- *Case 1*: All the N mesh routers $\{n_1, n_2, \ldots n_N\}$ were allocated with fixed positions, which were uniformly distributed in the range of [0, 2π] with in the circular area. The position of mesh client n_0 was at the center of the circular area, remaining fixed. The mesh client n_{N+1} was moving from the boundary of the circular area towards n0, with a constant speed 2.0 m/s.
- *Case 2*: The mesh routers were allocated with the mobility parameters described in section 5.4.1, starting from a random pause period between [0, 2] (seconds) and continuing to move with a random direction value between [0, 2π] and a random speed value between [1.0, 2.0] (m/s) towards this direction until it reaches the boundary of the mesh network with range R, as shown in Figure 5.3. The mesh client n_{N+1} was allocated with a constant speed 2.0 m/s from at the boundary towards the mesh client n_0 located and fixed at the center of the circular area.

In this test, the traffic data rate was set to 2.0 Mbps and the video sequence 2 in Table 5.2 was selected as the corresponding source video. The number of mesh routers was set to 20. The rest settings related to the mesh network topology remained the same as shown in Table 5.3.

The estimation and measurement results of the data rate impact study are shown in Table 5.7 in terms of the average value of the results and the standard deviation of the QoS parameters:

- *Energy consumption*: In case 1 when the mesh routers are static, the energy savings of AOC-MAC in comparison with the IEEE 802.11s and S-MAC are approximately 21.56% and 4.76%, respectively. In case 2 when the mesh routers are randomly moving, the energy savings of AOC-MAC in comparison with the IEEE 802.11s is approximately 17.03%, while the energy consumption rates of AOC-MAC and S-MAC are approximately the same. The average energy consumption rate of AOC-MAC in case 1 is 8.95% lower than in case 2.

TABLE 5.7 EFFECT OF MESH ROUTER MOBILITY ON AOC-MAC PERFORMANCE

Average Values	Case 1			Case 2		
	802.11s	S-MAC	AOC-MAC	802.11s	S-MAC	AOC-MAC
Energy Consumption (mWatts)	23.98	19.75	18.81	24.9	20.79	20.66
Frame Loss (%)	2.984	3.112	3.413	4.057	4.293	4.586
End-to-end Delay (Seconds)	1.356	1.445	1.538	1.433	1.608	1.732
MSSSIM	0.784	0.718	0.696	0.754	0.707	0.683
Standard Deviation	Case 1			Case 2		
	802.11s	S-MAC	AOC-MAC	802.11s	S-MAC	AOC-MAC
Frame Loss	1.806	1.784	1.713	1.896	1.897	1.864
End-to-end Delay	0.489	0.487	0.486	0.537	0.535	0.539
MSSSIM	0.141	0.176	0.183	0.153	0.178	0.185

- *Frame loss*: The average frame loss rate of AOC-MAC has increased to 3.41% in comparison with the 2.98% rate of the IEEE 802.11s MAC protocol and the 3.11% rate of S-MAC in case 1, respectively. In case 2, the average frame loss rate of AOC-MAC has increased to 4.59% in comparison with the 4.06% rate of the IEEE 802.11s MAC protocol and the 4.29% rate of S-MAC, respectively. The average frame loss rate of AOC-MAC in case 1 is 25.58% lower than in case 2.
- *End-to-end delay*: In case 1 when the mesh routers are static, the end-to-end delay of AOC-MAC has approximately 13.42% increase in comparison with the IEEE 802.11s and 6.44% increase in comparison with S-MAC. In case 2 when the mesh routers are randomly moving, the end-to-end delay of AOC-MAC has approximately 17.03% and 7.71% increase in comparison with the IEEE 802.11s and S-MAC, respectively. The average end-to-end delay of AOC-MAC in case 1 is 11.2% lower than in case 2.
- *Quality*: In case 1 when the mesh routers are static, the average MSSSIM value of AOC-MAC has approximately 11.22% decrease in comparison with the IEEE 802.11s and 3.06% decrease in comparison with S-MAC. In case 2 when the mesh routers are randomly moving, the end-to-end delay of AOC-MAC has approximately 9.41% and 3.39% decrease in comparison with the IEEE 802.11s and S-MAC, respectively. The average MSSSIM value of AOC-MAC in case 1 is 1.87% higher than in case 2.

Test results indicate that AOC-MAC achieves better performance in terms of both energy savings and QoS levels in the case when the mesh routers are with fixed position in comparison with the case when mesh routers are with random mobility, as indicated by the standard deviations of the results included in Table 5.7. The standard deviation of energy consumption rate is not presented as the energy is dropping almost linearly. AOC-MAC deployed at mesh routers with mobility results in higher standard deviation on frame loss, end-to-end delay and video quality, representing lower stability. It is clear that fixed mesh routers reduce the frequency of mesh network topology change, indicating more stable network connectivity during traffic delivery. However, the effect of mesh router mobility on transmission quality is not obvious, according to Table 5.7.

5.5 E-Mesh Testing Scenarios and Performance Analysis

To study the performance of E-Mesh within different wireless mesh network environments, separate tests were performed to study the impact of different weigh factor settings in the E-Mesh utility function as described in section 4.3.2.2 in Chapter 4, and different settings of mesh router mobility. Each scenario includes a specific experimental setup based on the topology illustrated in Figure 5.3. The performance of E-Mesh is evaluated in terms of the following parameters on each mesh router, in comparison with the performance of the IEEE 802.11s routing protocol:

- Average energy consumption rate
- QoS parameters such as video packet loss rate and network throughput
- Video quality assessment parameters: PSNR values

Tests are initialized with the parameters listed in Table 5.8.

TABLE 5.8 COMMON PARAMETERS USED IN E-MESH TESTING

Symbol	QUANTITY	value
D_{min}	Minimum distance between the mesh client and each mesh router	0 (meter)
D_{max}	Maximum distance between the mesh client and each mesh router	150 (meters)
E_{max}	Maximum amount of remaining energy of each mesh router	100 (Joule)
L_{min}	Minimum network traffic load of each mesh router	0 (Mbps)
L_{max}	Maximum network traffic load passing each mesh router	2 (Mbps)
N	Number of mesh routers	20
T	The overall simulation time	200 (s)

5.5.1 Simulation-based Energy Model

The energy model used in both scenarios is an extension of the energy model provided by NS-3, which measures the power of mesh devices by multiplying two main factors:

1) Voltage: The voltage is set in the initialization stage of the topology with a fixed value 3.0 V.
2) Radio current intensity: NS-3 supports five different working states of each mesh device in the physical layer. In each of them the mesh device has associated different current intensities. Our extended energy model includes an additional SLEEP state, relevant to our research:
   a) IDLE: the device is idle (current intensity I = 426μA)
   b) CCA_BUSY: the device has sensed the medium busy through the CCA mechanism (I = 426μA)
   c) TX: the device is sending a packet (I = 17.4mA)
   d) RX: the device is receiving a packet (I = 19.7mA)
   e) SWITCHING: the device is switching to another channel if it is multi-channel (I = 426μA)
   f) SLEEP: the device is off (I = 20uA)

5.5.2 Simulation Settings of Mesh Router Mobility

Test was based on the following two settings of mesh router mobility, which was introduced in section 5.4.3:

- *Case 1*: All the N mesh routers $\{n_1, n_2, \ldots n_N\}$ were allocated with fixed positions, which were uniformly distributed in the range of [0, 2π] with in the circular area. The position of mesh client n_0 was at the center of the circular area, remaining fixed. The mesh client n_{N+1} was moving from the boundary of the circular area towards n_0, with a constant speed 2.0 m/s.
- *Case 2*: The mesh routers were allocated with the mobility parameters described in section 5.4.1, starting from a random pause period between [0, 2] (seconds) and continuing to move with a random direction value between [0, 2π] and a random speed value between [1.0, 2.0] (m/s) towards this direction until it reaches the

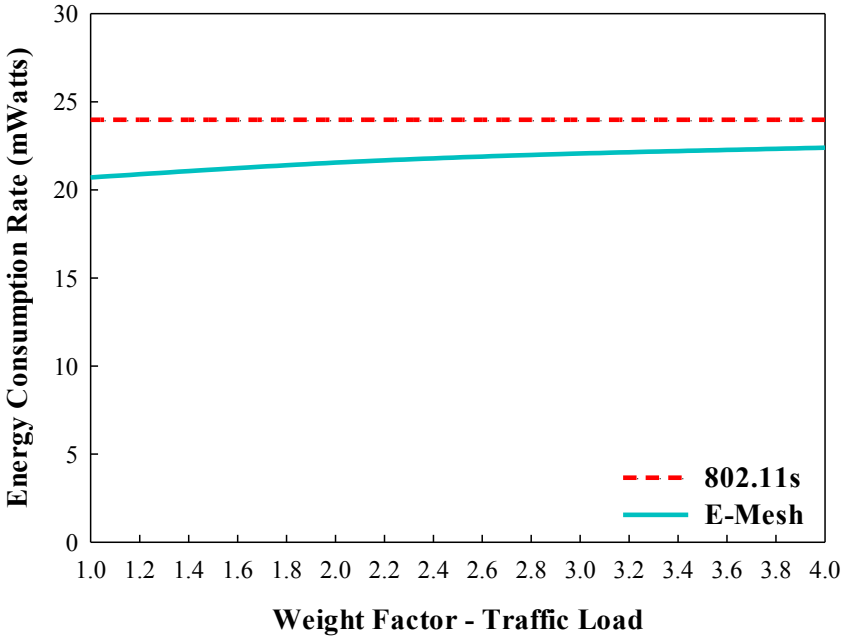

Fig.5.14.Energy consumption rates of 802.11s and E-Mesh with different weights on traffic load (static mesh routers)

boundary of the mesh network with range R, as shown in Figure 5.3. The mesh client n_{N+1} was allocated with a constant speed 2.0 m/s from at the boundary towards the mesh client n_0 located and fixed at the center of the circular area.

5.5.3 Impact of Traffic Load Weight on E-Mesh Performance

The network traffic load on the mesh routers is considered as one of the key parameters in the E-Mesh routing utility function, as mentioned in section 4.3.2.2 in Chapter 4. In the simulation-based tests, the weight of the network traffic in the E-Mesh utility function is controlled by the weight factor W_l. The purpose of this section was to study the E-Mesh performance with various values of W_l.

In this test, the value of W_l was varied from 1.0 to 4.0, representing the exponentially growth of the importance of the traffic load in the E-Mesh routing utility function. The values of W_e and W_d were set to 1.0 and remained fixed.

5.5.3.1 Impact of Traffic Load Weight on E-Mesh Performance with Static Mesh Routers

As shown in Figure 5.14, with the mesh router mobility settings in case 1, the average energy consumption rates of the IEEE 802.11s routing protocol remain the same, as HWMP is used as the default protocol without the influence from the E-Mesh utility function. On the other hand, the energy consumption rates of E-Mesh slightly increase along with the increase of the

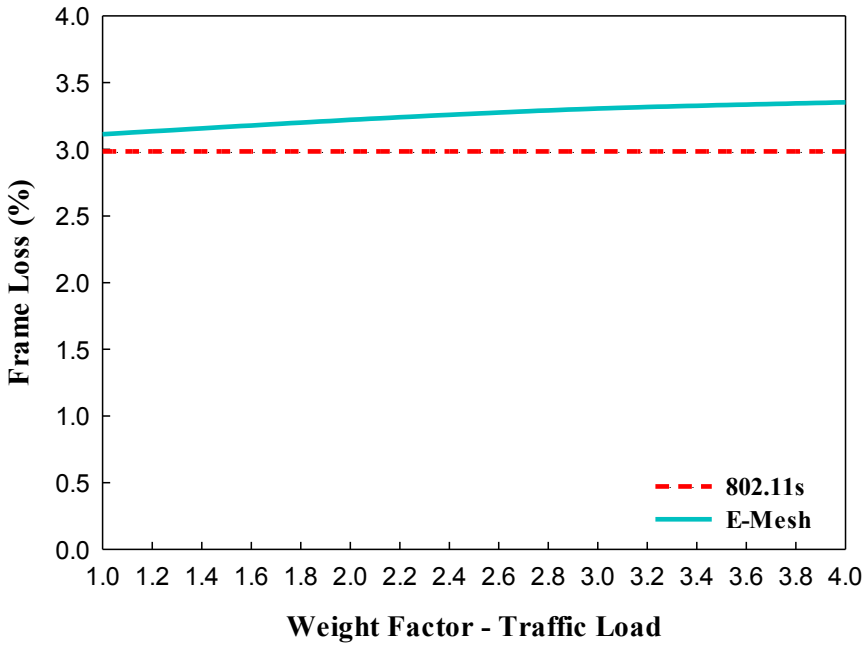

Fig.5.15. Frame loss rates of 802.11s and E-Mesh with different weights on traffic load (static mesh routers)

value of W_l, which results in deviations of selecting the active neighboring mesh routers with higher traffic load during the routing process, regardless of the remaining battery energy on those routers. With the value of W_l set to 1.0, 2.0, 3.0 and 4.0, E-Mesh has achieved approximately 13.64%, 10.13%, 7.96% and 6.59% energy savings in comparison with the IEEE 802.11s routing protocol, respectively.

Figure 5.15 illustrates the frame loss rates of the IEEE 802.11s routing protocol and E-Mesh with different values of W_l. It is shown that with the mesh router mobility settings in case 1, the frame loss rates of E-Mesh slightly increase along with the increase of the value of W_l, as higher value of W_l indicates higher importance of traffic load during mesh router selection and results in higher chance of traffic overloading and packet drop. With the value of W_l set to 1.0, 2.0, 3.0 and 4.0, E-Mesh has experienced approximately 4.32%, 7.94%, 10.79% and 12.36% increase of the average frame loss rate in comparison with the IEEE 802.11s routing protocol, respectively.

The transmission quality is estimated in terms of the PSNR value of the received data stream, which translates the effect of bit rate and loss on user perceived quality according to the formula [46] presented in equation (5.1). The relationship between various PSNR values and the

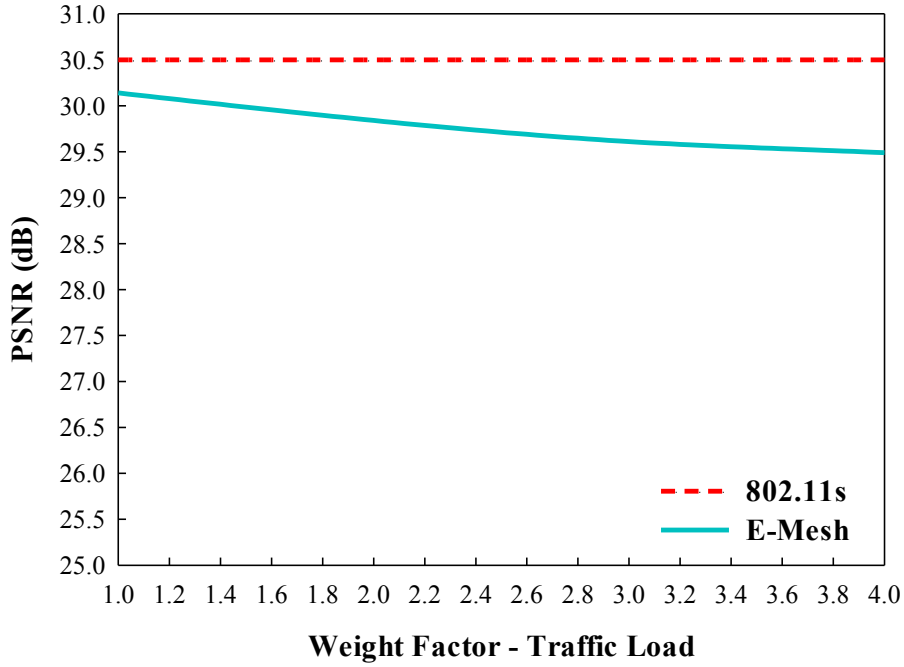

Fig.5.16. PSNR values of 802.11s and E-Mesh with different weights on traffic load (static mesh routers)

corresponding user perceived quality levels is illustrated in Table 2.2 in Chapter 2, as associated by the ITU T. P.800 standard [41].

$$PSNR = 20\,log_{10}(\frac{MAX\_Bitrate}{\sqrt{(EXP\_Thr - CRT\_Thr)^2}}) \quad (5.1)$$

In equation (5.1), *MAX_Bitrate* is the average bit rate of the data stream transmitted, *EXP_Thr* is the average throughput expected to be obtained and *CRT_Thr* is the actual measured average throughput. According to the parameter settings presented in Table 5.8, the value of *MAX_Bitrate* and *EXP_Thr* in equation (5.1) is 2 Mbps during simulation.

The PSNR values of the IEEE 802.11s routing protocol and E-Mesh are computed and illustrated in Figure 5.16. Figure 5.16 indicates that with the mesh router mobility settings in case 1, the PSNR values decrease along with the increase of the value of W_l for E-Mesh, as higher value of W_l indicates higher chance of packet drop and results in transmission quality decline. With the value of W_l set to 1.0, 2.0, 3.0 and 4.0, the transmission quality of E-Mesh remains roughly the same level in comparison with the IEEE 802.11s routing protocol, with approximately 0.4dB, 0.7dB, 0.9dB and 1.0 dB decrease, respectively.

It is clear that with the mesh router mobility settings in case 1, E-Mesh achieves considerable energy savings in comparison with the IEEE 802.11s routing protocol, while

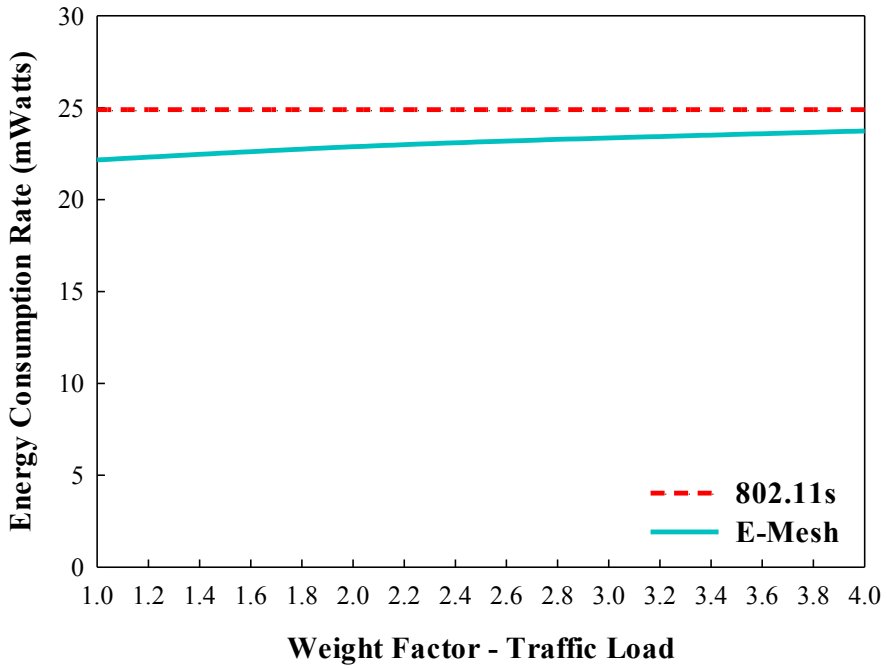

Fig.5.17.Energy consumption rates of 802.11s and E-Mesh with different weights on traffic load (moving mesh routers)

maintaining roughly the same transmission quality level with different values of W_l. The energy saving benefit of E-Mesh decreases along with the increase of the value of W_l, but still remains at a good level. When the increase of W_l exceeds a certain limit, the energy saving benefit does not overcome the quality decrease any more.

5.5.3.2 Impact of Traffic Load Weight on E-Mesh Performance with Moving Mesh Routers

As shown in Figure 5.17, with the mesh router mobility settings in case 2, the average energy consumption rates of the IEEE 802.11s routing protocol still remain the same, without the influence from the E-Mesh utility function. The energy consumption rates of E-Mesh slightly increase along with the increase of the value of W_l. With the value of W_l set to 1.0, 2.0, 3.0 and 4.0, E-Mesh has achieved approximately 11.01%, 8.11%, 6.18% and 4.66% energy savings in comparison with the IEEE 802.11s routing protocol, respectively.

Figure 5.18 illustrates the frame loss rates of the IEEE 802.11s routing protocol and E-Mesh with different values of W_l. It is shown that with the mesh router mobility settings in case 2, the frame loss rates of E-Mesh slightly increase along with the increase of the value of W_l. With the value of W_l set to 1.0, 2.0, 3.0 and 4.0, E-Mesh has experienced approximately

-

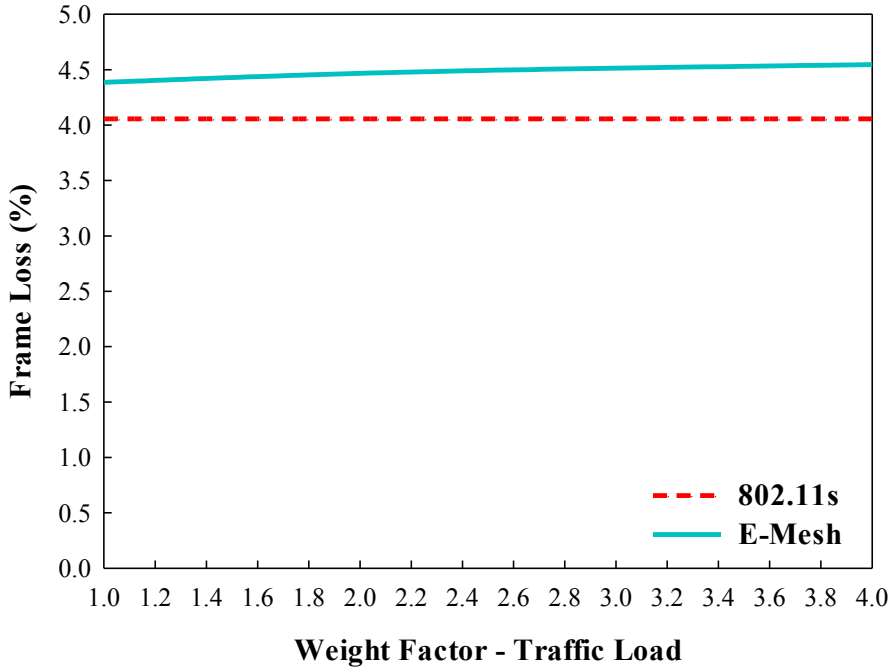

Fig.5.18. Frame loss rates of 802.11s and E-Mesh with different weights on traffic load (moving mesh routers)

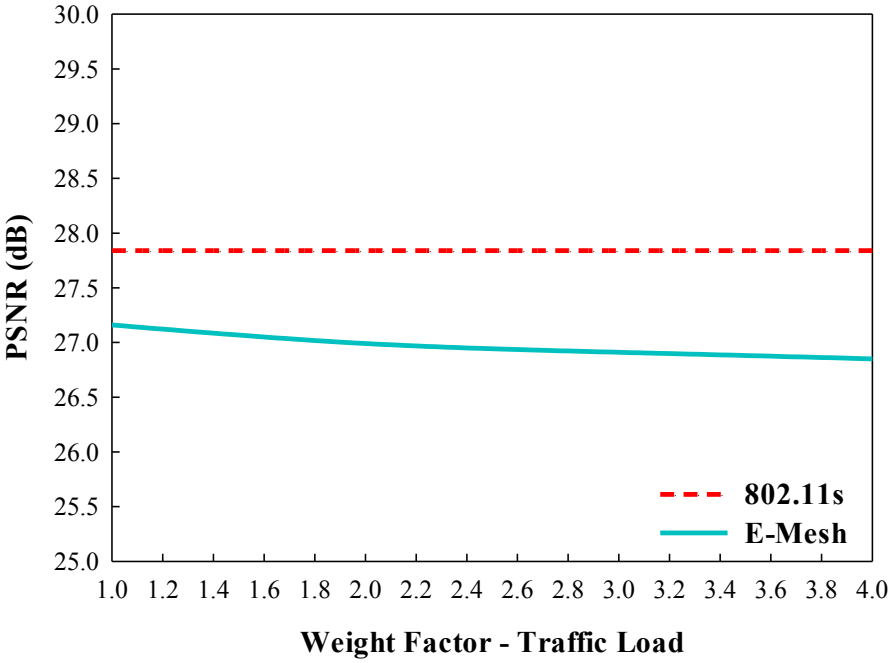

Fig.5.19. PSNR values of 802.11s and E-Mesh with different weights on traffic load (moving mesh routers)

8.11%, 10.14%, 11.26% and 12.05% increase of the average frame loss rate in comparison with the IEEE 802.11s routing protocol, respectively.

The PSNR values of the IEEE 802.11s routing protocol and E-Mesh are computed using the equation presented in section 5.5.3.1 and illustrated in Figure 5.19. Figure 5.19

indicates that with the mesh router mobility settings in case 2, the PSNR values of E-Mesh decrease along with the increase of the value of W_l. With the value of W_l set to 1.0, 2.0, 3.0 and 4.0, the transmission quality of E-Mesh remains roughly the same level in comparison with the IEEE 802.11s routing protocol, with approximately 0.7 dB, 0.8dB, 0.9dB and 1.0dB decrease, respectively.

It is clear that with the mesh router mobility settings in case 2, the energy saving benefit of E-Mesh in comparison with the IEEE 802.11s routing protocol is less obvious than in case 1, and decreases along with the increase of the value of W_l. Meanwhile, the QoS level of E-Mesh decreases in case 2 in comparison with in case 1, but in general the decrease of the QoS level does not overcome the energy saving benefit with appropriate values of W_l.

5.5.4 Impact of Remaining Energy Weight on E-Mesh Performance

The remaining energy on each mesh router in the wireless mesh network is another key parameter in the E-Mesh routing utility function for determining the routing strategy. In the simulation-based tests, the weight of the remaining energy in the E-Mesh utility function is controlled by the weight factor W_e. The purpose of this section was to study the E-Mesh

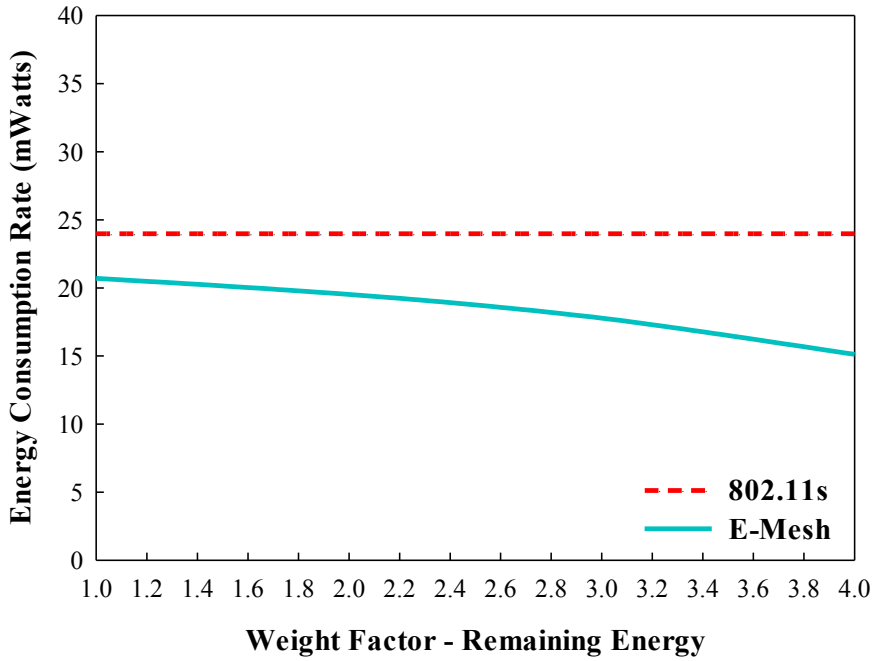

Fig.5.20.Energy consumption rates of 802.11s and E-Mesh with different weights on remaining energy (static mesh routers)

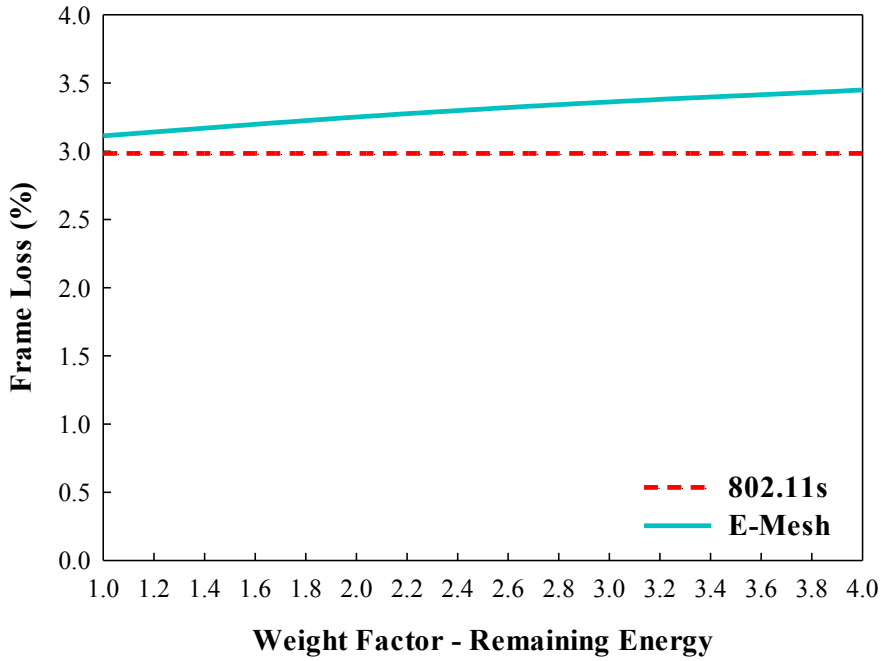

Fig.5.21. Frame loss rates of 802.11s and E-Mesh with different weights on remaining energy (static mesh routers)

performance with various values of W_e.

In this test, the value of W_e was varied from 1.0 to 4.0, representing the exponentially growth of the weight of the remaining energy of each mesh router in the E-Mesh routing utility function. The values of W_l and W_d were set to 1.0 and remained fixed.

5.5.4.1 Impact of Remaining Energy Weight on E-Mesh Performance with Static Mesh Routers

As shown in Figure 5.20, with the mesh router mobility settings in case 1, the average energy consumption rates of the IEEE 802.11s routing protocol remain fixed. The average energy consumption rates of E-Mesh slightly decrease along with the increase of the value of W_e, as higher value of W_e indicates deviations of selecting mesh routers with more remaining energy during routing process. With the value of W_e set to 1.0, 2.0, 3.0 and 4.0, E-Mesh has achieved approximately 13.64%, 18.56%, 25.85% and 36.54% energy savings in comparison with the IEEE 802.11s routing protocol, respectively.

Figure 5.21 illustrates the frame loss rates of the IEEE 802.11s routing protocol and E-Mesh with different values of W_e. It is shown that with the mesh router mobility settings in case 1, the frame loss rates of E-Mesh increase along with the increase of the value of W_e. With

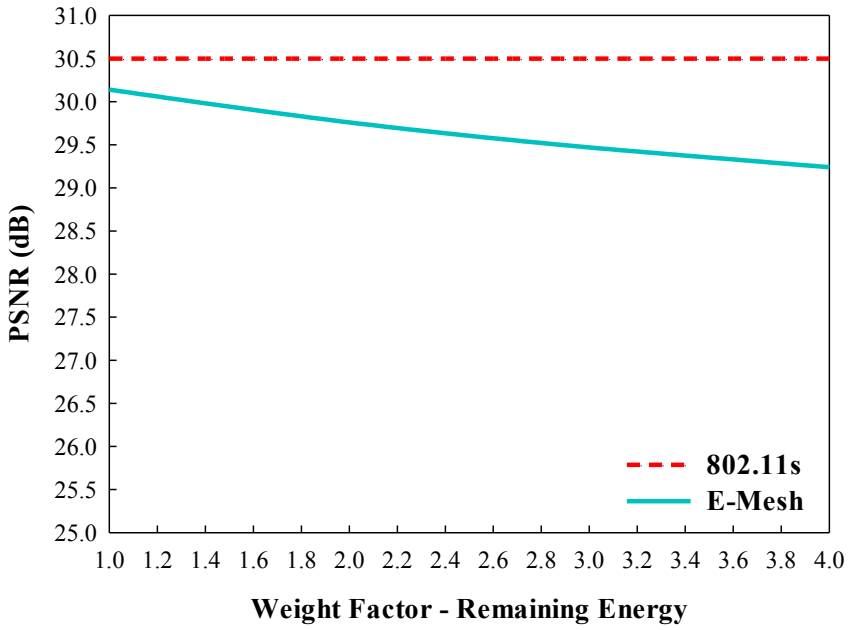

Fig.5.22. PSNR values of 802.11s and E-Mesh with different weights on remaining energy (static mesh routers)

the value of W_e set to 1.0, 2.0, 3.0 and 4.0, E-Mesh has experienced approximately 4.32%, 8.95%, 12.67% and 15.58% increase of the average frame loss rate in comparison with the IEEE 802.11s routing protocol, respectively.

The PSNR values of the IEEE 802.11s routing protocol and E-Mesh are computed using the equation presented in section 5.5.3.1 and illustrated in Figure 5.22. Figure 5.22 indicates that with the mesh router mobility settings in case 1, the PSNR values decrease along with the increase of the value of W_e for E-Mesh while the PSNR values of the 802.11s routing protocol remain the same. With different values of W_e, the transmission quality of E-Mesh decrease for 0.4dB, 0.8dB, 1.0dB and 1.3dB in comparison with the IEEE 802.11s routing protocol.

It is clear that with the mesh router mobility settings in case 1, the energy saving benefit of E-Mesh increases along with the increase of the value of W_e, as energy is consider with more weight during routing process. In this case, E-Mesh achieves considerable energy savings in comparison with the IEEE 802.11s routing protocol, while the transmission quality level remains approximately the same.

5.5.4.2 Impact of Remaining Energy Weight on E-Mesh Performance with Moving Mesh Routers

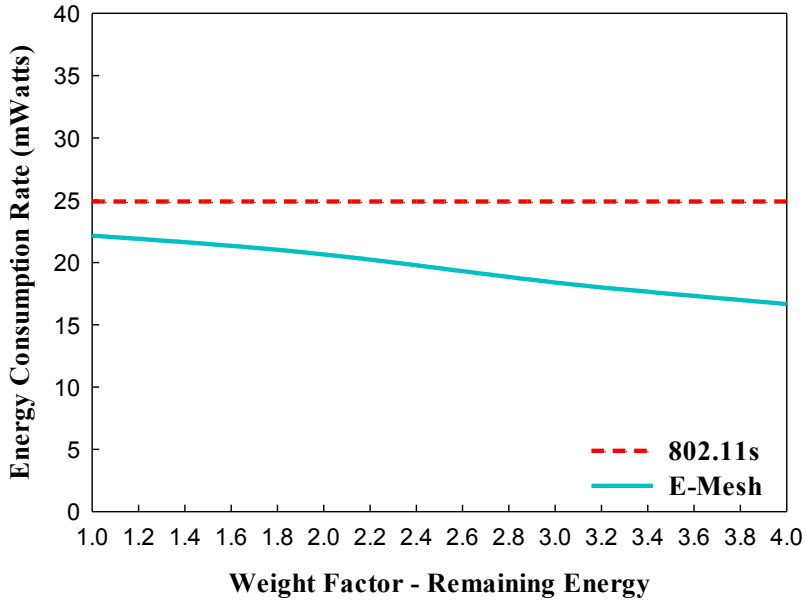

Fig.5.23.Energy consumption rates of 802.11s and E-Mesh with different weights on remaining energy (moving mesh routers)

As shown in Figure 5.23, with the mesh router mobility settings in case 2, the average energy consumption rates of E-Mesh decrease along with the increase of the value of W_e, while the average energy consumption rates of IEEE 802.11s routing protocol remain fixed. With the value of W_e set to 1.0, 2.0, 3.0 and 4.0, E-Mesh has achieved approximately 11.01%, 17.03%, 25.11% and 33.09% energy savings in comparison with the IEEE 802.11s routing protocol, respectively.

Figure 5.24 illustrates the frame loss rates of the IEEE 802.11s routing protocol and E-Mesh with different values of W_e. It is shown that with the mesh router mobility settings in case 2, the frame loss rates of E-Mesh slightly increase along with the increase of the value of W_e. With the value of W_e set to 1.0, 2.0, 3.0 and 4.0, E-Mesh has experienced approximately 8.11%, 10.82%, 12.69% and 14.05% increase of the average frame loss rate in comparison with the IEEE 802.11s routing protocol, respectively.

The PSNR values of the IEEE 802.11s routing protocol and E-Mesh are computed using the equation presented in section 5.5.3.1 and illustrated in Figure 5.25. Figure 5.25 indicates that with the mesh router mobility settings in case 2, the PSNR values of E-Mesh decrease along with the increase of the value of W_e and the PSNR values of the IEEE 802.11s routing protocol remain the same. With the value of W_e set to 1.0, 2.0, 3.0 and 4.0, the

-

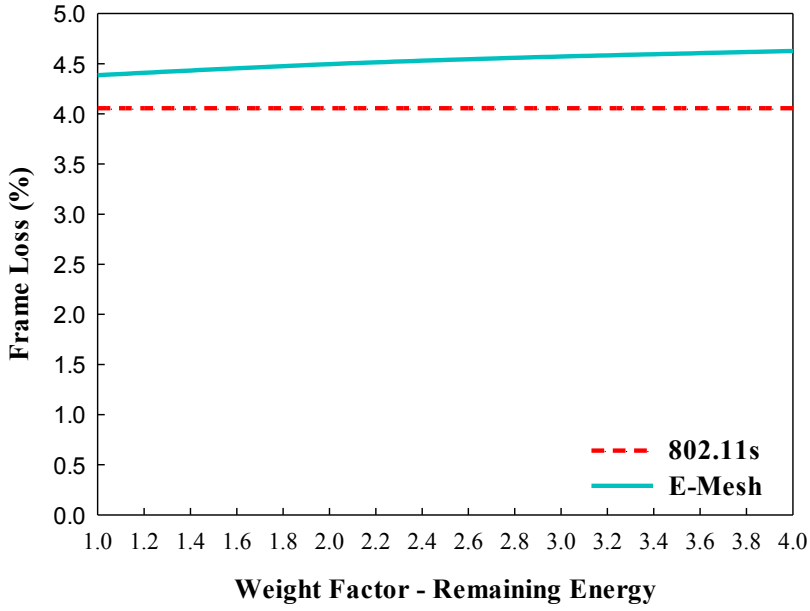

Fig.5.24. Frame loss rates of 802.11s and E-Mesh with different weights on remaining energy (moving mesh routers)

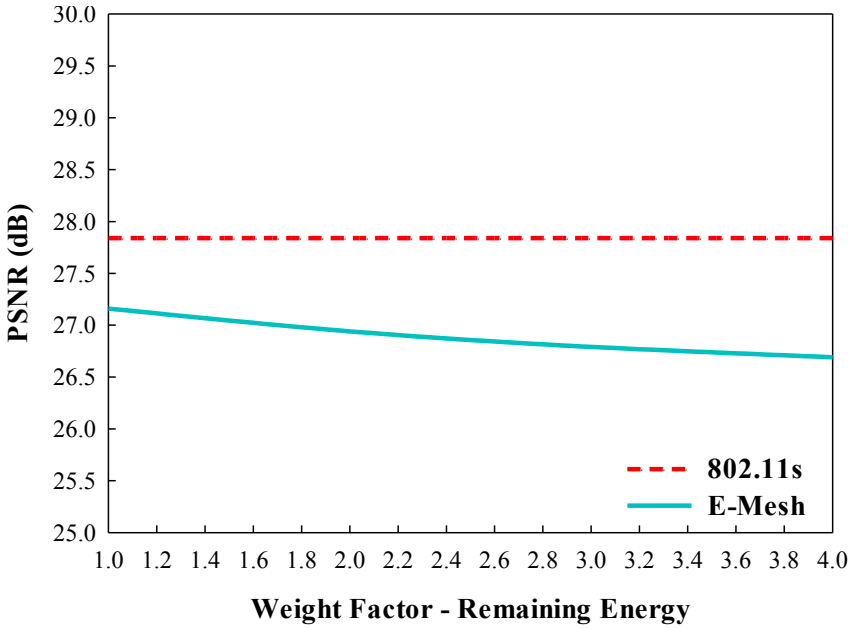

Fig.5.25. PSNR values of 802.11s and E-Mesh with different weights on remaining energy (moving mesh routers)

transmission quality of E-Mesh has approximately 0.7dB, 0.9dB, 1.0dB and 1.2dB decrease in comparison with the IEEE 802.11s routing protocol.

It is clear that E-Mesh achieves significant energy savings in comparison with the IEEE 802.11s routing protocol, regardless of the mesh router mobility. The energy saving benefit of E-Mesh increases along with the increase of the value of W_e, while the QoS level of E-Mesh

decreases in case 2 in comparison with in case 1, but still remains in a good level.

5.5.5 Impact of Mesh Router Distance Weight on E-Mesh Performance

The distance between mesh routers in the wireless mesh network is the third key parameter in the E-Mesh routing utility function. During data forwarding in the mesh network, mesh routers with shorter distance with each other are with stronger transmission power, according to the propagation loss model. In the simulation-based tests, the weight of the distance between mesh routers in the E-Mesh utility function is controlled by the weight factor W_d. The purpose of this section was to study the E-Mesh performance with various values of W_d.

In this test, the value of W_d was varied from 1.0 to 4.0, representing the exponentially growth of the weight of the distance between mesh routers in the E-Mesh routing utility function. The values of W_l and W_e were set to 1.0 and remained fixed.

5.5.5.1 Impact of Mesh Router Distance Weight on E-Mesh Performance with Static Mesh Routers

As shown in Figure 5.26, with the mesh router mobility settings in case 1, the average energy consumption rates of the IEEE 802.11s routing protocol do not change while the average energy consumption rates of E-Mesh decrease along with the increase of the value of W_d, as higher value of W_d indicates lower transmission power. With the value of W_d set to 1.0, 2.0, 3.0 and 4.0, E-Mesh has achieved approximately 13.64%, 14.26%, 14.72% and 15.01% energy savings in comparison with the IEEE 802.11s routing protocol, respectively.

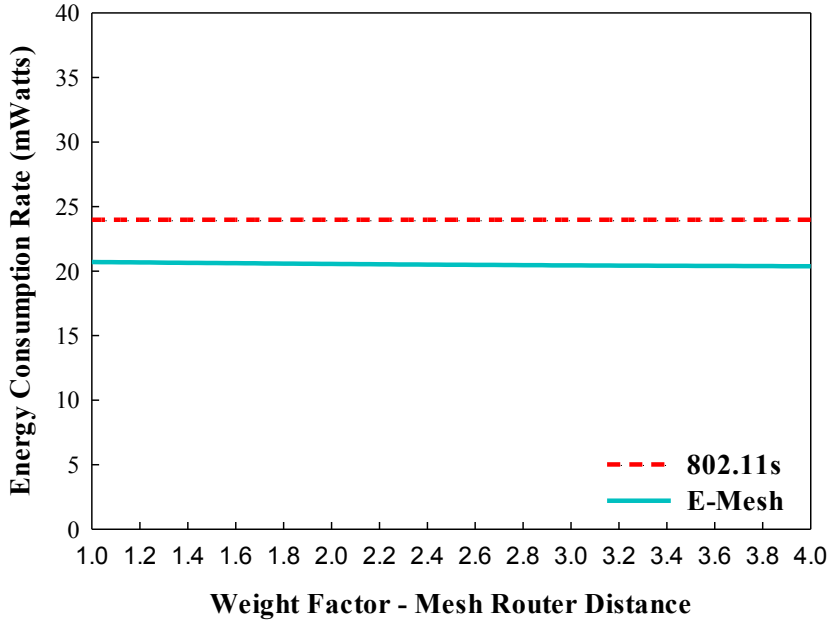

Fig.5.26.Energy consumption rates of 802.11s and E-Mesh with different weights on mesh router distance (static mesh routers)

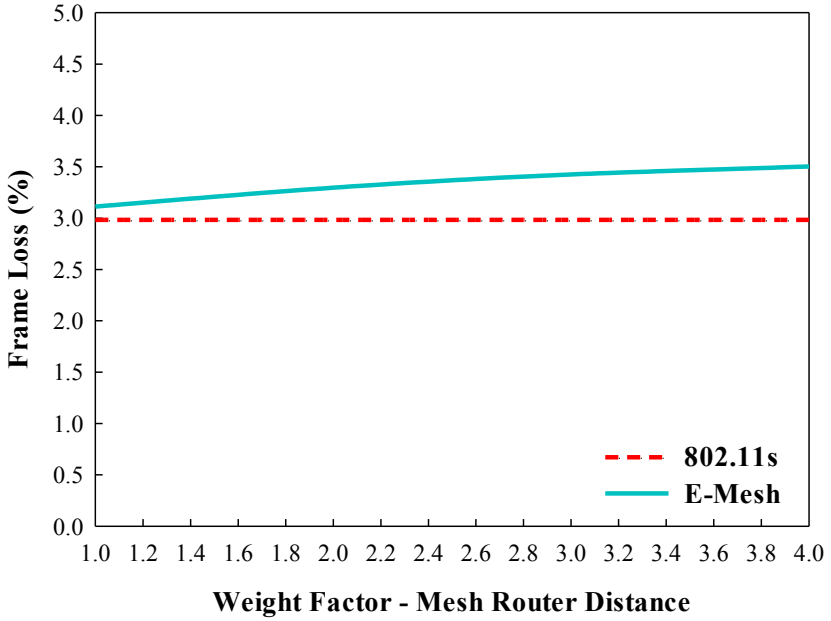

Fig.5.27. Frame loss rates of 802.11s and E-Mesh with different weights on mesh router distance (static mesh routers)

Figure 5.27 illustrates the frame loss rates of the IEEE 802.11s routing protocol and E-Mesh with different values of W_d. It is shown that with the mesh router mobility settings in case 1, the frame loss rates of E-Mesh slightly increase along with the increase of the value of W_d while the frame loss rates of the IEEE 802.11s routing protocol stay in the same level. With the value of W_d set to 1.0, 2.0, 3.0 and 4.0, E-Mesh has experienced approximately 4.32%,

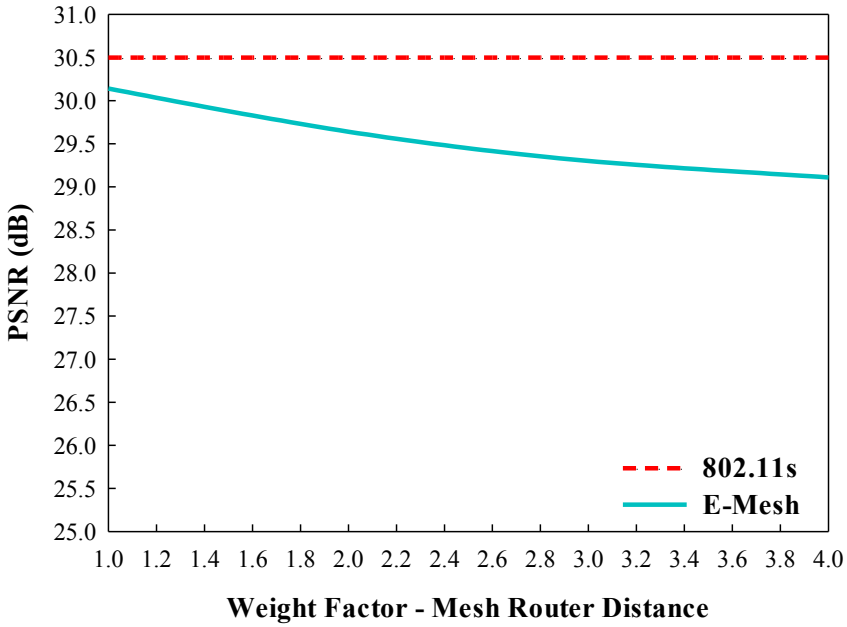

Fig.5.28. PSNR values of 802.11s and E-Mesh with different weights on mesh router distance (static mesh routers)

10.49%, 14.81% and 17.39% increase of the average frame loss rate in comparison with the IEEE 802.11s routing protocol, respectively.

The PSNR values of the IEEE 802.11s routing protocol and E-Mesh are computed using the equation presented in section 5.5.3.1 and illustrated in Figure 5.28. Figure 5.28 indicates that with the mesh router mobility settings in case 2, the PSNR values of E-Mesh slightly decrease along with the increase of the value of W_d, but roughly remain at a stable level. With the value of W_d set to 1.0, 2.0, 3.0 and 4.0, the transmission quality of E-Mesh remains roughly the same level in comparison with the IEEE 802.11s routing protocol, with approximately 0.4dB, 0.8dB, 1.2dB and 1.4dB decrease.

It is clear that with the mesh router mobility settings in case 1, E-Mesh achieves energy savings in comparison with the IEEE 802.11s routing protocol, which increases along with the increase of the value of W_d, while maintaining roughly the same transmission quality levels.

5.5.5.2 Impact of Mesh Router Distance Weight on E-Mesh Performance with Moving Mesh Routers

As shown in Figure 5.29, with the mesh router mobility settings in case 2, the average energy consumption rates of the IEEE 802.11s routing protocol and E-Mesh slightly decrease along with the increase of the value of W_d. With the value of W_d set to 1, 2, 3 and 4, E-Mesh has

-

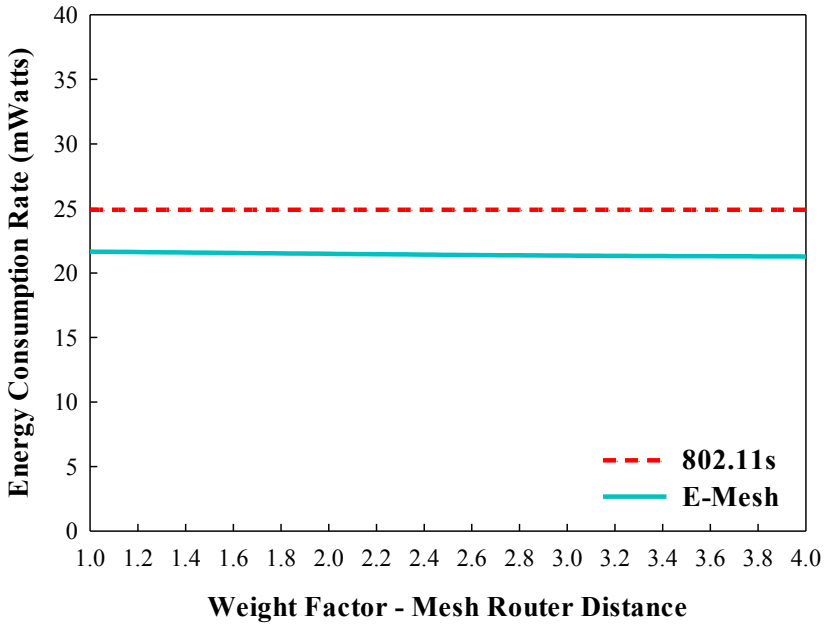

Fig.5.29.Energy consumption rates of 802.11s and E-Mesh with different weights on mesh router distance (moving mesh routers)

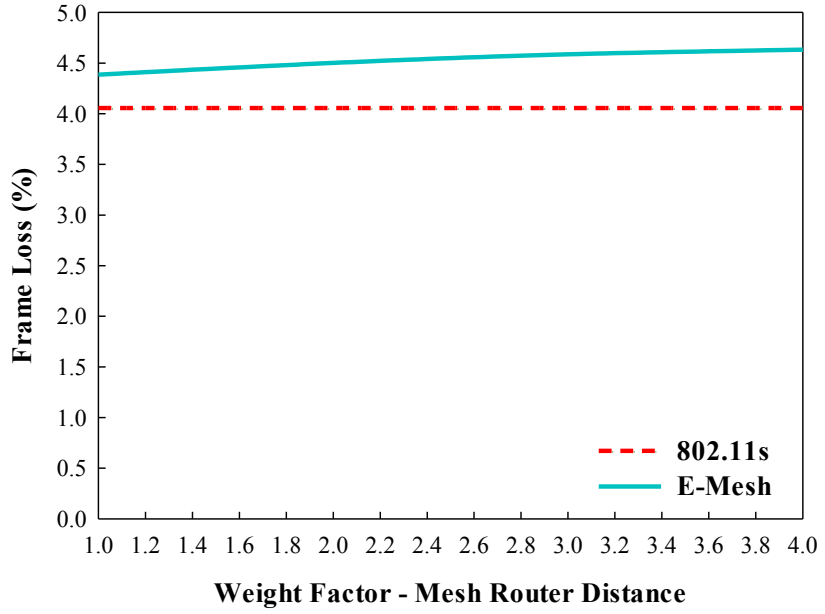

Fig.5.30. Frame loss rates of 802.11s and E-Mesh with different weights on mesh router distance (moving mesh routers)

achieved approximately 13.01%, 13.69%, 14.26% and 14.54% energy savings in comparison with the IEEE 802.11s routing protocol, respectively.

Figure 5.30 illustrates the frame loss rates of the IEEE 802.11s routing protocol and E-Mesh with different values of W_d. It is shown that with the mesh router mobility settings in case 2, the frame loss rates of E-Mesh slightly increase along with the increase of the value of

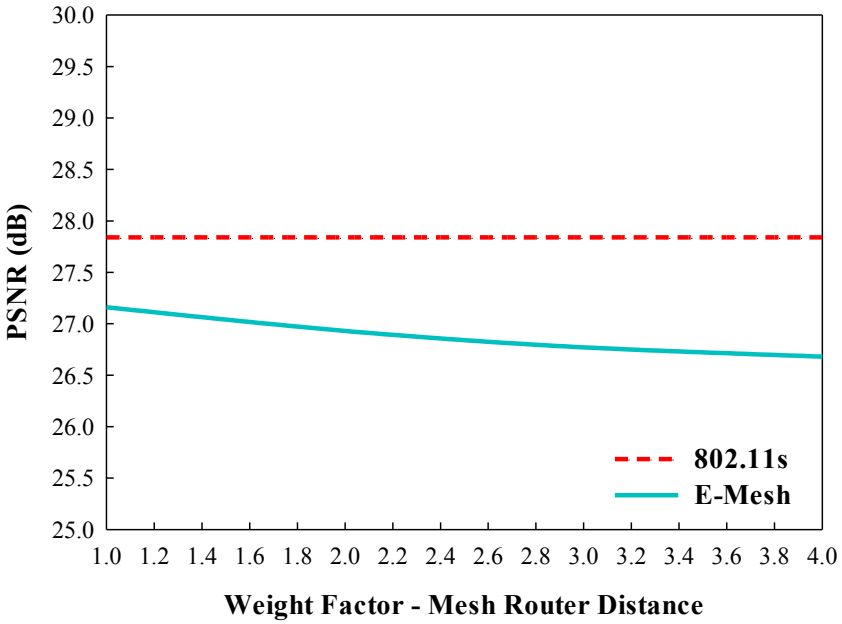

Fig.5.31. PSNR values of 802.11s and E-Mesh with different weights on mesh router distance (moving mesh routers)

W_d. With the value of W_d set to 1.0, 2.0, 3.0 and 4.0, E-Mesh has experienced approximately 7.51%, 10.96%, 13.06% and 14.19% increase of the average frame loss rate in comparison with the IEEE 802.11s routing protocol, respectively.

The PSNR values of the IEEE 802.11s routing protocol and E-Mesh are computed using the equation presented in section 5.5.3.1 and illustrated in Figure 5.31. Figure 5.31 indicates that with the mesh router mobility settings in case 2, the PSNR values of E-Mesh decrease along with the increase of the value of W_d. With the value of W_d set to 1.0, 2.0, 3.0 and 4.0, the transmission quality of E-Mesh remains roughly the same level in comparison with the IEEE 802.11s routing protocol, with approximately 0.7dB, 0.9dB, 1.1dB and 1.2dB decrease.

It is clear that with the mesh router mobility settings in case 2, the energy saving benefit of E-Mesh in comparison with the IEEE 802.11s routing protocol is roughly the same with case 1, regardless of the value of W_d.

5.6 eMTCP Testing Scenarios and Performance Analysis

5.6.1 eMTCP Testing Scenarios

The following four test cases are considered with the different parameters presented in Table 5.9:

TABLE 5.9 DETAILS OF FOUR TEST CASES OF EMTCP

Case	1	2	3	4
Number of nodes	2	3	3	3
Case description	data sender and receiver	2 UE nodes (data sender and receiver) and 1 eNB node	2 UE nodes (data sender and receiver) and 1 eNB node	2 UE nodes (data sender and receiver) and 1 eNB node
Distance between base station and receiver (m)	60	60	60	60
Aggregate data transmission rate (Mbps)	11	11	11	11
Battery capacity (Joule)	300	300	300	300
Physical link between data sender and receiver	WiFi	LTE	WiFi + LTE	WiFi + LTE
Transport layer protocol	TCP	TCP	MPTCP	eMTCP + MPTCP
Simulation time (s)	150	150	150	150

- *Case 1*: A single Wi-Fi link is established between WN_0 and WN_2, which is also shared by the other data sink nodes. The distances from WN_0 to WN_2 and to the base stations of LTE and Wi-Fi are set to the same 60 meters, respectively. The initial energy of the battery of WN_2 is set to 300 Joules. Data stream is sent via the Wi-Fi link with the aggregate rate of 11 Mbps using TCP as the transport layer protocol. Simulation time is 150 seconds.
- *Case 2*: Apart from WN_0 and WN_2, an extra eNB node is added as a part of the single LTE link between them instead of the Wi-Fi link used in case 1. Other settings remain the same as in case 1.
- *Case 3*: Both Wi-Fi and LTE links are used simultaneously for multipath data transmission and MPTCP is used as the transport layer protocol instead of TCP. Other settings remain the same as in case 2.
- *Case 4*: eMTCP is deployed to complement MPTCP. Other settings remain the same as in case 3.

In all four cases, constant bit-rate (CBR) data streams are used as input in the simulation, modeling video traffic. The data packet size was 1040 bytes which is a multiple of 26 bytes (data splicing in the output stream was employed in the NS-3 implementation of MPTCP) [112].

The NS-3 implementation of MPTCP used involves modifications of the TCP socket structure definition and the corresponding application-layer and network-layer protocols. The re-defined TCP socket used in this implementation includes the setting of TCP receive buffer, from which data stream is taken out to the sub-flows and then sent to the application layer. In simulations the size of the TCP receive buffer is set according to the following equation [10]:

$$S_{buffer} = 2 \times \text{sum}(BW_i) \times RTT_{max} \quad (5.2)$$

In equation (5.2), S_{buffer} represents the size of the TCP receive buffer, BW_i represents the default bandwidth set for sub-flow i (in this case, $i \in \{0, 1\}$) and RTT_{max} represents the maximum round-trip time across all the sub-flows. Setting the TCP receive buffer in the simulation using this formula avoids the sub-flows from stalling when MPTCP fast retransmission scheme is triggered on any of them.

When using the bandwidth and round-trip time values for LTE and Wi-Fi links shown in Figure 5.4, the TCP receive buffer size S_{buffer} calculated by the formula from equation (5.2) is 2.55 Mbytes.

Based on the settings described above, the following two test scenarios are designed for data transmission performance assessment:

- *Scenario C1*: studies the influence of different traffic off-loading percentage on the energy efficiency by varying it between 0% and 100%.
- *Scenario C2*: studies the energy consumption, energy efficiency and delivery performance in terms of average throughput and estimated user-perceived quality when delivering video data for the four test cases.

In each scenario, the performance of eMTCP was evaluated and compared against the single-path TCP, MPTCP and the MPTCP-based multi-path scheduler proposed by Nokia [82], using the corresponding parameters listed in Table 5.9. A simple prototype of the multi-path scheduler was implemented in NS-3 to be used for testing any type of application. The prototype mainly involves a MDP-based model which does the transmission handover between multiple interfaces used by MPTCP every Δt time units based on the throughput in Δt and the interface states. In each handover process, new sub-flows are established for the newly selected interface and all the previous sub-flows are torn down. The MDP-based model was

implemented with the following elements:

- *State* – a *k+1* tuple array, with the first k state variables $\{s_1, s_2, \ldots s_k\}$ defined as the energy states of the *k* wireless interfaces correspondingly and the state variable s_{k+1} defined as the observed throughput in Δt time units.
- *Action* – which interface between the *k* interfaces is selected
- *Reward Function* – defined as the sum of energy consumption of the *k* interfaces

The value of Δt was set to 1 second according to the original test settings presented in [82].

5.6.2 eMTCP Performance Analysis

The performance of eMTCP is evaluated in terms of the energy efficiency on the smartphone, with the four test cases described in section 5.6.1. The impact of traffic load balancing between the LTE and Wi-Fi paths on the energy efficiency of eMTCP-deployed smartphone is also investigated.

As shown in Figure 5.32, the energy efficiency increases when the traffic off-loaded from LTE to Wi-Fi increases from 0% to approximately 24% of the queued data in the TCP receiver buffer. When the traffic off-loading share increases from 24% to 100% (which indicates that all the traffic is off-loaded to the Wi-Fi link), the energy efficiency declines as the data size allocated to the Wi-Fi link exceeds its capacity, which causes throughput decrease. The observation that there is a value with the highest energy efficiency determined setting 24% as

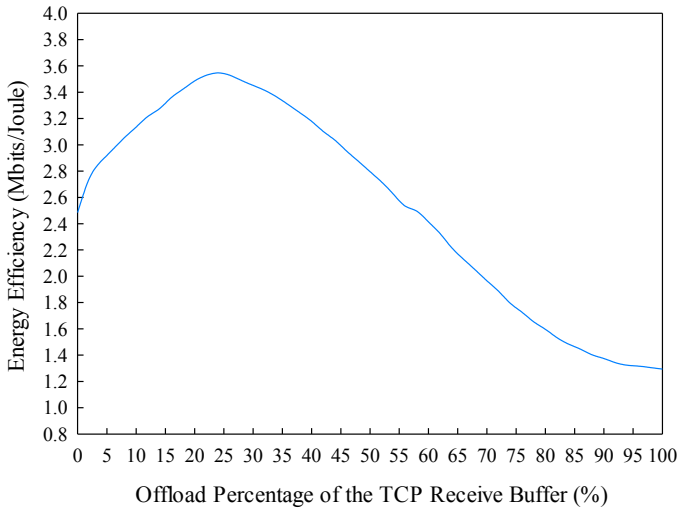

Fig.5.32. Change of energy efficiency according to change of traffic off-loading percentage

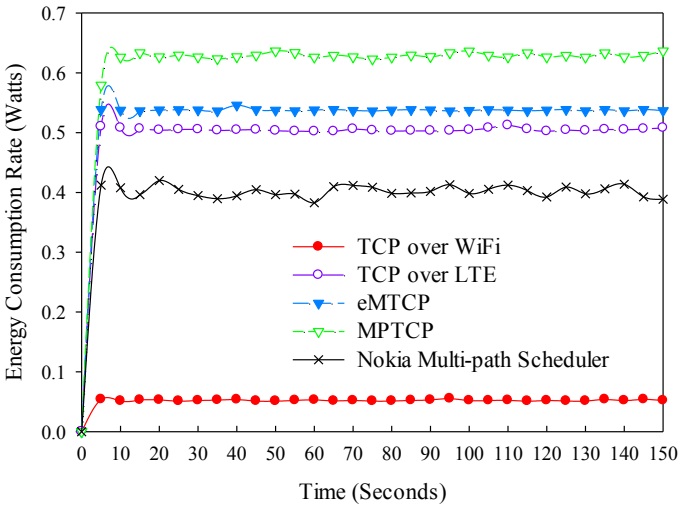

Fig.5.33. Energy consumption rates of single-path TCP, MPTCP, eMTCP and the Nokia Multi-path Scheduler

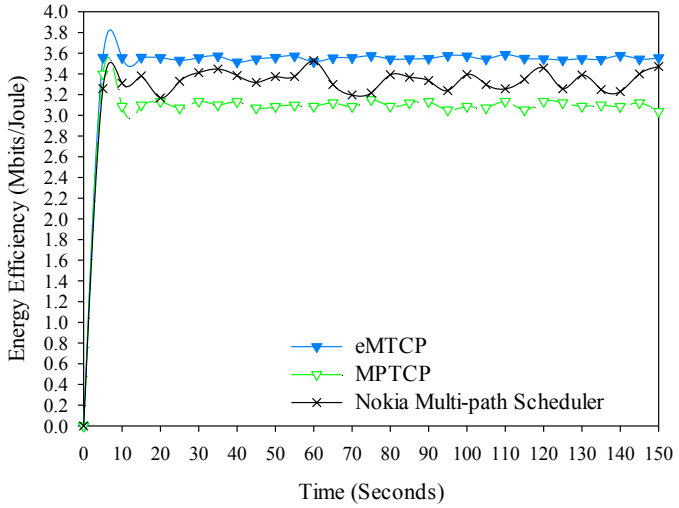

Fig.5.34. Energy efficiency of eMTCP, MPTCP and the Nokia Multi-path Scheduler

the default traffic off-loading percentage for the eMTCP performance evaluation.

Figure 5.33 and Figure 5.34 show how the energy consumption and energy efficiency when employing eMTCP are 14.2% and 14.1% respectively lower than when MPTCP was used, The downside of these improvements was a 2.1% decrease in the average transmission throughput, as indicated in Figure 5.35. Figure 5.35 also shows how the average transmission throughput of eMTCP is roughly 2.26 times that of TCP over Wi-Fi and 2.05 times that of TCP over LTE. This clearly shows the data rate benefit of multi-path transmissions in comparison with single-path data transfers. The energy consumption of the Nokia multi-path scheduler is roughly 25.4% lower than eMTCP. However, the average throughput of eMTCP is 42.34% higher, which results in the 10.1% improvement on the energy efficiency in comparison with

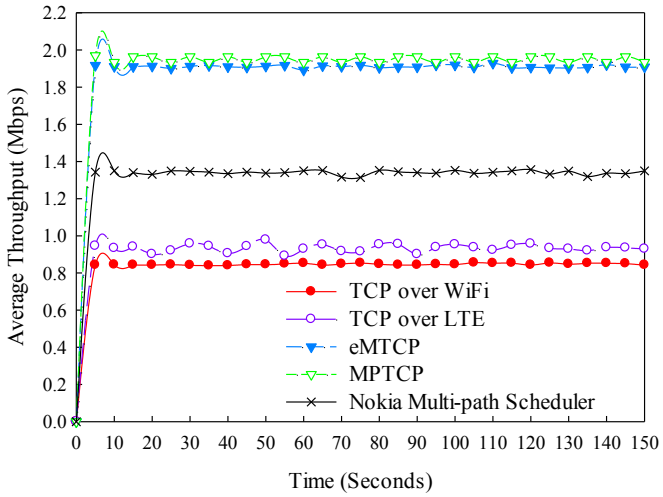

Fig.5.35. Throughput of single-path TCP, MPTCP, eMTCP and the Nokia Multi-path Scheduler

the Nokia multi-path scheduler.

The experiments have also studied the performance of video-type data delivery using CBR data streams to simulate real video streams. The performance is measured in terms of the PSNR values of the simulated video streams, which translate the effect of throughput and loss on user-perceived quality according to equation (5.1) in section 5.5.3.1. The values of *MAX_Bitrate* and *EXP_Thr* in equation (5.1) are 1 Mbps for case 1 and 2 and 2 Mbps for case 3 and 4 (as a dual-path approach is used). The PSNR values are computed and shown in Figure 5.36 and Table 5.10.

It can be noted that eMTCP's excellent energy efficiency and energy consumption results are balanced by a PSNR value with 5.54 dB lower than that of MPTCP but slightly higher than that of the Nokia multi-path scheduler. However the value of 27.03 dB still places eMTCP's estimated user-perceived quality at "Fair" ITU T. P.800 level. The PSNR standard deviation of eMTCP shown in Table 5.10 is much smaller in comparison with that of MPTCP, indicating that as eMTCP results in lower PSNR fluctuations, there is important user benefit in favor of eMTCP. This is explained by the 24% traffic off-loading rate which leads to a better utilization of the TCP receiver buffer and determines smooth throughput and PSNR. The PSNR level of eMTCP is 12.79% higher than that resulted by employing single-path TCP data transfers over LTE and 66.09% higher in comparison with that of TCP over Wi-Fi. This clearly demonstrates the quality improvement our multi-path solution has against the two single-path

-

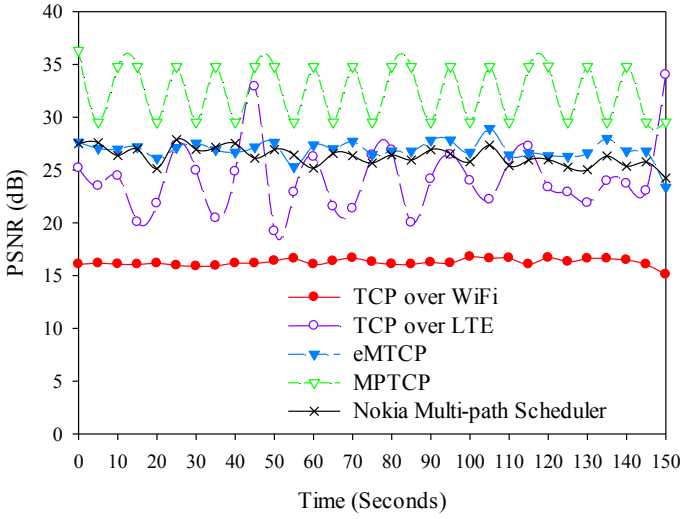

Fig.5.36. Estimated PSNR of single-path TCP, MPTCP, eMTCP and the Nokia Multi-path Scheduler approaches.

The transmission performance in the four cases is also evaluated in terms of the estimated lifespan of device battery, as shown in Table 5.10. By using TCP over LTE there is with 8.71 times shorter battery lifespan in comparison with the duration when employing Wi-Fi, but the signal coverage is much larger than in the Wi-Fi case. When both Wi-Fi and LTE interfaces are used for multipath data transmissions, it is clear that using eMTCP has a 16.51% improvement on the battery lifespan in comparison with the original MPTCP. Although the battery lifespan of eMTCP is approximately 25% shorter than the Nokia multi-path scheduler, the bandwidth benefit of eMTCP overcomes the latter.

TABLE 5.10 PERFORMANCE EVALUATION OF THE TRANSPORT LAYER PROTOCOLS

	TCP over WiFi	TCP over LTE	eMTCP	MPTCP	Nokia Multi-path Scheduler
Energy Consumption Rate (Watts)	0.052	0.505	0.539	0.628	0.402
Average Throughput (Mbps)	0.846	0.934	1.910	1.951	1.341
PSNR (dB)	16.274	23.964	27.029	32.572	26.285
PSNR Standard Deviation	0.263	2.815	0.690	2.712	0.881
Estimated Battery Life-span (Seconds)	5769.23	594.06	556.59	477.71	746.27

5.7 eMTCP-BT Testing Scenarios and Performance Analysis

5.7.1 eMTCP-BT Testing Scenarios

The four types of application traffic: (1) video streaming; (2) VoIP service; (3) web browsing; and (4) file downloading are used as traffic input for testing. In the simulation the application traffic is generated from packet trace files which are captured with the Wireshark software [113] during real data delivery scenarios. The detailed parameters of the four application traffic types are listed in Table 5.11 together with those of the network topology shown in Figure 5.5.

TABLE 5.11 DETAILS OF SIMULATION PARAMETERS OF EMTCP-BT SCENARIOS

Application Type	VoIP	Web Browsing	Video Streaming	File Downloading
Traffic Description	5-min Skype voice session	5-min surfing the Internet webpages	5-min online video clip playing on YouTube	5-min downloading large file from remote server via HTTP
Traffic Burst Level	High		Low	
Average Data Rate (Mbps)	0.06	0.01	2	1
Average Packet Size (Bytes)	150	600	1460	1540
Traffic Duration (s)	300	300	300	300
Distance between data sender and receiver (m)	60	60	60	60
Initial Battery capacity (Joule)	300	300	300	300

The following three scenarios are designed for performance assessment in terms of energy efficiency of the traffic distribution between the LTE and Wi-Fi channels:

- *Scenario D1*: uses 300-second high bursty traffic: VoIP and web browsing. The average bit rate is 60 Kbps for VoIP and 10 Kbps for web browsing. The average packet size is 150 bytes for VoIP and 600 bytes for web browsing.
- *Scenario D2*: makes use of 300-second low bursty traffic: video streaming and file downloading. The average bit rate is 2 Mbps for video streaming and 1 Mbps for file downloading. The average packet size is 1460 bytes and 1540 bytes, respectively.
- *Scenario D3*: contains 300-second traffic of all the four types already described in

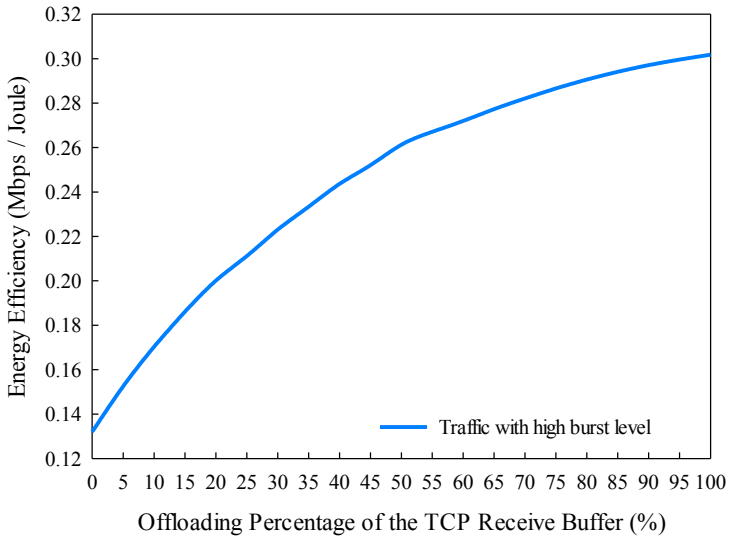

Fig.5.37. Change of average energy efficiency according to change of off-loading amount for high bursty traffic

scenarios *D1* and *D2* and with the same settings.

In each of the three scenarios, the traffic performance measured in terms of energy efficiency is evaluated for MPTCP, eMTCP and eMTCP-BT as transport layer protocols in turn.

5.7.2 eMTCP-BT Performance Analysis

Similar with eMTCP, the performance of eMTCP-BT is evaluated in terms of the energy efficiency on the smartphone, with different burstiness levels of application traffic investigated in the three scenarios described in section 5.7.1. In the three test scenarios, the traffic off-loading percentage ranges between 0% and 100%. eMTCP uses a fixed off-loading percentage of approximately 24% between LTE and Wi-Fi regardless of traffic burstiness level, which is non-optimal in terms of energy efficiency, while eMTCP-BT determines the optimal percentage. The original MPTCP protocol performs no traffic off-loading.

Figure 5.37 shows how the energy efficiency increases when the traffic off-loading percentage increases from 0% (i.e. no traffic off-loading) to 100%. In this case, the employment of eMTCP-BT (with the 100% optimal off-loading percentage in this scenario) results in 91.68% and 15.95% improvement in energy efficiency in comparison with MPTCP and eMTCP, respectively, as shown in Figure 5.38.

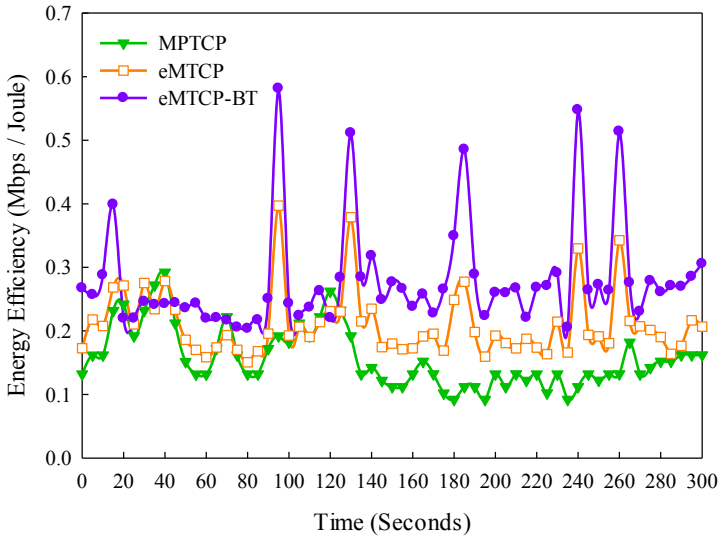

Fig.5.38. Energy efficiency of MPTCP, eMTCP and eMTCP-BT for high bursty traffic

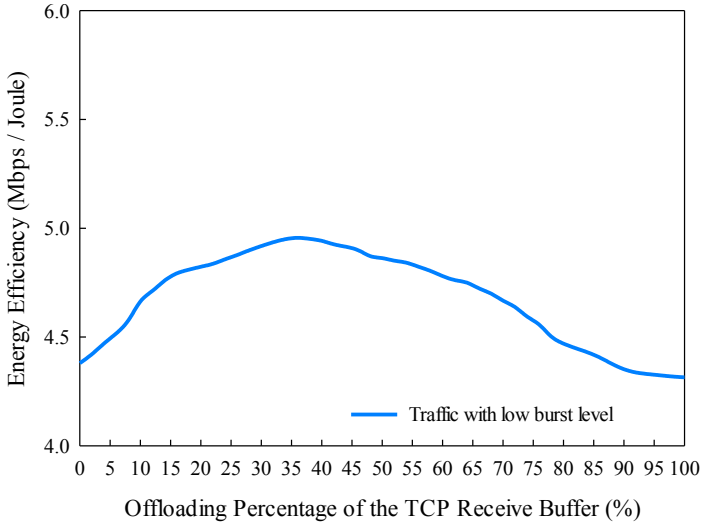

Fig.5.39. Change of average energy efficiency according to change of off-loading amount for low bursty traffic

The same investigation is performed in the second scenario for the low bursty applications. Figure 5.39 shows how the energy efficiency increases when the traffic off-loaded from LTE to Wi-Fi increases from 0% to approximately 36%. When the off-loading percentage grows from 36% to 100%, the energy efficiency decreases as the data size allocated to the Wi-Fi link exceeds its capacity and causes overall traffic throughput reduction. As a result, in this scenario, the optimal traffic off-loading percentage from LTE to Wi-Fi determined by eMTCP-BT is 36%. As shown in Figure 5.40, in this case the energy efficiency of using eMTCP-BT is with 43.45% and 5.77% better than those of MPTCP and eMTCP, respectively.

The benefit of deploying eMTCP-BT in the third scenario is indicated in Figure 5.42. The energy efficiency increases with 22.69% and 10.32% in comparison with MPTCP and

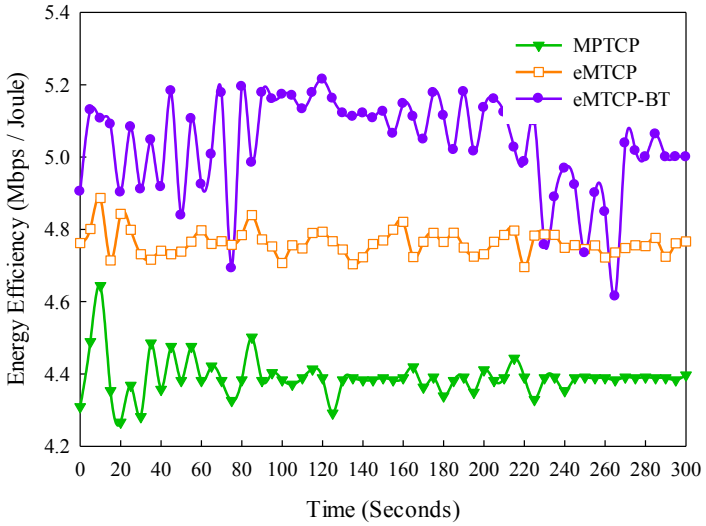

Fig.5.40. Energy efficiency of MPTCP, eMTCP and eMTCP-BT for low bursty traffic

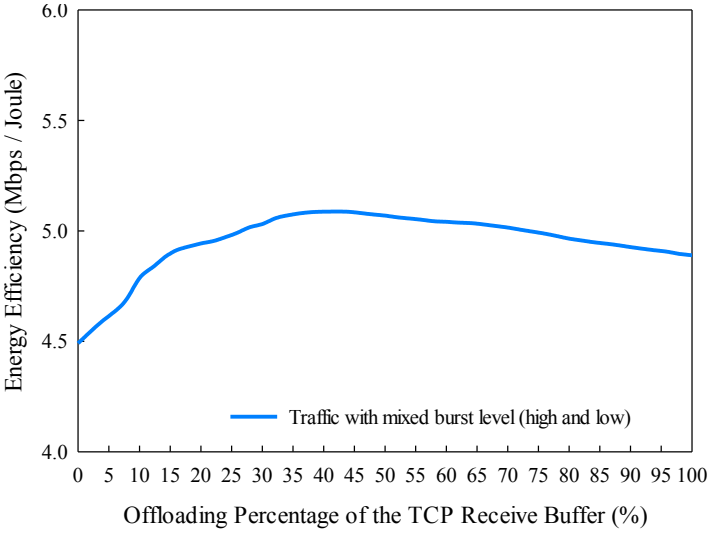

Fig.5.41. Change of average energy efficiency according to change of off-loading amount for mixed bursty traffic

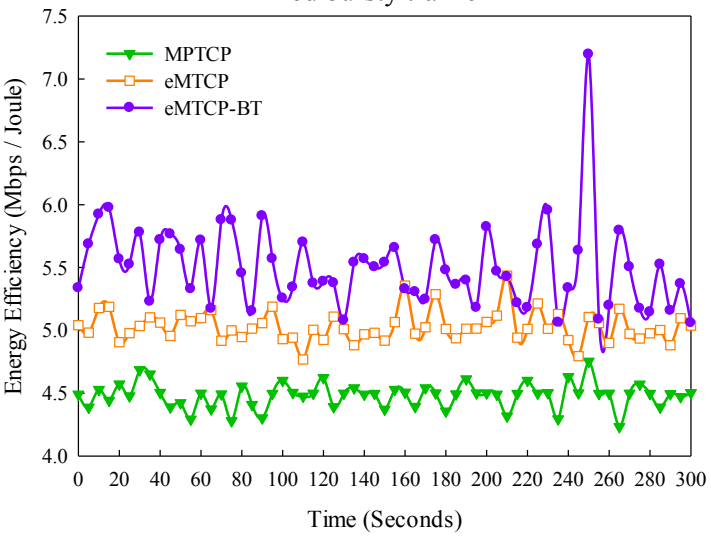

Fig.5.42. Energy efficiency of MPTCP, eMTCP and eMTCP-BT for mixed bursty traffic

eMTCP, respectively. Similar to the case in the second scenario, at approximately 42% of the

TABLE 5.12 PERFORMANCE EVALUATION IN TERMS OF ENERGY EFFICIENCY FOR EMTCP-BT, EMTCP AND MPTCP

Scenario	**Scenario 1 – Traffic with high burstiness level**		**Scenario 2 – Traffic with low burstiness level**		**Scenario 3 – Traffic with mixed burstiness level**	
Transport-layer Protocol	**Average Energy Efficiency (Mbps/Joule)**	**Traffic Off-loading Percentage (%)**	**Average Energy Efficiency (Mbps/Joule)**	**Traffic Off-loading Percentage (%)**	**Average Energy Efficiency (Mbps/Joule)**	**Traffic Off-loading Percentage (%)**
MPTCP	0.1574	0	4.390	0	4.483	0
eMTCP	0.2104	24	4.763	24	5.031	24
eMTCP-BT	0.3018	100	5.038	36	5.499	42

data queued in the TCP receiver buffer, the energy efficiency reaches the maximum level, which is determined by eMTCP-BT. Moreover, as the high bursty traffic is mixed with the low bursty traffic, the optimal traffic off-loading percentage increases (as seen in in Figure 5.41 in comparison with Figure 5.39) due to the influence from the growing tendency of the optimal traffic off-loading percentage for the high bursty traffic.

The benefit in terms of energy efficiency in the three scenarios is concluded in Table 5.12. It is obvious that applications with different burstiness level significantly affect the optimal traffic off-loading percentage. The results show clearly how significant energy saving is achieved with no negative effect in terms of quality of service (i.e. the throughput has not been affected) when eMTCP-BT determines the optimal traffic off-loading percentage.

5.8 Chapter Summary

This chapter presents the settings of simulation-based test environment of the proposed solutions introduced in Chapter 4. Scenarios with different settings of condition parameters are designed for the validation of the proposed wireless network topology which involves the usage of the wireless mesh network and the cellular network. In simulation environments for the mesh-based solutions (AOC-MAC and E-Mesh), comparison with the existing IEEE 802.11s protocol and two corresponding mesh network solutions are provided in terms of energy saving and QoS performance of mesh routers. Likewise, in simulation environments for the MPTCP-based solutions (eMTCP and eMTCP-BT), comparison with the existing MPTCP protocol and a MPTCP-based scheduler solution are provided in terms of benefits on energy efficiency of the smartphone.

CHAPTER 6

Experimental Testing: Environment Set-up and Test Result Analysis

Abstract

This chapter presents the prototyping-based experimental tests which further assess the four proposed solutions: (1) AOC-MAC; (2) E-Mesh; (3) eMTCP and (4) eMTCP-BT, and the corresponding results. In Chapter 5, the performance of the four proposed solutions has been evaluated by network modeling and simulations. The same network topologies and similar tests were implemented in the real-life test-bed introduced in this chapter. The performance of the four proposed solutions is evaluated via both objective and subjective tests.

6.1 Introduction

In this thesis, the mesh-network-based solutions AOC-MAC and E-Mesh provide energy savings at mesh routers and maintain good transmission quality levels, while the multi-path heterogeneous-wireless-network-based solutions eMTCP and eMTCP-BT offer energy efficiency awareness which balances energy consumption and transmission quality at end user mobile devices. The simulation-based tests presented in Chapter 5 have provided performance evaluation for all the four solutions in terms of energy consumption rate, transmission QoS parameters (e.g. loss rate, delay) and estimated transmission quality. Although quality metrics such as MSSSIM and PSNR were used in the simulation-based tests, quality evaluation based on actual measurements and perceptual evaluation performed is to confirm the simulation results. For this purpose, real-life test-beds have been set-up and prototyping of the four proposed solutions have been done.

This chapter focuses on the performance evaluation of the four solutions in terms of the video delivery quality. For each solution, several video clips are transmitted over the corresponding wireless network environment to an end-user mobile device (a smartphone). The delivered video clips are saved at the smartphone and evaluated using objective and subjective

video quality assessment metrics.

This chapter is structured as follows. First, the real-life test-bed set-up process is presented in details, including the topology set-up, equipment and software used, solution prototype implementation and video clip information. Next, the network-delivered video clips at the smartphone are evaluated in terms of objective and subjective video quality assessment metrics. Finally, the evaluation results are compared with the simulation-based results and the fairness of the evaluation is assessed.

6.2 Experimental Test-Bed Set-up

6.2.1 General Topology

In this context, the prototyping of the four solutions is performed via emulation and makes use of the NS-3 Tap Bridge [114] mechanism, which is provided as a particular NS-3 module. This enables the integration of real-life Internet hosts into NS-3 simulations. The Tap Bridge module connects the inputs and outputs of a virtual NS-3 device to the inputs and outputs of a real-life network device, generating a link between two communicating net devices with the traffic delivered over the NS-3 topology. In general, three basic operating modes are used in the NS-3 Tap Bridge module:

- *ConfigureLocal*: In this mode the configuration of the tap device is NS-3 configuration-centric. Configuration information is taken from a device in the NS-3 simulation and a tap device matching the NS-3 attributes is automatically created. In this case, a host is made to appear as if it was directly connected to a simulated NS-3 network.
- *UseLocal*: This mode works in a similar principle with the *ConfigureLocal* mode. The difference is that an existing tap device previously created and configured by the user is used for building the connection between the virtual simulation node and the actual net device.
- *UseBridge*: In this mode, the module makes use of an existing configuration to create the connection between the virtual simulation node and the actual net device. The configuration is done by logically extending a Linux bridge to the NS-3 simulation topology.

In the tests of this thesis, the *ConfigureLocal* mode is used.

Using the NS-3 Tap Bridge module, the emulation test-bed topology is illustrated in Figure 6.1, and consists of a multimedia server, a client host machine and the "Bridge" host located between the server host and the client host. The multimedia server host and the client host are installed with one single Ethernet card. The "Bridge" host is installed with two Ethernet cards *Eth0* and *Eth1*, connected to the multimedia server host and the client host using Ethernet cables, respectively. For each of the four solutions in this thesis, the NS-3 implementation is deployed at the "Bridge" host, in which the NS-3 server node in the simulation topology is connected with the multimedia server host and the NS-3 client node in the simulation topology is connected with the client host, using the Tap Bridge module. This ensures that the solution implementation has impact on the traffic delivery from the multimedia server host to the client host. Figure 6.2 further presents the photo of the test-bed based on the topology illustrated in Figure 6.1.

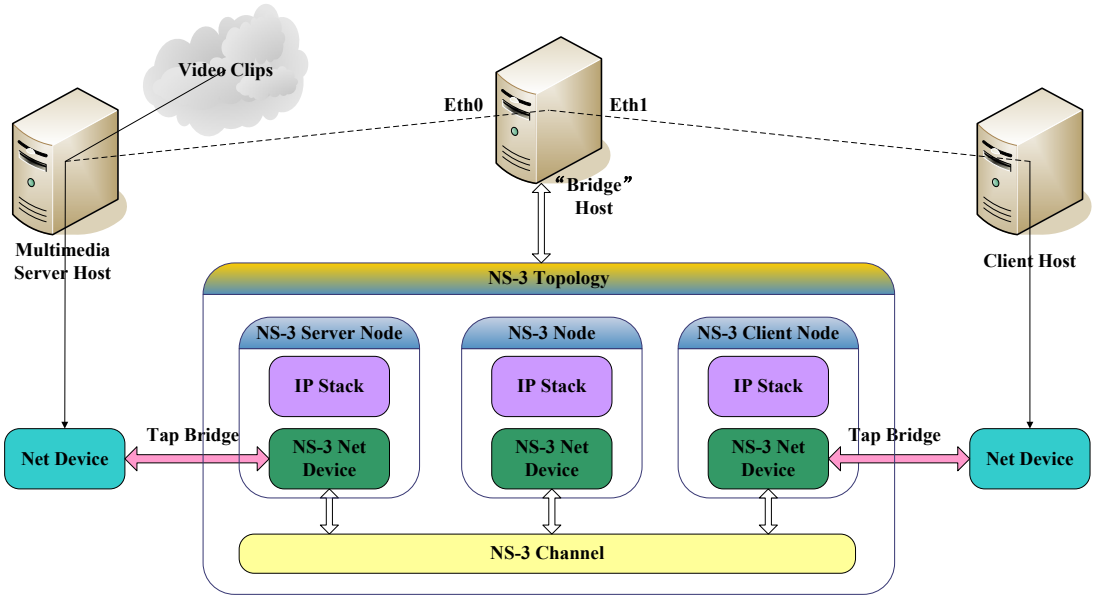

Fig.6.1. Experimental real-life test-bed topology used

6.2.2 Equipment and Software Specifications

The hardware equipment involved in the tests is listed below:

- *Multimedia server host*: a desktop with Ubuntu 12.04, Intel Core i7-3770 at 3.48GHz and NetXtreme BCM5722 Gigabit Ethernet PC card
- *Client host*: a desktop with Ubuntu 12.04, Intel Core i7-3770 at 3.48GHz and NetXtreme BCM5722 Gigabit Ethernet PC card

Fig.6.2. Photo of the real test bed environment

- *"Bridge" host*: a desktop with Ubuntu 12.04, Intel Core i7-3770 at 3.48GHz and two Ethernet cards:
  - NetXtreme BCM5722 Gigabit Ethernet PC
  - 82579LM Gigabit Network Connection
- *2 KRONE PremisNET CATEGORY 5e Ethernet cables*

The software used in the tests is listed below:

- *Video LAN Client (VLC)*[1]: an open-source video player supporting multiple operating systems and most of the existing codecs. VLC is deployed at both the multimedia server host and the client host, used for video traffic sending and receiving.
- *MSU Video Quality Measurement Tool* [111]: an objective video quality assessment software which supports most of the objective video quality assessment metrics such as PSNR, MSE, VQM and MSSSIM. It requires the original video and the delivered video to be simultaneous inputs of the video quality assessment metrics.

6.2.3 Video Sequences

[1] Video LAN Client – http://www.videolan.org/vlc

As presented in Chapter 5, the simulation-based tests of AOC-MAC have investigated the impact of different data rates on performance, involving video streams with different parameters. Accordingly, for the experimental test of AOC-MAC in this chapter, four video sequences are used as the original video source stored in the multimedia server host, with the characteristics illustrated in Table 6.1. For the experimental tests of E-Mesh and eMTCP, video sequence 2 in Table 6.1 is selected as the original video source.

TABLE 6.1VIDEO CLIPS DELIVERED FOR REAL-LIFE TEST-BED

Video Sequence Number	Duration (seconds)	Encoding Codec	Audio Codec	Overall Bit Rate (Kbps)	Resolution (pixels×pixels)	Frame Rate (fps)	Color Space
1	666	MPEG4	MPEG	308	352×288	30	YUV
2	399	MPEG4	Audio	1026	576×240	25	YUV
3	841	MPEG4	138 Kbps	2000	1920×1040	23.976	YUV
4	1529	MPEG4	48 KHz	1339	1280×720	23.976	YUV

The simulation-based test of eMTCP-BT presented in Chapter 5 involves different types of applications (i.e., video streaming, VoIP, web browsing and file downloading). As there are no common quality assessment metrics for the VoIP, web browsing and file downloading services, only the quality assessment of video streaming is considered for eMTCP-BT in this thesis. eMTCP-BT also uses the video sequence 2 in Table 6.1 as the original video source.

6.3 Experimental Scenarios

The video delivery performance of the four solutions (AOC-MAC, E-Mesh, eMTCP and eMTCP-BT) is assessed in real-life tests. In the simulation-based tests presented in Chapter 5, comparison in terms of performance is made between AOC-MAC, S-MAC and the IEEE 802.11s MAC protocol; E-Mesh and the IEEE 802.11s routing protocol; eMTCP, MPTCP, TCP and the Nokia Multi-path Scheduler; and finally eMTCP-BT, eMTCP and MPTCP, with impacts caused by different tested conditions. Therefore, the test scenarios for real-life tests for the four solutions are designed similarly.

6.3.1 Experimental Scenarios for AOC-MAC

To investigate the video transmission quality of AOC-MAC, the following test cases are designed:

- *Case A1*: The four video clips are delivered from the multimedia server host to the

client host, offering different data rates. The corresponding NS-3 AOC-MAC scenarios described in section 5.4.1 are deployed and simulated on the "Bridge" host.

- *Case A2*: The video sequence 2 in Table 6.1 is delivered from the multimedia server host to the client host. The corresponding NS-3 AOC-MAC scenario described in section 5.4.2 is deployed and simulated on the "Bridge" host, with different settings of mesh router numbers.
- *Case A3*: The video sequence 2 in Table 6.1 is delivered from the multimedia server host to the client host. The corresponding NS-3 AOC-MAC scenario described in section 5.4.3 is deployed and simulated on the "Bridge" host, with different settings of mesh router mobility.

6.3.2 Experimental Scenarios for E-Mesh

To investigate the video transmission quality of E-Mesh, the following test cases are designed:

- *Case B1*: The video sequence 2 in Table 6.1 is delivered from the multimedia server host to the client host. The corresponding NS-3 E-Mesh scenario described in section 5.5.3 is deployed and simulated on the "Bridge" host, with different settings of the traffic load weight and the mesh router mobility set to as follows:
  - *Static*: mesh routers have fixed positions.
  - *Randomly Moving*: mesh routers are moving with uniformly distributed speeds and directions.
- *Case B2*: The video sequence 2 in Table 6.1 is delivered from the multimedia server host to the client host. The corresponding NS-3 E-Mesh scenario described in section 5.5.4 is deployed and simulated on the "Bridge" host, with different settings of the remaining energy and the mesh router mobility set to as follows:
  - *Static*: mesh routers have fixed positions.
  - *Randomly Moving*: mesh routers are moving with uniformly distributed speeds and directions.
- *Case B3*: The video sequence 2 in Table 6.1 is delivered from the multimedia server host to the client host. The corresponding NS-3 E-Mesh scenario described

in section 5.5.5 is deployed and simulated on the "Bridge" host, with different settings of the mesh router distance weight and the mesh router mobility set to as follows:

- *Static*: mesh routers have fixed positions.
- *Randomly Moving*: mesh routers are moving with uniformly distributed speeds and directions.

6.3.3 Experimental Scenarios for eMTCP

To investigate the video transmission quality of eMTCP, the following test cases are designed:

- *Case C1*: The video sequence 2 in Table 6.1 is delivered from the multimedia server host to the client host. The NS-3 eMTCP test case 1 described in section 5.6.1 is deployed and simulated on the "Bridge" host.
- *Case C2*: The video sequence 2 in Table 6.1 is delivered from the multimedia server host to the client host. The NS-3 eMTCP test case 2 described in section 5.6.1 is deployed and simulated on the "Bridge" host.
- *Case C3*: The video sequence 2 in Table 6.1 is delivered from the multimedia server host to the client host. The NS-3 eMTCP test case 3 described in section 5.6.1 is deployed and simulated on the "Bridge" host.
- *Case C4*: The video sequence 2 in Table 6.1 is delivered from the multimedia server host to the client host. The NS-3 eMTCP test case 4 described in section 5.6.1 is deployed and simulated on the "Bridge" host.

6.3.4 Experimental Scenarios for eMTCP-BT

- *Case D1*: The video sequence 2 in Table 6.1 is delivered from the multimedia server host to the client host. MPTCP is implemented in the NS-3 topology deployed and simulated on the "Bridge" host.
- *Case D2*: The video sequence 2 in Table 6.1 is delivered from the multimedia server host to the client host. eMTCP is implemented in the NS-3 topology deployed and simulated on the "Bridge" host, with a traffic off-loading percentage of 20%.
- *Case D3*: The video sequence 2 in Table 6.1 is delivered from the multimedia

server host to the client host. eMTCP-BT is implemented in the NS-3 topology deployed and simulated on the "Bridge" host.

6.4 Objective Video Quality Assessment

6.4.1 Objective Video Quality Assessment Metrics

PSNR [42] and MSSSIM [44] are selected as the objective video quality assessment metrics for the delivered video quality in AOC-MAC test scenarios. For the delivered video quality measurement of E-Mesh, eMTCP and eMTCP-BT, PSNR is used. The delivered video quality is affected by QoS parameters such as packet loss and end-to-end delay. In general, higher traffic throughput and lower loss indicate better received video quality, but this is not guaranteed.

Figure 6.3 illustrates the quality of the original and received videos affected by the QoS parameters.

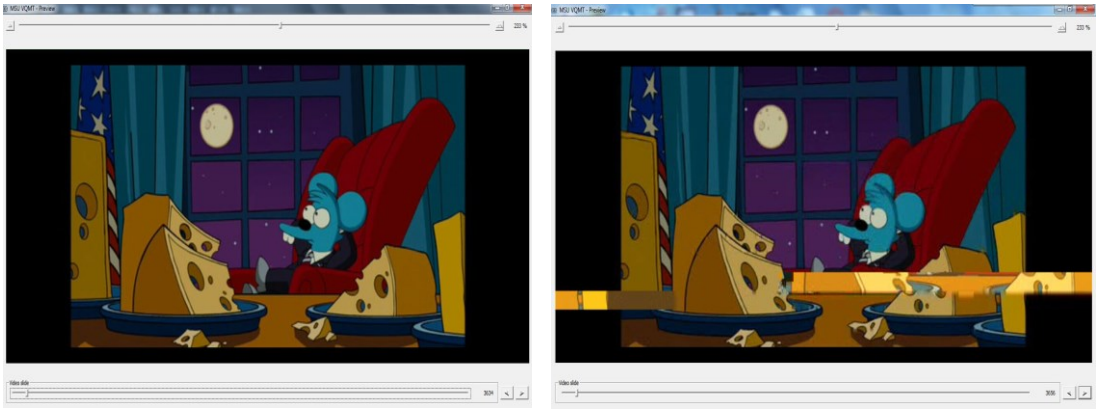

(a) Source video frame (b) Received video frame

Fig.6.3. An example of the quality of the original and received videos

6.4.2 Result Analysis

As mentioned in section 6.3, the experimental tests for each of the four solutions are designed and run individually. Therefore, the separate result analysis is presented accordingly in this section.

6.4.2.1 Result Analysis for the Video Delivery with AOC-MAC

Figure 6.4 and Figure 6.5 illustrate the PSNR and MSSSIM values measured in test case *A1*. Figure 6.4 shows that video delivered with AOC-MAC has slightly lower average PSNR in comparison with the IEEE 802.11s MAC protocol and S-MAC with different data

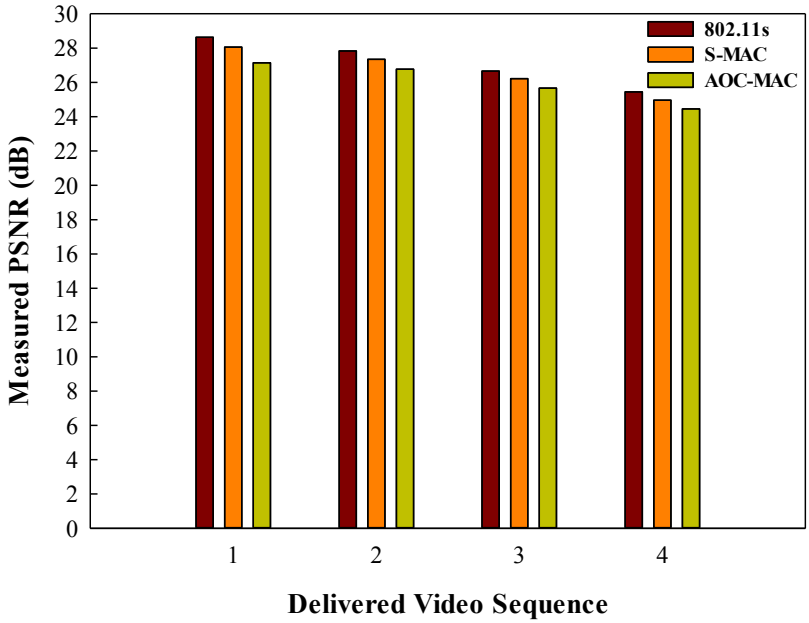

Fig.6.4.PSNR achieved using 802.11s, S-MAC and AOC-MAC with variable data rates

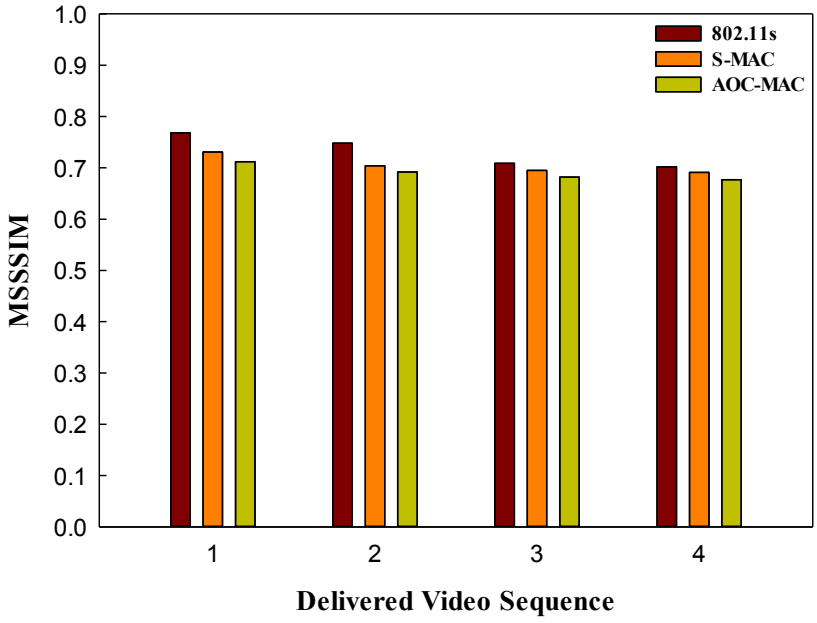

Fig.6.5.MSSSIM achieved using 802.11s, S-MAC and AOC-MAC with variable data rates

rates (1Mbps, 2 Mbps, 5.5 Mbps and 10 Mbps). For example, when the video sequence 1 in Table 6.1 is delivered, the PSNR of AOC-MAC has decreased by approximately 5.2% and 3.3% in comparison with the IEEE 802.11s MAC protocol and S-MAC, respectively. Similar results are illustrated in Figure 6.5, suggesting the 7.3% and 2.6% decrease of the received video quality in terms of MSSSIM when AOC-MAC is used in comparison with the IEEE 802.11s MAC protocol and S-MAC, respectively.

The PSNR and MSSSIM results measured in test case *A2* are illustrated in Figure 6.6

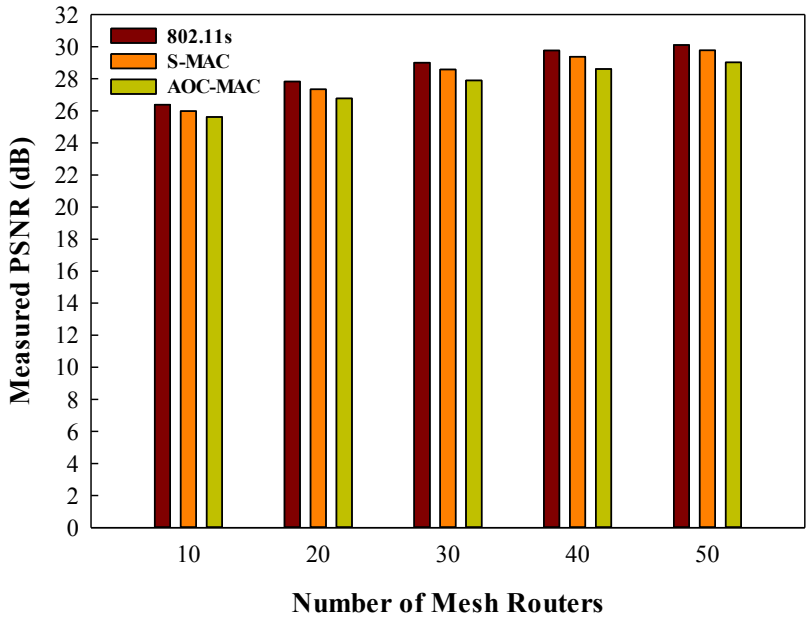

Fig.6.6.PSNR achieved using 802.11s, S-MAC and AOC-MAC with variable mesh router numbers

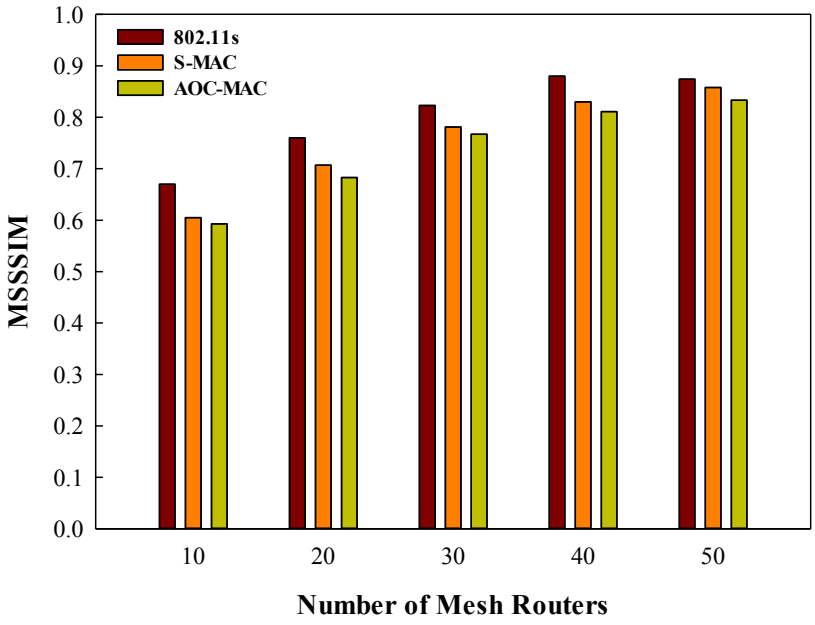

Fig.6.7.MSSSIM achieved using 802.11s, S-MAC and AOC-MAC with variable mesh router numbers

and Figure 6.7. Figure 6.6 shows the increase of the average PSNR of the received videos along with the increase of the number of mesh routers in the simulated mesh network. For different mesh router numbers, the average PSNR of the received videos using AOC-MAC has decreased in comparison with the IEEE 802.11s MAC protocol and S-MAC. For instance, when 20 mesh routers are set in the simulated mesh network, the average PSNR of the received videos using AOC-MAC has decreased 3.8% and 2.1% compared against the IEEE 802.11s MAC protocol

and S-MAC, respectively. In Figure 6.7, the average MSSSIM of the received videos increases along with the increase of the number of mesh routers in the simulated mesh network. Also, the MSSSIM decrease of AOC-MAC in comparison with the other two MAC protocols is shown in Figure 6.7. For instance, the decrease of the average MSSSIM of the received videos using AOC-MAC is roughly 10.1% in comparison with the IEEE 802.11s MAC protocol and 3.4% in comparison with S-MAC.

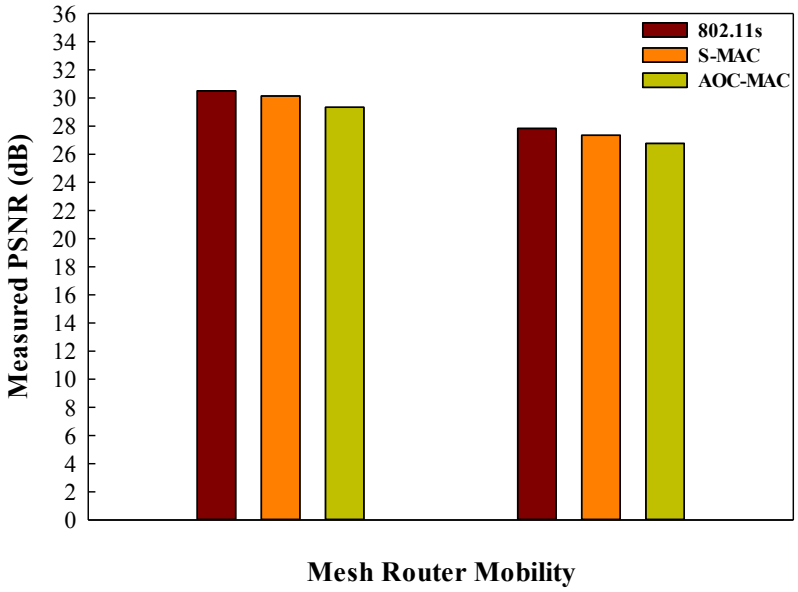

Fig.6.8.PSNR achieved using 802.11s, S-MAC and AOC-MAC with variable mesh router mobility

Figure 6.8 and Figure 6.9 illustrate the PSNR and MSSSIM values measured in test case *A3*. It is shown in Figure 6.8 that when the mesh routers are randomly moving, the video delivered with the three MAC solutions has lower average PSNR than when the mesh routers are static. When 802.11s is used, the PSNR of the received video has 8.7% decrease when the mesh routers are randomly moving compared against when the mesh routers are static. When S-MAC is used, the PSNR of the received video has 9.3% decrease when the mesh routers are randomly moving compared against when the mesh routers are static. When AOC-MAC is used, the PSNR of the received video has 8.6% decrease when the mesh routers are randomly moving compared against when the mesh routers are static. In general, AOC-MAC has approximately 3.8% and 2.7% lower average PSNR in comparison with the IEEE 802.11s MAC protocol and S-MAC when the mesh routers are static, respectively. When the mesh routers are moving,

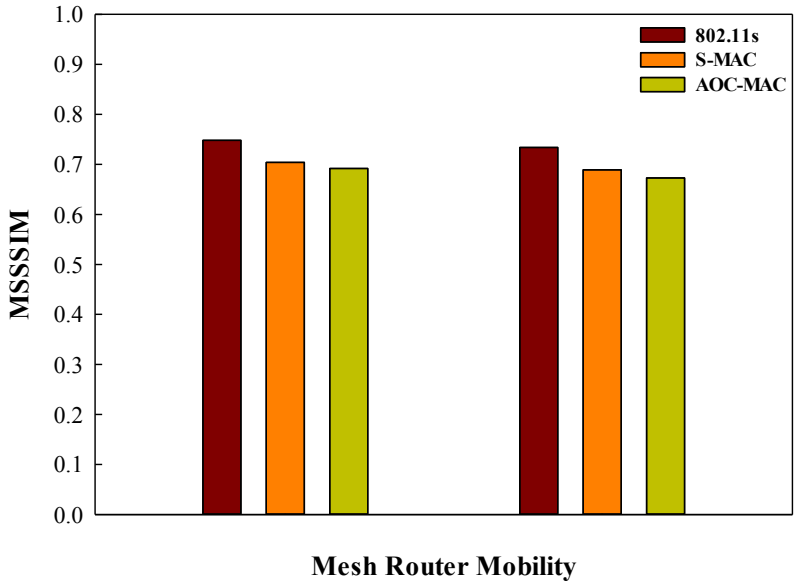

Fig.6.9.MSSSIM achieved using 802.11s, S-MAC and AOC-MAC with variable mesh router mobility

AOC-MAC has approximately 3.8% and 2.1% lower average PSNR in comparison with the IEEE 802.11s MAC protocol and S-MAC, respectively. Similar comparison in terms of MSSSIM is shown in Figure 6.9. When 802.11s is used, the MSSSIM of the received video has 1.87% decrease when the mesh routers are randomly moving compared against when the mesh routers are static. When S-MAC is used, the MSSSIM of the received video has 2.13% decrease when the mesh routers are randomly moving compared against when the mesh routers are static. When AOC-MAC is used, the MSSSIM of the received video has 2.89% decrease when the mesh routers are randomly moving compared against when the mesh routers are static. In general, AOC-MAC has approximately 7.5% and 1.7% lower average MSSSIM in comparison with the IEEE 802.11s MAC protocol and S-MAC when the mesh routers are static, respectively. When the mesh routers are moving, AOC-MAC has approximately 8.3% and 2.3% lower average MSSSIM in comparison with the IEEE 802.11s MAC protocol and S-MAC, respectively.

The measured PSNR and MSSSIM values of the received videos for AOC-MAC test cases are concluded in Table 6.2. Although the received video quality is slightly lower on comparison with the IEEE 802.11s MAC protocol and S-MAC, AOC-MAC achieves significant energy savings on the mesh routers according to the simulation test results presented in section 5.4 in Chapter 5.

TABLE 6.2PSNR AND MSSSIM VALUES WITH 802.11S, S-MAC AND AOC-MAC

			802.11s	S-MAC	AOC-MAC	802.11s	S-MAC	AOC-MAC
			PSNR (dB)			MSSSIM (0-1)		
Test Case A1	Data Rate (Mbps)	**1**	28.63	28.06	27.14	0.768	0.731	0.712
		2	27.84	27.34	26.77	0.748	0.704	0.692
		5.5	26.66	26.22	25.67	0.709	0.695	0.682
		10	25.45	24.97	24.46	0.702	0.691	0.677
Test Case A2	Number of Mesh Routers	**10**	26.38	25.98	25.62	0.670	0.605	0.593
		20	27.84	27.34	26.77	0.760	0.707	0.683
		30	29.00	28.58	27.90	0.823	0.781	0.767
		40	29.77	29.38	28.61	0.880	0.830	0.811
		50	30.11	29.77	29.03	0.874	0.858	0.833
Test Case A3	Mesh Router Mobility	**Static**	30.50	30.14	29.34	0.748	0.704	0.692
		Moving	27.84	27.34	26.77	0.734	0.689	0.683

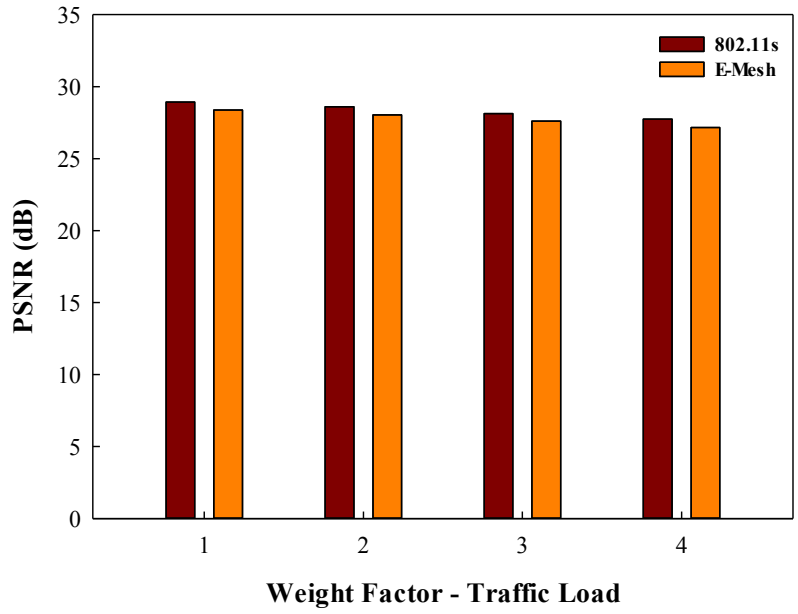

Fig.6.10.PSNR achieved using 802.11s and E-Mesh with variable weights on traffic load when the mesh routers are static

6.4.2.2 Result Analysis for the Video Delivery with E-Mesh

Figure 6.10 and Figure 6.11 illlustrates the measured PSNR results of the received videos for the E-Mesh experimental test case *B1* with different weights on the traffic load, when the mesh routers are static and moving, respectively. In Figure 6.10, when the mesh routers are static, the PSNR of the received video slight decreases along with the increase of the traffic load weight factor value, but in general it remains at a stable level. In this case, the PSNR of the

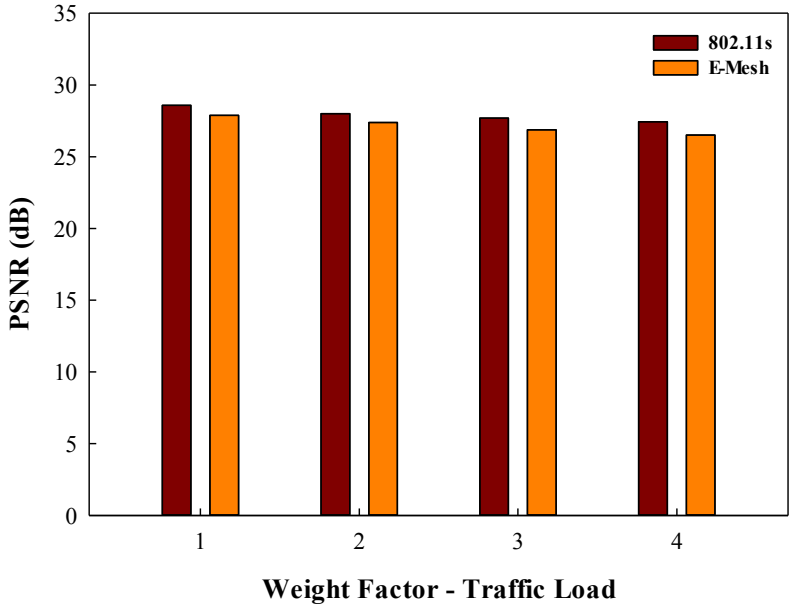

Fig.6.11.PSNR achieved using 802.11s and E-Mesh with variable weights on traffic load when the mesh routers are moving

received video using E-Mesh has decreased approximately 1.9%, 1.95%, 1.85% and 2.09% with the traffic load weight factor value 1.0, 2.0, 3.0 and 4.0, respectively, in comparison with the IEEE 802.11s routing protocol. In Figure 6.11, when the mesh routers are moving, the PSNR of the received video again slight decreases along with the increase of the traffic load weight factor value. In this case, the PSNR of the received video using E-Mesh has decreased approximately 2.4%, 2.17%, 2.96% and 3.35% with the traffic load weight factor value 1.0, 2.0, 3.0 and 4.0, respectively, in comparison with the IEEE 802.11s routing protocol. In general, the average PSNR of the received video is lower when the mesh routers are moving, in comparison with when the mesh routers are static, as the mobility of mesh routers decreases the stability of the network connectivity. With the traffic load weight factor value 1.0, 2.0, 3.0 and 4.0, the PSNR of the received video using the IEEE 802.11s routing protocol is roughly 1.21%, 2.1%, 1.56% and 1.08% lower when the mesh routers are moving, while the PSNR of the received video using E-Mesh is roughly 1.76%, 2.32%, 2.68% and 2.39% lower when the mesh routers are moving.

Figure 6.12 and Figure 6.13 illlustrates the measured PSNR results of the received videos for the E-Mesh experimental test case *B2* with different weights on the remaining energy

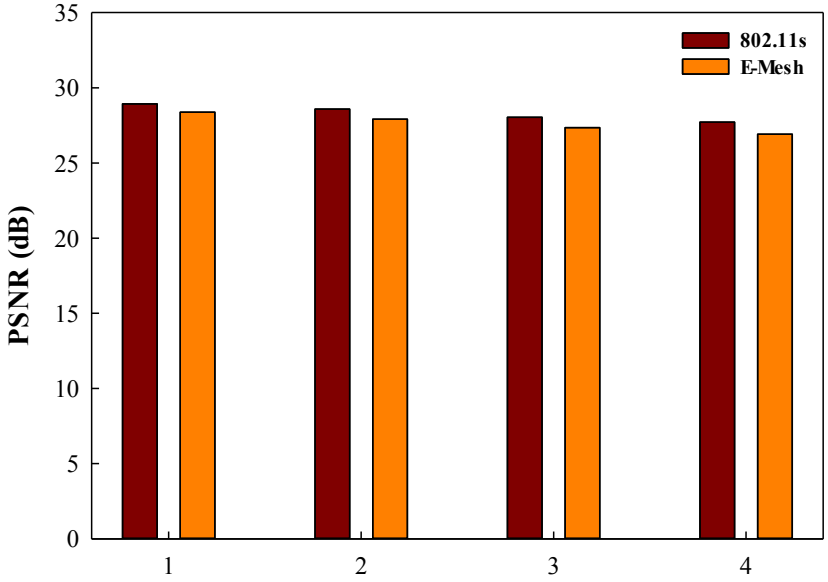

Fig.6.12.PSNR achieved using 802.11s and E-Mesh with variable weights on remaining energy when the mesh routers are static

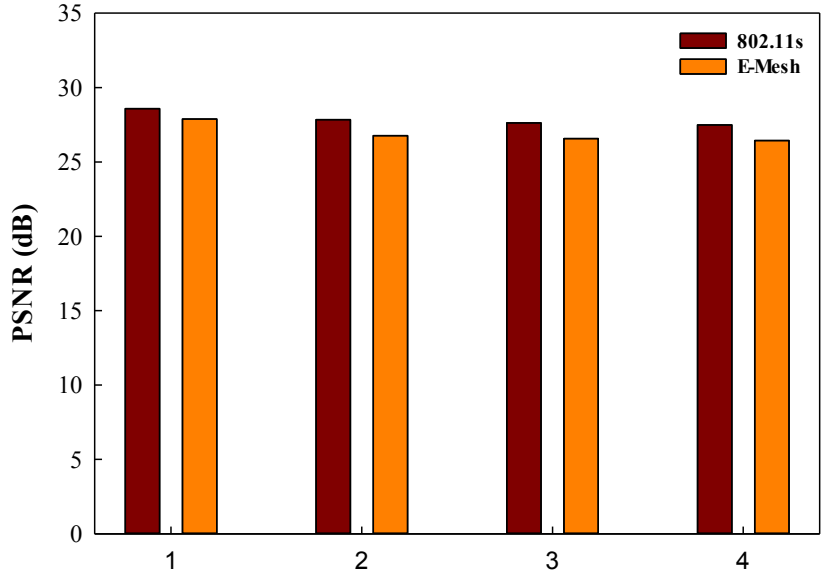

Fig.6.13.PSNR achieved using 802.11s and E-Mesh with variable weights on remaining energy when the mesh routers are moving

of mesh routers, when the mesh routers are static and moving, respectively. In Figure 6.12, when the mesh routers are static, the PSNR of the received video slight decreases along with the increase of the remaining energy weight factor value, but in general it remains at a stable level. In this case, the PSNR of the received video using E-Mesh has decreased approximately 1.9%, 2.32%, 2.46% and 2.89% with the remaining energy weight factor value 1.0, 2.0, 3.0 and 4.0, respectively, in comparison with the IEEE 802.11s routing protocol. In Figure 6.13, when the

mesh routers are moving, the PSNR of the received video again slight decreases along with the increase of the remaining energy weight factor value. In this case, the PSNR of the received video using E-Mesh has decreased approximately 2.4%, 3.84%, 3.83% and 3.82% with the remaining energy weight factor value 1.0, 2.0, 3.0 and 4.0, respectively, in comparison with the IEEE 802.11s routing protocol. In general, the average PSNR of the received video is lower when the mesh routers are moving, in comparison with when the mesh routers are static. With the remaining energy weight factor value 1.0, 2.0, 3.0 and 4.0, the PSNR of the received video using the IEEE 802.11s routing protocol is roughly 1.21%, 2.59%, 1.46% and 0.79% lower when the mesh routers are moving, while the PSNR of the received video using E-Mesh is roughly 1.76%, 4.08%, 2.85% and 1.75% lower when the mesh routers are moving.

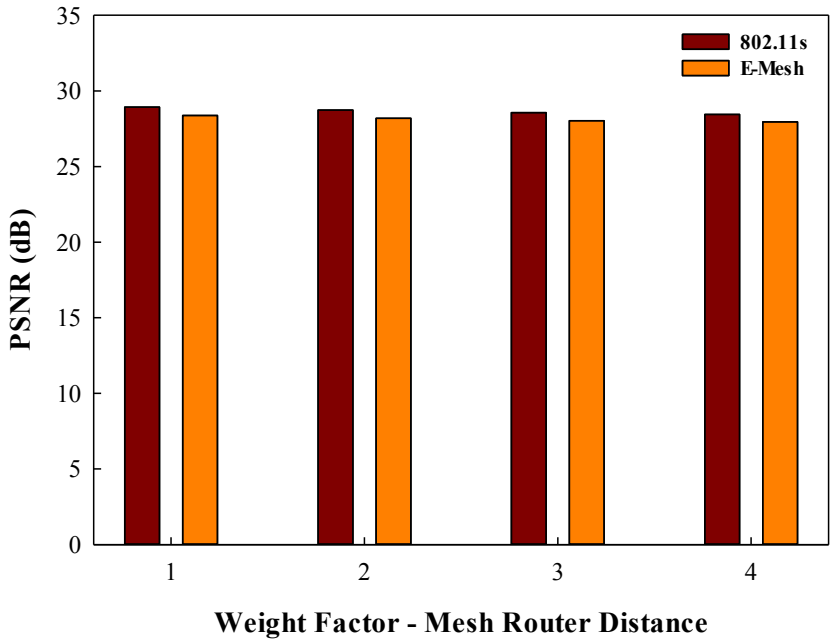

Fig.6.14.PSNR achieved using 802.11s and E-Mesh with variable weights on mesh router distance when the mesh routers are static

Figure 6.14 and Figure 6.15 illlustrates the measured PSNR results of the received videos for the E-Mesh experimental test case *B3* with different weights on the mesh router distance, when the mesh routers are static and moving, respectively. In Figure 6.14, when the mesh routers are static, the PSNR of the received video slight decreases along with the increase of the mesh router distance weight factor value, but in general it remains at a stable level. In this case, the PSNR of the received video using E-Mesh has decreased approximately 1.9%, 1.88%,

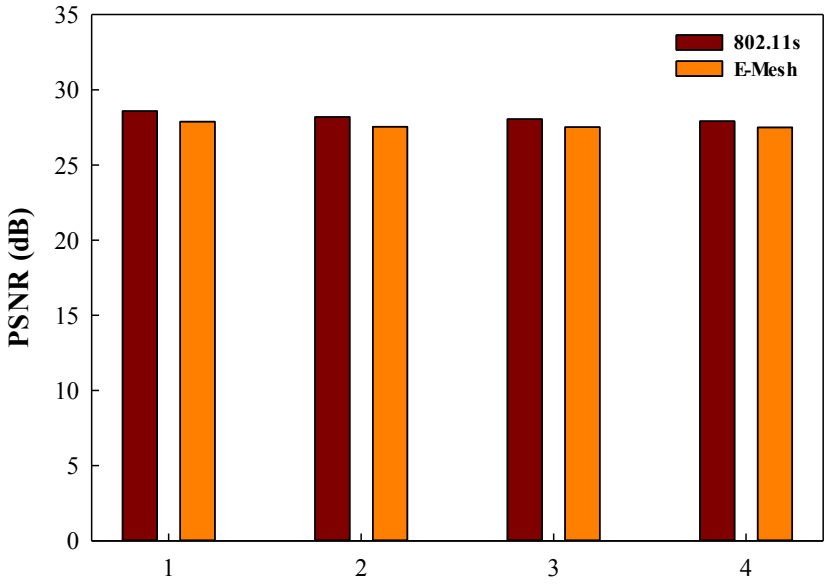

Fig.6.15.PSNR achieved using 802.11s and E-Mesh with variable weights on mesh router distance when the mesh routers are moving

1.86% and 1.76% with the mesh router distance weight factor value 1.0, 2.0, 3.0 and 4.0, respectively, in comparison with the IEEE 802.11s routing protocol. In Figure 6.15, when the mesh routers are moving, the PSNR of the received video again slight decreases along with the increase of the mesh router distance weight factor value. In this case, the PSNR of the received video using E-Mesh has decreased approximately 2.4%, 2.27%, 1.89% and 1.45% with the mesh router distance weight factor value 1.0, 2.0, 3.0 and 4.0, respectively, in comparison with the IEEE 802.11s routing protocol. In general, the average PSNR of the received video is lower when the mesh routers are moving, in comparison with when the mesh routers are static. With the mesh router distance weight factor value 1.0, 2.0, 3.0 and 4.0, the PSNR of the received video using the IEEE 802.11s routing protocol is roughly 1.21%, 1.88%, 1.79% and 1.9% lower when the mesh routers are moving, while the PSNR of the received video using E-Mesh is roughly 1.76%, 2.27%, 1.82% and 1.61% lower when the mesh routers are moving.

The measured PSNR values of the received videos for E-Mesh test cases are concluded in Table 6.3. Although the PSNR values demonstrate the decrease of received video quality when E-Mesh is deployed, good level of energy saving is achieved in comparison with the IEEE 802.11s routing protocol, according to the simulation test results presented in section 5.5 in Chapter 5.

TABLE 6.3 PSNR VALUES WITH 802.11S AND E-MESH

E-Mesh Test Cases			PSNR (dB)			
			802.11s		E-Mesh	
			Static	Moving	Static	Moving
E-Mesh Utility Function Weight Factor	Traffic Load	1.0	28.87	28.42	28.31	27.75
		2.0	28.44	27.82	27.89	27.24
		3.0	28.01	27.54	27.47	26.69
		4.0	27.63	27.28	26.99	26.37
	Remaining Energy	1.0	28.87	28.42	28.31	27.75
		2.0	28.45	27.69	27.74	26.59
		3.0	27.91	27.45	27.19	26.44
		4.0	27.58	27.35	26.73	26.26
	Mesh Router Distance	1.0	28.87	28.42	28.31	27.75
		2.0	28.59	28.02	28.04	27.41
		3.0	28.42	27.88	27.82	27.34
		4.0	28.27	27.72	27.79	27.37

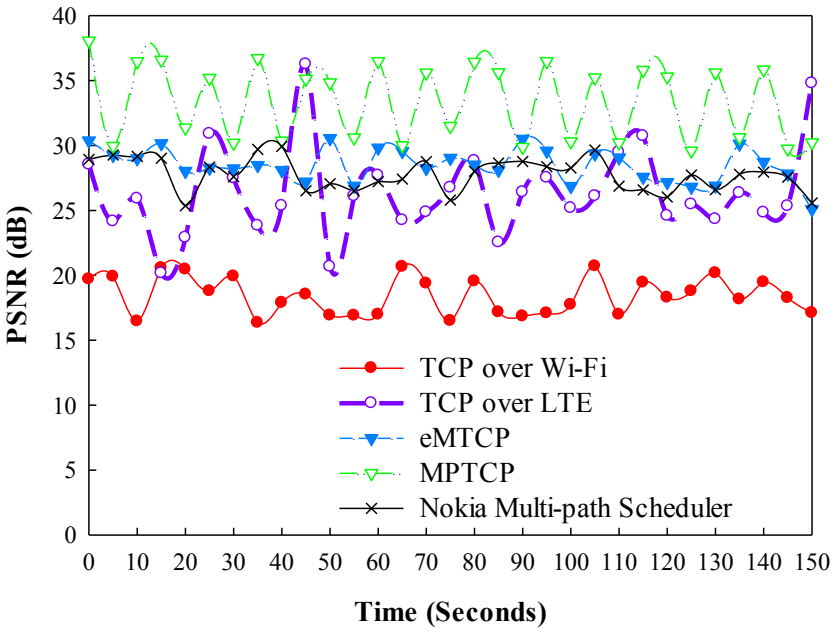

Fig.6.16.PSNR values of eMTCP test cases

6.4.2.3 Result Analysis for the Video Delivery with eMTCP

The measured PSNR values for the eMTCP experimental test cases are illustrated in Figure 6.16 and Table 6.4. As The average measured PSNR of the received video in test case *C4* (in which eMTCP is used) is 35.5% higher in comparison with the average PSNR in test case *C1* (in which TCP is used over Wi-Fi); 7.38% higher in comparison with the average PSNR in test case *C2* (in which TCP is used over LTE); 14.73% lower in comparison with the average

TABLE 6.4 PSNR VALUES WITH EMTCP TEST CASES

	Solution				
	TCP over Wi-Fi	**TCP over LTE**	**MPTCP**	**eMTCP**	**Nokia Multi-path Scheduler**
Average PSNR (dB)	18.42	26.39	33.42	28.50	27.77
Standard Deviation of PSNR	1.434	3.481	2.936	1.306	1.266

PSNR in test case *C3* (in which MPTCP is used over LTE and Wi-Fi); and 2.6% higher in comparison with the average PSNR when using the Nokia multi-path scheduler. The measurement of the standard deviations of the PSNR values indicate that the test scenaio with eMTCP deployed is with less transmission fluctuation in comparison with the scenario with MPTCP deployed. Also, the slight decrease of PSNR does not overcome the energy efficiency improvement when eMTCP is deployed, according to the simulation test results presented in section 5.6 in Chapter 5.

6.4.2.4 Result Analysis for the Video Delivery with eMTCP-BT

The measured PSNR values for the eMTCP experimental test cases are illustrated in Figure 6.17 and Table 6.5. As The average measured PSNR of the received video in test case *D3* (in which eMTCP-BT is used) is 23.2% higher in comparison with the average PSNR in test

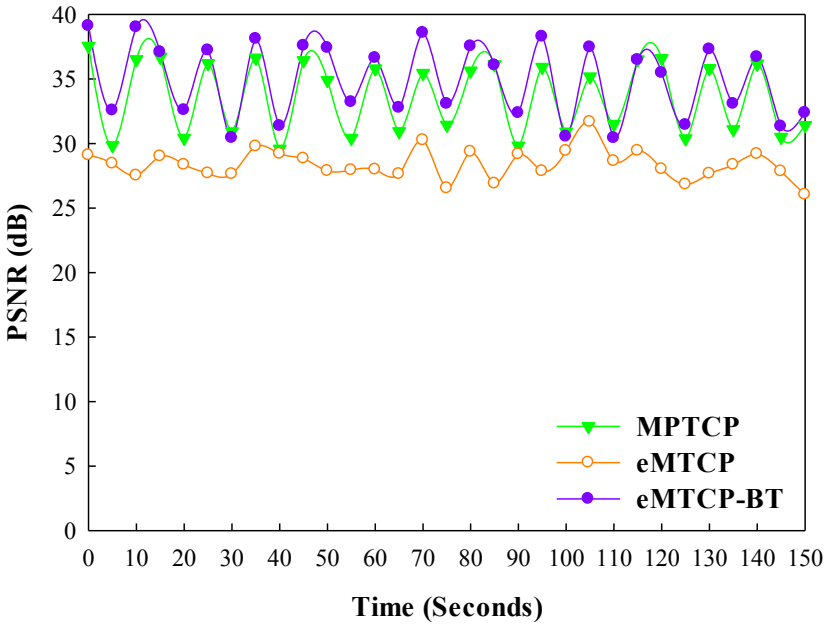

Fig.6.17. PSNR values of eMTCP-BT test cases

TABLE 6.5 PSNR VALUES WITH EMTCP-BT TEST CASES

	Solution		
	MPTCP	**eMTCP**	**eMTCP-BT**
Average PSNR (dB)	33.66	28.39	34.95
Standard Deviation of PSNR	2.837	1.159	3.175

case *D2* (in which eMTCP is used) and 3.83% higher in comparison with the average PSNR in test case *D1* (in which MPTCP is used). The measurement of the standard deviations of the PSNR values indicate that eMTCP-BT results in higher received video quality (and higher energy efficiency as presented in section 5.7 in Chapter 5) in comparison with MPTCP and eMTCP, but also causes higher traffic fluctuation.

6.5 Subjective Video Quality Assessment

In previous sections, objective video quality assessment metrics such as PSNR and MSSSIM are used for measuring the received video quality for the real-life experimental tests. However, the results from the objective video quality assessment metrics do not correlate perfectly with the user perceived quality from human vision, which behaves non-linearly. This section presents the investigation of the performance of the four proposed solutions using subjective video quality assessment. MOS [41] is selected for the subjective video quality measurement. The quality scale for MOS is presented in Table 2.2 in Chapter 2, with the value 5 indicating the "excellent" quality and 1 indicating the "bad" quality. The same four video sequences listed in Table 6.1 are transmitted from the multimedia server host to the client host, over the "Bridge" host where the prototyping of the four proposed solutions are deployed within NS-3. The delivered video clips are obtained based on the same test cases described in the objective video quality assessment in section 6.4.

6.5.1 Subjective Test Set-up

The Absolute Category Rating (ACR) [115] is selected as the methodology used in the subjective tests. This method involves the following manner: 20 users (12 males and 8 females) were invited to watch the video clips received in the test cases in a separate room without any disturbance from outside. The age of each user is distributed between 24 to 40 years old. The occupations of the users include technicians, students, business people, engineer, etc. Each user was required to watch the video clips received in each test case in the order which the cases are

described in section 6.3. After watching all the received video clips, each user was asked to rate the quality of each video clips based on the MOS metric by filling a questionnaire presented to the subjects on papers, which was handed out to the user before watching the video clips. During the subjective test, any video clip presented to a user will never repeat to the same user, in order to prevent user boredom according to the ITU-T Rec.P.911 [116]. This is a well-documented testing methodology also employed in the validation of related solutions in [117] and [118].

Based on the set-up regulated above, video clips received using the prototyping of the four proposed solutions are evaluated by users.

6.5.2 Result Analysis

Similar with the objective test result analysis presented in section 6.4.2, the separate result analysis is presented for each individual proposed solution in this section. The video clips generated in all the test cases for the four proposed solutions are completed by each user. The MOS value for the quality assessment of each video clip is computed as the average value rated from the 20 users.

6.5.2.1 Result Analysis for the Video Delivery with AOC-MAC

Figure 6.18 illustrates the average MOS values measured for test case *A1*, which shows that video delivered with AOC-MAC has slightly lower average MOS in comparison with the IEEE 802.11s MAC protocol and S-MAC with different data rates (1Mbps, 2 Mbps, 5.5 Mbps and 10 Mbps). When the video sequence 1 to 4 in Table 6.1 is delivered, the average MOS of AOC-MAC has decreased by approximately 8.57% and 3.03%; 6.06% and 3.12%; 6.45% and 3.33% and finally 3.45% and 3.57% in comparison with the IEEE 802.11s MAC protocol and S-MAC, respectively. Also, Figure 6.18 shows the decrease of MOS along with the increase of the data rate of the delivered video.

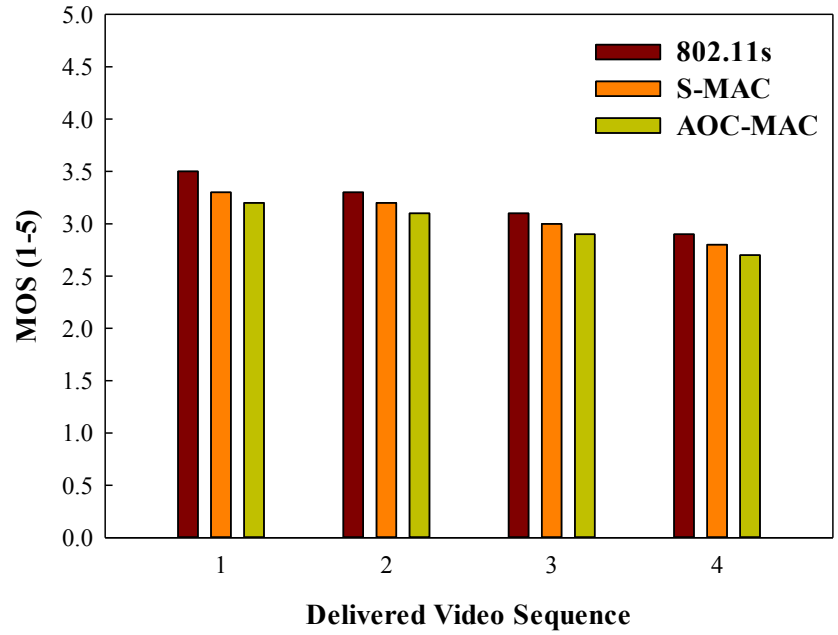

Fig.6.18.MOS achieved using 802.11s, S-MAC and AOC-MAC with variable data rates

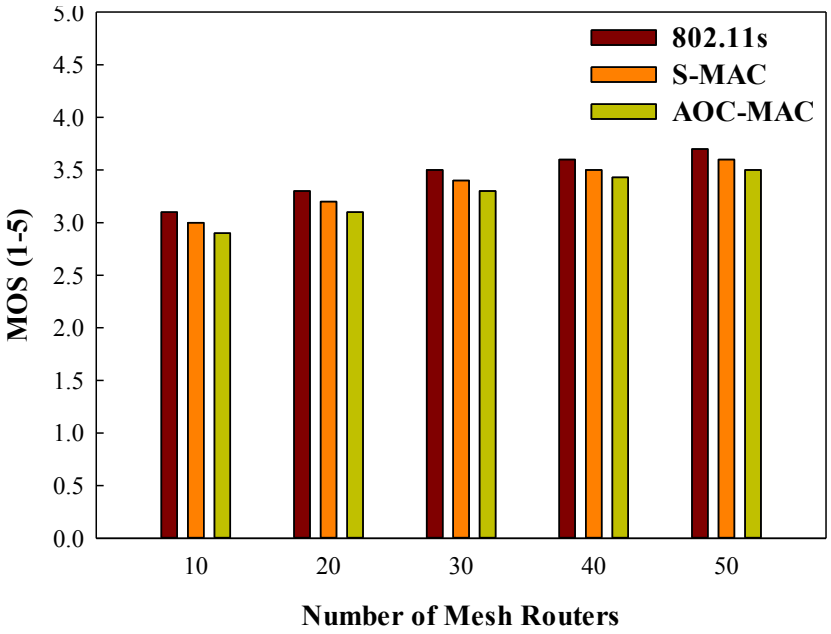

Fig.6.19.MOS achieved using 802.11s, S-MAC and AOC-MAC with variable mesh router numbers

The average MOS values measured in test case *A2* are illustrated in Figure 6.19, which shows the increase of the average MOS of the received videos along with the increase of the number of mesh routers in the simulated mesh network. For different mesh router numbers, the average MOS of the received videos using AOC-MAC has decreased in comparison with the IEEE 802.11s MAC protocol and S-MAC. When 10, 20, 30, 40 and 50 mesh routers are set in the simulated mesh network, the average MOS of the received videos using AOC-MAC has decreased 6.45% and 3.33%; 6.06% and 3.13%; 5.71% and 2.94%; 5.56% and 2.86%; and

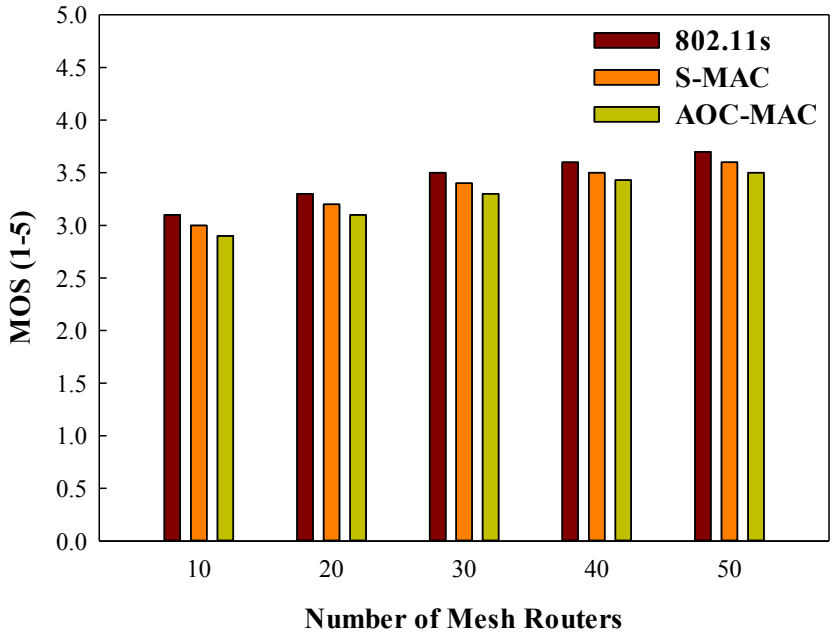

Fig.6.20.MOS achieved using 802.11s, S-MAC and AOC-MAC with variable mesh router mobility

finally 5.41% and 2.78% compared against the IEEE 802.11s MAC protocol and S-MAC, respectively. Also, Figure 6.19 shows the decrease of MOS along with the increase of the data rate of the delivered video. It is clear that the impact of AOC-MAC on the decrease of received video quality is less significant with higher number of mesh routers.

Figure 6.20 illustrates the MOS values measured in test case *A3*, which shows that when the mesh routers are randomly moving, the video delivered with the three MAC solutions has lower average MOS than when the mesh routers are static. When 802.11s is used, the MOS of the received video has 13.16% decrease when the mesh routers are randomly moving compared against when the mesh routers are static. When S-MAC is used, the MOS of the received video has 13.51% decrease when the mesh routers are randomly moving compared against when the mesh routers are static. When AOC-MAC is used, the MOS of the received video has 11.43% decrease when the mesh routers are randomly moving compared against when the mesh routers are static. In general, AOC-MAC has approximately 7.89% and 5.41% lower average MOS in comparison with the IEEE 802.11s MAC protocol and S-MAC when the mesh routers are static, respectively. When the mesh routers are moving, AOC-MAC has approximately 6.06% and 3.13% lower average PSNR in comparison with the IEEE 802.11s MAC protocol and S-MAC, respectively.

TABLE 6.6 MOS VALUES WITH 802.11S, S-MAC AND AOC-MAC

			802.11s	S-MAC	AOC-MAC
			MOS (1-5)		
Test Case A1	Data Rate (Mbps)	**1**	3.5	3.3	3.2
		2	3.3	3.2	3.1
		5.5	3.1	3.0	2.9
		10	2.9	2.8	2.7
Test Case A2	Number of Mesh Routers	**10**	3.1	3.0	2.9
		20	3.3	3.2	3.1
		30	3.5	3.4	3.3
		40	3.6	3.5	3.4
		50	3.7	3.6	3.5
Test Case A3	Mesh Router Mobility	**Static**	3.8	3.7	3.5
		Moving	3.3	3.2	3.1

The measured MOS values of the received videos for AOC-MAC test cases are concluded in Table 6.6. Although the received video quality is slightly lower on comparison with the IEEE 802.11s MAC protocol and S-MAC, AOC-MAC achieves significant energy savings on the mesh routers according to the simulation test results presented in section 5.4 in Chapter 5.

6.5.2.2 Result Analysis for the Video Delivery with E-Mesh

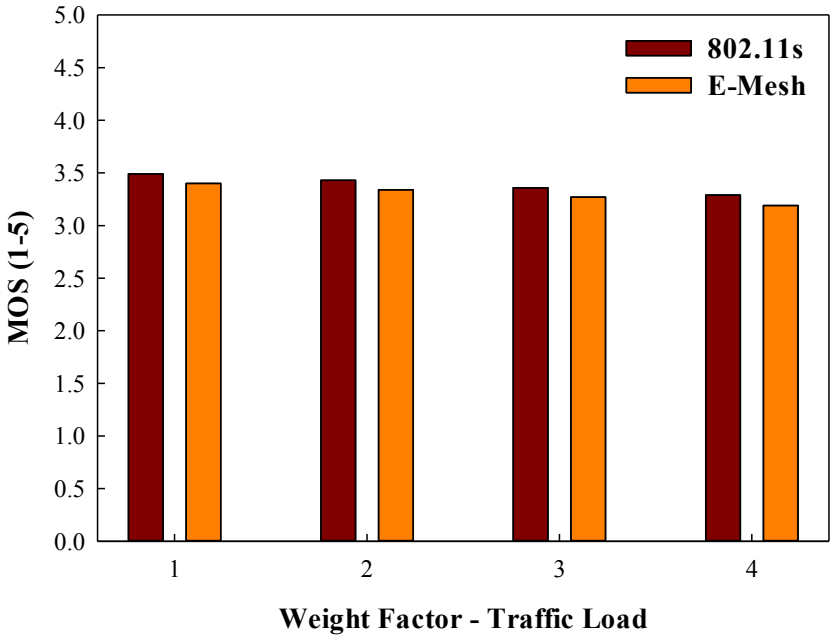

Fig.6.21.MOS achieved using 802.11s and E-Mesh with variable weights on traffic load when the mesh routers are static

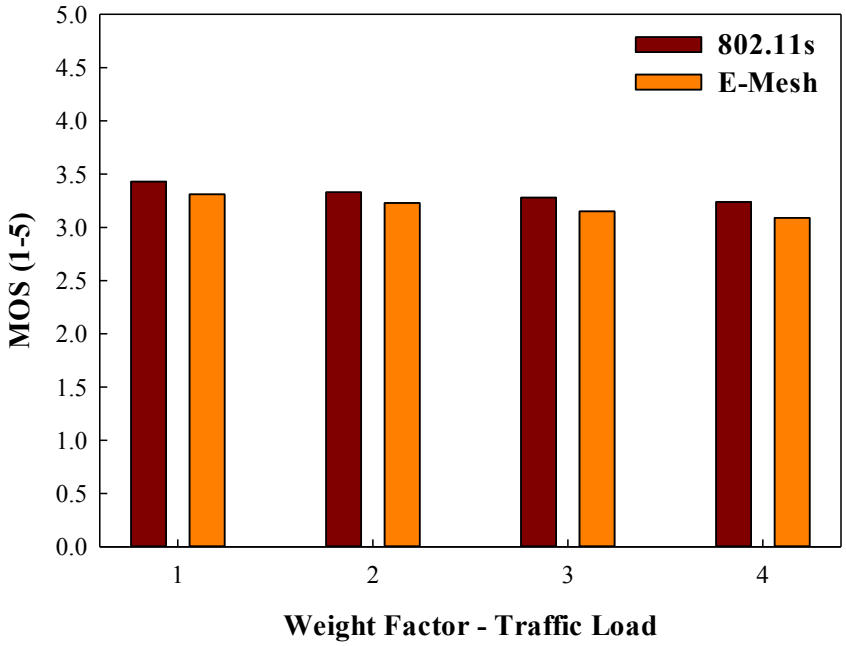

Fig.6.22.MOS achieved using 802.11s and E-Mesh with variable weights on traffic load when the mesh routers are moving

Figure 6.21 and Figure 6.22 illustrates the measured MOS results of the received videos for the E-Mesh experimental test case *B1* with different weights on the traffic load, when the mesh routers are static and moving, respectively. In Figure 6.21, when the mesh routers are static, the MOS of the received video slight decreases along with the increase of the traffic load weight factor value, but in general it remains at a stable level. In this case, the MOS of the received video using E-Mesh has decreased approximately 2.58%, 2.62%, 2.68% and 3.04% with the traffic load weight factor value 1.0, 2.0, 3.0 and 4.0, respectively, in comparison with the IEEE 802.11s routing protocol. In Figure 6.22, when the mesh routers are moving, the MOS of the received video again slight decreases along with the increase of the traffic load weight factor value. In this case, the MOS of the received video using E-Mesh has decreased approximately 3.5%, 3%, 3.96% and 4.63% with the traffic load weight factor value 1.0, 2.0, 3.0 and 4.0, respectively, in comparison with the IEEE 802.11s routing protocol. In general, the average MOS of the received video is lower when the mesh routers are moving, in comparison with when the mesh routers are static, as the mobility of mesh routers decreases the stability of the network connectivity. With the traffic load weight factor value 1.0, 2.0, 3.0 and 4.0, the MOS of the received video using the IEEE 802.11s routing protocol is roughly 1.72%, 2.92%, 2.38% and 1.52% lower when the mesh routers are moving, while the MOS of the received

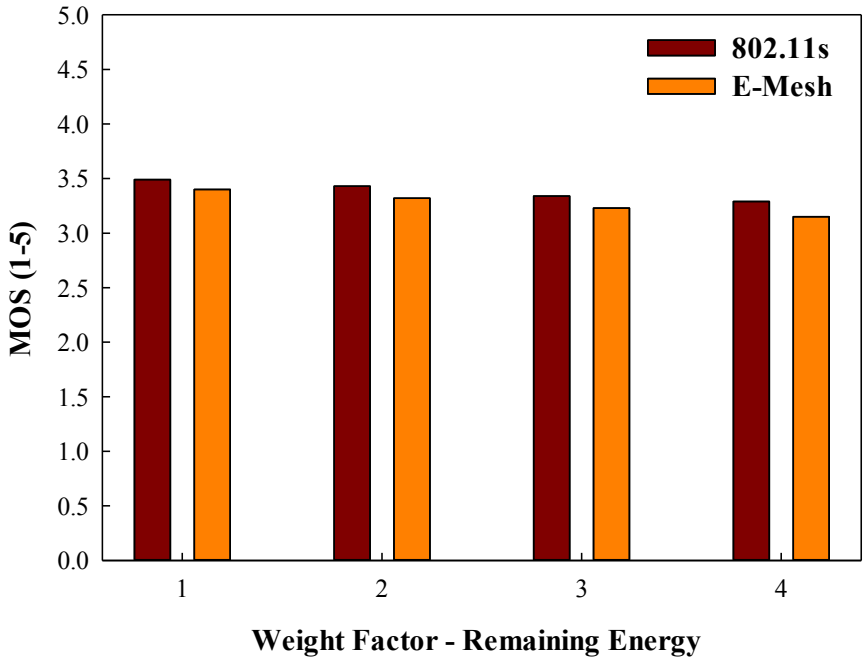

Fig.6.23.MOS achieved using 802.11s and E-Mesh with variable weights on remaining energy when the mesh routers are static

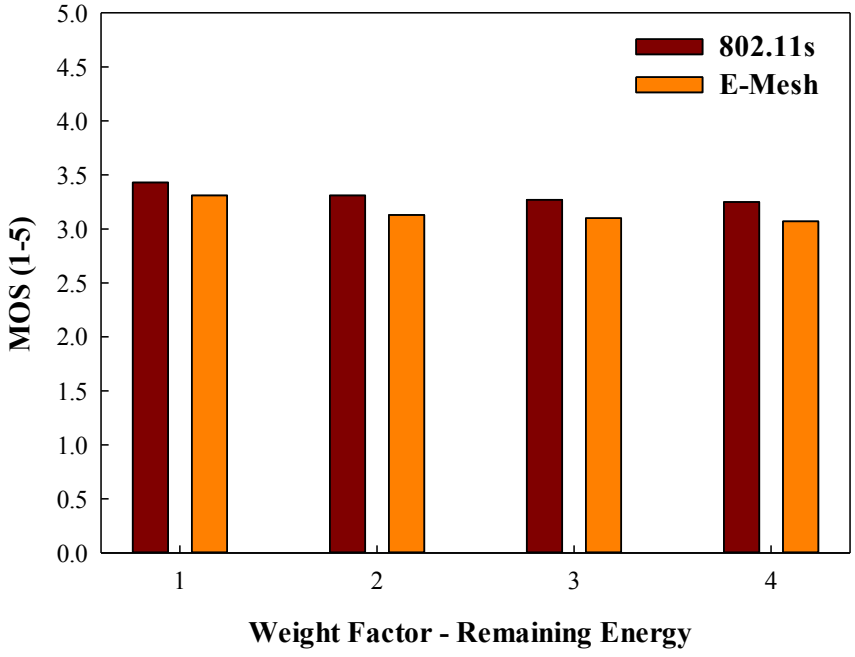

Fig.6.24.MOS achieved using 802.11s and E-Mesh with variable weights on remaining energy when the mesh routers are moving

video using E-Mesh is roughly 2.65%, 3.29%, 3.67% and 3.13% lower when the mesh routers are moving.

Figure 6.23 and Figure 6.24 illlustrates the measured MOS results of the received videos for the E-Mesh experimental test case *B2* with different weights on the remaining energy of mesh routers, when the mesh routers are static and moving, respectively. In Figure 6.23,

when the mesh routers are static, the MOS of the received video slight decreases along with the increase of the remaining energy weight factor value, but in general it remains at a stable level. In this case, the MOS of the received video using E-Mesh has decreased approximately 2.58%, 3.21%, 3.29% and 4.26% with the remaining energy weight factor value 1.0, 2.0, 3.0 and 4.0, respectively, in comparison with the IEEE 802.11s routing protocol. In Figure 6.24, when the mesh routers are moving, the MOS of the received video again slight decreases along with the increase of the remaining energy weight factor value. In this case, the MOS of the received video using E-Mesh has decreased approximately 3.5%, 5.44%, 5.2% and 5.54% with the remaining energy weight factor value 1.0, 2.0, 3.0 and 4.0, respectively, in comparison with the IEEE 802.11s routing protocol. In general, the average MOS of the received video is lower when the mesh routers are moving, in comparison with when the mesh routers are static. With the remaining energy weight factor value 1.0, 2.0, 3.0 and 4.0, the MOS of the received video using the IEEE 802.11s routing protocol is roughly 1.72%, 3.5%, 2.1% and 1.22% lower when the mesh routers are moving, while the MOS of the received video using E-Mesh is roughly 2.65%, 5.72%, 4.02% and 2.54% lower when the mesh routers are moving.

Figure 6.25 and Figure 6.26 illlustrates the measured MOS results of the received

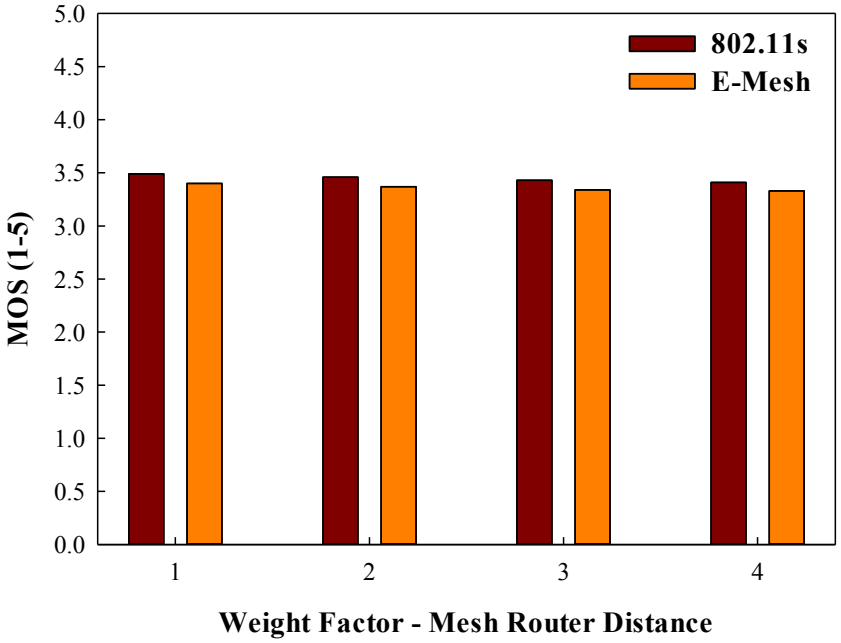

Fig.6.25.MOS achieved using 802.11s and E-Mesh with variable weights on mesh router distance when the mesh routers are static

videos for the E-Mesh experimental test case *B3* with different weights on the mesh router distance, when the mesh routers are static and moving, respectively. In Figure 6.25, when the mesh routers are static, the MOS of the received video slight decreases along with the increase of the mesh router distance weight factor value, but in general it remains at a stable level. In this case, the MOS of the received video using E-Mesh has decreased approximately 2.58%, 2.6%, 2.62% and 2.35% with the mesh router distance weight factor value 1.0, 2.0, 3.0 and 4.0, respectively, in comparison with the IEEE 802.11s routing protocol. In Figure 6.26, when the mesh routers are moving, the MOS of the received video again slight decreases along with the increase of the mesh router distance weight factor value. In this case, the MOS of the received video using E-Mesh has decreased approximately 3.5%, 3.26%, 2.69% and 2.21% with the mesh router distance weight factor value 1.0, 2.0, 3.0 and 4.0, respectively, in comparison with the IEEE 802.11s routing protocol. In general, the average MOS of the received video is lower when the mesh routers are moving, in comparison with when the mesh routers are static. With the mesh router distance weight factor value 1.0, 2.0, 3.0 and 4.0, the MOS of the received video using the IEEE 802.11s routing protocol is roughly 1.72%, 2.6%, 2.62% and 2.64% lower when the mesh routers are moving, while the MOS of the received video using E-Mesh is roughly 2.65%, 3.26%, 2.69% and 2.4% lower when the mesh routers are moving.

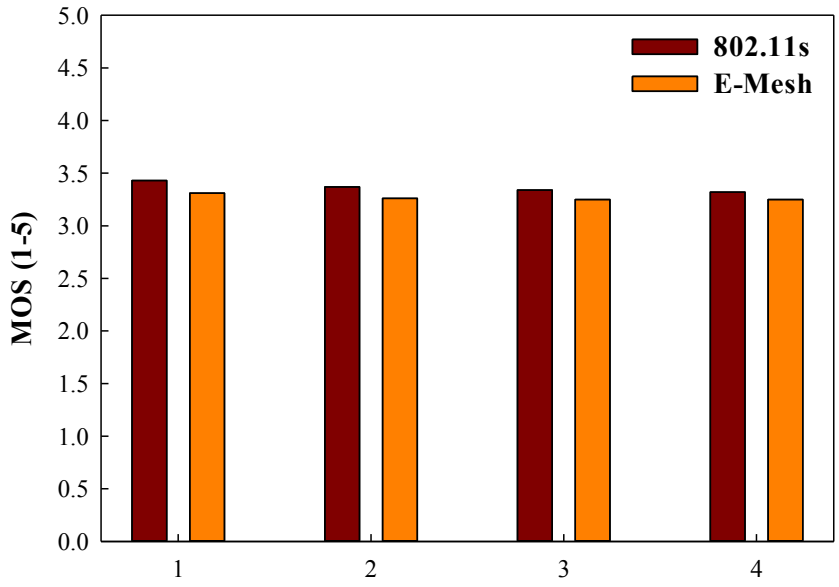

Fig.6.26.MOS achieved using 802.11s and E-Mesh with variable weights on mesh router distance when the mesh routers are moving

TABLE 6.7 MOS VALUES WITH 802.11S AND E-MESH

E-Mesh Test Cases			MOS (1-5)			
			802.11s		E-Mesh	
			Static	Moving	Static	Moving
E-Mesh Utility Function Weight Factor	Traffic Load	1.0	3.49	3.43	3.40	3.31
		2.0	3.43	3.33	3.34	3.23
		3.0	3.36	3.28	3.27	3.15
		4.0	3.29	3.24	3.19	3.09
	Remaining Energy	1.0	3.49	3.43	3.40	3.31
		2.0	3.43	3.31	3.32	3.13
		3.0	3.34	3.27	3.23	3.10
		4.0	3.29	3.25	3.15	3.07
	Mesh Router Distance	1.0	3.49	3.43	3.40	3.31
		2.0	3.46	3.37	3.37	3.26
		3.0	3.43	3.34	3.34	3.25
		4.0	3.41	3.32	3.33	3.25

The measured MOS values of the received videos for E-Mesh test cases are concluded in Table 6.7. Although the MOS values demonstrate the decrease of received video quality when E-Mesh is deployed, good level of energy saving is achieved in comparison with the IEEE 802.11s routing protocol, according to the simulation test results presented in section 5.5 in Chapter 5.

6.5.2.3 Result Analysis for the Video Delivery with eMTCP

The measured MOS values for the eMTCP experimental test cases are illustrated in Figure 6.27 and Table 6.8. As The average measured MOS of the received video in test case *C4* (in which eMTCP is used) is 96.6% higher in comparison with the average PSNR in test case *C1* (in which TCP is used over Wi-Fi); 10.23% higher in comparison with the average PSNR in test case *C2* (in which TCP is used over LTE); 19.34% lower in comparison with the average PSNR in test case *C3* (in which MPTCP is used over LTE and Wi-Fi); and 3.64% higher in comparison with the average PSNR when using the Nokia multi-path scheduler. The measurement of the standard deviations of the MOS values indicate that the test scenaio with eMTCP deployed is with less transmission fluctuation in comparison with the scenario with MPTCP deployed. Also, the decrease of MOS does not overcome the energy efficiency improvement when eMTCP is deployed, according to the simulation test results presented in section 5.6 in Chapter 5.

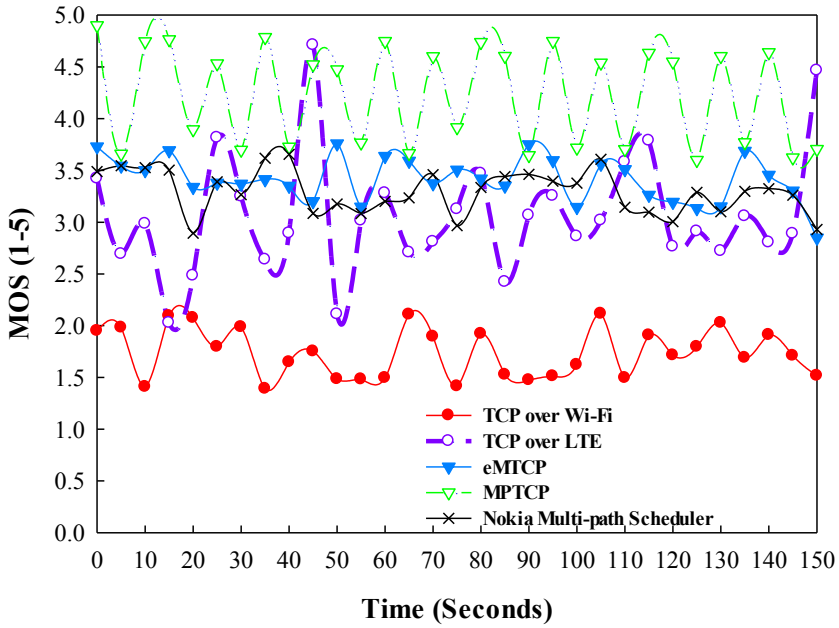

Fig.6.27.MOS values of eMTCP test cases

TABLE 6.8 MOS VALUES WITH EMTCP TEST CASES

	Solution				
	TCP over Wi-Fi	**TCP over LTE**	**MPTCP**	**eMTCP**	**Nokia Multi-path Scheduler**
Average MOS (1-5)	1.74	3.07	4.24	3.42	3.30
Standard Deviation of MOS	0.239	0.580	0.489	0.217	0.211

6.5.2.4 Result Analysis for the Video Delivery with eMTCP-BT

The measured MOS values for the eMTCP experimental test cases are illustrated in Figure 6.28 and Table 6.9. As The average measured MOS of the received video in test case *D3* (in which eMTCP-BT is used) is 32.06% higher in comparison with the average MOS in test case *D2* (in which eMTCP is used) and 4.91% higher in comparison with the average MOS in test case *D1* (in which MPTCP is used). The measurement of the standard deviations of the MOS values indicate that eMTCP-BT results in higher received video quality (and higher energy efficiency as presented in section 5.7 in Chapter 5) in comparison with MPTCP and eMTCP, but also causes higher traffic fluctuation.

6.6 Results Comparison

The delivered video quality has been investigated for the four proposed solutions using both objective and subjective metrics. In general, AOC-MAC, E-Mesh and eMTCP causes more

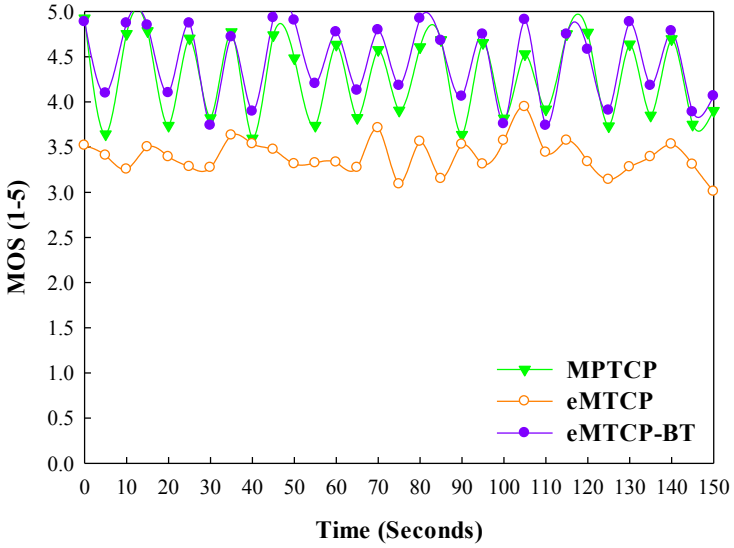

Fig.6.28.MOS values of eMTCP-BT test cases

TABLE 6.9 MOS VALUES WITH EMTCP-BT TEST CASES

	Solution		
	MPTCP	**eMTCP**	**eMTCP-BT**
Average MOS (1-5)	4.28	3.40	4.49
Standard Deviation of MOS	0.473	0.193	0.488

or less received video quality decrease in comparison with the IEEE 802.11 MAC protocol and S-MAC; the IEEE 802.11 routing protocol; and MPTCP, respectively. However, the decreased video quality is still in a good level assessed by the objective and subjective metrics. eMTCP-BT provides a slight video quality increase in comparison with MPTCP and a significant video quality increase in comparison with eMTCP.

6.7 Chapter Summary

This chapter presents the performance analysis of the four proposed solutions: 1) AOC-MAC; 2) E-Mesh; 3) eMTCP; and 4) eMTCP-BT, based on comparison between existing solutions in terms of video transmission quality, which is evaluated by objective and subjective video quality assessment metrics. Real-life test-bed is described for the video quality assessment for the four proposed solutions, including equipment and software specifications, video sequence selection and experimental scenario design. PSNR (and MSSSIM specifically for AOC-MAC) is selected as the objective video quality assessment metric and MOS is selected as the subjective video assessment metric. In objective tests, the MSU video quality assessment tool is used for result collection. In subjective tests, 20 users are invited for rating video quality.

CHAPTER 7

Conclusions and Future Work

In this chapter, the conclusions of this thesis are presented alongside limitations of the work and possible future research work directions.

7.1 Conclusions

7.1.1 Overview

The rapid development of the wireless communication technologies enables support for more powerful and affordable wireless devices. Due to the significantly increasing popularity of network-based services based on heterogeneous wireless technologies, especially applications with rich-media contents, ensuring the stability of application service quality and the power source lifespan for mobile devices remains an essential challenge. Research works focusing on energy awareness of content delivery in mobile wireless networks develop very fast, aiming at achieving high data transmission quality for network users and low energy consumption for both users at their terminals and network operators of wireless devices at the same time.

7.1.2 Contributions

In these circumstances, this thesis presents an energy-aware solution for both network operators and mobile users for the purpose of energy saving and maintaining good application service quality levels, by proposing four major contributions:

- **AOC-MAC**: an energy-aware mesh router duty cycle management scheme which adaptively adjusts the sleep-periods of router devices in a wireless mesh network. AOC-MAC is a MAC-layer solution which controls the sleep-periods of mesh routers according to the condition of application traffic delivery detected by the E-Mesh solution. In general, the sleep-periods of idle mesh routers are increased in order to save energy. On the other hand, the sleep-periods are reduced for the mesh routers changing from idle to busy, in order to maintain the stability of network connection and traffic delivery for good QoS levels.
- **E-Mesh**: an energy-adaptive routing algorithm for router devices in a wireless

mesh network. E-Mesh consists of a novel utility function for obtaining the optimal route for traffic delivery in terms of energy consumption level, network load and connection stability for each mesh router, based on the classic OLSR algorithm. E-Mesh also works in conjunction with AOC-MAC via informing it with the detection result of the network connection condition and traffic delivery state.

- **eMTCP**: an energy-aware traffic load balancing scheme for rich-media content delivery to end-user mobile devices in heterogeneous wireless networks. eMTCP makes use of the IETF-proposed multi-path TCP transport-layer protocol for multi-path wireless connection maintenance, by which the transmission bandwidth is significantly increased. The issue of extra energy consumption on MPTCP-based mobile devices is caused by using multiple wireless radio access technologies and is solved by off-loading traffic from the more energy-consuming radio interfaces to others. Traffic off-loading is achieved by the co-operation of the sub-flow interface state detector module and the off-loading controller module of eMTCP. The sub-flow interface state detector observes the physical-layer traffic receiving and idle states of the wireless radio interfaces used on mobile devices. The off-loading controller module performs the off-loading activity according to the state observation results from the sub-flow interface state detector module. As a result, eMTCP makes increase in energy efficiency on mobile devices.
- **eMTCP-BT**: an energy-efficiency-oriented traffic load balancing scheme extending the traffic off-loading scheme of eMTCP. eMTCP-BT performs an innovative distribution of the overall traffic for its delivery via the available wireless radio interfaces and paths on mobile devices, according to the traffic characteristics of the running applications. The traffic distribution on each wireless content delivery path is adaptively managed for obtaining the highest energy efficiency for mobile devices. The adaptive management of traffic distribution in eMTCP-BT is provided by adding a traffic classification module to co-operate with the sub-flow interface state detector module and the off-loading controller module of eMTCP. The traffic classification module categorizes the burstiness level of the

application traffic on mobile devices and the classified traffic burstiness level information is sent to the off-loading controller module as an important factor for traffic off-loading percentage decision making. By using this mechanism, eMTCP-BT further increases energy efficiency on mobile devices as the energy-efficiency-optimal traffic off-loading percentage is adaptively achieved.

7.1.3 Testing

The performance analysis of the proposed solution was performed via simulations using Network Simulator 3 (NS-3) and real-life experimental tests using objective and subjective quality assessment metrics. Simulation models and prototypes for AOC-MAC, E-Mesh, eMTCP and eMTCP-BT were developed with the corresponding algorithms implemented.

AOC-MAC was analyzed in terms of the trade-off between energy consumption and traffic delivery performance on wireless mesh routers. It was compared against the duty cycle management scheme in the existing IEEE 802.11s MAC mechanism and an existing duty cycle management scheme S-MAC, with the same parameter settings of a multi-router mesh network. Performance analysis was investigated with the impact of various traffic data rates, number of mesh routers and mesh router mobility.

Simulation-based test results show that AOC-MAC sacrifices little QoS in terms of approximately up to 5% higher frame loss, 6%-12% higher delay and 8% lower video quality, for a significant 21.56% and a 11.18% energy saving in comparison with the IEEE 802.11s MAC protocol and S-MAC, respectively, with various settings of traffic data rates, number of mesh routers and mesh router mobility. Also, the energy saving and quality drop of AOC-MAC increase along with the increase of traffic data rate and decrease along with the increase of the number of mesh routers in the mesh network, while the energy saving and quality drop of AOC-MAC is roughly 8.95% and 1.87% lower when the mesh routers are static than when the mesh routers are moving. Experimental test results show that AOC-MAC achieves approximately the same video transmission quality level in comparison with the IEEE 802.11s MAC protocol and S-MAC.

E-Mesh was also analyzed in terms of energy consumption rate, QoS and video-related transmission quality. Comparison was made between an IEEE 802.11s multi-router mesh

network with E-Mesh deployed and another mesh network with the same parameter settings but without E-Mesh deployed. Performance analysis was investigated with the impact of various settings of the traffic load, remaining energy and mesh router distance weight factors in the utility function described in section 4.4.2.2 in Chapter 4.

The advantage of E-Mesh against the IEEE 802.11s routing protocol is demonstrated by observing its performance with different settings of the weight factors via simulation-based test results. When the mesh routers are static, E-Mesh achieves up to a significant 22.9% energy saving, in return of a 9.65% increased loss and a 0.7-dB decreased PSNR, in comparison with the IEEE 802.11s routing protocol, with various settings of traffic load, remaining energy and mesh router distance weight factors. When the mesh routers are moving, the energy saving benefit of E-Mesh is up to 19.8%, in return of a 13% increased loss and a 1-dB decreased PSNR. The energy-quality balance of E-Mesh is further illustrated by the experimental test results, indicating that approximately the same video transmission quality level is achieved.

The energy efficiency on end user wireless mobile devices was selected as the performance evaluation parameter for eMTCP, which was compared against MPTCP with no traffic load balancing mechanisms and against a Multi-path Scheduler solution proposed by Nokia, in order to prove its benefit on energy efficiency. Meanwhile it was also compared against the classic single-path TCP in order to demonstrate its benefit in terms of transmission bandwidth improvement.

As the simulation-based tests show, the energy efficiency of eMTCP has a 10.1% improvement in comparison with the Nokia Multi-path Scheduler solution, while it experiences about 15% energy consumption in comparison with MPTCP from using multiple radio access interfaces by traffic off-loading, with simply 2% throughput reduction. Meanwhile, eMTCP ensures almost doubled bandwidth usage via the multi-path feature in comparison with single-path TCP. Experimental test results of eMTCP show that the video transmission quality slightly decreases (lower of 5 dB) in comparison with MPTCP, but approximately the same video transmission quality level is achieved in comparison with the Nokia Multi-path Scheduler solution.

To analyze the performance of eMTCP-BT, the best traffic off-loading proportion which obtained the highest energy efficiency on mobile devices is considered. The usage of

various types of applications with different traffic burstiness levels were done in simulations to observe the best traffic off-loading percentage under different application usage circumstances. eMTCP-BT was compared against eMTCP, with the best traffic off-loading percentage against the sub-optimal traffic off-loading percentage.

Simulation-based test results demonstrate that the adaptation of traffic off-loading percentage provided by eMTCP-BT brings significant improvement on the energy efficiency of mobile devices with different application usage. Meanwhile, comparison against MPTCP and classic single-path TCP was also kept in simulations in order to prove that eMTCP-BT still has the benefits on high bandwidth and low energy cost. The fact that the video transmission quality of eMTCP-BT remains approximately the same level in comparison with MPTCP and slightly increases (higher of 6 dB) in comparison with eMTCP, is illustrated via the experimental test results.

7.2 Current Work Limitations and Future Work Directions

The main purpose of the work presented in this thesis is to propose solutions for energy-performance trade-off during content delivery to mobile devices in heterogeneous wireless networks. These solutions include a duty-cycle/routing management scheme for mesh devices in wireless mesh networks and a traffic load balancing scheme for end user mobile devices in heterogeneous wireless networks. Apart from saving energy at both the network operators of routers and the wireless networked mobile devices, the aim of the proposed solutions is also to offer better user experience of application service during the energy-aware content delivery.

The work included in this thesis is with several limitations. First, the solutions are heuristic-designed based on mainly modeling and simulation of the wireless network topologies. Second, although the solutions succeed to achieve a good energy-performance trade-off and result in good energy savings while improving user perceived quality in comparison with other solutions, the work in this thesis does not claim to have found the optimum solution in a general manner. For example, the ping-pong effect exists in AOC-MAC as described in section 4.2.1.2 in Chapter 4. Third, the investigation on the performance of different wireless technologies is limited only to Wi-Fi and LTE, while there are still many other technologies worth to be

included in the research, such as 3G and WiMAX.

Consider these limitations, several additional research directions can be identified for the further progress of the work described in this thesis. One of the most important directions is the investigation on performance of the proposed solution in a more complex heterogeneous wireless network environment. As most of the wireless networks today are with multi-user environments, it is important to find a good trade-off between energy consumption of multiple wireless devices of different users and the service quality of multiple applications. The principles and experimental tests of the proposed work in this thesis focus more on a multi-source single-client/user manner, which is not often the case in real-life scenarios. It is necessary for further evaluation of the performance of the proposed solution on multi-user multi-device scenarios.

Another possibility of further development on the proposed solution is to introduce more types of wireless radio access technologies in the heterogeneous network environment of the proposed solution. The main contributions in this thesis mainly focus on the 4G LTE and the Wi-Fi technologies, while there are still many radio access technologies used by most of the wireless mobile devices today. One of the examples is the still popular 3G technology. It is important to study the performance of 3G connection in multi-path transmission conditions. As MPTCP supports multi-path connections with up to 5 sub-channels, it is possible to add an extra 3G sub-flow to eMTCP and eMTCP-BT and to investigate the performance of content delivery and energy consumption of connections with more sub-channels. Also, the impact of multiple sub-channels on the wireless radio access technologies needs to be investigated (e.g. 2 sub-channel for LTE and 3 sub-channels for Wi-Fi, deployed simultaneously in a heterogeneous wireless network, using MPTCP).

Optimization based on the four proposed solutions is another possible future work direction. As mentioned in Chapter 4, it is possible to solve the ping-pong effect of the AOC-MAC algorithm with a delay decision on changing the parameters related to mesh router sleep-periods. Alternatively, hysteresis methods can be used to avoid the ping-pong effect.

Last but not the least, the attempt of using more advanced mathematical models in traffic off-loading proportion adaptation in eMTCP-BT is also worth to mention. Many mathematical models are developed for traffic classification. The work in [119] proposes a

comprehensive study on the traffic classification models in terms of complexity and classification accuracy. Among all the mathematical models studied in this work, the ones with better accuracy are obviously more valuable for the proposed solution in this thesis, as they have positive impacts on the condition of a mixture of application traffic with multiple burstiness levels.

APPENDIX
Perceptual Test Instructions

Acknowledgement

Appreciate your support for the video perceptual test organized by the Performance Engineering Lab, School of Electronic Engineering, Dublin City University, Ireland.

Test Motivations

The purpose of the perceptual test is to make performance evaluation for the four proposed solutions: AOC-MAC, E-Mesh, eMTCP and eMTCP-BT in terms of video transmission quality.

Test Guidelines

To complete the perceptual tests, you are encouraged to finish one test case which takes around 20 minutes. You are also recommended to start the test according to the following guidelines:

1. Filling the **Personal Information Form**.
2. Filling the **Questionnaire** while watching 10 video clips. Each video clip is 20-seconds long. During the playback of each short video clip, you are asked to rate the video quality in terms of MOS.
3. The rating is supposed to be finished immediately when one video clip ended.
4. You are not allowed to change the distance from the device screen too much.

Personal Information Form

Please check "√" for your choice _____

User No:

Gender:	(A) Male		(B) Female
Age:			
Working type:	(A) Computer Science (B) Engineering (C) Education (D) Finance (E) Others (Please specify:_____)		
Do you use glasses?	(A) Yes		(B) No
Do you have visual disabilities, such as colour blindness and colour weakness?	(A) Yes		(B) No
How often do you watch streaming videos?	(A) Every day (B) Twice/week (C) Once/week (D) Once/month (E) Never		
Which device is your favourite to watch video?	(A) Laptop	(B) Tablet	(C) Smartphone
How familiar are you with wireless multimedia delivery?	(A) Expert	(B) Familiar	(C) Not familiar
How familiar are you with video quality assessment?	(A) Expert	(B) Familiar	(C) Not familiar
Which network do you use	(A)	(B)	(C) Ethernet with cable

most to watch video?	Wi-Fi	3G/4G	
Which is your favourite movie type?	(A) Action (B) Horror (C) Comedy (D) Cartoon (E) Crime (F) Romance (G) Other		

Guidlines for Rating the Video Quality

Rating	Description
	Mean Opinion Score
1	Bad
2	Poor
3	Fair
4	Good
5	Excellent

Questionnaire for user

User No: _____

Video Clip	MOS				
1	1	2	3	4	5
2					
3					
4					
5					
6					
7					
8					
9					
10					

BIBLIOGRAPHY

[1] IEEE 802.11a-1999, IEEE Standard for Local and Metropolitan Area Networks Specific Requirements – Part 11: Wireless LAN Medium Access Control (MAC) and Physical Layer (PHY) Specifications High Speed Physical Layer in the 5 GHz Band, 1999.

[2] 3GPP TS 25.800, “Technical Report on UMTS Heterogeneous Networks”.

[3] 3GPP TS 36.201, "Evolved Universal Terrestrial Radio Access (E-UTRA); Long Term Evolution (LTE) physical layer".

[4] Cisco Systems, Inc., “Cisco Visual Networking Index: Global Mobile Data Traffic Forecast Update, 2013-2018”, 2014. [Online]. Available: http://www.cisco.com/c/en/us/solutions/collateral/service-provider/visual-networking-index-vni/white_paper_c11-520862.html.

[5] Celtra, Inc., “The Evolution of Mobile Displaying Advertising”, 2013. [Online]. Available: http://www.celtra.com/infographic?v=86.

[6] ANSI/IEEE Std 802.11, 1999 Edition (R2003), ―Part 11: Wireless LAN Medium Access Control (MAC) and Physical Layer (PHY) Specifications‖, June 2003.

[7] International Electronic Commission, “Electrical Energy Storage”, 2011. [Online]. Available: http://www.iec.ch/whitepaper/pdf/iecWP-energystorage-LR-en.pdf.

[8] COST IC1004, “Scientific Challenges towards 5G Mobile Communications”, 2013. [Online]. Available: http://www.ic1004.org/uploads/Documents/COST%20IC1004%20White%20Paper%20on%20Mobile%20Comms%20Challenges%20towards%205G%20%20-%202013.pdf.

[9] T. Clausen, P. Jacquet, “Optimized Link State Routing Protocol”, Hipercom, *RFC-3626*, Oct. 2003.

[10] A. Ford, C. Raiciu, M. Handley, S. Barre, J. Iyengar, “Architectural Guidelines for Multipath TCP Development”, *RFC 6182,* Mar. 2011.

[11] K. Pahlavan, P. Krishnamurphy, “Principles of Wireless Networks: A Unified Approach”, Prentice Hall, 2002

[12] IEEE 802.15.1-2005, IEEE Standard for Information technology-- Local and metropolitan area networks-- Specific requirements-- Part 15.1a: Wireless Medium Access Control (MAC) and Physical Layer (PHY) specifications for Wireless Personal Area Networks

(WPAN), 2005.

[13] Charles D. Knutson, Jeffrey M. Brown, "IrDA Principles and Protocols: The IrDA Library", Vol. 1, May 2004.

[14] J.G.Andrews and A.Ghosh, "Fundamentals of WiMAX: Understanding Broadband Wireless Networking", Prentice Hall PTR, 2007.

[15] IEEE 802.16e-2004, IEEE Standard for Local and Metropolitan Area Networks Part 16: Air Interface for Fixed Broadband Wireless Systems, Jul. 2004.

[16] Rohde & Schwarz, "IEEE 802.16m Technology Introduction, White paper", 2010. [Online]. Available: http://cdn.rohde-schwarz.com/pws/dl_downloads/dl_application/ application_notes/ 1ma167/1MA167_3e_IEEE_80216m_technology.pdf.

[17] IEEE 802.11a-1999 - IEEE Standard for Information technology-- Local and metropolitan area networks-- Specific requirements-- Part 11 : Wireless LAN Medium Access Control (MAC) and Physical Layer (PHY) specifications High-speed Physical Layer in the 5 GHz Band, Jun.,2003.

[18] IEEE 802.11b-1999 - IEEE Standard for Information technology-- Local and metropolitan area networks-- Specific requirements-- Part 11 : Wireless LAN Medium Access Control (MAC) and Physical Layer (PHY) specifications : Higher-Speed Physical Layer Extension in the 2.4 GHz Band, Jun. 2003.

[19] IEEE 802.11g-2003 - IEEE Standard for Information technology-- Local and metropolitan area networks-- Specific requirements-- Part 11: Wireless LAN Medium Access Control (MAC) and Physical Layer (PHY) Specifications: Further Higher Data Rate Extension in the 2.4 GHz Band, 2003.

[20] IEEE 802.11n-2009 - IEEE Standard for Information technology-- Local and metropolitan area networks-- Specific requirements-- Part 11: Wireless LAN Medium Access Control (MAC)and Physical Layer (PHY) Specifications Amendment 5: Enhancements for Higher Throughput, 2009.

[21] Cisco Systems, Inc., "802.11ac: The Fifth Generation of Wi-Fi", Technical White Paper, Aug.2012. [Online]. Available: http://www.cisco.com/c/en/us/products/collateral/wireless/ aironet-3600-series/white_paper_c11-713103.pdf.

[22] IEEE 802.11ad-2012 - IEEE Standard for Information technology--Telecommunications

and information exchange between systems--Local and metropolitan area networks--Specific requirements-- Part 11: Wireless LAN Medium Access Control (MAC) and Physical Layer (PHY) Specifications Amendment 3: Enhancements for Very High Throughput in the 60 GHz Band, 2012.

[23] IEEE 802.11s-2011 - IEEE Standard for Information Technology--Telecommunications and information exchange between systems--Local and metropolitan area networks--Specific requirements Part 11: Wireless LAN Medium Access Control (MAC) and Physical Layer (PHY) specifications Amendment 10: Mesh Networking, 2011.

[24] Petersen, Julie K., "The Telecommunications Illustrated Dictionary", Second Edition, 2002

[25] Radisys, "Trillium 3G Wireless Software", White Papar, 2010. [Online]. Available: http://go.radisys.com/rs/radisys/images/paper-trillium-3g-wireless.pdf.

[26] V.H.Mac Donald, "Advanced Mobile Phone Service: The Cellular Concept", *The Bell System Technical Journal*, Vol. 58, No. 1, Jan. 1979.

[27] P. Nicopolitidis, "*Wireless networks*", John Wiley and Sons, 2003.

[28] W. Webb, "*The Future Wireless Communications*," John Wiley and Sons, 2007.

[29] 3GPP TS 133.102, "Universal Mobile Telecommunications System (UMTS); 3G Security; Security Architecture".

[30] Nokia, "Long Term HSPA Evolution: Mobile Broadband Evolution beyond 3GPP", release 10, 2010. [Online]. Available: http://www.nokiasiemensnetworks.com/sites/default/files/document/HSPA_evolution_white_paper_low_res_141220.pdf.

[31] S. Parkvall, E. Dahlman, A. Furuskär, Y. Jading, M. Olsson, S. Wänstedt, K. Zangi, "LTE-Advanced – Evolving LTE towards IMT-Advanced", *IEEE Vehicular Technology Conference (VTC)*, 2008

[32] 3GPP TS 36.201, "Evolved Universal Terrestrial Radio Access (E-UTRA); Long Term Evolution (LTE) physical layer".

[33] Rohde & Schwarz, "LTE Advanced Technology Introduction, White paper", 2013. [Online]. Available: http://cdn.rohde-schwarz.com/pws/dl_downloads/dl_application/application_notes/1ma232/1MA232_1E_LTE_Rel11.pdf.

[34] Ericsson, "5G Radio Access: Research and Vision", Jun. 2013. [Online]. Available: http://www.ericsson.com/res/docs/whitepapers/wp-5g.pdf.

[35] ITU-T Recommendation X.200, "Data Networks and Open System Communications: Open Systems Interconnection – Model and Notation", Jul. 1994.

[36] M.-S. Kim, Y. J. Won, and J. W. Hong, "Characteristic analysis of internet traffic from the perspective of flows," Comput. Commun., vol.29, pp. 1639–1652, Jun. 2006.

[37] R. Stewart, "Stream control transmission protocol", IETF RFC 4960, Sept.2007.

[38] ITU-T Recommendation E.800, "Definitions of terms related to quality of service", Apr. 2009.

[39] ITU-T Recommendation X.902, "Information technology - Open Distributed Processing - Reference Model: Foundations", Jun. 1996

[40] ITU-T Recommendation X.641, "Information technology - Quality of service: framework", Jul. 1998

[41] ITU-T Recommendation P.800, "Methods for subjective determination of transmission quality", Aug. 1996

[42] Q. Huynh-Thu, M. Ghanbari, "Scope of validity of PSNR in image/video quality assessment", *Electronic Letters*, Vol. 44, Jun. 2008.

[43] E. Lehmann, G. Casella, "Theory of Point Estimation", 2nd Edition, 1998.

[44] Z. Wang, A. C. Bovik, H. R. Sheikh, E. P. Simoncelli, "Image quality assessment: From error visibility to structural similarity", *IEEE Transactions on Image Processing*, Vol. 13, No. 4, pp. 600-612, Apr. 2004.

[45] M. Pinson and S. Wolf, "A New Standardized Method for Objectively Measuring Video Quality", *IEEE Transactions on Broadcasting*, Vol. 50, No.3, pp. 312-322, Sept. 2004.

[46] S.-B. Lee, G.-M. Muntean, Alan F. Smeaton, "Performance-Aware Replication of Distributed Pre-Recorded IPTV Content", *IEEE Transactions on Broadcasting*, Vol.55, No. 2, pp.516-526, Jun. 2009.

[47] Kevin McClaning, Tom Vito, "Radio Receiver Design", Noble Publishing, 2000.

[48] G. Y.Li, Z. Xu, C. Xiong, C. Yang, S. Zhang, Y. Chen, S. Xu, "Energy-efficient wireless communications: tutorial, survey, and open issues", *IEEE Wireless Communications*, Vol. 18, Dec. 2011.

[49] A. Rice and S. Hay, "Measuring mobile phone energy consumption for 802.11 wireless networking", *Pervasive and Mobile Computing*, Vol. 6, Issue 6, Dec. 2010, pp. 593–606.

[50] W. Ye, J. Heidemann, D. Estrin, "An Energy-Efficient MAC Protocol for Wireless Sensor Networks", IEEE INFOCOM, New York, USA, vol.3, pp. 1567-1576, Jun. 2002.

[51] T. van Dam, K. Langendoen, "An Adaptive Energy-Efficient MAC Protocol for Wireless Sensor Networks", *ACM SenSys*, Los Angeles, USA, pp.171-180, Nov. 2003.

[52] G. Lu, B. Krishnamachari, C. S. Raghavendra, "An Adaptive Energy-Efficient and Low-Latency MAC for Data Gathering in Wireless Sensor Networks", *IPDPS*, Santa Fe, USA, pp. 224, April 2004.

[53] S. Du, A. K. Saha, D. B.Johnson, "RMAC: A Routing-Enhanced Duty-Cycle MAC Protocol for Wireless Sensor Networks", *IEEE INFOCOM*, Anchorage USA, pp. 1478-1486, May 2007.

[54] T. Zheng, S. Radhakrishnan, V. Sarangan, "PMAC: an adaptive energy-efficient MAC protocol for wireless sensor networks", *IPDPS*, Denver, USA, pp. 8, April 2005.

[55] M. Buettner, G. V. Yee, E. Anderson, R. Han, "X-MAC: a short preamble MAC protocol for duty-cycled wireless sensor networks", *ACM SenSys*, Boulder, USA, pp. 307-320, Oct.-Nov. 2006.

[56] Y. Sun, O. Gurewitz, D. B. Johnson, "RI-MAC: A Receiver-Initiated Asynchronous Duty Cycle MAC Protocol for Dynamic Traffic Loads in Wireless Sensor Networks", *ACM SenSys* Raleigh USA, pp.1-14, 2008.

[57] M. Benveniste, "QoS for Wireless Mesh: MAC Layer Enhancements", International Journal On Advances in Internet Technology, Vol. 2, No. 1, 2009.

[58] IEEE 802.11e-2005, IEEE Standard for Information technology — Telecommunications and information exchange between systems — Local and metropolitan area networks — Specific requirements Part 11: Wireless LAN Medium Access Control (MAC) and Physical Layer (PHY) specifications Amendment 8: Medium Access Control (MAC) Quality of Service Enhancements, Nov. 2005.

[59] B. Raman, K. Chebrolu, "Design and Evaluation of a new MAC Protocol for Long-Distance 802.11 Mesh Networks", *MOBICOM*, Cologne, Germany, Aug-Sept 2005, pp. 156-169.

[60] Z.J.Haas, J.Deng, "Dual Busy Tone Multiple Access (DBTMA) – A Multiple Access Control Scheme for Ad-hoc Networks", *IEEE Transactions on Communications*, Vol. 50,

Jun. 2002.

[61] M.M.Rana, K.E.U.Ahmed, R.Karim, H.M.Tareque, M.I.Hasan, "An Adaptive and Efficient MAC Protocol for Wireless Mesh Networks: An Extension of Maca-P", *IEEE International Conference on Computer Engineering and Technology (ICCET)*, Jan. 2009

[62] Acharya, A., Misra, A., Bansal, S, "Design and analysis of a cooperative medium access scheme for wireless mesh networks," *BROADNETs 04*, 2004, pp.621-631.

[63] S.Shankar, Mihaela van der Schaar, "Performance Analysis of Video Transmission Over IEEE 802.11a/e WLANs", *IEEE Transactions on Vehicular Technology*, Vol. 56, Jul. 2007.

[64] H. Jiao, Frank Y. Li, "A Mini-Slot-based Cooperative MAC Protocol for Wireless Mesh Networks", *IEEE Globecom Workshops*, Miami, USA, Dec 2010, pp. 89-93.

[65] R. Santamaria, O. Bourdeau, T. Anjali, "MAC-ASA: A New MAC Protocol for WMNs", *ICCCN*, Hawaii, USA, Aug 2007, pp. 973-978.

[66] F. Huang, Y. Yang, "Energy Efficient Collision Avoidance MAC Protocol in Wireless Mesh Access Networks", IWCMC, Hawaii, USA, Aug 2007, pp.272-277.

[67] A. Hassanzadeh, R. Stoleru, B. Shihada, "Energy Efficient Monitoring for Intrusion Detection in Battery-Powered Wireless Mesh Networks", *Proceedings of the 10th international conference on Ad-hoc, mobile, and wireless networks*, 2011.

[68] J. McQuillan, I. Richer, E. Rosen, "The New Routing Algorithm for the ARPANET", IEEE Transactions on Communications, Vol. 38, no. 5, pp. 711-719, 1980.

[69] R.E.Korf, "Linear-Space Best-First Search: Summary of Results", *Proceedings of the tenth national conference on Artificial intelligence*, 1992.

[70] A. Schrijver, "On the history of combinatorial optimization (till 1960)", 1960.

[71] M. Kubale, "Graph Colorings", American Mathematical Society, 2004.

[72] G. B. Mathews, "On the partition of numbers", *Proceedings of the London Mathematical Society*, Vol.28, pp. 486–490.

[73] S. Kirkpatrick, C. D. Gelatt Jr, M. P. Vecchi, "Optimization by Simulated Annealing", *Science*, vol. 220, No. 4598, pp. 671-680, May 1983.

[74] James R. Norris, "Markov chains", *Cambridge University Press*, 1998.

[75] E. Rozner, J. Seshadri, Y. Mehta, L. Qiu, "Simple Opportunistic Routing Protocol for

Wireless Mesh Networks", *IEEE Workshop on Wireless Mesh Networks,* pp. 1024–1030, 2006.

[76] D. Krishnaswamy, H. Shiang, J. Vicente, W. S. Conner, S. Rungta, W. Chan, and K. Miao, "A Cross-Layer Cross-Overlay Architecture for Proactive Adaptive Processing in Mesh Networks", *IEEE Workshop on Wireless Mesh Networks*, pp. 1050–1058, 2006.

[77] C. Liu, Y. Shu, and L. Zhang, "Backup Routing for Multimedia Transmissions over Mesh Networks", *IEEE International Conference on Communications (ICC)*, pp. 3829–3834, 2007.

[78] C. Xu, E. Fallon, Y. Qiao, L. Zhong, and G. Muntean, "Performance Evaluation of Multimedia Content Distribution Over Multi-Homed Wireless Networks", *IEEE Transactions on Broadcasting*, Vol. 57, No. 2, pp. 204–215, 2011.

[79] Zhenhui Yuan, Gabriel-Miro Muntean, "A Prioritized Adaptive Scheme for Multimedia Services over IEEE 802.11 WLANs", *IEEE Transactions on Network and Service Management*, Vol. 10, Dec. 2013.

[80] E. Nordmark, M. Bagnulo, "Shim6: Level 3 Multihoming Shim Protocol for IPv6", RFC 5533, Internet Engineering Task Force, Jun. 2009.

[81] J. Arkk, I. van Beijnum, "Failure Detection and Locator Pair Exploration Protocol for IPv6 Multihoming", Internet draft, IETF, Dec. 2006.

[82] C. Pluntke, L. Eggert, and N. Kiukkonen, "Saving Mobile Device Energy with Multipath TCP", *Proceedings of the sixth international workshop on MobiArch*, 2011.

[83] Ronald A. Howard, "Dynamic Programming and Markov Processes", 1960.

[84] T. A. Le, C. S. Hong, M. A. Razzaque, S. Lee, H. Jung, "ecMTCP: An Energy-Aware Congestion Control Algorithm for Multipath TCP", *IEEE Communications Letters*, Vol. 16, No. 2, pp. 275 -277, Feb. 2012.

[85] M. Li, A. Lukyanenko, Y. Cui, "Network coding based multipath TCP", *2012 IEEE Conference on Computer Communications Workshops (INFOCOM WKSHPS)*, Orlando, US, Mar. 2012, pp. 25 -30.

[86] C. Paasch, G. Detal, F. Duchene, C. Raiciu, O. Bonaventure, "Exploring Mobile/Wi-Fi Handover with Multipath TCP", *ACM SIGCOMM workshop on Cellular Networks*, Helsiki, Finland, Aug.2012, pp.31-36.

[87] Cisco white paper, “Cisco Visual Networking Index: Globel Mobile Data Traffic Forecast Update, 2012-2017”, Feb. 2013. [Online]. Available: http://www.cisco.com/en/US/ solutions/collateral/ns341/ns525/ns537/ns705/ns827/white_paper_c11 -520862.pdf.

[88] K. Samdanis, “Traffic Offload Enhancements for eUTRAN”, *IEEE Communication Surveys & Tutorials*, Sep. 2012.

[89] 3GPP TR 23.829 Rel-10, “Local IP Access and Selected IP Traffic Offload (LIPA-SIPTO)”, Oct. 2011.

[90] B. Han, P. Hui, V. S. A. Kumar, M. V. Marathe, J. Shao, and A. Srinivasan, “Mobile Data Offloading through Opportunistic Communications and Social Participation”, *IEEE Transactions on Mobile Computing*, Vol. 11, No. 5, pp. 821–834, May.2012.

[91] X. Zhuo, W. Gao, G. Cao, S. Hua, “An Incentive Framework for Cellular Traffic Offloading”, *IEEE Transsactions on Mobile Computing*, Vol. 99, pp. 1, Jan. 2013.

[92] M. Gupta, S.C. Jha, A.T. Koc, R. Vannithamby, “Energy Impact of Emerging Mobile Internet Applications on LTE Networks: Issues and Solutions”, *IEEE Communications Magazine*, Vol. 51, No. 2, Feb. 2013.

[93] R. Palit, K. Naik, A. Singh, “Impact of Packet Aggregation on Energy Consumption in Smartphones”, *Wireless Communications and Mobile Computing Conference (IWCMC)*, pp. 589-594, July 2011.

[94] Chi-Chen Lee, Jui-Hung Yeh, Jyh-Cheng Chen, “Impact of Inactivity Timer on Energy Consumption in WCDMA and cdma2000”, *IEEE Wireless Telecommunications Symposium*, 2004

[95] G. Anastasi, M. Conti, E. Gregori, A. Passarella, “802.11 power-saving mode for mobile computing in Wi-Fi hotspots: Limitations, enhancements and open issues,” *Wireless Networks*, Vol. 14, No. 6, pp. 745–768, Jan. 2007.

[96] R. Wang, J. Tsai, C. Maciocco, T. C. Tai, J. Wu, “Reducing Power Consumption for Mobile Platforms via Adaptive Traffic Coalescing”, *IEEE Journal on Selected Areas in Communications*, Vol. 29, No. 8, pp. 1618–1629, 2011.

[97] Y. Song, B. Ciubotaru, G.-M. Muntean, “Q-PASTE: A Cross-Layer Power Saving Solution for Wireless Data Transmission”, *IEEE International Conference on Communications Workshops (ICCW)*, 2013.

[98] M. Altamimi, R. Palit, K. Naik, A. R. Nayak, "Energy-as-a-Service (EaaS): On the Efficacy of Multimedia Cloud Computing to Save Smartphone Energy", *IEEE 5th International Conference on Cloud Computing (CLOUD)*, pp. 764-771, June 2012.

[99] M. Kennedy, H. Venkataraman, G.-M. Muntean, "Battery and Stream-Aware Adaptive Multimedia Delivery for wireless devices", *IEEE 35th Conference on Local Computer Networks (LCN)*, pp. 843-846, Oct. 2010.

[100] Ns3::LogDistancePropagationLossModel Class Reference, Network Simulator 3 [Online]. Available: http://www.nsnam.org/docs/release/3.13/doxygen/classns3_1_1_ log_distance_ propagation_loss_model.html

[101] Theodore S. Rappaport, "Wireless Communications: Principles and Practice", 2nd Edition, CA: Prentice Hall, 2002.

[102] A. R. Jensen, M. Lauridsen, P. Mogensen, T. B. Sørensen, and P. Jensen, "LTE UE Power Consumption Model for System Level Energy and Performance Optimization", *IEEE Vehicular Technology Conference (VTC Fall)*, Sept.2012.

[103] Ns3::WiFiRadioEnergyModel Class Reference, Network Simulator 3 [Online]. Available: http://www.nsnam.org/doxygen/classns3_1_1_wifi_radio_energy_model.html.

[104] Y. Chen, T. Farley, N. Ye, "QoS Requirements of Network Applications on the Internet", *Information-Knowledge-Systems Management*, Vol. 4, Issue 1, pp. 55 – 76, Jan. 2004.

[105] J. R. Quinlan, "Simplifying decision trees", *International Journal of Man-Machine Studies - Special Issue: Knowledge Acquisition for Knowledge-based Systems. Part 5*, Vol. 27, Issue 3, pp. 221 - 234, Sept. 1987.

[106] Breiman L, Friedman JH, Olshen RA, Stone CJ., "Classification and Regression Trees", Chapman &Hall (Wadsworth, Inc.): New York, 1984.

[107] Network Simulator 3 [Online]. Available: http://www.nsnam.org.

[108] Ns3::YansWiFiPhy Class Reference, Network Simulator 3 [Online]. Available: http://www.nsnam.org/doxygen/classns3_1_1_yans_wifi_phy.html

[109] Ns3::LteSpectrumPhy Class Reference, Network Simulator 3 [Online]. Available: http://www.nsnam.org/doxygen/classns3_1_1_lte_spectrum_phy.html

[110] J.Klaue, B.Rathke, A.Wolisz, "EvalVid – A Framework for Video Transmission and

Quality Evaluation", *Performance TOOLS 2003*, Urbana, USA, Sept. 2003, pp. 255-272.

[111] MSU Video Quality Measurement Tool, [Online]. Available: http://www.compression.ru/video/quality_measure/video_measurement_tool_en.html.

[112] MPTCP-NS3 Project, [Online]. Available: http://code.google.com/p/mptcp-ns3.

[113] Wireshark, [Online]. Available: http://www.wireshark.org.

[114] Ns3::TapBridge Class Reference, Network Simulator 3 [Online]. Available: http://www.nsnam.org/doxygen/classns3_1_1_tap_bridge.html#details.

[115] ITU-T Recommendation P.910, "Subjective Video Quality Assessment Methods for Multimedia Applications", Aug, 1996.

[116] ITU-T Recommendation P.911, "Subjective Audiovisual Quality Assessment Methods for Multimedia Applications", Dec, 1998.

[117] R. Trestian, "User-Centric Power-Friendly Quality-based Network Selection Strategy for Heterogeneous Wireless Environments", PhD thesis, Dublin City University, 2012, [Online]. Available: http://doras.dcu.ie/16783/1/Ramona_Trestian_-_PhD_Thesis_Final.PDF

[118] Z. Yuan, "Quality of Service Differentiation for Multimedia Delivery in Wireless LANs", PhD thesis, Dublin City University, 2012, [Online]. Available: http://doras.dcu.ie/17317/1/Thesis_Zhenhui_Yuan_-_Final_29_aug_2012.pdf

[119] H. Kim, M. Fomenkov, U. C. S. Diego, K. Lee, "Internet Traffic Classification Demystified: Myths, Caveats and the Best Practices", *Proceedings of the 2008 ACM CoNEXT Conference*, 2008.